

People's Democratic Republic of Algeria.

وزارة التعليم العالي و البحث العلمي

Ministry of Higher Education and Scientific Research

جامعة الجيلالي بونعاما بخميس مليانة

University of Djilali Bounaama Khemis Miliana

Faculty of Science and Technology

Department of Materials Sciences



Final Study Thesis

*In order to obtain a **Master's** degree in Chemistry*

Specialization: Pharmaceutical Chemistry

Theme

Anticancer study of ginger and Cinnamon against cyclin-Dependent Kinase-2 (CDK2) : An molecular Docking approach

In front of the jury composed of:

- Dr B. MKHANEG **President**
- Dr M. HAMMOUDI **Supervisor**
- Dr M. FIZIR **Examiner**

Presented by :

- Miss MEDANI Khadidja
- Miss DAHAS Manal

Année universitaire : 2022 / 2023

DEDICATION

Today, as I stand on the threshold of a new chapter in my life, I cannot help but reflect on the incredible journey that has led me here. Each step, every triumph, and even the occasional stumble, has been shaped by your unwavering support and love. On this momentous occasion of my graduation, I want to dedicate a heartfelt expression of gratitude to each and every one of you.

To my dearest parents, you have been my guiding stars, always lighting the way and nurturing my dreams. Your love has been a constant source of strength, and your sacrifices have been immeasurable. From the earliest days of my education, you instilled in me a thirst for knowledge and a belief in my own abilities. You were my cheerleaders, my confidants, and my rock. I owe my accomplishments to your unwavering faith in me, and I am forever grateful for the love and values you have bestowed upon me.

To my four knights, Abd Elmalek , Lotfi , Fawzi and Younes, you were the pillars of my strength and my pillar in this life. Thank you for being the best brothers.

To my sweet brother's wife Manal, and our new prince Raid , your presence has deeply touched and enriched my life.

A special dedication to all the Medani families.

To my cherished childhood friend, you who bloomed in my life like beautiful roses, Warda .

To my dear friend and invaluable companion, Manal, who has stood by my side through the moments of laughter and tears, supporting me unconditionally. Together, we have weathered the highs and lows, and I am forever grateful for our unwavering bond.

To our exceptional supervisor, Mr. HAMMOUDI, we attribute the completion of this thesis to your unwavering support and guidance. Without your encouragement and expertise, this achievement would not have been possible. We express our deepest gratitude and appreciation.
Thank you, sir

To Dr. BENZAID and to all my teachers, you are the true architects of my education. Your dedication, patience, and guidance have shaped my mind and inspired a deep passion for learning within me. I am forever thankful for your presence in my educational journey.

To the entire cohort of the 2022/2023 Pharmaceutical Chemistry Master's program,
Rihab ;Rabab; Sabrina ;Salma ;Amira ;Amal and Mawloud ,with whom I shared unparalleled experiences and created cherished memories that will forever hold a special place in my heart.

Finally, to all those I love and who love me, both near and far.

DEDICATION

I would like to dedicate this thesis to:

My grandparents,

For always loving encouragement and supporting me; your dua is the secret of my success. I am so blessed to have them in my life .

My parents,

As well as everything that I do, I would be honor to dedicate this thesis to my parents. The two person that gave the tools and values necessary to be where I am standing today. My parents support me on every step I make, and decision I take: but is necessary to understand that they let me take my decisions alone in order for me to learn from my personal mistake. I will never finish to thank my father and my mother for all the opportunities that they have offer and gave me, for all the teachings that they have told me and for every advise that come out of their mouth. I am so graceful with them, I hope that I can make you proud the same way I am proud of having you as my parents.

My siblings,

Meriem Hanaa, Maha and Mohamed Rayan , thank you for sharing with me all the moments of joy and sadness for being my confidant and my moral support. May god keep us for each other.

All my uncles and aunts ,

Special thank and gratitude to my uncle benyoucef for his help during my work in this thesis. I will never thank you enough for being here for me.

My incredible friends,

Rihab; Nadia “beti”; Wafa; Meriem; Sabrina; Rabab; Selma; Amira; Amel; mouloud . Your friendship and laughter have made this journey memorable and enjoyable thank you for your mental and emotional support in my life .

And my partner in this reserch MEDDANI Khadidja .

This thesis would not have been possible without the encougement of our supervisor Mr. HAMMOUDI .

This thesis is dedicated to all of you. Thank you for your love, support, and belief in me.

ACKNOWLEDGEMENT

First and foremost, we would like to thank GOD Almighty who has granted countless blessing, knowledge, and opportunity to us, so that we have been finally able to accomplish this modest work.

We would like to thank our supervisors Dr. HAMMOUDI for his guidance, knowledge, and expertise have been instrumental in shaping our understanding of our respective fields. He had not only provided us with the necessary tools and academic resources but also challenged us to think critically, explore new ideas, and push the boundaries of our knowledge. His commitment to our intellectual growth and development has inspired us to strive for greatness.

we would like to give special thanks to universitas Djilali Bounaâma (UDBKM) for giving me the opportunity to complete my studies successfully and I give many thanks to the faculty of sciences and technology, Department of Material Sciences, administration staff and lecturers for their kindness and cooperation with me during my studies at the university.

A special thanks to the dean of the Faculty Dr. BENZAID for his help duran this research and for always opening his door for us and for listening to us and encouraging us. We also appreciate his valuable advice.

We are truly grateful and thankful to Dr. KORAN for generously shared her time and wisdom. her insightful feedback ,constructive criticism and her help to redact this thesis.

We would also like to express my deepest appreciation to Dr B. MKHANEG and Dr M. FIZIR for serving as members of the jury . I also want to thank you for your brilliant comments and suggestions, thanks to you.

To each and every professor who has contributed to our education and growth, we offer our sincerest thanks. Your influence will forever be etched in our minds and hearts. We are privileged to have been your students, and we carry the lessons you have taught us as we embark on our future endeavors.

Finally, we would also like to thank all those who participated directly or indirectly in the realization of this thesis.

ملخص:

السرطان هو السبب الرئيسي للوفاة ، وغالبا ما تفشل علاجات السرطان الحالية في تحقيق النتائج المثلى بسبب الآثار الجانبية المبلغ عنها وتطور مقاومة العلاج. الهدف من عملنا هو دراسة النشاط المضاد للسرطان للزنجبيل والقرفة ضد السيكلين المعتمد على كيناز 2. هذا البحث عبارة عن دراسة في سيليكو عشرة مركبات من الزنجبيل (6-جنجرول، 8-جنجرول، 10-جنجرول، 6-بارادول و 6-شوغاؤل). ومن القرفة (سينامالدهيد، اوجينول، او-اسيتات السيناميل، السيناملدهيد المتناظر و حمض البروتوكاتيكويك. وللتنبؤ بنشاط هذه العناصر، استخدمنا عدة طرق حسابية (اداة الباس عبر الانترنت، دروليتو، نماذج حركية الدواء للجزيئات الصغيرة عبر الانترنت. تم الحصول على بنية المستقبل المستهدف من قاعدة بيانات البروتين، والتي تعمل كمستودع لهياكل البروتين المحددة تجريبيا. للحصول على بنية متوقعة للمستقبل السيكلين المعتمد على الكيناز 2، استخدمنا 4 طرق مختلفة للنمذجة: سويس مودال، الفاداتاباز، صانع الهيكل القائم على التطور و روبينا، تشير النتائج المتحصل عليها الى ان نموذج سويس اظهر تفوقا في المقارنات القائمة على قاعدة بيانات البروتين، بينما تفوقت روبينا في نتائج طاقة الارتباط الحر بعد ذلك قمنا بالالتحاق الجزيئي باستخدام برنامج اوتودوك 4.2.6 الذي يستهدف السيكلين المعتمد على الكيناز 2. تكشف البيانات التي تم الحصول عليها ان حمض البروتوكاتيكويك و6-شوجاؤل لهما تقربقوي مع المستقبل، مع طاقة الارتباط الحر 5.7- و5.4-. سرعة حرارية /مول، وثابت تثبيط 60715 و1339 نانومتر على التوالي، عند مقارنة نتائج مع عقار روسكوفيتين، نجد ان النتائج كانت متقاربة، حيث تقدر طاقة الارتباط الحر ب5.9- سرعة حرارية /مول و ثابت تثبيط 21250 نانومتر. على اساس نتائج الدراسة يمكن الاستنتاج ان مركبات الزنجبيل و القرفة لديها القدرة على ان تكون مرشحة و اعدة لعقاقير مكافحة السرطان، حيث يكون افضل مرشح هو حمض البروتوكاتيكويك يليه 6-شوجاؤل. ومع ذلك هناك حاجة الى دراسات إضافية تجريبية على مركبات الفلافونويد و احماض الفينوليك للزنجبيل و القرفة.

الكلمات المفتاحية: السرطان، للزنجبيل، القرفة، السيكلين المعتمد على كيناز، في سيليكو، النمذجة.

Résumé :

Le cancer est l'une des principales causes de décès, et les traitements anticancéreux existants échouent souvent à atteindre des résultats optimaux en raison des effets secondaires signalés et du développement de résistance au traitement. L'objectif de notre travail est d'étudier l'activité anticancéreuse du gingembre et de la cannelle contre la cycline dépendante de la kinase 2 (CDK2). Cette recherche est une étude *in silico* de dix composés du gingembre (6-gingérol, 8-gingérol, 10-gingérol, 6-paradol, 6-shogaol) et de la cannelle (Cuminaldéhyde, Eugénol, (E)-acétate de cinnamyle, trans-Cinnamaldéhyde, Acide protocatéchique). Pour prédire l'activité de ces substances, nous avons utilisé plusieurs méthodes computationnelles (Pass online, PKCSM, Drulito). La structure du récepteur cible CDK2 a été obtenue à partir de la Banque de données sur les protéines (PDB), qui sert de référentiel pour les structures protéiques déterminées expérimentalement. Pour obtenir une structure prédite du récepteur CDK2, nous avons utilisé quatre méthodes de modélisation différentes: Swiss-Model, la base de données AlphaFold, ESM (Evolutionary-based Structure Maker) et Robetta, nos résultats indiquent que Swiss-Model a montré une supériorité dans les comparaisons basées sur PDB, tandis que Robetta s'est distingué dans les résultats ΔG . Ensuite, nous avons effectué un docking moléculaire en utilisant le programme AutoDock 4.2.6 en ciblant la CDK2.

Les données obtenues révèlent que l'Acide protocatéchique et le 6-shogaol présentent une forte affinité pour la CDK2, avec une énergie libre de liaison (ΔG) de -5,7 et -5,4 kcal/mol, et une constante d'inhibition (K_i) de 15 607 et 9 133 nm, respectivement, lorsqu'on compare les résultats de ΔG avec le médicament roscovitine, nous constatons que les résultats sont très proches, estimés à -5,9 kcal/mol, et une constante d'inhibition (K_i) de 21250 nm. On peut conclure que les composés

du gingembre et de la cannelle ont le potentiel d'être des candidats médicamenteux anticancéreux prometteurs, où le meilleur candidat est l'Acide protocatéchuique (cannelle), suivi du 6-shogaol (gingembre). Cependant, des études supplémentaires sur les composés flavonoïdes, Acides phénoliques du gingembre et de la cannelle sont nécessaires.

Mots clés: Cancer, Gingembre, Cannelle, Cycline dépendante de la kinase 2 (CDK2), In silico, Modélisation .

Abstract :

One of the causes of death is cancer. Existing anti-cancer treatments often fail to achieve optimal outcomes due to reported side effects and the development of treatment resistance. The objective of our work is to study the anticancer activity of ginger and cinnamon against cyclin dependent kinase 2. This research is an in silico study of ten compounds from ginger (6-gingerol ; 8-gingerol ; 10-gingerol ; 6-paradol ; 6-shogaol) and cinnamon (Cuminaldehyd ; Eugenol ; (E)-cinnamyl acetate ; transCinnamaldehyde ; Protocatechuic Acid) , to predict the activity spectrum of substances we used Pass online, DruLiTo, PKCSM . The structure of the CDK2 target receptor was obtained from the Protein Data Bank (PDB), which serves as a repository for experimentally determined protein structures. To obtain a predicted structure of the CDK2 receptor, four different methods of modeling were employed: Swiss-Model, AlphaFold database, ESM (Evolutionary-based Structure Maker), and Robetta, our findings indicate that Swiss-Model showed superiority in PDB-based comparisons, while Robetta excelled in ΔG results. Molecular docking was carried out by the AutoDock 4.2.6 program on CDK2 targeting. From the data obtained, Protocatechuic Acid and 6-shogaol have a high affinity for CDK2 with a free energy of binding (ΔG) -5.7 and -5.4 kcal/mol and an inhibition constant (K_i) of 15607 and 9133nm , when compared with a roscovitine drug, we find that the results of ΔG are very close, estimated at -5.9Kcal/mol with K_i of 21250 nm . It can be concluded that the compounds from ginger and cinnamon. Album has the potential as a promising anti-cancer drug candidate, where the best candidate is the Protocatechuic Acid (cinnamon) then 6-Shogaol (ginger). However, further studies of flavonoid and Phenolic acids compounds from ginger and cinnamon are needed.

Key words: Cancer, Ginger, Cinnamon, Cyclin dependent kinase2, In silico, Modeling.

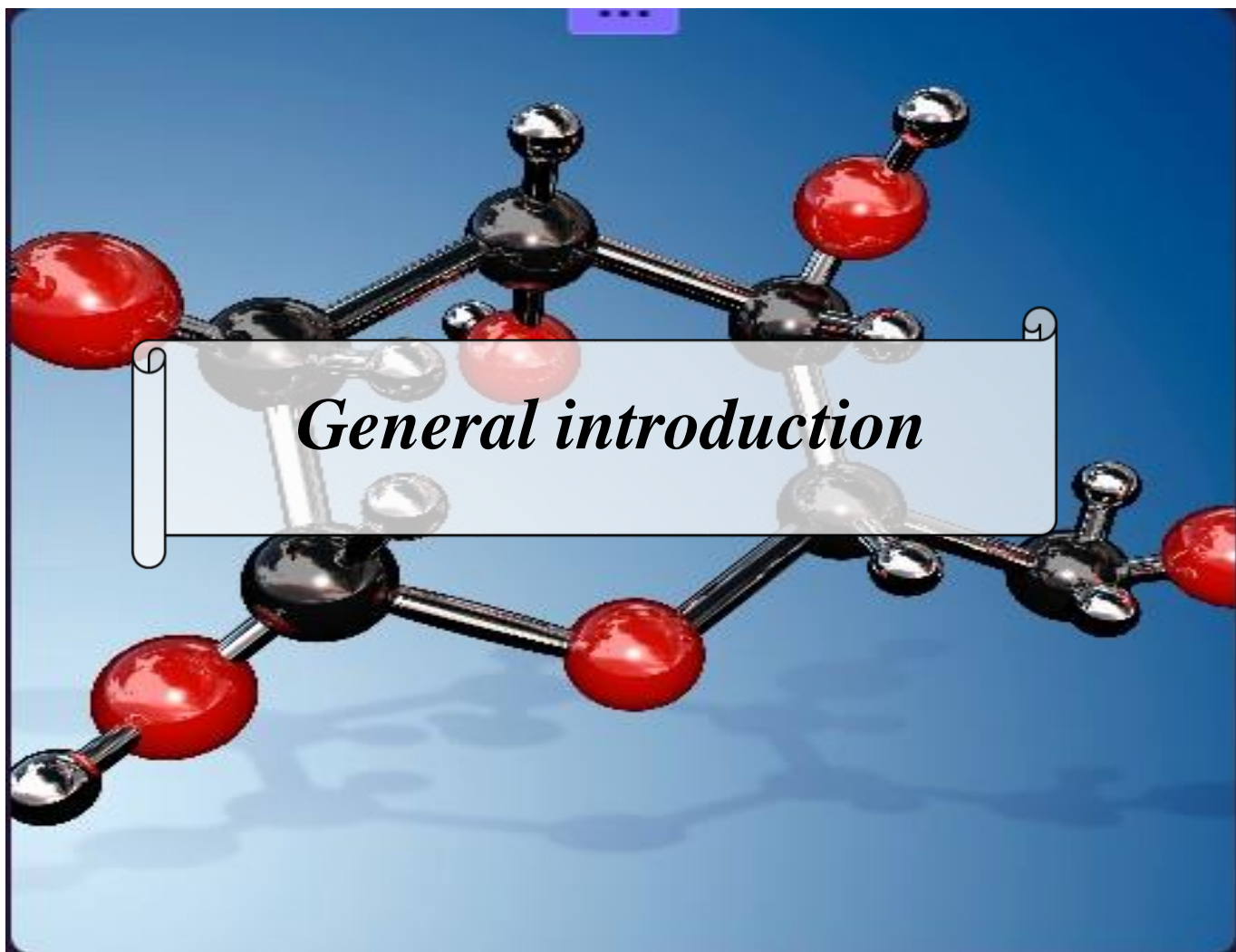
General introduction	1
.....	3
<i>Bibliographic studies</i>.....	4
Chapter 1 : Medicinal plants	5
1.1. Introduction	6
1.2. Medicinal plants	6
1.3. Significances of medicinal plants to human beings	7
1.3.1. Plant primary metabolites	7
1.3.2. Plant secondary metabolites	7
1.4. Characteristics of medicinal plants	8
1.5. Future of medical plants.....	8
1.6. Cinnamon	9
1.6.1. Clinical significance of cinnamon	10
1.6.2. Chemical composition of cinnamon	11
1.6.3. Anti-cancer properties of cinnamon	12
1.7. Ginger.....	13
1.7.1. Clinical significance of ginger.....	14
1.7.2. Chemical composition of ginger.....	15
1.7.3. Anti-cancer properties of ginger.....	18
1.8. Conclusion.....	21
Chapter 2 : Cancer , Cyclin depepent kinase.....	22
2.1. Introduction	23
2.2. Cancer.....	23
2.2.1. General information.....	23
2.2.2. Definition of cancer	24
2.2.3. Property of cancer cells	24
2.2.4. Cancer statistics	26
2.3. Different types of cancer-related to cyclin dependent kinase 2 :	26
2.3.1. Breast cancer.....	27
2.3.1.1 Epidemiology.....	27
2.3.2. Lung cancer	28
2.3.2.1. Epidemiology.....	28

2.3.3. Colon cancer	28
2.3.3.1. Epidemiology.....	29
□ Global statistics.....	29
2.4. Cyclin Dependent Kinase.....	29
2.4.1. General information of cyclin-dependent kinases	29
2.4.2. Nomenclature and classification of cyclin dependent kinase	30
2.4.3. General structure.....	31
2.4.4. Activity of cyclin-dependent kinases	32
2.4.5. cyclin-dependent kinases inhibitor	33
2.5.Cyclin-Dependent Kinase 2 enzyme.....	34
2.5.1. Catalytic domain.....	34
2.5.2. Action mechanism	35
2.5.3. Inhibitor of cyclin-dependent kinase 2	36
2.6. Conclusion.....	36
Chapter 3: In silico.....	38
3.1. Introduction	38
3.2. In silico.....	38
3.3. Quantitative structure-activity relationship (QSAR).....	39
3.4. Molecular docking.....	40
3.4.1. The principle of docking	41
3.4.2. The importance of the docking.....	41
3.4.3. The most popular docking programs.....	42
3.5. Autodock	43
3.6. Autodock Vina	43
3.7. Discovery studio.....	44
3.8. Modeling	46
3.8.1. Swiss model.....	46
3.8.2. Alphadatabase	47
3.8.3. Evolutionary scale modeling.....	47
3.8.4. Robetta	47
3.9. Pharmacokinetics	48
3.9.1 Drug likeness tool.....	48

3.9.2. Pharmacokinetics models for small molecules (PKCSM).....	49
3.9.3. Pass online	50
2.7. Conclusion.....	51
Chapter 4: Materials and methods.....	53
4.1. Introduction	53
4.2. Apparatus and reagents	54
4.3. Extraction methods.....	54
4.3.1 Steam distillation (Hydrodistillation).....	55
4.4. Characteristics of the essential oil.....	57
4.4.1. Organoleptic properties	57
4.4.2 Physico-chemical properties.....	57
4.4.2.1. Relative density	57
4.4.2.2. pH value.....	58
4.4.2.3. Acid value (neutralization number).....	58
4.4.2.4. Ester value	59
4.4.2.5. Saponification Value.....	61
4.4.3. Biochemical activity	61
4.4.3.1 Determination of total flavonoids:.....	61
4.4.3.2. Antioxidant activitie.....	62
4.4.3.Antibacterial activity :Determination of the minimum inhibitory concentration of ginger and cinnamon essential oils.....	63
4.4.3.1. Selection of bacterial and fungal strains for culture media:.....	64
4.4.3.2. Bacterial suspension preparation.....	64
4.4.3.3. Preparation of cinnamon and ginger essential oil dilutions.....	65
4.5. In Silico anticancer study	67
4.5.1. Micro-computer	67
4.5.2. Moleculer docking.....	70
4.5.2.1. Preparation of the receptor/target and ligand for the docking	70
4.5.2.2. Ligand preparation	71
4.5.2.3. Preparation of docking parameter file.....	73
4.5.2.4. Running autodock vina	75
4.5.2.5. Evaluation of docking and virtual screening	76
4.5.3. Modeling.....	76

4.6. Pharmacokinetics	83
4.6.1. Drug likeness tool ‘Drulito’	83
4.6.2. Pharmacokinetics models for small molecule(PKCSM)	86
4.6.3. Pass Online	87
4.7. Conclusion.....	87
Chapter 5:Results and discusion	89
5.1. Introduction	89
5.2. Extraction “Hydrodistillation”	89
5.3. Characteristics of essential oil.....	91
5.3.1. Organoleptic properties	91
5.3.2. Physico-chemical properties of essential oil	92
5.3.3.1. Relative density	92
5.3.3.2. pH value.....	92
5.3.3.3. Acid value (neutralization number).....	93
5.3.3.4. Ester value	95
5.3.3.6. Saponification value	97
5.3.4. Biochemical activity	98
5.3.4.1. Flavonoids test	98
5.3.4.2. Antioxidant activity	100
5.3.5. Antibacterial activitiy.....	102
5.4. In Silico anti-cancer study.....	109
5.4.1. Moleculer docking:	109
5.4.1.1. Protein data bank	116
5.4.1.2. Swiss model	123
5.4.1.3. Alphadatabase	130
5.4.1.4. Evolutionary scale modeling ESM	136
5.4.1.5. Robetta	142
5.4.2. Comparison of Interaction Results	149
5.5. Pharmacokinetics	150
5.5.1. Drug likeness tool.....	150
5.5.2. Pharmacokinetics models for small molecules.....	152
5.5.3. Pass online	154

5.6. Conclusion.....	156
General conclusion	158
Appendices	
Bibliographic references	
List of Tabs	
List of Figs	
List of equation	
List of abbreviation	



General introduction

General introduction

The world relied predominantly on manual processes and traditional problem-solving approaches. Tasks that consuming and required significant human effort. The introduction of Artificial intelligence by the mathematician Alan Turing has brought about remarkable advancements, transforming various industries and shaping our daily lives [1]. The AI leverages computers and machines to mimic the problem-solving and decision-making capabilities of the human mind. According to the McKinsey Global Institute, the rapid development and increasing applications of AI across various industries have captured widespread attention and have the potential to transform the way we live and work [2, 3].

In recent years, the pharmaceutical sector has experienced a significant increase in data digitalization. However, this digitalization poses challenges in effectively acquiring, analyzing, and applying knowledge to address complex clinical problems [4]. To tackle these challenges, the use of AI has emerged as a promising solution, leveraging its ability to handle large volumes of data through enhanced automation [5]. AI is a technology-driven system that incorporates advanced tools and networks to simulate human intelligence, without completely replacing human involvement [6, 7]. By utilizing software and systems capable of interpreting and learning from input data, AI can independently make decisions to achieve specific objectives.

The process of discovering new drugs encounters numerous challenges. One significant challenge lies in the low success rate of bringing a new drug to the market, as many potential candidates fail during preclinical and clinical trials. This can be attributed to the complexity of biological systems, which makes it difficult to fully comprehend their intricacies. Pharmaceutical research generates vast amounts of valuable data and knowledge; however, effectively transferring this knowledge within and between organizations can be a challenging task. Furthermore, the development of a new drug is a complex and costly endeavor, often spanning several years and incurring expenses amounting to billions of dollars [8]. the timeline and cost involved in discovering and developing anticancer drugs are substantial. The process often takes many years, involving extensive research, laboratory testing, preclinical studies, clinical trials, and regulatory approvals. The expenses associated with these activities can be substantial and can fail to demonstrate efficacy or safety in clinical trials [9].

Cyclin-Dependent Kinases, are enzymes responsible for regulating cellular processes and the cell cycle [10]. CDK2, a prominent member of the CDK family, plays a critical role in facilitating the transition of cells from the G1 phase to the S phase. Targeting CDK2 activity has emerged as a potential strategy in cancer treatment, showing promise in enhancing cancer therapy [11].

In our study, we have chosen Cinnamon and ginger, which is among the many herbal medicines used as an anticancer against Cyclin-Dependent Kinase-2 (CDK2)

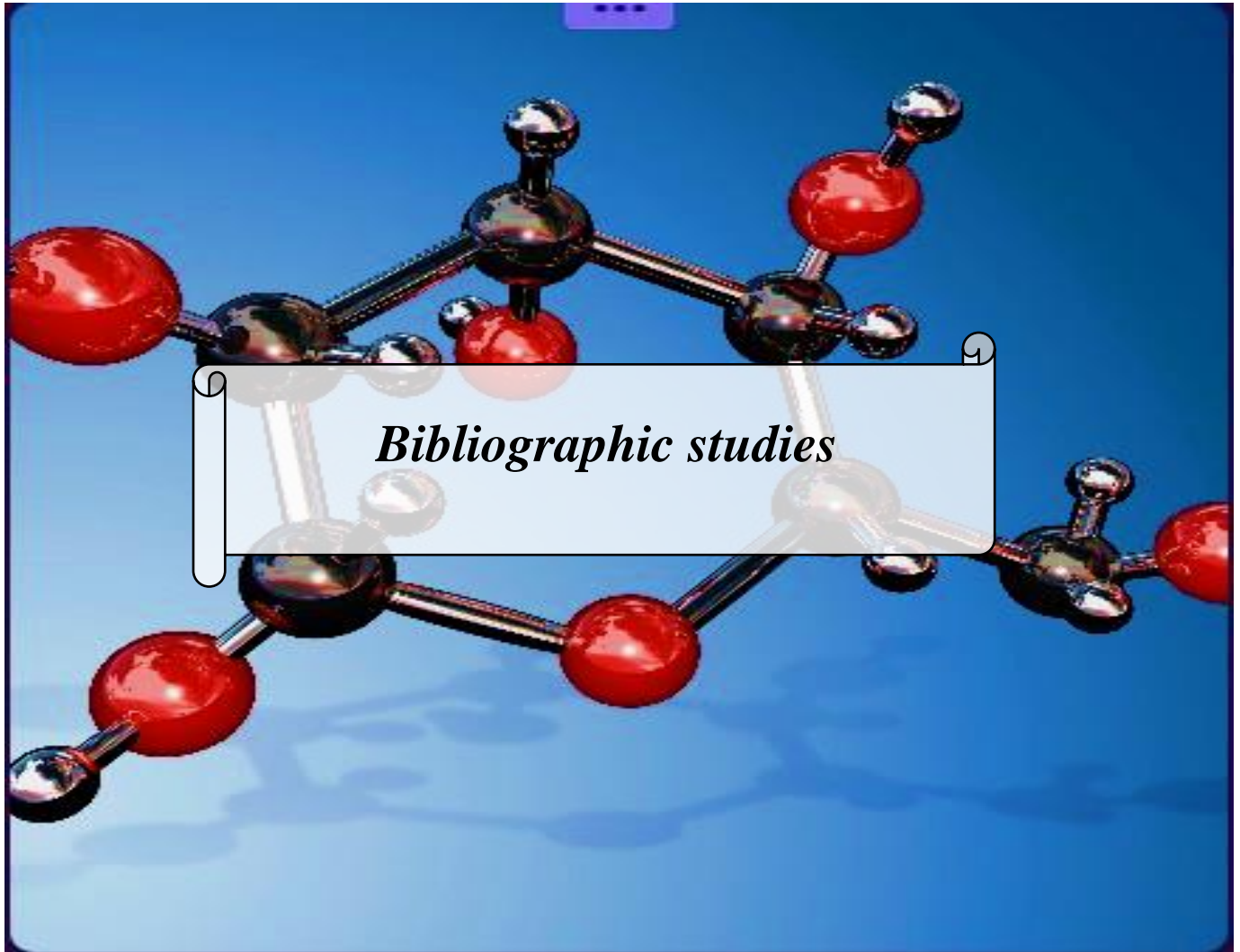
In this context we aim to answer the following questions:

- ❖ Do interactions genuinely occur between CDK2 and the compounds found in cinnamon and ginger?
- ❖ What is the fate of the compounds from cinnamon and ginger in the human body?
- ❖ How can we propose new modelities for predicting protein target of CDK2 contributing to the advancement of drug discovery and therapeutic interventions?
- ❖ In the context of the potential anticancer properties of cinnamon and ginger, is it worth exploring the possibility of identifying common compounds and the presence of similar classes of compounds, such as flavonoids, phenols acid, polyphenols ?

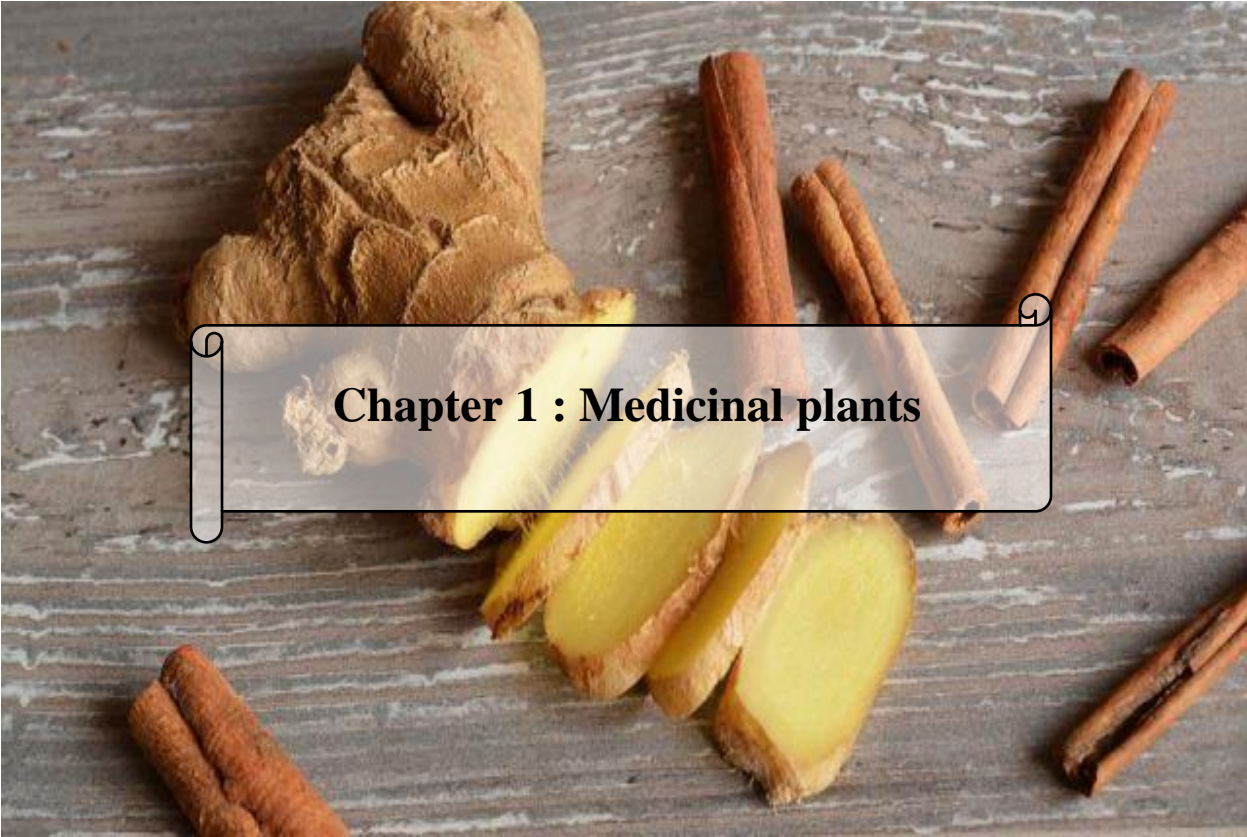
To answer this question, this thesis is divided into three parts. The first part is a literature review, which includes general information about medicinal plants, specifically focusing on cinnamon and ginger. It also explores the relationship between cancer and CDK2 and examines the *in silico* approach used in medicinal plant research.

The second part of the thesis is an experimental study. It begins with a description of the extraction methods employed and provides physico-chemical characterizations of cinnamon and ginger extracts. Furthermore, it delves into the investigation of the antibacterial and biochemical activities of the cinnamon and ginger extracts through experimental methods. The study also applies an *in silico* approach to explore the potential anticancer activity of the extracts. Additionally, a pharmacokinetics study is conducted to analyze the behavior of specific compounds found in cinnamon and ginger. Lastly, the study includes the modeling of the target of CDK2 to gain further insights into its interaction with the compounds.

The third and final part of the thesis consists of a conclusion that provides a general summary of the findings and their implications. It serves to consolidate the results obtained throughout the study and draw meaningful conclusions from them.



Bibliographic studies



Chapter 1 : Medicinal plants

Chapter 1: Medicinal plants

1.1. Introduction

Cinnamon and ginger, renowned for their medicinal properties, have been extensively researched due to their potential health benefits. Cinnamon is derived from the bark of Cinnamomum trees, while ginger comes from the root of the Zingiber officinale plant. Both plants possess therapeutic properties and are widely utilized in traditional and modern medicine [12].

1.2. Medicinal plants

Medicinal plants, which encompass a variety of plants used in herbalism with medicinal properties, play a critical role in the development of human cultures worldwide and are considered a rich resource for drug development and synthesis. Some plants, such as ginger, green tea, and walnuts, are also recommended for their nutritional and therapeutic values. The active ingredients derived from medicinal plants are used in various drugs, including aspirin and toothpaste. Traditional medicinal systems and developing countries rely heavily on medicinal plants for primary healthcare needs [13]. UNESCO (United Nations Educational, Scientific, and Cultural Organization) has noted that medicinal plant use is increasing in industrialized societies for traditional herbal remedies and drug development. Developing countries, such as those in Africa, have a wealth of medicinal plants, including Phytolacca dodecandra, Catharanthus roseus, Ricinus communis, and Harpagophytum procumbens, which are used for various medicinal purposes. The medicinal plant trade has grown in volume and exports, and it is a major source of valuable foreign exchange for most developing countries. The development and commercialization of medicinal plant-based industries in developing countries require the availability of facilities and information regarding bioprocessing, extraction, purification, and marketing of the industrial potential of medicinal plants. Recent estimates suggest that over 9,000 plants have known medicinal applications in various cultures and countries [14, 15].

1.3. Significances of medicinal plants to human beings

Medicinal herbs are crucial to the evolution of human culture, including religion and many ceremonies. Many contemporary medications, like aspirin, are made inadvertently from therapeutic plants, and many food crops like garlic, have therapeutic properties.

New medications can be derived from medicinal plants. More than 250 000 different species of flowering plants are thought to exist. Understanding plant toxicity and defending people and animals against natural poisons are two benefits of studying medicinal plants. Plant metabolic engineering, for instance, is protected by the cultivation and preservation of therapeutic plants. Plant species produce metabolites, particularly secondary chemicals, which are responsible for the therapeutic actions of plants. Among the plant metabolites are primary metabolites and secondary metabolites.

The term "phytotherapy" refers to using plants or plant extracts for therapeutic purposes, particularly ones that are not often consumed. Various secondary metabolic products are discovered in plants, and phytochemistry is the study of phytochemicals produced by plants, and it describes these compounds' isolation, purification, identification, and structure [16].

1.3.1. Plant primary metabolites

Every plant produces organic molecules that perform metabolic processes necessary for plant development and growth. Include lipids, fatty acids, steroids, nucleotides, amino acids, and carbs [16].

1.3.2. Plant secondary metabolites

Organic substances made by the plant kingdom have no obvious roles in the growth and development of plants. Produced throughout a plant's growth in distinct plant families, specific groups of plant families, or in certain tissues, cells, or developmental stages. Include phenolics, terpenoids, and specific nitrogen metabolites (such as on-protein amino acids, amines, cyanogenic glycosides, glucosinolates, and alkaloids) Fig1.1 [16].

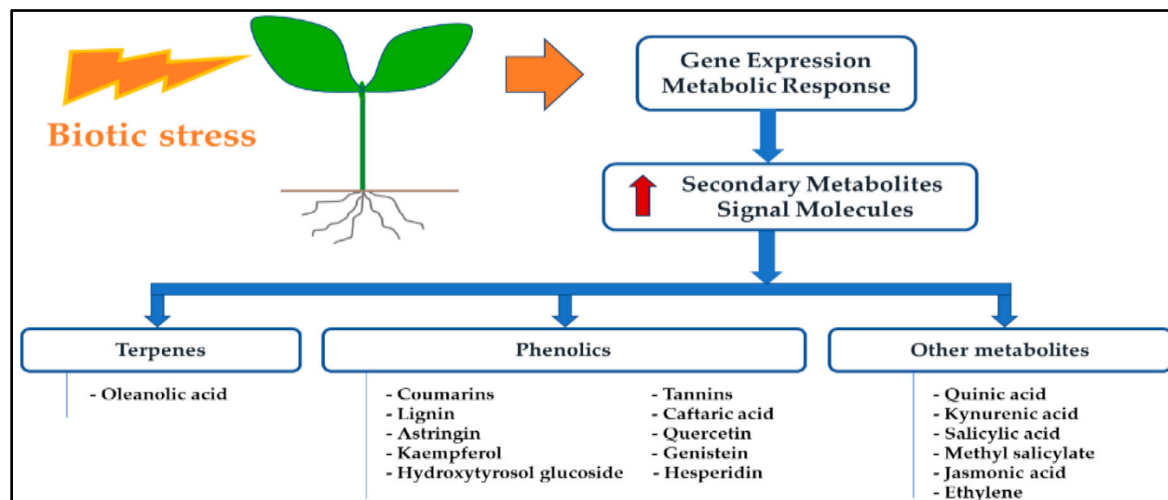


Fig.1.1 Secondary metabolites [17]

1.4. Characteristics of medicinal plants

Plants have many characteristics when used as a treatment, including:

- Synergic medicine- The ingredients of plants all interact simultaneously, so their uses can complement or damage others or neutralize their possible negative effects.
- Support of official medicine- In treating complex cases like cancer diseases the components of the plants proved to be very effective [18, 19].
- Preventive medicine- It has been proven that the component of plants is also characterized by their ability to prevent the appearance of some diseases. This will help to reduce the use of chemical remedies, which will be used when the disease is already present, i.e., reduce the side effect of synthetic treatment [20].

1.5. Future of medical plants

More than 100,000 plants still need to be identified or have yet to have their medicinal properties thoroughly researched and studied. The medical efficacy of plants and herbs should be evaluated in current and future studies because it is projected that they will play a significant role in the medical profession, particularly in treating serious diseases like cancer [19].

1.6. Cinnamon

Looking through any cookbook will reveal that cinnamon is among the most commonly used spices in the world. Cinnamon is a common ingredient in everyday family meals and exceptional delights, including breakfast rolls, spiced cookies, pudding and pies, quickbreads, and chutneys. Cinnamon ranks as the second-most significant spice (next to black pepper) [21]. Cinnamon comes from the Greek word *Kinnamon*, which means sweet wood. Probably derived from the Hebrew word *quinamom*, this name has a Semitic origin. In addition to having the meaning "sweet wood," the names "kayu manis" in Malayan and Indonesian also have this meaning. An old spelling of this term could have impacted Hebrew and Greek. Names derived from the Latin *canella* include Dutch (*kaneel*), French (*cannelle*), Italian (*Cannella*), and Spanish (*Canela*) (meaning small tube or pipe, referring to the form of cinnamon quills) (Rq : in arabic we say *Qurfar*). Originally, the Chinese cinnamon, well-liked in northern India before the Ceylon cinnamon became well-known, was referred to by the Hindi name *dalchini*, which means Chinese wood. The Greek name *Kasia*, which originates in the Hebrew word *qeshiiah*, has given rise to the name *Cassia*. One of the wide varieties of *Cinnamomum* is *Cinnamomum verum* (syn. *C. zeylanicum*), also known as "genuine" cinnamon or Ceylon cinnamon and native to Sri Lanka. Another variety is *Cinnamomum cassia*, which comes from several places. Other species include Chinese cinnamon (syn. *C. aromaticum*), a native of China and Vietnam; Indonesian cassia (syn. *C. burmannii*), originating from Sumatra and Java regions; Indian cassia (syn. *C. tamala*), originating from North Eastern India; and Saigon cassia (syn. *C. loureiroi*) from Vietnam; The bark can be powdered and is typically a golden brown color [13]. It has been demonstrated that this spice has a number of useful qualities. It is applied to Fight internal cancer-causing radicals. A spice called that can lower the risk of colon cancer. Both Parkinson's disease and attention deficit disorder are treated with cinnamon. Impotence and erectile dysfunction in men may be simultaneously cured with cinnamon. In addition to regulating the amount of bad cholesterol, cinnamon is a spice that can increase the body's HDL(High-Density Lipoprotein), or "good" cholesterol, in addition to regulating the amount of bad cholesterol. The common cold is warded off when cinnamon is consumed because it has anti-inflammatory qualities that prevent phlegm development. For people with type 2 diabetes, the delayed release of carbs in the body is beneficial [21].

1.6.1. Clinical significance of cinnamon

For centuries, cinnamon has been used as a spice and medicinal agent [22]. Medicinally, it has been used to alleviate digestive issues such as dyspepsia, anorexia, and vomiting and for anecdotal purposes such as treating bleeding ulcers and various cancers [20]. Recent research has mainly focused on cinnamon's antidiabetic and antilipidemic properties, although more investigation is needed to determine the optimal therapeutic benefit and dosing parameters (Fig 1.2). Cinnamon is abundant in polyphenol antioxidants, which possess anti-inflammatory effects that can reduce disease risk [23]. In addition, cinnamon has been demonstrated to enhance key risk factors linked to heart diseases, such as cholesterol, triglycerides, and blood pressure. Studies involving animals have shown that cinnamon may improve conditions such as Alzheimer's and Parkinson's, although its effectiveness in humans remains to be seen. Additionally, animal and test-tube studies suggest that cinnamon may provide protection against cancer, and its antifungal and antibacterial properties, mainly cinnamaldehyde, may help to reduce infections, tooth decay, and bad breath. Although human research in this area is limited, preliminary test-tube studies indicate that cinnamon could safeguard against specific viruses [24].

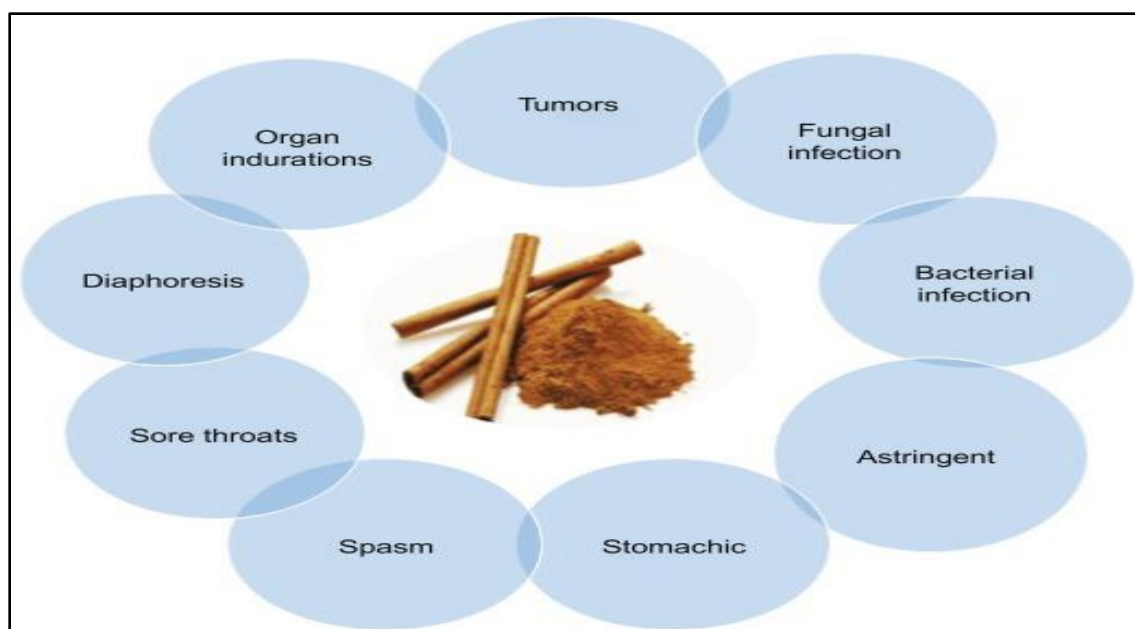


Fig.1.2 Clinical Significance of Cinnamon [25]

1.6.2. Chemical composition of cinnamon

Cinnamon is made up of many resinous substances, such as cinnamaldehyde, cinnamate, cinnamic acid (Fig 1.3), and many essential oils (Tab 1.1) [25]. Cinnamaldehyde, produced by the absorption of oxygen, is reportedly responsible for the spicy flavour and aroma. As cinnamon ages, the color darkens, enhancing the resinous components. Numerous essential oils have been identified as being present, including trans-cinnamaldehyde, cinnamyl acetate [26].

Tab.1.1 Chemical constituents of different parts of cinnamon [12]

Parts of cinnamon	Chemical constituents
Bark	Cinnamaldehyde: 65.00 to 80.00% Eugenol: 5.00 to 10.00%
Root bark	Camphor: 60.00%
Fruit	Trans-cinnamyl acetate (42.00 to 54.00%) Caryophyllene (9.00 to 14.00%)
c.zeylanicum buds	Terpene hydrocarbons: 78.00% Alpha-Bergamotene: 27.38% Alpha-Copaene: 23.05% Oxygenated terpenoids: 9.00%
C. zeylanicum flowers	(E)-Cinnamyl acetate: 41.98% Trans-alpha-Bergamotene: 7.97% Caryophyllene oxide: 7.20%

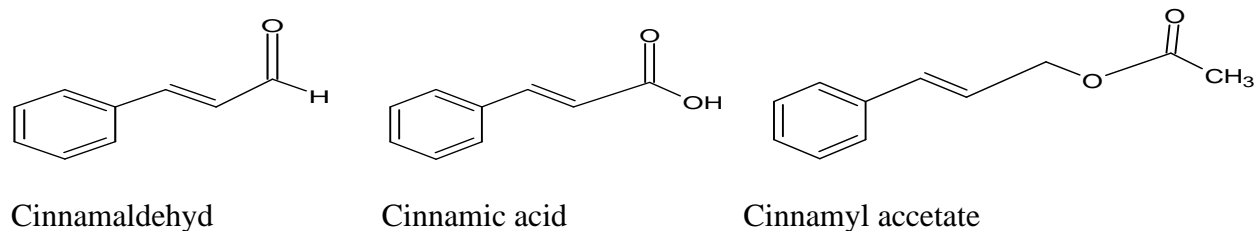


Fig.1.3 Cinnamyl group-containing compounds [26]

1.6.3. Anti-cancer properties of cinnamon

Cinnamon bark extract has been found to significantly prevent the activation of the EBV-EA (Epstein-Barr Virus - Early Antigens) early antigen, which is a factor that initiates tumor growth. In vivo and in vitro studies have shown promising trends in the anti-cancer effects of cinnamon bark extract on cutaneous and lung tumors. 2-hydroxy cinnamaldehyde, isolated from the stem bark of cinnamon, was investigated for its effect on Farnesyl-protein-transferase, an enzyme involved in the onset of tumor formation. An experimental liver and lung metastasis reveals antimetastatic potential in a cinnamon multiherbal formulation. Anti-tumor activities may be implied by research on vitamins' antioxidant and immunomodulatory abilities [24].

Cinnamaldehyde's anti-cancer effects were determined to be caused by the development of reactive oxygen species (ROS)-mediated mitochondrial permeability transition and subsequent cytochrome C release. It was found that increased caspase-3 activity and a decrease in mitochondrial transmembrane potential in HL-60 cells indicate that *C. cassia* caused cell death. The authors developed cinnamaldehydes and related compounds from various cinnamic acids based on the 2-hydroxycinnamaldehyde isolated from the bark of *C. Cassenamaldehyde* analogues, such as HCT15 and SK-MEL-2 cells, were found to be more cytotoxic than human solid tumor cells. Saturated aldehydes had lower cytotoxicity. The main structural element of the extracellular and basement membranes, type IV collagen, was degraded by matrix metalloproteinase-9 (MMP-9). In tumor tissues, there was an increase in this enzyme's activity, however, it was moderately inhibited by the *C. Cassena* water extract, hexane and chloroform fractions, and fractions. A significant MMP-19 inhibition was discovered in the *C. cassia* butanol fraction [27].

1.7. Ginger

Ginger (*Zingiber officinal*) is a member of the ginger family native to Southeast Asia. Indigenous peoples of Asia (especially China and India) have consumed ginger in various ways for centuries, both as a spice and sweetener in local cuisines and as a herbal remedy for many ailments. In particular, ginger is said to have healing properties in traditional Chinese, Indian and Ayurvedic medicine. It is a cough suppressant due to its expectorant and expectorant properties. Ginger relieves pain, treats nausea, vomiting, and poisoning, and improves digestion [26]. Currently, ginger is known to have antioxidant, anti-inflammatory, and anti-tumour properties, and its effectiveness in the prevention and treatment of gastrointestinal, cardiovascular, respiratory, and nervous system diseases has been confirmed by multiple studies. Rhizomes are the edible parts of plants [28]. The nutritional value of ginger is attributed to the bioactive compounds contained in the rhizome, such as gingerols (GNs), gingerols (SGs), paradols, and zingiberene. Volatile phenolic compounds in fresh ginger rhizomes, mainly 6-GN and 4-, 8-, 10-, and 12-GN, endow ginger with a pungent smell and unique aroma [26]. These compounds are sensitive to pH and temperature changes, and gingerol is rapidly converted to the corresponding 6, 8 and 10 SG during processes that require extreme heat, such as drying and baking. Extracts and processing methods from rhizomes vary widely in chemical composition and related properties, and dried ginger plays a key role in antioxidant activity [28].

Dried Ginger Powder is also known as Sonth in Hindi, Sonti in Telugu, Soonth in Gujarati, Suntha in Marathi, and Suntha in Kannada, Called Shunti. The main phenolic compound in ginger is mainly gingerol, the active ingredient of fresh ginger. Other important polyphenols are abundant in active phytochemicals, such as shogaole, paradole, cerumbone, zingerone, gingerol, and 1-dehydro-(10)-gingerdione. Ginger can be obtained from ginger by heat treatment or long-term storage, and Paradols can form Shogaols upon hydration. In addition, ginger fiber also contains polysaccharides, lipids and organic acids. The active compounds of ginger play a vital role in various biological activities such as anti-inflammatory, anti-tumor, antibacterial, and antioxidant. Therefore, dried ginger rhizomes are the primary source of 6-SG, the most famous dehydration product. Recent studies have shown that 6-SG has better biological effects compared to 6-GN

and has no associated side effects. Therefore, shuntha is medically considered more effective than ginger [29].

1.7.1. Clinical significance of ginger

Many herbs and spices possess a range of biochemical and pharmacological activities, including anti-inflammatory and antioxidant properties, which are thought to contribute to their antimutagenic and anti-cancer activities [30]. Spice ginger mainly contains the phenolic substance gingerol, which has various pharmacological effects such as anti-inflammation, anti-oxidation, and anti-apoptosis. Since tumor promotion is closely related to inflammation and oxidative stress, compounds with anti-inflammatory and/or antioxidant properties may serve as anti-cancer agents. Ginger is important in treating several ailments, including gastrointestinal complications, upset stomach, diarrhea, rheumatism, nausea, colds, fever, and dizziness. Ginger also has antineoplastic and chemopreventive properties [31].

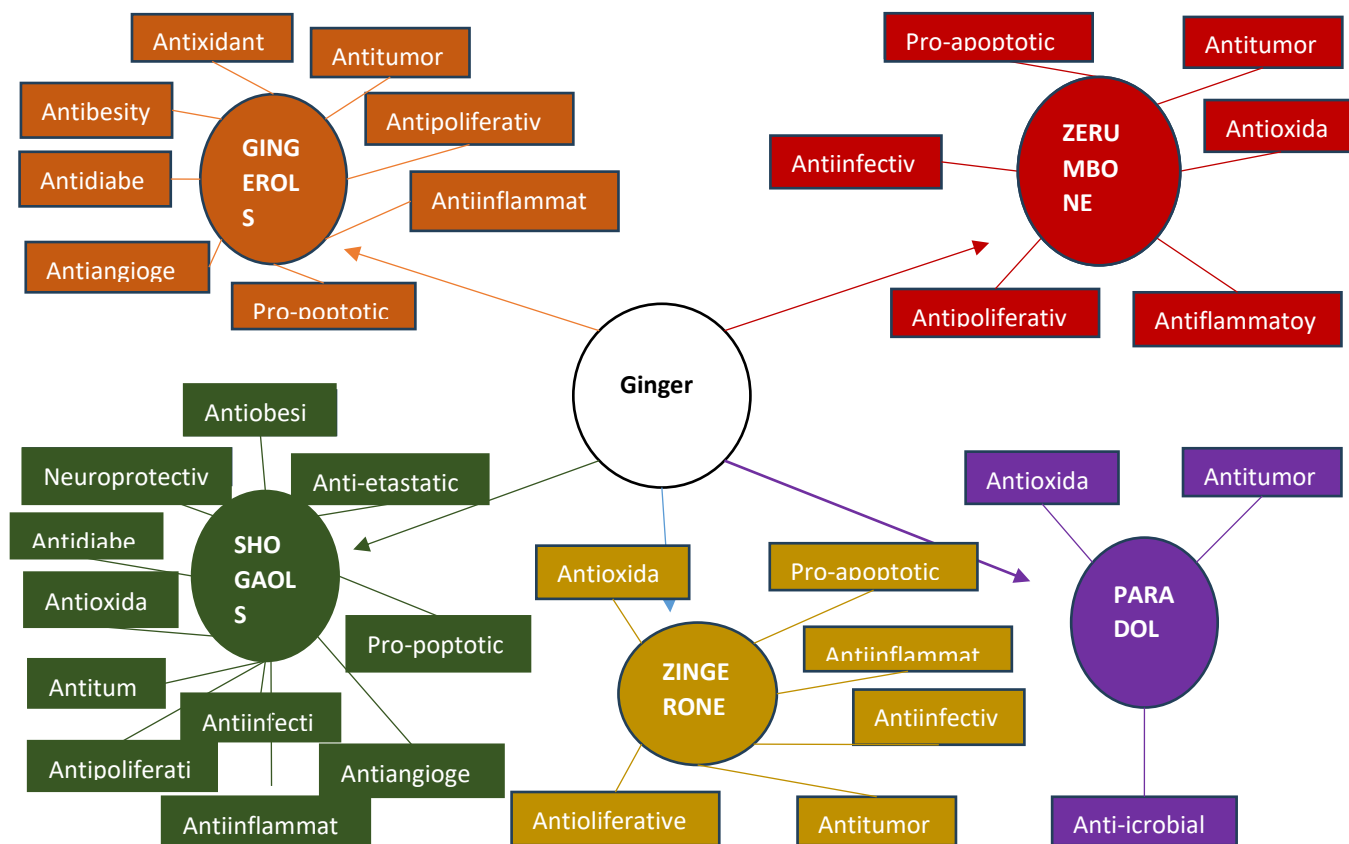


Fig.1.4 Clinical Significance of Ginger [28].

1.7.2. Chemical composition of ginger

Ginger contains numerous constituents that vary depending on its place of origin and whether they are fresh or dry. The odor of ginger mainly depends on the volatile oil's pharmacological activities, which yield mainly monoterpenoids and sesquiterpenoids [32]. The pungency of fresh ginger comes from gingerols, a homologous series of phenols, with 6-gingerol being the most abundant. The pungency of dry ginger mainly comes from shogaols, dehydrated forms of gingerols formed during thermal processing. Sixty-three compounds have been identified in organically grown fresh ginger, including gingerols, shogaols, 3-dihydroshogaols, paradols (Fig1.5) [33]. dihydroparadols, acetyl derivatives of gingerols, gingerdiols, mono- and di-acetyl derivatives of gingerdiols, 1-dehydrogingerdiones, diarylheptanoids, and methyl ether derivatives of some of these compounds. Ginger also contains diarylheptanoids, reported as fresh and dry ginger components. The significant cytotoxic and apoptotic activities against human promyelocytic leukemia cells of several ginger constituents, including some diarylheptanoids and gingerol-related compounds [34].

It can be presented in two chemical groups: volatile and non-volatile. The volatile oil composition is mainly composed of sesquiterpene hydrocarbons, zingiberene (35%), curcumene (18%) and farnesene (10%), and a small amount of bisabolene and b-sesquiphellandrene. At least 40 monoterpenoids are present in small amounts, of which 1,8-cineole, neral, borneol, linalool, and geraniol are the most common. These volatile oil constituents contribute to ginger's unique aroma and flavor. Ginger contains bioactive compounds, including non-volatile stimulant compounds such as gingerol, gingerol, shogaol, and zingerone, which produce a sensation of heat. Ginger contains zingiberene and 6-gingerol, which are important components of gastric medicine. Gingerol has been identified as the main active ingredient in fresh rhizomes and is a series of chemical homologues with varying lengths of their linear alkyl chains [32].

Furthermore, gingerol, the dehydrated form of gingerol, is the principal pungent constituent in dried ginger. Paradol is similar to gingerol and is produced by the hydrogenation of shogaol . In addition to the extractable oleoresins, ginger contains many fats, vitamins, carbohydrates, waxes and minerals. Ginger rhizome also contains zingiberin, a powerful proteolytic enzyme (Tab1.2) [33].

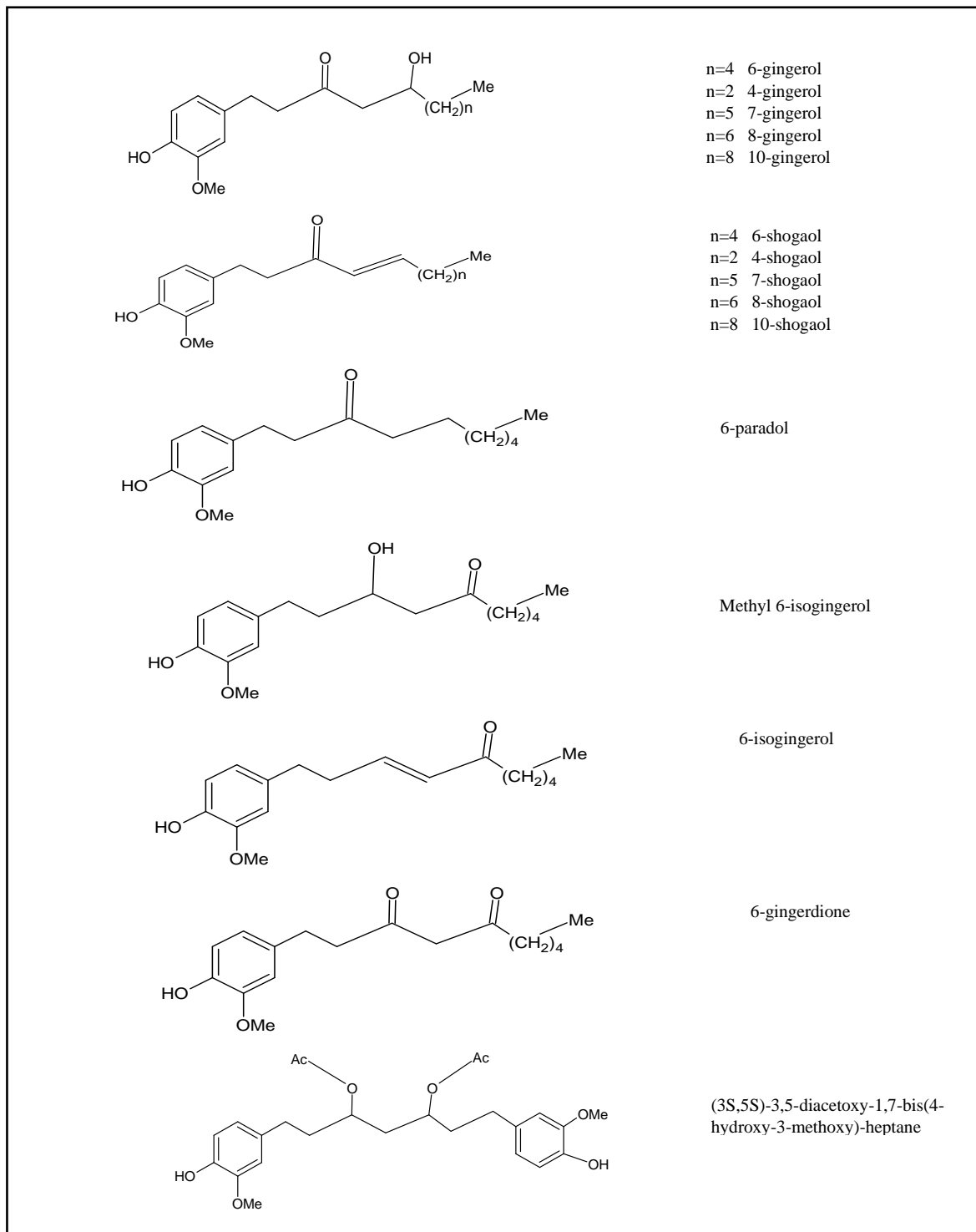


Fig.1.5 Major chemical constituents of ginger [33].

Tab.1.2 The Chemical Composition of Ginger [33]

Chemical composition (in %)	Carbohydrates: 60 -70%	Protein: 9%	Fatty Oil: 3 - 6%	Crude fiber: 3 - 8%	Ash: 8%	Water: 9 - 12%	Volatile oil: 2 - 3%
Volatile oil consists : the monoterpenes & sesquiterpenes	1) α -farnesene α - zingiberene. β -bisabolene. β -elemene. β phellandrene, B esquiphellandrenebomeol ,camphene. cincole,curcumene. geraniol geranyl acetate. limonene, linalool, terpenes, terphineol, zingiberenol zingiberol,						
Non-Volatile Oil Contains	Gingerols, paradols Shogaols, zingerone. (Pungent compounds).		A series of homologs with linear alkyl chains-13-6). (8), (10), and (12). gingerols; and having a side-chain with (7-10), (12), (14), or (16) carbon atoms.				
Other Constituents	Capsaicin, diarylheptanoids gala ctosylglycerols. galanolactone. gingediol, ginger protease. gingerglycolipids, gingesulfonic acid, monoacyldi vitamins, neral, phytosterols						
Uses of Ginger	Spice, Antioxidant, anti- inflammatory antineoplastic. chemopreventive. antiangiogenic, antimetastatic, activates- apoptosis, anticancer			Fever, antipyretic Cold, Antimicrobial, Hypoglycaemic. Hepatoprotective,Diuretic, Hypocholesterolenic. Broad spectrum of antihelminthic effect. Heart condition, Rheumatic complaints			

1.7.3. Anti-cancer properties of ginger

Ginger is rich in various active components 6-gingerol, an important spicy component of ginger has potent anti-angiogenic activity both in vitro and in vivo. 6-gingerol can inhibit tumor growth and metastasis through its anti-angiogenic activity [35]. Topical Application of 6-Gingerol Inhibits COX-2 Expression and NF- κ B (Nuclear Factor-kappa B) DNA (Deoxyribonucleic Acid) Binding Activity in Mouse Skin Pathway-Shogaol Effectively Inhibits NF- κ B Activation, Reduces Secreted Components of VEGF (Vascular Endothelial Growth Factor) and IL-8 (Interleukin-8) Regulates Ovarian Cancer Cell Angiogenesis in Vitro Secretion of factor, an effective chemopreventive food [36].

A novel anti-cancer drug, β -elemene, extracted from the ginger plant induces mitochondrial cytochrome c release-mediated apoptosis in non-small cell lung cancer cells. β -Elemene induces caspase-3, -7-, and -9 activity, reduces Bcl-2 expression, causes cytochrome c release, and increases cleaved caspase-9 and poly(ADP-ribose) polymerase in cells [37]. Enzyme activity enhancement of glutathione reductase (GR), glutathione peroxidase (GPX), and glutathione S-transferase (GST) can inhibit intestinal carcinogenesis by ginger supplementation. Ginger is very effective in reducing colon cancer [38]. Ginger and its constituent 6-gingerol Fight ovarian cancer in the body. Ginger inhibits necrosis Factor kappa-B (NF- κ B) and interleukin 8 (IL-8) inhibition [39].

6-gingerol can effectively inhibit the growth of colon tumors in mice [40]; 6-gingerol can resist skin, breast, and ovarian cancer [39] ; 6-gingerol and 6-shogals inhibit gastric cancer.

The pharmacokinetic properties of ginger constituents, including 6-shogaol, 6-gingerol, 8-gingerol, and 10-gingerol, were studied on humans for their potential as anti-cancer agents. Additionally, 6-paradol exhibited anti-cancer activity against skin cancer.

Extracts of ginger were found to reduce the elevated expression of tumor necrosis factor-alpha (TNF- α) and NF- κ B in liver cancer of rats, thereby acting as an antioxidant and suppressing liver carcinogenesis [41]. Three ginger compounds, including 6-, 8-, and 10-shagaols, were observed to be much more robust against tumor growth, particularly in H-1299 human lung cancer cells. Among these, 6-shagaol was found to be a potential agent against cancer.

Zerumbone was found to suppress the growth of colon and lung cancer growth in mice and activate apoptosis, inhibit NF- κ B activation in osteoclastogenesis in mice, induce apoptosis in colon cancer, and inhibit gastric cancers. Two important target-specific mechanisms in cancer therapy, telomerase and c-Myc inhibition, were identified. The ginger extract was found to be a potential agent in cancer prevention and maintenance therapy [42].

Anti-metastasis activity of 6-shogaol was observed in vitro and was active against breast cancer. The pharmacokinetic properties of anti-cancer agents identified from some important medicinal herbs were also studied. Two Bangladeshi ginger varieties (Fulbaria and Syedpuri) were used to determine their antioxidant and anti-cancer activities against MCF-7 and MDA-MB-231, two human breast cancer cell lines.

Fresh ginger contains various phytochemicals with biological activities relevant to diseases associated with reactive oxygen species (ROS). About 29 phenolic compounds were isolated from the root bark of fresh ginger, and their structures were fully characterized. These compounds were examined for their anti-cancer activity against nine human tumor cell lines, with three compounds, including 6-shogaol, 10-gingerol, and enone-diarylheptanoids analogue of curcumin, exhibiting cytotoxic properties in cell lines. Terpenoids of ginger were found to induce apoptosis by activation of protein 53 in endometrial cancer cells, while the ginger root was found to be effective on COX-1 in colon cancer. The primary compound of ginger, 6-shogaol, was active in cancer cells [43] as it show in the (Tab 1.3).

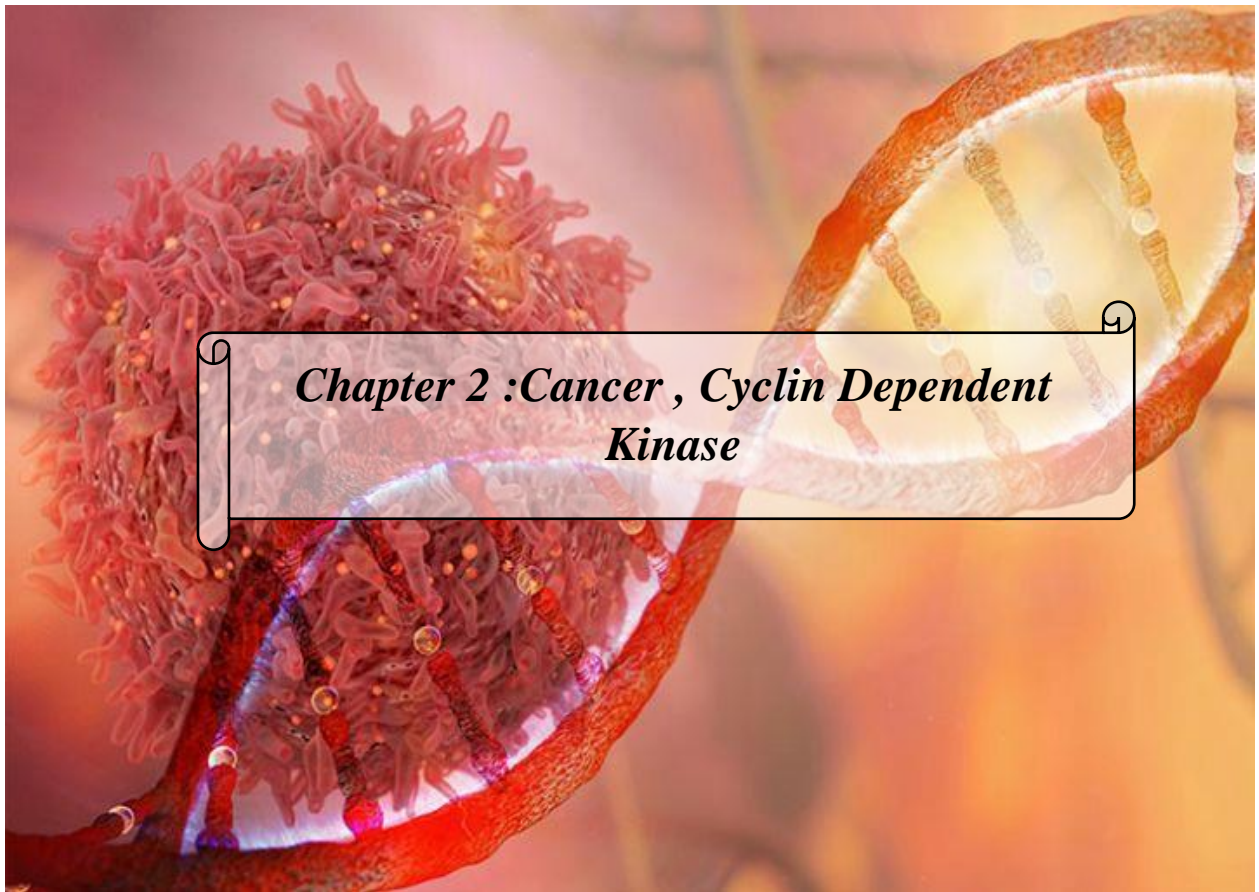
Tab.1.3 Anticancer Activity of Ginger [35-43]

S. No	Compound Name	Cancer	Mechanism
01	β -Elemene	Non-small-cell lung cancer cells	release of cytochrome c
02	Ginger- whole and 6-gingerol	Ovarian cancer	Inhibition NF- κ B; tumor growth
03	Ginger extract	Liver cancer	Reduced the elevated expression of

			TNF- α and NF- κ B
04	6-gingerol	Breast cancer	Inhibits cell adhesion invasion motility
		Skin cancer.	Enhances apoptosis
		Colon cancer	Inhibition of leukotriene activity
05	Zerumbone	Lung and colon cancer	It suppresses modulatory mechanisms of growth and induces apoptosis. Reduces the expression of NF- κ B.
		Colon cancer	Activation of extracellular signal-regulated kinase 1/2 p38 mitogen-activated protein kinase
		Osteoclastogenesis	Blocks NF-kappa B expression.
		Cancer cell	Anti-cancer
06	6-Shogaol	Lungs cancer	Inhibition of AKT
		Breast cancer	Anti-metastasis
07	Ginger-Flavonoids	Breast cancer	Antioxidant activity
08	Enone-diaryl heptanoid, 6-Shogaol, [10]-gingerol,	Liver/against nine human tumor cells (lines)	Inhibition of lipid peroxidation, antioxidant activity, cytotoxic
09	Terpenoids	Endometrial Cancer Cells	Induce apoptosis by activation of p53

1.8. Conclusion

the medicinal plants cinnamon and ginger offer a range of notable health benefits. Cinnamon exhibits antioxidant properties, helps regulate blood sugar levels, possesses anti-inflammatory effects, promotes heart health, and has antimicrobial properties. On the other hand, ginger aids in digestive health, reduces inflammation, provides pain relief, supports the immune system, and possesses anti-nausea properties. Incorporating these powerful spices into our diets or using them in various forms can potentially enhance our overall well-being.



*Chapter 2 :Cancer , Cyclin Dependent
Kinase*

Chapter 2: Cancer, Cyclin dependent kinase

2.1. Introduction

Cancer, a devastating disease characterized by uncontrolled cell growth, poses significant challenges globally. It can arise from various factors such as genetics, carcinogen exposure, and unhealthy habits. Advancements in cancer research are vital for improved prevention, detection, and treatment, considering its impact on physical, emotional, social, and economic aspects [44].

The understanding of cyclin-dependent kinases (CDKs), particularly CDK2, is crucial as these enzymes regulate the cell cycle and play a key role in transitioning cells for DNA replication. Targeting abnormal CDK2 activity with selective inhibitors has emerged as a potential strategy for cancer treatment. By blocking abnormal CDK2 in tumor cells while sparing normal cells, this approach holds promise for advancing cancer therapy and highlights CDK2's significance in controlling the cell cycle and disease [45] [46].

2.2. Cancer

2.2.1. General information

Cancer is a collection of diseases characterized by the abnormal proliferation of cells, which, if left unchecked, can progress and eventually lead to premature death. It occurs in any part of the body and affects individuals from diverse socio-economic backgrounds, races, and ages [47].

Cancer is the primary cause of morbidity and mortality globally, with an estimated 9.6 million deaths in 2018, accounting for one in six deaths.

According to World Health Organization “WHO”. In males, the most common cancers are lung, prostate, colorectal, stomach, and liver, while in females, they are breast, colorectal, lung, cervical, and thyroid cancer.

Unhealthy lifestyle habits adoption such as inadequate physical activity, reduced intake of fruits and vegetables, and increased use of tobacco, fast food, and alcohol are expected to increase the incidence of cancer further [48].

2.2.2. Definition of cancer

Cancer is a broad category of illnesses in which abnormal cells grow uncontrollably, potentially originating from any organ or tissue in the body. The cells often breach their usual boundaries, filtering adjacent areas of the body and may spread to other organs, a process known as metastasis, which is a significant contributor to cancer-related mortality. Other frequently used terms for cancer include malignant tumor and neoplasm [49].

Human cells usually grow and divide in an orderly process to create new cells as needed and die when they become old or damaged. However, sometimes this process goes awry, and abnormal or damaged cells can multiply and form lumps of tissue known as tumors. Tumors can be either benign or malignant. Benign tumors do not invade nearby tissue and are usually not life-threatening but may cause severe symptoms. Malignant tumors, on the other hand, can spread to other parts of the body and are often life-threatening. Neoplasm refers to an abnormal tissue mass that grows uncontrollably even when stimuli for growth are removed. Early detection and proper treatment can increase the chances of survival for many types of cancer.

2.2.3. Property of cancer cells

Malignant tumors possess specific characteristics, including uncontrolled growth, the ability to invade nearby tissues, and the potential to spread to other parts of the body (metastasis) as illustrated in Fig 2.1.

These traits arise from a variety of genetic changes that occur within cancer cells, such as the ability to proliferate without standard growth signals, resistance to signals that would generally limit growth, evasion of cell death mechanisms, development of new blood vessels to support tumor growth, invasion of neighboring tissues, and failure to repair damaged DNA (as depicted in Fig 2.2) [48].

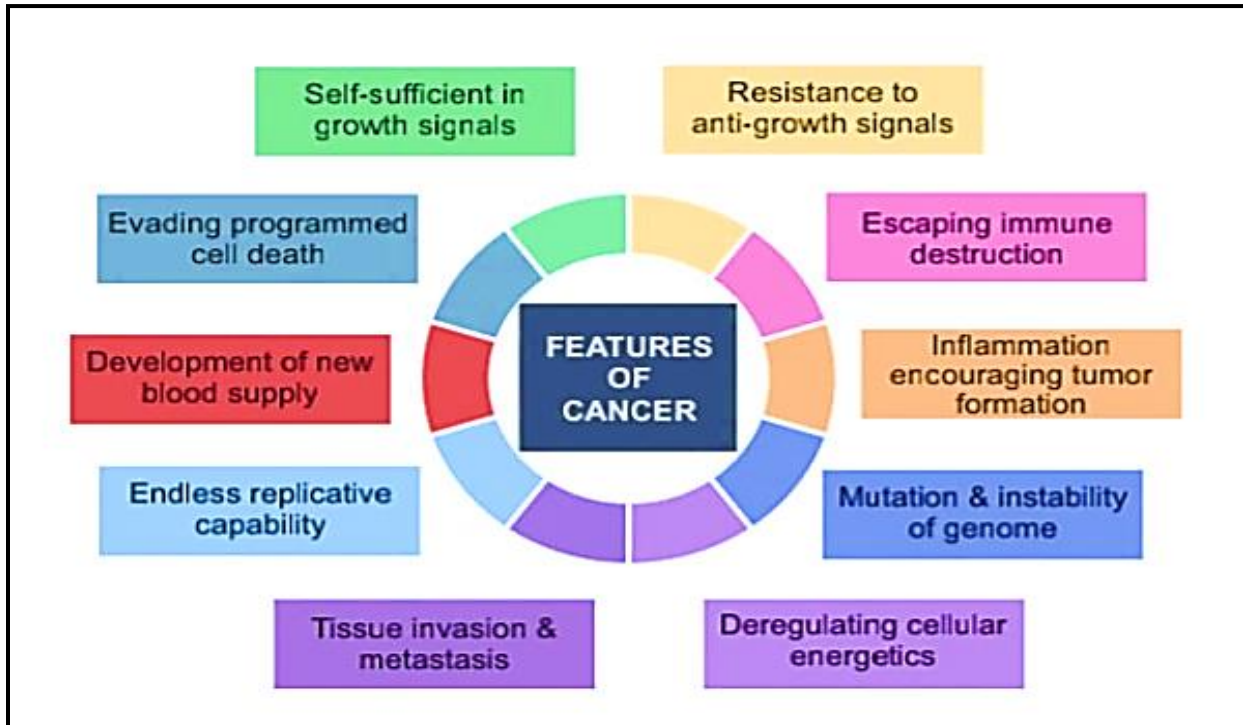


Fig.2.1 Features of Cancer - Major changes occurring in a cell undergoing malignant change [48]

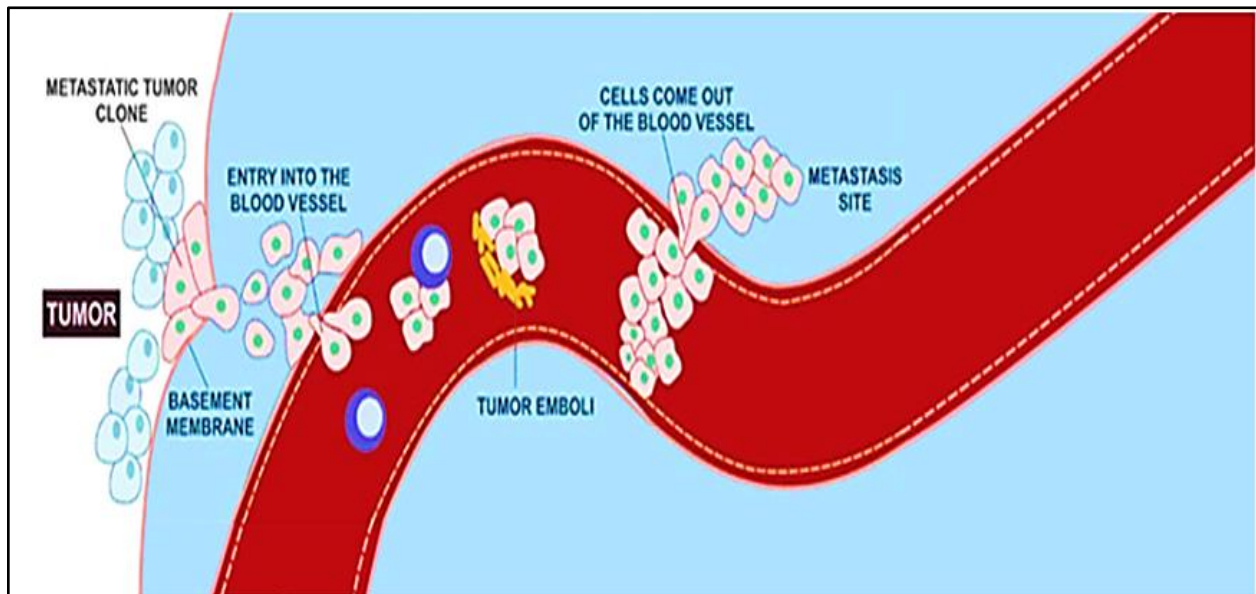


Fig.2.2 Schematic diagram depicting how metastasis from tumor occurs [48]

2.2.4. Cancer statistics

The number of cancer cases revealed by Professor Kamal Bouzid, head of oncology at Mustapha Pacha Hospital, is chilling. In 2019, 50,000 new cases and 20,000 deaths were recorded in Algeria, according to the Arabic-language newspaper Echourouk. The number of cases is expected to increase in the coming years, with breast cancer topping the list with 12,000 new cases in Algeria, followed by colon cancer, which has seen a terrifying resurgence in recent years. « Echourouk » . The medical budget deficit in Algeria significantly affects patients, who are left without power in the face of drugs and cancer treatment shortages, notes Kamel Bouzid, who explains that the problem has worsened in the past year. The professor also said that by 2025, 60,000 new cases would be recorded annually in Algeria, wxpected to rise to 70,000 cases per year by 2030 [50].

2.3. Different types of cancer-related to cyclin dependent kinase 2

The three most common types of cancer in terms of incidence are lung cancer, breast cancer in women, and colorectal cancer. These three types of cancer also rank among the top five in terms of mortality, with lung cancer being the most deadly, followed by colorectal and breast cancer. Together, these three types of cancer account for one-third of the incidence and mortality of cancer worldwide as showed in the Fig 2.3 (World Health Organization 2018).

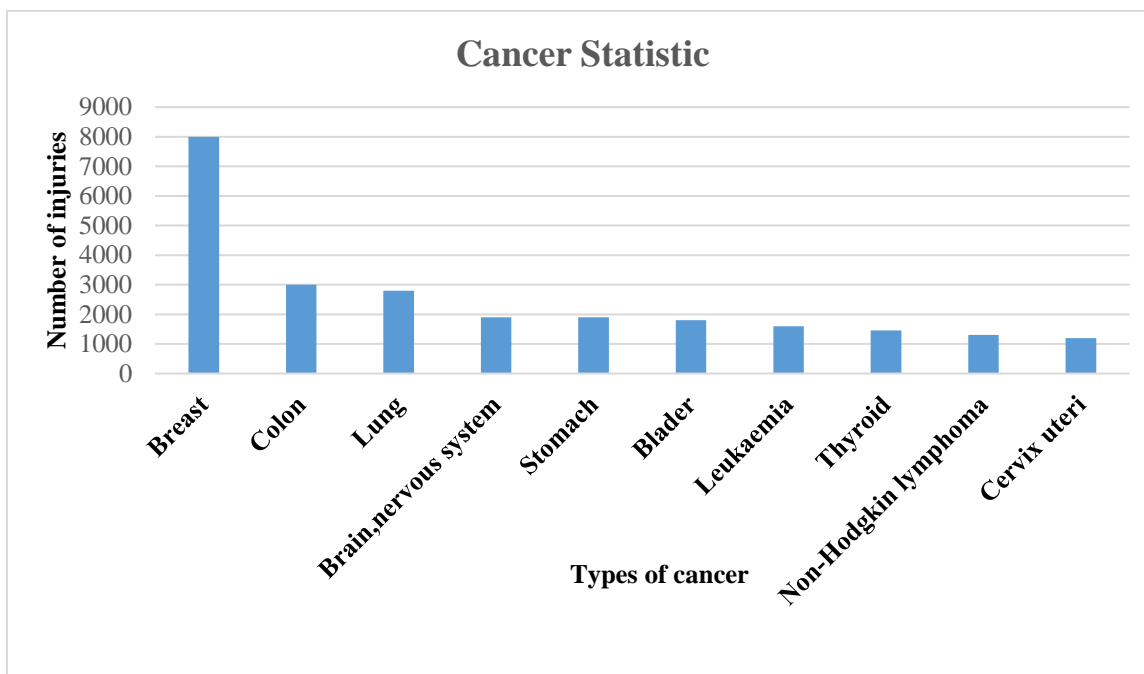


Fig.2.3 Top 10 Cancers by Incidence-Current Rates in Algeria [51]

2.3.1. Breast cancer

Breast cancer develops in the breast's milk-secreting cellular units, known as the ducto-lobular units, primarily in women. In other words, it is a cancer of the mammary gland. Eight out of ten cases of breast cancer occur in women over 50 [52].

2.3.1.1 Epidemiology

➤ Global statistics

In 2020, more than 2.2 million breast cancer cases were reported, making it the most common cancer. Nearly one in twelve women will develop breast cancer in their lifetime. Breast cancer is the leading cause of cancer-related deaths among women, with approximately 685,000 women dying in 2020. Most cases and deaths from breast cancer occur in low- and middle-income countries. **WHO 2020.**

➤ **National statistics**

Breast cancer is the most common cancer among women in Algeria, with an estimated 12,500 new cases and 3,400 deaths in 2020. The incidence rate of breast cancer in Algeria is relatively low at 20.3 cases per 100,000 population [53].

2.3.2. Lung cancer

Bronchopulmonary cancer is a malignant tumor that can arise at the junction of the main branches, in one of the bronchi, or the periphery of the lung in the alveoli. Cancerous cells can spread to lymph nodes through lymphatic vessels (lymphatic dissemination) or to other organs through blood vessels (hematogenous dissemination), leading to the formation of metastases [54].

2.3.2.1. Epidemiology

➤ **National statistics**

In Algeria, there were an estimated 4,800 new cases and 4,400 deaths from lung cancer in 2020, with an incidence rate of 3.8 cases per 100,000 population. Risk factors for lung cancer, such as smoking and pollution exposure, may also vary across different populations [55].

➤ **Global statistics**

Lung cancer is the second most common cancer worldwide, the most common cancer in men and the second most common cancer in women.

There were more than 2.2 million new cases of lung cancer in 2020 [44].

2.3.3. Colon cancer

Colon cancer arises from mutations in the cells' genes within the inner layer of the colonic wall, leading to the growth of benign tumors called adenomas or adenomatous polyps. These polyps can later become cancerous tumors, invading the colonic wall and spreading to distant sites. The adenoma-cancer sequence takes several years to develop, and screening can help diagnose colon

cancer at an earlier stage and prevent it by removing adenomatous polyps during a colonoscopy [56].

2.3.3.1. Epidemiology

➤ Global statistics

According to the World Health Organization's data, colorectal cancer is ranked as the third most prevalent cancer globally. In 2020, it was estimated that approximately 1.93 million new cases were diagnosed, resulting in 935,000 deaths. The incidence of colorectal cancer varies across different regions, with the highest rates in developed nations. Typically, the risk of developing this cancer increases with age, with over 90% of cases being detected in individuals over 50. Men are marginally more susceptible to colorectal cancer than women.

➤ National statistics

In Algeria, there were an estimated 8,300 new cases and 4,200 deaths from colorectal cancer in 2020. The incidence rate of colorectal cancer in Algeria is relatively low at 6.4 cases per 100,000 population. The development of colorectal cancer can be influenced by lifestyle, diet, and genetics, which may differ between populations [55].

2.4. Cyclin Dependent Kinase

2.4.1. General information of cyclin-dependent kinases

Genetic and biochemical investigations in model organisms like yeasts and frogs led to the initial discovery of CDKs.

All known eukaryotes have cyclin-dependent kinases (CDKs), a family of 20 serine/threonine protein kinases that are relatively tiny proteins with molecular weights between 34 and 40 kDa [57]. that CDKs play crucial roles in essential cellular and molecular processes, including metabolism, gene transcription, mRNA splicing, cell migration, senescence, and death. They need physical interaction with a cyclin partner, as suggested by their name, and post-translational changes to become catalytically active and phosphorylate their protein substrates [46].

Constitutive or uncontrolled hyperactivity of these kinases caused by cyclin or CDK amplification, overexpression, or mutation contributes to the growth of cancer cells, and abnormal activity of these kinases has been found in many different types of human malignancies. These kinases are consequently interesting pharmacological targets for creating anti-cancer therapies and indicators of proliferation [58].

2.4.2. Nomenclature and classification of cyclin dependent kinase

The family of cyclin-dependent kinases includes 20 members that recently have been renamed CDK1 through to CDK20 [59].

The study of the evolution of the CDK family in mammals has enabled categorizing of these enzymes into three subfamilies related to cell cycle regulation (CDK1, CDK4, and CDK5) and five subfamilies related to transcriptional regulation (CDK7, CDK8, CDK9, CDK11, and CDK20). These CDKs typically associate with one or a few cyclins, which impart specific functional roles to the resulting complexes.

The human cyclin family (regulatory subunits of CDKs) consists of approximately 29 proteins grouped into three main groups: the cyclin b group, mainly cell cycle-associated CDKs, the cyclin i group, partners of CDK5, and the cellular cyclin c group, significant partners of transcriptional CDKs (as illustrated in the Fig 2.4) [60].

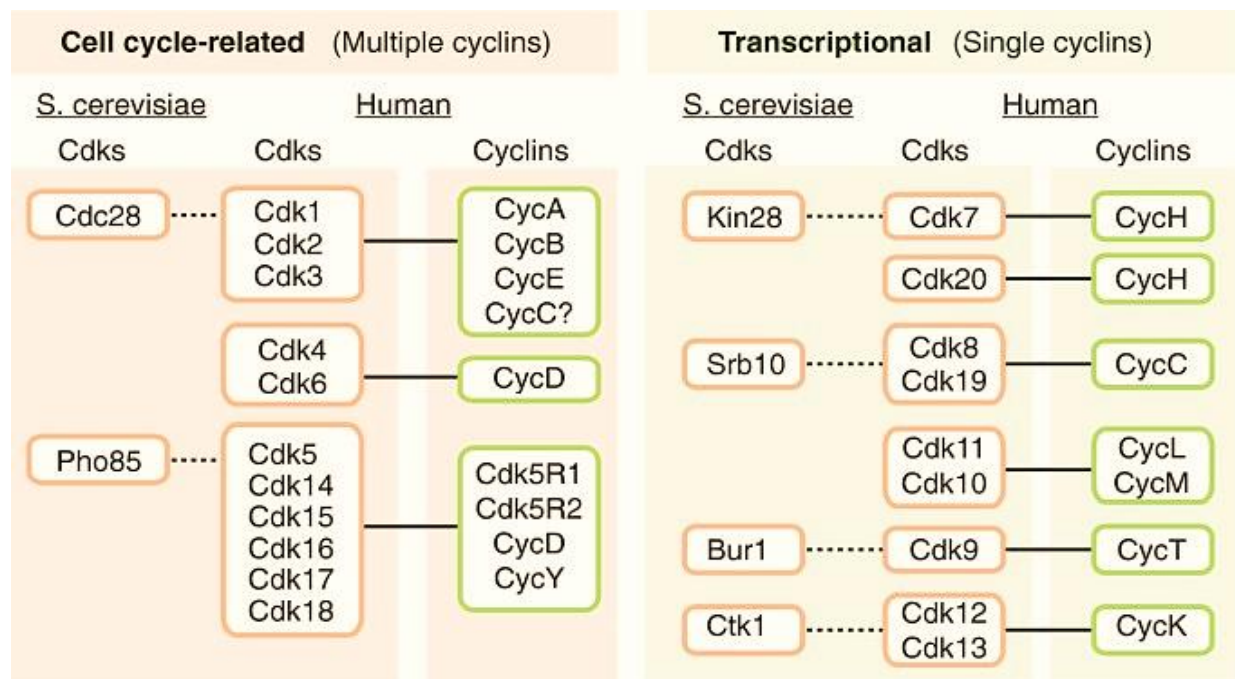


Fig.2.4 Classification of CDKs [57]

2.4.3. General structure

CDKs are proline-directed serine/threonine protein kinases that prefer the S/TPXK/R sequence due to a hydrophobic pocket near the catalytic site that accommodates proline (+1 position). However, the requirement for basic residues at the +3 position must be maintained in CDK4 or transcriptional CDKs that showed a less stringent S/TPX consensus. Other family members, such as CDK7 or CDK9, are not necessarily proline-targeted and can also phosphorylate residues without +1-proline [61].

CDKs range in size from approximately 250 amino acid residues, containing only the serine/threonine kinase catalytic domain, to proteins of over 1,500 residues, with variable-length amino- and/or carboxy-terminal extensions (Fig 2.5). Like all kinases, CDKs have a bilobed structure. The amino-terminal lobe contains β -sheets, while the carboxy-terminal lobe is rich in α -helices, with the active site in the middle. The N lobe contains a glycine-rich repressive element (G loop) and a unique main helix - the C helix (containing the PSTAIRE sequence in CDK1). The C lobe contains an activation fragment extending from the DFG motif (D145 in CDK2; EMBL: AK291941) to the APE motif (E172 in CDK2) and

phosphorylation-sensitive residues in the so-called T-loop (T160 in CDK2). In the cyclin-free monomeric form, the catalytic CDK gap is closed by a T-loop, preventing enzymatic activity [57].

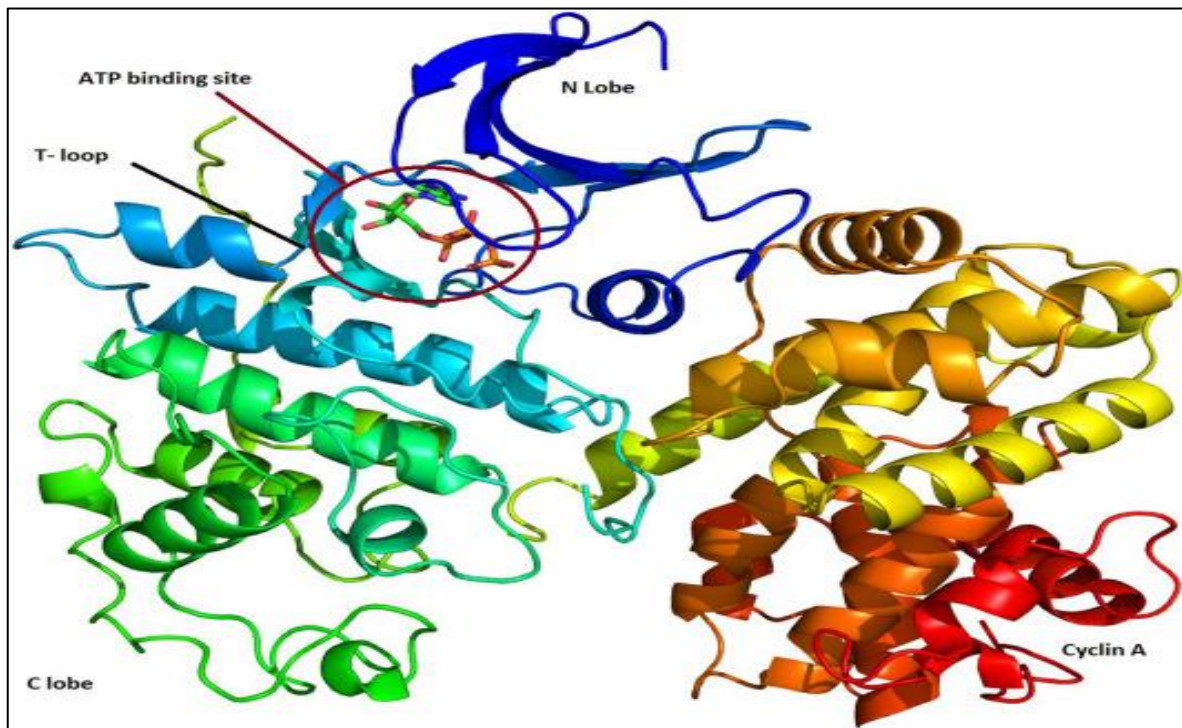


Fig.2.5 Representation of CDK2 as a prototype CDK protein bound with cyclin A and ATP and Tloop helps activate the ATP binding site when it gets bound to the CDK [47, 58, 62]

2.4.4. Activity of cyclin-dependent kinases

Different CDK-cyclin complexes are generated during cell cycle progression, each of which acts at a specific time point in the cell cycle [46].

In particular, the CDK4/6 cyclin D complex is activated during the G1 phase of the cell cycle. It is responsible for the phosphorylation of members of the pRb protein family (pRb, p107, and p130), which transform into repressive transcriptional complexes. These complexes are subsequently phosphorylated by CDK2-cyclin E, disrupting them and inducing the transcription of genes encoding proteins required for DNA replication and mitosis.

The CDK2-cyclin E complex is also involved in triggering DNA replication. CDK2 Cyclin A is subsequently activated and is required for DNA replication during the S phase of the cell cycle.

Finally, CDK1-cyclin A and CDK1-cyclin B are involved in the initiation and progression of mitosis [61-63].

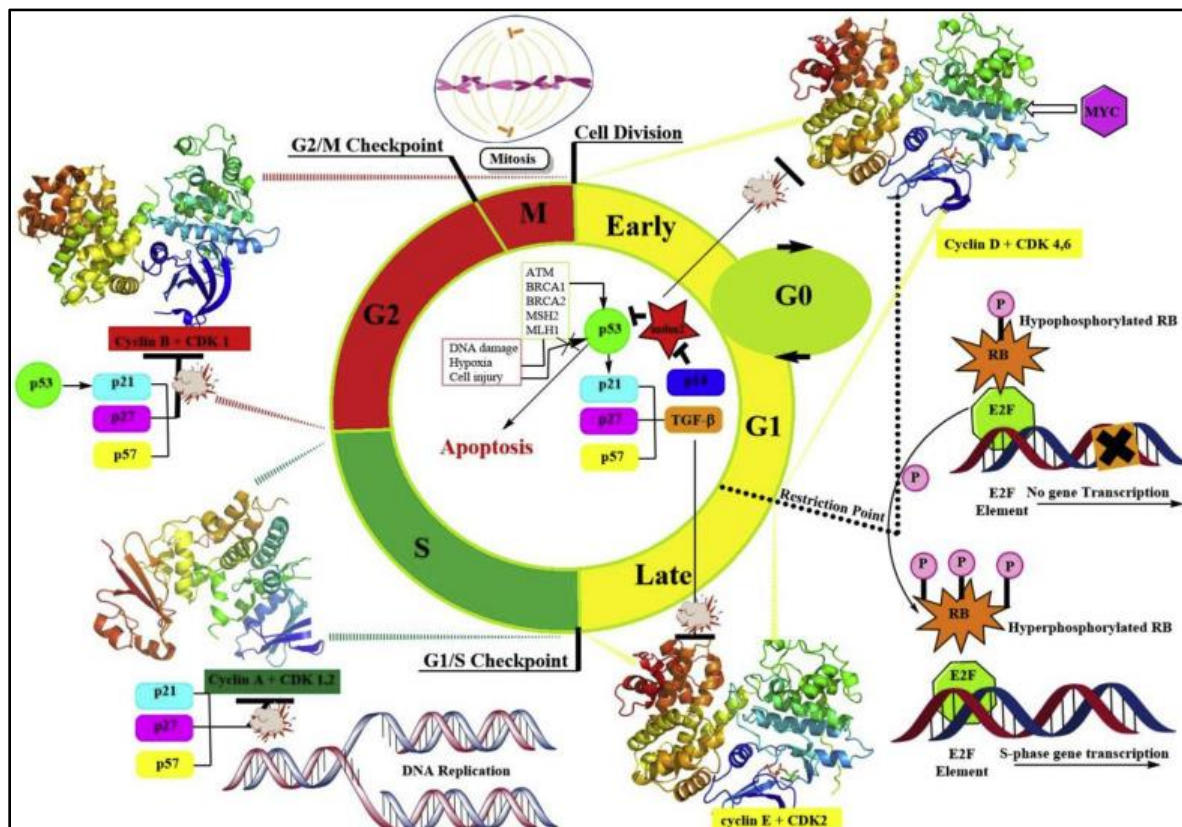


Fig.2.6 Illustrative view of cell cycle along with CDKs involved in cell cycle progression [62].

2.4.5. cyclin-dependent kinases inhibitor

Approximately 20 chemical classes of CDK inhibitors are available; they are analogues of purines, pyrimidines and natural metabolites isolated from microbial strains and their derivatives. Flavopiridol, roscovitine, staurosporine, purvalanol, and alsterpaullone are some potential drug candidates that have been clinically tested and inhibit CDK activity. Specificity is the biggest problem with these currently available antagonists, and they do not have CDK-only specificity; most of these inhibitors have multiple CDK targets.

For example, R-roscovitine inhibits CDK1, CDK2, CDK5, CDK7 and CDK9.

The development of specific kinase inhibitors is critical to minimizing the unwanted side effects of these drugs [64].

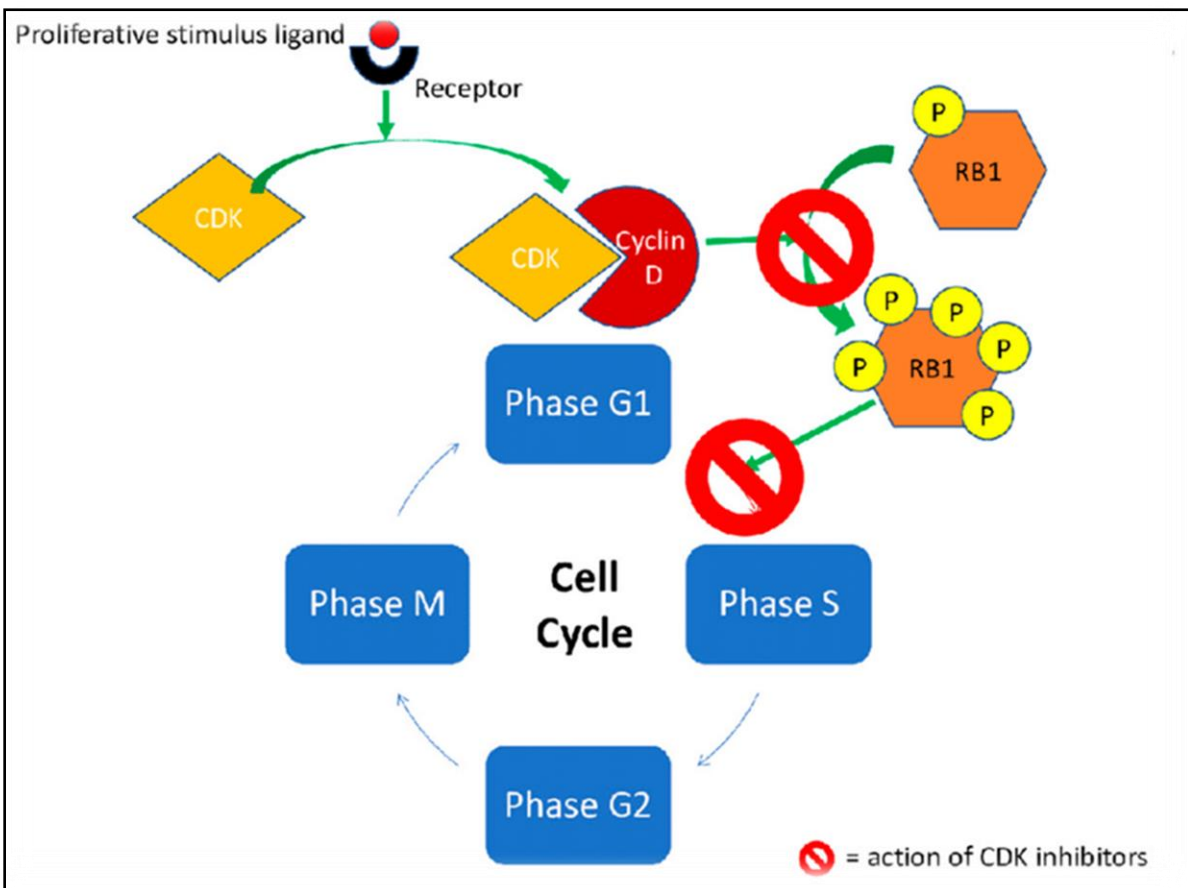


Fig.2.7 inhibitors CDKs [61]

2.5.Cyclin-Dependent Kinase 2 enzyme

CDK2 Human Recombinant is produced in e. coli as a single non-glycosylated polypeptide chain of 306 amino acids (1-298 amino acids) with a molecular weight of 35 kda [65].

2.5.1. Catalytic domain

Cyclin-dependent kinase 2 is structured in two lobes. The lobe beginning at the N-terminus (N-lobe) contains many beta sheets, while the C-terminus lobe (C-lobe) is rich in alpha helices. CDK2 becomes active when a cyclin protein (A or E) binds at the active site between the N and C lobes of the kinase, [59] CDK2 undergoes phosphorylation: activates threonine 160 and represses threonine 14 and tyrosine 15. when cyclin A is degraded, the CDK2-cyclin A complex develops kinase activity from the late to mid-G1 phase. The kinase activity of the CDK2-cyclin E complex

is also present in the early G1 phase, peaks at the onset of the S phase and then disappears [65, 66]. This kinase likely binds to cyclin E and is essential for initiating DNA replication [45].

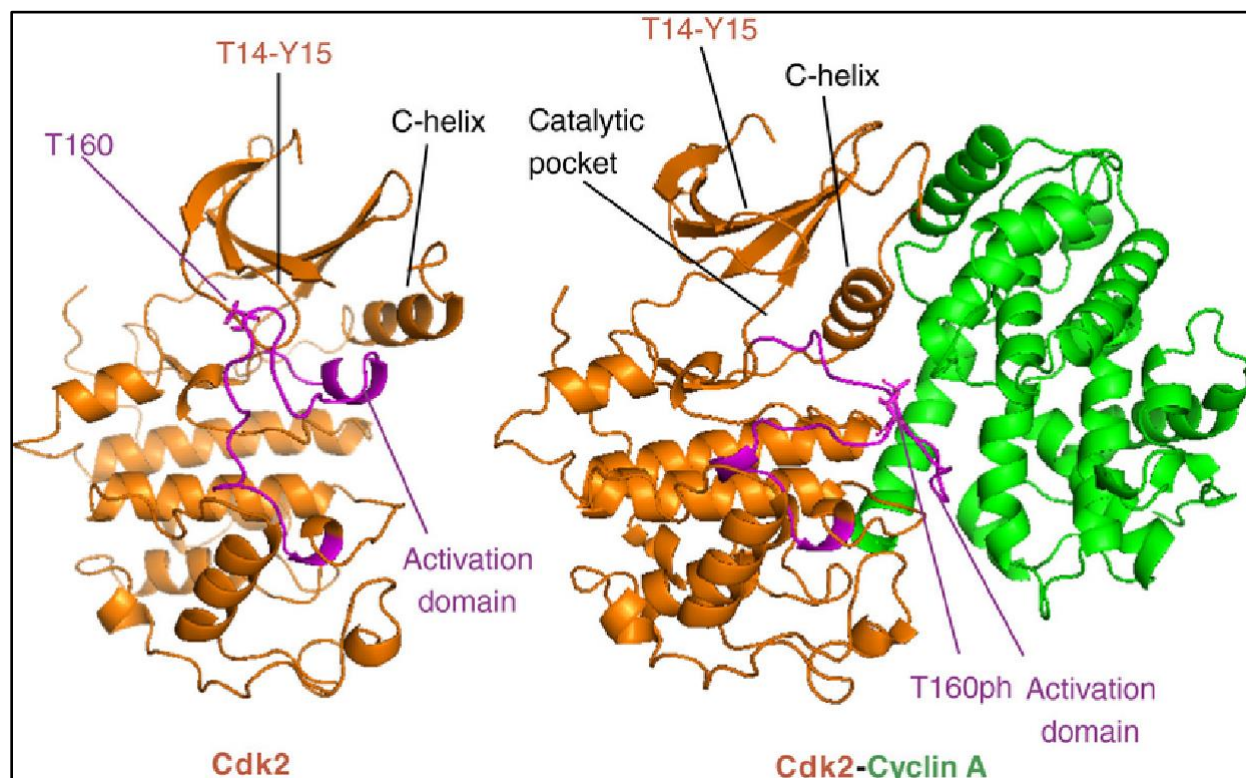


Fig.2.8 Crystallographic structure of CDK2 without and with cyclin [57]

2.5.2. Action mechanism

The protein CDK2 binds the transcription factor E2F, responsible for the expression of several genes involved in DNA replication. In late G1-phase cells, several researchers have found that CDK2 forms a complex with cyclin E, E2F, and a protein called p107, which is associated with a retinoblastoma susceptibility gene called pRB. During the S phase, cyclin E is replaced by cyclin A in this complex [67]. The CDK2-cyclin A complex can also directly bind to E2F-1, a member of the E2F family, without the participation of p107. In contrast to CDK2-cyclin E, CDK2-cyclin A can phosphorylate E2F-1, thereby losing its affinity for DNA and its activity as a transcription factor [68].

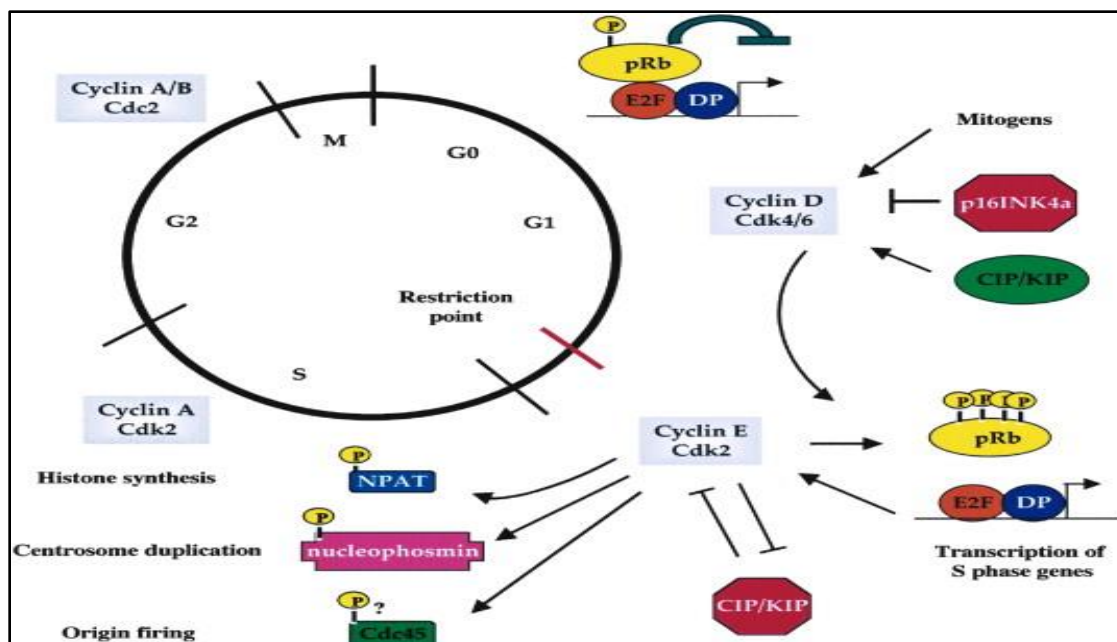


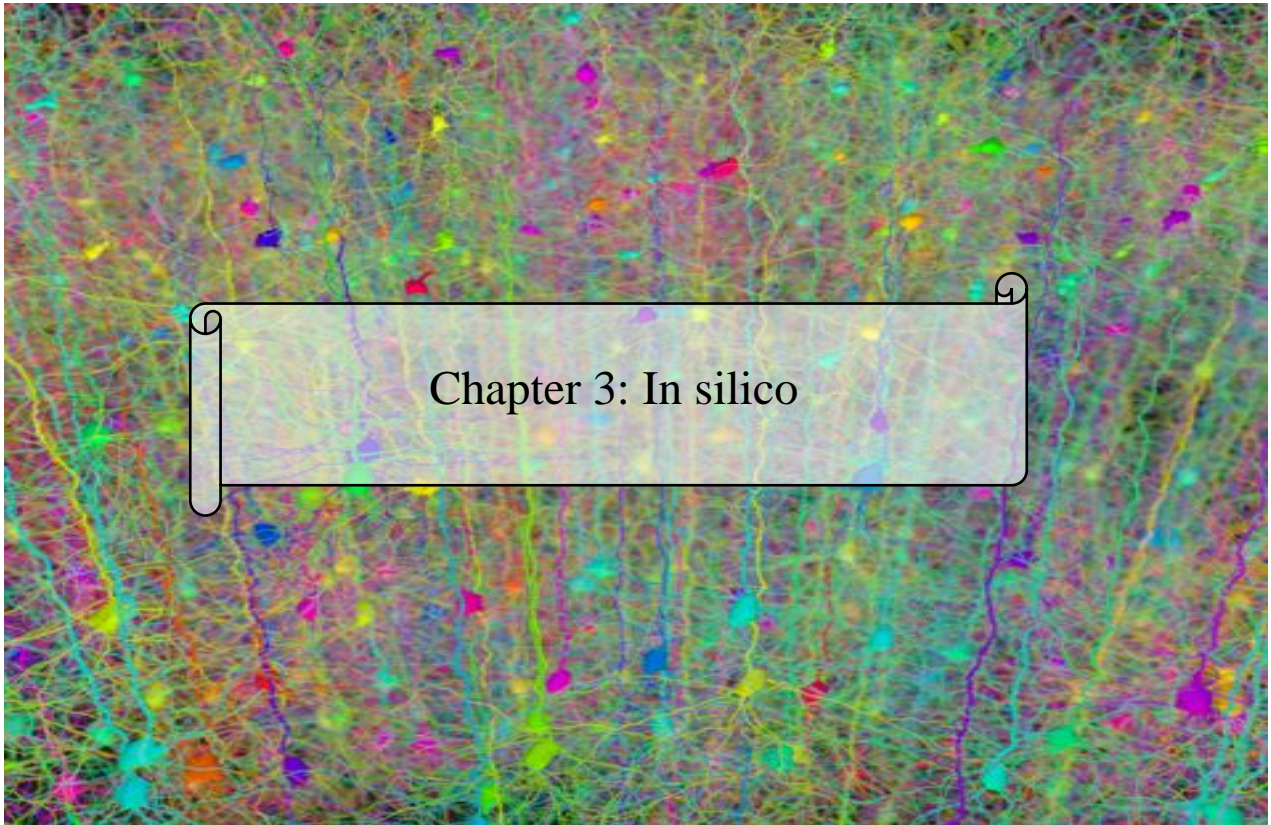
Fig.2.9 Action mechanism of CDK2 at the cell level [69]

2.5.3. Inhibitor of cyclin-dependent kinase 2

The co-crystallization of inhibitors with CDK2 has significantly advanced our understanding of the mechanisms of action of these molecules. Seven inhibitors, including isopentenyl adenine [70], olomoucine [70], roscovitine [71], purvalanol [72], a flavopiridol derivative [73], indirubin-3'-monoxime [74], and staurosporine [74], have been co-crystallized with CDK2 in addition to ATP.

2.6. Conclusion

In conclusion, this chapter sheds light on the intricate relationship between cell cycle regulation and tumor development in cancer is highlighted, with CDK2, a key regulator, being a potential therapeutic intervention target. Understanding CDK2's role in tumor development allows researchers to develop targeted therapies targeting cancer cells while minimizing harm to healthy tissues. This knowledge holds promise for transforming cancer care and improving patient outcomes.



Chapter 3: In silico

3.1. Introduction

Docking, a computational technique in molecular biology and drug discovery, plays a vital role in predicting and analyzing interactions between small molecules and target proteins or biomolecular structures. By identifying potential drug candidates and understanding their mode of action, docking greatly aids in virtual screening and accelerating the development of new pharmaceuticals [24].

Protein structure prediction by modeling is a computational method utilized to forecast the three-dimensional structure of proteins based on their amino acid sequences. By comparing target protein sequences to known structures and refining the predictions, this technique provides valuable insights into protein function and finds applications in various scientific fields [13].

3.2. In silico

In silico prediction methods have gained popularity in drug discovery processes, as they are cheaper and less time-consuming than obtaining experimental data through in vivo and in vitro methods [75].

"In silico" is a term used to describe computer-based or simulated processes [76]. In drug discovery, in silico drug designing involves using computer-based models to tailor combinations of chemical responses to fit specific treatment profiles, as opposed to the traditional method of trial-and-error testing on animals [77]. A drug is a substance used for diagnosis, treatment, or prevention of a disease or as a component of medication. Drug discovery aims to rapidly develop effective treatments for both endogenous and exogenous diseases [78]. Drug design involves creating small molecules that are complementary in shape and charge to the target biomolecule, allowing them to bind to it [79]. Identifying potential drug targets is crucial in the research and development of drug molecules at an early stage. While experimental techniques are limited by throughput, accuracy, and cost, the development of in silico target identification algorithms has gained attention globally due to its speed and low cost [80]. Computational tools offer the advantage of delivering new drug candidates quickly and cost-effectively [81].

3.3. Quantitative structure-activity relationship (QSAR)

Chemical structure and biological activity are supposedly related by quantitative structure-activity relationship (QSAR) models, which are quantitative regression techniques. Numerous scientific fields, such as chemistry, biology, and toxicology, have made substantial use of the quantitative structure-activity connection and related techniques [81, 82]. QSAR models are now considered as a scientifically reliable technique for predicting and categorizing the biological activities of untested compounds in both drug discovery and environmental toxicology [83].

QSAR has unavoidably cemented itself as a crucial tool in the pharmaceutical sector as we approach the new millennium, from lead identification and optimization through lead development [84, 85]. For instance, it's becoming more common to employ QSAR as a screening and enrichment method early in the drug discovery process to weed out molecules without druglike qualities or substances that are likely to cause a hazardous reaction from further development. The extension of QSAR outside the pharmaceutical sector to human and environmental regulatory bodies for application in toxicology is predicted under this emerging scenario.

The development of QSAR during the past ten years has been enabled by advancements in computer hardware and software. Improvements in QSAR methodologies and related software have been largely driven by the enormous financial incentives within the pharmaceutical industry alone to speed up the drug discovery process and increase success odds by enhancing the drug pipeline with more potent and less toxic candidates. Its widespread adoption has been further sparked by the incorporation of QSAR modeling with current developments in hardware and software for data storage and administration. The QSAR software's algorithms have also significantly improved, especially in relation to the vast and expanding set of descriptors used to describe molecule structure and properties.

The core tenet of QSAR is that differences in the structural, physical, and chemical features of a group of compounds that have a common mechanism of action are linked with variations in their biological activity [86]. A statistically validated QSAR model is capable of predicting the biological activity of a new chemical within the same series instead of the time-consuming and labor-intensive processes of chemical synthesis and biological evaluation because it is

presumably that these structurally related properties of a chemical can be determined by experimental or computational means much more efficiently than its biological activity using in vitro or in vivo approaches. When used wisely, QSAR can result in significant time, financial, and human resource savings.

3.4. Molecular docking

Molecular docking is the placement of molecules in a known three-dimensional structural database one by one at the active site of the target molecule. By optimizing the position and conformation of the acceptor compound, the dihedral angle of the inner rotatable bond, and the side chain and backbone of the amino acid residue of the acceptor, the optimal conformation of the acceptor small molecule compound and the target macromolecule is sought and predicted. A combination of mode, affinity, and a method for simulating intermolecular interactions by selecting a ligand with optimal affinity for the receptor that is close to the natural conformation by a scoring function [87].

Molecular docking (or molecular bonding) is one of the most SBDD (Structure-Based Drug Design) is used to predict (in silico) the structure of a molecular complex from isolated molecules, in which different approaches are combined to study the modes of interaction between the two molecules (ligand protein) or (protein-protein) at a time when the methods Each experiment has its own limitations and remains difficult and costly to put into practice. place (in vitro). Docking is generally used to generate models that allow Predict the interaction between two molecules based on their coordinates. atomic and three-dimensional structures (3D) and suggest modes of binding Responsible for protein inhibition perform accurately bonding studies on needs the X-ray modeled structure, high-resolution NMR with a known/predicted bond in the biomolecule . There are 148 827 proteins available in The Protein Data Bank (PDB) [88]. Docking software is a very useful tool in biology, pharmacy and medicine. Because most of the active ingredients are small molecules (ligand) that interact with a biological target of therapeutic interest. As the macromolecular receptor is most often a protein, the term Docking alone is commonly used to refer to a “protein-ligand docking” [89].

3.4.1. The principle of docking

Molecular Docking may refer to a problem of optimization according to a numerical value that would account for the more or less favorable conformation of two entities.

The total free energy of the protein-ligand system. This numerical value will later be called a docking score (or simply a score). Its definition is essential to any molecular docking program as determines the outcome of prediction. In fact, there are different ways to obtain this score depending on the quality of the docking molecule [90].

3.4.2. The importance of the docking

Molecular recognition including enzyme-substrate, drug -protein, drug-nucleic acid, protein-nucleic acid, and protein-protein interactions play important roles in many biological processes such as signal transduction, cell regulation, and other macromolecular assemblies. Therefore, determination of the binding mode and affinity between the constituent molecules in molecular recognition is crucial to understanding the interaction mechanisms and to designing therapeutic interventions [91]. Due to the difficulties and economic cost of the experimental methods for determining the structures of complexes, computational methods such as molecular docking are desired for predicting putative binding modes and affinities. In molecular docking, based on the protein structures, thousands of possible poses of association are tried and evaluated; the pose with the lowest energy score is predicted as the “best match”, the binding mode. Since Kuntz and colleagues’ pioneering work , significant progress has been made in docking research to improve the computational speed and accuracy. Among them, protein-ligand docking is a particularly vibrant research area because of its importance to structure-based drug design [92].

A protein-ligand docking program consists of two essential components, sampling and scoring. Sampling refers to the generation of putative ligand binding orientations/conformations near a binding site of a protein and can be further divided into two aspects, ligand sampling and protein flexibility.

Scoring is the prediction of the binding tightness for individual ligand orientations/conformations with a physical or empirical energy function. The top orientation/conformation, namely the one with the lowest energy score, is predicted as the binding mode.

3.4.3. The most popular docking programs

More than 30 docking software are currently available (Fig 3.1) . These molecular docking programs include: GOLD, FlexX, DOCK, AutoDock, MOE or UCSF. Chimera and Molegro Virtual Docker (MVD) .(Tab 3.1)

The use of docking programs has led to many successes in the field of Discovery of new bioactive molecules [87].

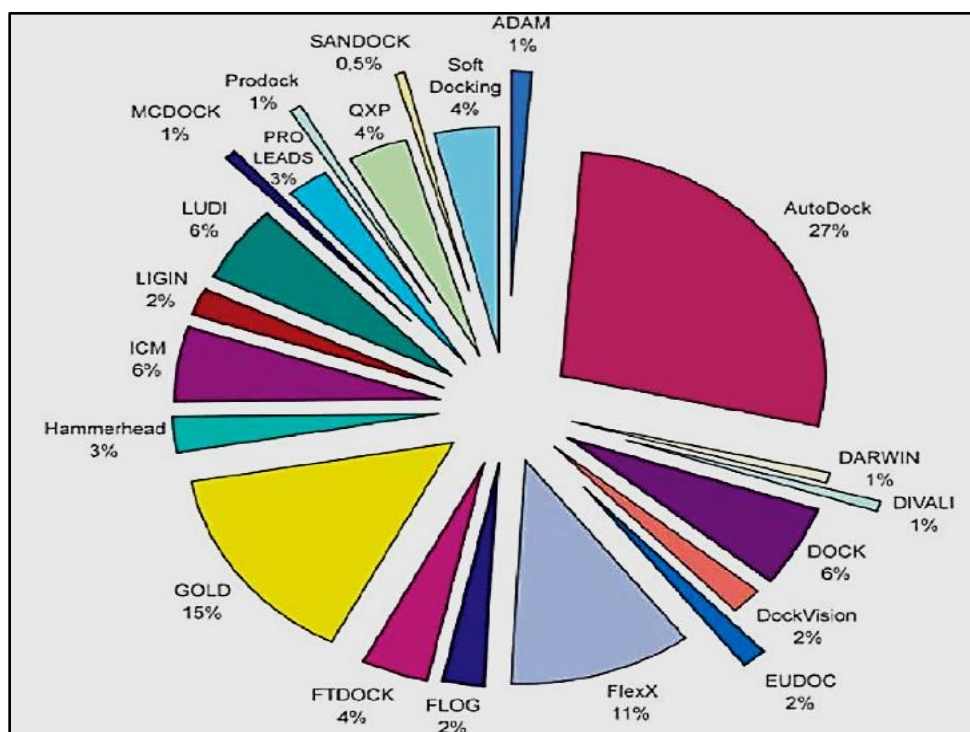


Fig.3.1 Molecular bonding purchase of docking programs [87]

Tab.3.1 Web site of the main molecular docking programs [87]

Nam	Editteur	Web site
AutoDock	Scripps	http://www.scripps.edu/mb/olson/doc/autodock/
Dock	UCSF	http://dock.compbio.ucsf.edu/
FlexX	BioSolveIT	http://www.biosolveit.de/FlexX/
Fred	OpenEyes	http://www.eyesopen.com/products/applications/fred.html

Glide	Schrodinger	http://www.schrodinger.com/Products/glide.html
Gold	CCDC	http://www.cede.cam.ac.uk/products/life_sciences/gold/
ICM	Molsoft	http://www.molsoft.com/products.html
LigandFit	Accelrys	http://www.accelrys.com/cerius2/c2ligandfit.html
Surflex	Biopharmics	http://www.biopharmics.com/products.html

3.5. Autodock

Autodock is an example of the latter, more physically detailed, flexible docking technique. Previous releases of Autodock combine a rapid grid-based method for energy evaluation, precalculating ligand-protein pairwise interaction energies so that they may be used as a look-up Tab during simulation, with a Monte Carlo simulated annealing search for optimal conformations of ligands. Autodock has been applied with great success in the prediction of bound conformations of enzyme (inhibitor complexes, peptide) antibody complexes, and even protein-protein interactions; these and other applications have been reviewed elsewhere.

Autodock is often used to obtain unbiased dockings of flexible inhibitors in enzyme active sites: in computer-assisted drug-design, novel modifications of such lead molecules can be investigated computationally. Like many other computational approaches, Autodock performs well in predicting relative quantities and rankings for series of similar molecules; however, it has not been possible to estimate in Autodock whether a ligand will bind with a millimolar, micromolar, or nanomolar binding constant. Earlier versions of Autodock used a set of traditional molecular mechanics force-field parameters that were not directly correlated with observed binding free energies [87].

3.6. Autodock Vina

AutoDock Vina, a new program for molecular docking and virtual screening, has been presented. Vina uses a sophisticated gradient optimization method in its local optimization procedure. The calculation of the gradient effectively gives the optimization algorithm a “sense of direction” from

a single evaluation. By using multithreading, Vina can further speed up the execution by taking advantage of multiple CPUs (Central Processing Unit) or CPU cores.

The evaluation of the speed and accuracy of Vina during flexible redocking of the 190 receptor-ligand complexes making up the AutoDock 4 training set showed approximately two orders of magnitude improvement in speed and a simultaneous significantly better accuracy of the binding mode prediction. In addition, AUTODOCK Vina can achieve near-ideal speed-up by utilizing multiple CPU cores [93].

3.7. Discovery studio

Discovery Studio is a software suite designed for scientific research in the fields of chemistry, biology, and materials science. It is developed by Dassault Systèmes BIOVIA and includes a wide range of tools and modules for molecular modeling, visualization, and simulation.

Molecular modeling: Discovery Studio includes a variety of tools for building, editing, and optimizing molecular structures. These tools can be used to create new compounds or modify existing ones, and can help researchers explore the properties and behavior of molecules at a structural level [94].

Virtual screening: Discovery Studio includes several tools for virtual screening of large compound libraries, including ligand-based and structure-based approaches.

These tools can help researchers identify potential drug candidates based on their predicted binding affinity and other properties .

Molecular dynamics simulation: Discovery Studio includes a module for molecular dynamics simulation, which can be used to simulate the behavior of molecules over time. This can be helpful for understanding how molecules interact with each other and with their environment, and for predicting their properties and behavior under different conditions [88].

Visualization and analysis: Discovery Studio includes powerful tools for visualizing and analyzing molecular structures and properties. These tools can help researchers explore complex data sets and generate insightful visualizations and graphics.

Overall, Discovery Studio is a versatile and powerful software suite that can be used for a wide range of scientific research applications. Its many features and modules make it a valuable tool for researchers in chemistry, biology, and materials science, among other fields [95].

Examples of drugs that have been discovered using docking techniques:

Docking can be a powerful tool in drug discovery, allowing researchers to quickly and efficiently screen large numbers of potential drug molecules for their ability to bind to a target protein. This is a few examples of drugs that have been discovered using docking techniques in the field of cancer:

1-Gefitinib (Iressa): This drug was developed to treat non-small cell lung cancer (NSCLC) and works by inhibiting the activity of the epidermal growth factor receptor (EGFR). Docking studies were used to identify the binding site of gefitinib on the EGFR protein and optimize its structure for maximum binding affinity [96].

2-Sorafenib (Nexavar): This drug was developed to treat kidney cancer and works by inhibiting the activity of several proteins involved in cell growth and division. Docking studies were used to identify the binding site of sorafenib on the protein kinase RAF and optimize its structure for maximum binding affinity [97].

3-Venetoclax (Venclexta): This drug was developed to treat chronic lymphocytic leukemia (CLL) and works by inhibiting the activity of the protein B-cell lymphoma 2 (BCL-2), which helps cancer cells survive. Docking studies were used to identify the binding site of venetoclax on BCL-2 and optimize its structure for maximum binding affinity [98].

4-Olaparib (Lynparza): This drug was developed to treat ovarian cancer and works by inhibiting the activity of the protein poly (ADP-ribose) polymerase (PARP), which helps repair damaged DNA. Docking studies were used to identify the binding site of olaparib on PARP and optimize its structure for maximum binding affinity [99].

5-Acalabrutinib (Calquence): This drug was developed to treat mantle cell lymphoma and works by inhibiting the activity of the protein Bruton's tyrosine kinase (BTK). Docking studies were used to identify the binding site of acalabrutinib on BTK and optimize its structure for maximum binding affinity [100].

3.8. Modeling

3.8.1. Swiss model

SWISS-MODEL is a widely used web-based tool in structural bioinformatics that employs homology modeling techniques to generate reliable 3D models of protein structures. It provides a user-friendly interface that allows users to generate models based on templates from the Protein Data Bank or a user-defined template library. The SWISS-MODEL pipeline involves template selection, target-template alignment, model building, model quality assessment, and visualization, which are essential in generating high-quality models. The resulting models are suitable for various applications, such as protein structure prediction, drug discovery, and understanding of protein function [101].

Protein structure homology modeling has become a routine technique for generating 3D models of proteins when experimental structures are unavailable. Fully automated servers such as SWISS-MODEL generate reliable models without requiring complex software packages or large database downloads, making them accessible to non-specialists. SWISS-MODEL was established 20 years ago as the first fully automated server for protein structure homology modeling and has continuously improved. Conserved ligands such as essential cofactors or metal ions in the model [102]. Recently, SWISS-MODEL's functionality has been expanded to model oligomeric structures of target proteins and include evolutionarily conserved ligands such as essential cofactors or metalions in the model [102].



Fig.3.2 Swiss Model [103]

3.8.2. Alphadatabase

The Alpha Database, also known as the AlphaFold Protein Structure Database (AFDB), is a collection of predicted protein structures generated by the AlphaFold2 algorithm. It serves as a valuable resource for researchers and scientists seeking information about protein structures [104]. The database incorporates various algorithms and tools to enhance its functionality. For instance, the CCTOP (Consensus Constrained TOPology Prediction), TOPCONS2, and DeepTMHMM algorithms are utilized to differentiate between transmembrane (TM) and non-TM proteins. CCTOP, in particular, is employed to predict the topology of TM proteins, with the SignalP6 algorithm replacing the older version of signal peptide prediction. The structures in the database are segmented into fragments based on their Predicted Alignment Error matrix, using the Agglomerative Clustering function from the Sklearn Python package. Additionally, the DSSP algorithm is applied to identify helical residues within the protein structures, while the TMDET (TransMembrane Protein DETection) algorithm helps in detecting the membrane plane in both the complete AlphaFold structures and their fragments. Overall, the Alpha Database provides a comprehensive collection of protein structure predictions, enhancing our understanding of protein architecture and aiding in various biological and biomedical research endeavors [105].

3.8.3. Evolutionary scale modeling

Evolutionary scale modeling is a powerful approach for predicting protein structures, especially for challenging proteins that are difficult to study experimentally. It complements traditional experimental techniques like X-ray crystallography and nuclear magnetic resonance spectroscopy [106]. By utilizing evolutionary information and analyzing related protein sequences, this method offers a rapid and cost-effective way to generate structural models. It provides valuable insights into protein structure and function, aiding in understanding biological processes and enabling drug design and discovery [107].

3.8.4. Robetta

Robetta is an Internet service that automates protein structure prediction and analysis using genomic data. It employs a fully automated procedure to generate models for entire protein

sequences, regardless of homology to known structures. Robetta identifies domains and builds models using comparative modeling for homologous domains and the Rosetta de novo prediction method for non-homologous domains [108]. It can also utilize NMR constraints for structure determination. Robetta's tools have applications in structural genomics, aiding in the determination of challenging protein structures and identifying energetically important side-chains in protein-protein interfaces. The ultimate goal of Robetta is to provide high-quality structural information to support research, infer protein function, and assist in drug design [109].

3.9. Pharmacokinetics

3.9.1 Drug likeness tool

A drug-likeness tool is a computational method that can be accessed online or downloaded as standalone software packages used in drug discovery to predict the pharmacological properties of small molecules based on their chemical structure. These tools analyze the structural and physicochemical properties of small molecules and generate predictions about their pharmacological properties, including factors such as oral bioavailability, absorption, distribution, metabolism, and excretion (ADME), as well as potential toxicity and drug-drug interactions.

The primary objective of drug-likeness tools is to identify small molecules with a high probability of serving as safe and effective drug candidates, which can help reduce the time and cost associated with experimental drug discovery [110]. Various drug-likeness tools are available, which use different algorithms and statistical models to generate predictions. Some of the most commonly used drug-likeness tools include Lipinski's Rule of Five, which predicts oral bioavailability based

on molecular weight, the number of hydrogen bond donors and acceptors, and lipophilicity, and the Molecular Weight, Hydrogen Bond Donor and Acceptor, Lipophilicity, and RotaTab Bonds (MW-HD-LR) rule, which predicts drug-likeness based on similar parameters. Other commonly used rules include the MDDR-like rule, Veber rule, Ghose filter, BBB rule, CMC-50-like rule, and Quantitative Estimate of Drug-likeness (QED) [111]

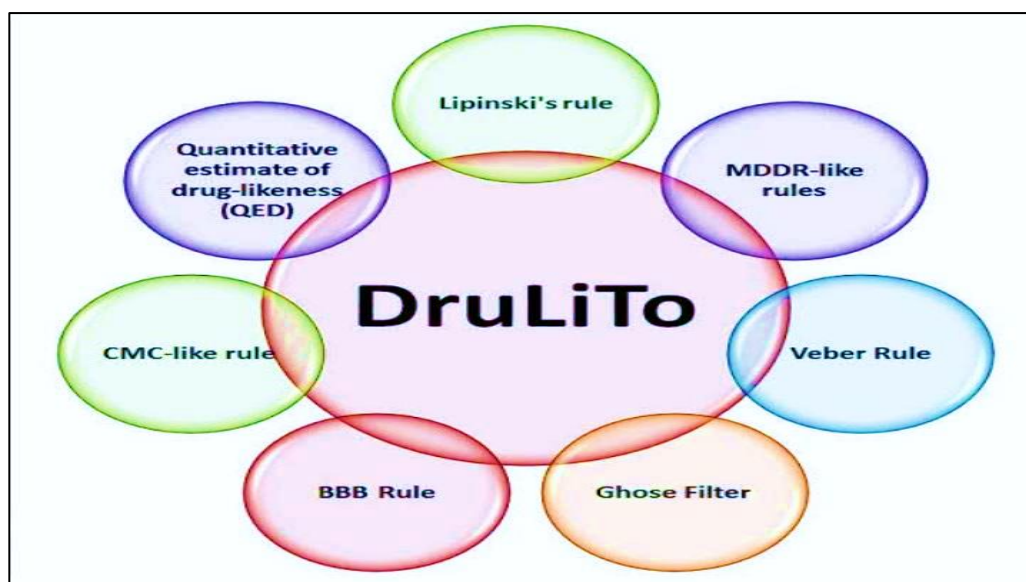


Fig.3.3 Drug likeness tools [111]

3.9.2. Pharmacokinetics models for small molecules (PKCSM)

Pharmacokinetics models for small molecules (PKCSM) is a powerful computational tool used in drug discovery to predict the pharmacokinetic properties of small molecules. This graph-based signature approach enables the prediction of ADME (absorption, distribution, metabolism, and excretion) properties and toxicity profiles of small molecules, aiding in identifying potential drug candidates. PKCSM utilizes a distance-based graph signature method, adapted from the Cutoff Scanning concept, to represent small molecules' chemical structure and atomic pharmacophores. This enables the development of 30 predictors divided into five major classes: absorption, distribution, metabolism, excretion, and toxicity [112].

PKCSM has shown a high accuracy rate of 83.8% in predicting mutagenicity in external validation datasets. Additionally, PKCSM can predict several endpoints, such as LD50, Ames test, maximum daily dose, and hepatotoxicity, making it a valuable tool for drug development [113].

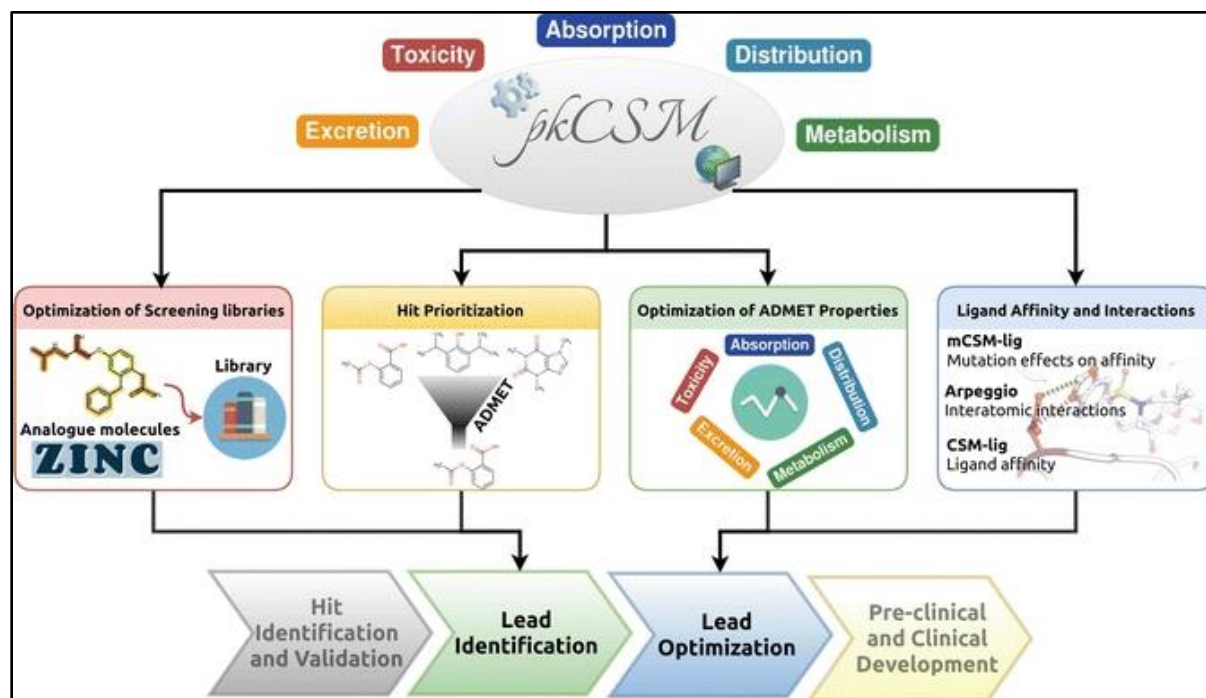


Fig.3.4 Pharmacokinetics models for small molecules [113].

3.9.3. Pass online

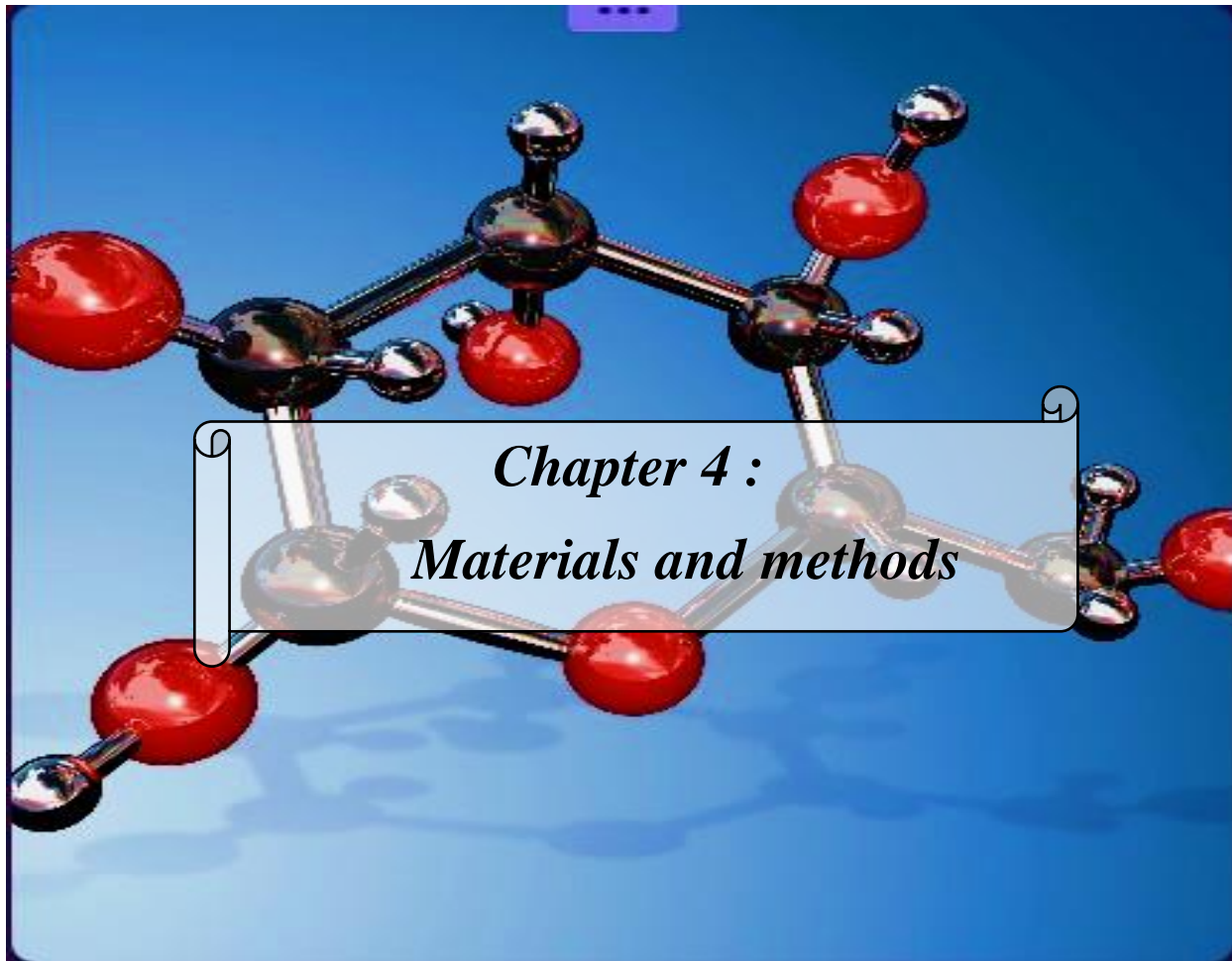
The software program PASS is a freely accessible web resource that predicts the biological activity profiles of organic compounds based on their structural formulas. It provides simultaneous predictions of many types of biological activity (over 4,000 types of biological activity predictions with average accuracy above 95%), allowing for evaluation of the general biological potential of drug-like molecules [114].

PASS is based on analyzing the structure-activity relationships in a training set containing information on more than 300,000 organic compounds. The program predicts biological activity profiles for chemical compounds in a standardized representation and uses a naïve Bayes classifier as its mathematical approach. A PASS prediction results in a list of probable biological activities

arranged in descending order of P_a - P_i values. P_a is the probability of belonging to the class of "actives", and P_i is the probability of belonging to the "inactive" [115].

3.10. Conclusion

Docking and protein structure prediction are crucial in drug discovery and protein analysis. These techniques identify potential interactions between molecules and target proteins, aiding in drug design and optimization. Docking predicts binding affinities, selectivity, and modes of action, accelerating drug development. Protein structure prediction provides insights into folding, dynamics, and function, aiding in understanding biological processes and disease mechanisms. Together, these techniques and studies drive advancements in pharmaceutical research, leading to the development of safer and more effective drugs. By combining computational approaches, protein analysis, and pharmacokinetic investigations.



Chapter 4 :
Materials and methods

Chapter 4: Materials and methods

4.1. Introduction

In this chapter, we will discuss the methods used included the extraction and quality identification of ginger and cinnamon oils, as well as the evaluation of their biochemical properties, antibacterial activity and inhibition of CDK2.

Current research indicates that cinnamon and ginger essential oil may offer therapeutic advantages as an anticancer. To completely understand the activities and processes of cinnamon and ginger oil's possible anticancer effect, additional in-silico research are required.

We identify potential enzymatic processes by which various cinnamon and ginger essential oil components may exert effects, mostly utilising in silico molecular modelling. Additionally, models will offer estimated binding affinities that project the possibility of a target and ligand interacting spontaneously. These models provide a foundation for additional in vitro and in vivo validation.

Our study uses essential oil of Algerian ginger from Biskra, Indian cinnamon *C. tamala*, Indonesian cinnamon *C. burmannii* and chains cinnamon *C. cassia*. The part used of cinnamon in this study is the barks. Both are known for their medicinal characteristics, great use by the population, and interesting therapeutic virtues.

Our research project was conducted at Dr Zibouche's medical centre in Ain Defla's level of the analytical laboratory and the process engineering laboratory of Khemis Miliana.

4.2. Apparatus and reagents

In this part, all apparatus and reagents used in this study are summarised in Tab 4.1:

Tab.4.1: Apparatus and reagents .

Plants materials	Laboratory materials	Microbiological material
<ul style="list-style-type: none"> -Indonesian cinnamon sticks. - Chinese cinnamon sticks. - Indian cinnamon sticks. -Algerian ginger. 	<ul style="list-style-type: none"> -Flask (1000 ml)+Beaker. -Bunsen burner+incubator. -Separatory funnel (250 ml). -Erlenmeyer flask with stopper vacuum filtration. -Rotary vacuum evaporator. -Eppendorf Tubes (1.5 ml). -Electronic Balance. -pH-indicator strips pH meter. -Magnetic Stirrer. -Holes wooden test tube. -Micropipette - Pipette tips. -Test tubes. -UV-Visible Spectrophotometer. -Volumetric flasks. - Flask 50 ml. -Burette. -Magnetic hotplate stirrer. 	<ul style="list-style-type: none"> -Sabouraud culture medium -Mueller Hinton culture medium -Petri dish -strains of bacteria and yeasts : *<i>Escherichia coli</i> *<i>Staphylococcus aureus</i> *<i>Candida albicans</i>

4.3. Extraction methods

This part is devoted to extracting the essential oil of cinnamon and ginger obtained from the shop. The extraction method is presented in the Fig 4.1:

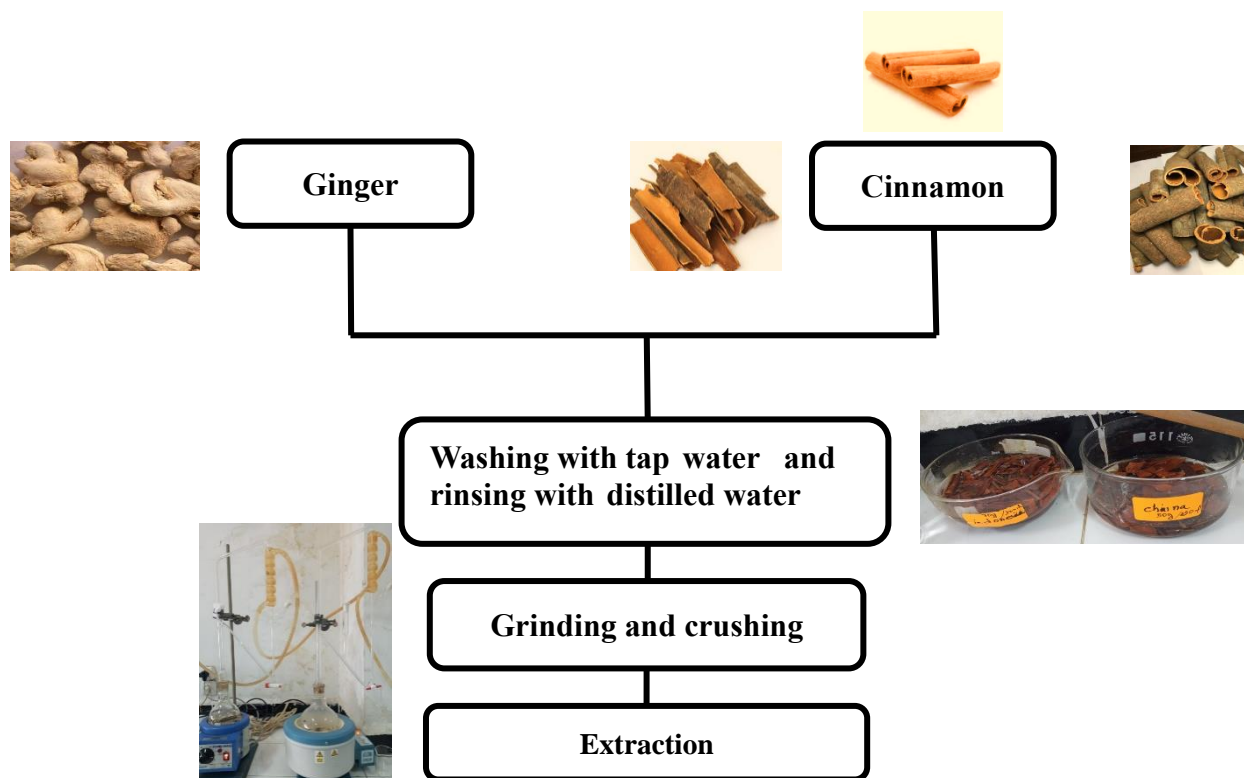


Fig.4.1 Flowchart representing the preparation of the plants.

4.3.1 Steam distillation (Hydrodistillation)

Steam distillation is the extraction method used for most commercial essential oils today. This brings many advantages: shorter extraction times, lower energy consumption and better oil quality [1].

The cinnamon bark and ginger utilised in the study were crushed from a supermarket. Next, it was washed with deionised water for 5 minutes. Fifty grams of the resulting powder of cinnamon and 70 grams of the resulting powder of ginger were placed in a 500 millilitres distillation flask along with 250 millilitres of distilled water. This flask was connected via a glass tube to a steam generator and a condenser to extract the oil as show in Fig 4.2 .

The essential oils were then distilled with boiling water for 2 to 3 hours, and the recovered mixture was allowed to settle before the oil was withdrawn. The product obtained from the steam distillation was separated using a separatory funnel. The essential oils settled at the top layer

and were repeatedly separated until no oil remained in the funnel (Fig 4.3). The essential oils were then stored in a refrigerator at 4 °C [116].



Fig.4.2 Steam extraction process



Fig.4.3 Separation the essential oil of cinnamon

The essential oil yield percentage was determined by dividing the weight of essential oils by the weight of bark powder [117].

The yield was calculated using the equation bellow:

$$\text{Yield(\%)} = \left(\frac{M_{E.O}}{B_m} \right) \times 100 \quad (\text{Eq.4. 1})$$

Where:

- $M_{E.O}$: Mass of the extracted oil (g)
- B_m : Initial plant biomass (g)

4.4. Characteristics of the essential oil

During this study, the quality and composition of the extracted cinnamon essential oils were evaluated by analysing their organoleptic and physico-chemical properties. These properties serve as a means to verify and monitor the quality of the essential oils.

4.4.1. Organoleptic properties

The organoleptic test involved scoring assessments of taste, texture, colour, and aroma to evaluate the sensory properties of the essential oils.

4.4.2 Physico-chemical properties

4.4.2.1. Relative density

Relative density, denoted as RD, is a dimensionless quantity representing the ratio of the mass of a specific volume of oil at 20 °C to the mass of an equal volume of distilled water at 20 °C [118].

- **Procedure**

To determine the relative density (RD), an electrical balance is used to consecutively weigh equal amounts of oil and water at a temperature of 20 °C.

Relative density is calculated as follows:

$$RD = \frac{(m_2 - m_0)}{(m_1 - m_0)} \quad (\text{Eq.4. 2})$$

With:

- RD: The value of the relative density according to the standards.
- m_0 : The mass in grams of empty eppendorf.
- m_1 : The mass in grams of eppendorf, filled with distilled water.
- m_2 : The mass, in grams of eppendorf, filled with the EO.

4.4.2.2. pH value

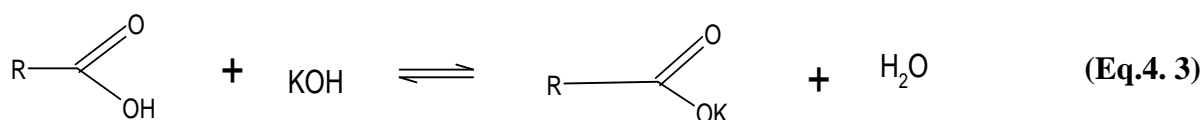
In chemistry, pH, the "potential of hydrogen," is a scale employed to indicate the acidity or basicity of an aqueous solution. Acidic solutions with higher concentrations of H⁺ ions are characterised by lower pH values than basic or alkaline solutions [119].

In our study, we are utilizing the colorimetric method for measuring pH. This method involves using pH papers to visually determine the acidity or basicity of the solution under investigation.

4.4.2.3. Acid value (neutralization number)

The acid value, denoted as AV, is a number expressed in milligrams representing the quantity of potassium hydroxide required to neutralise the free acids present in 1 gram of substance [120] [97].

Potassium hydroxide reacts with the acid according to the following reaction:



The principle is to neutralize the free acids using a titrated ethanolic solution of potassium hydroxide.

The procedure involves introducing 1 gram of essential oil into a flask and adding 5 ml of ethanol. Then, agitation is performed, followed by titration with a titrated ethanolic solution of potassium hydroxide (C (KOH) = 0.1 mol/L) in the presence of phenolphthalein (a coloured indicator) as show in Fig.4.4. The liquid's light yellow colour (the essential oil colour) changes to pink upon neutralisation. The volume of KOH used for neutralisation is read directly from the burette.

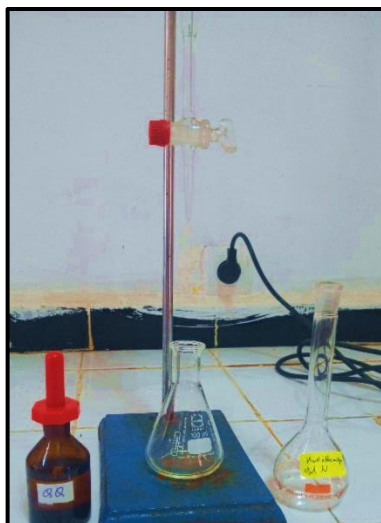


Fig.4.4 Volumetric analysis process

The acid value is expressed by the formula:

$$AV = \frac{56.11 \times M \times V}{W} \quad (\text{Eq 4.4})$$

Where:

- 56.11: Molar mass of KOH (g/mol).
- M: Molarity of the base (mol).
- V: Volume of titre for EO sample (ml).
- W: Weight of essential oil sample (g).

4.4.2.4. Ester value

The ester value, denoted as EV, is the number of milligrams of potassium hydroxide required to neutralise the acids released by the hydrolysis of esters contained in one gram of oil[98].

Hydrolysis of esters is achieved by heating under defined conditions in the presence of a titrated ethanolic solution of potassium hydroxide, and the excess is titrated with a titrated solution of hydrochloric acid.



The procedure involves adding 1 g of the ester (HE) and 25 ml of a 0.5 M alcoholic solution of potassium hydroxide (KOH) to a 100 ml flask. The mixture is refluxed for 1 hour. After cooling the solution, 20 ml of distilled water and 5 drops of phenolphthalein are added. The excess KOH is titrated with a 0.5 N hydrochloric acid (HCl) solution until the pink colour disappears. A blank operation is performed under the same conditions as before (as illustrated in Fig 4.5).

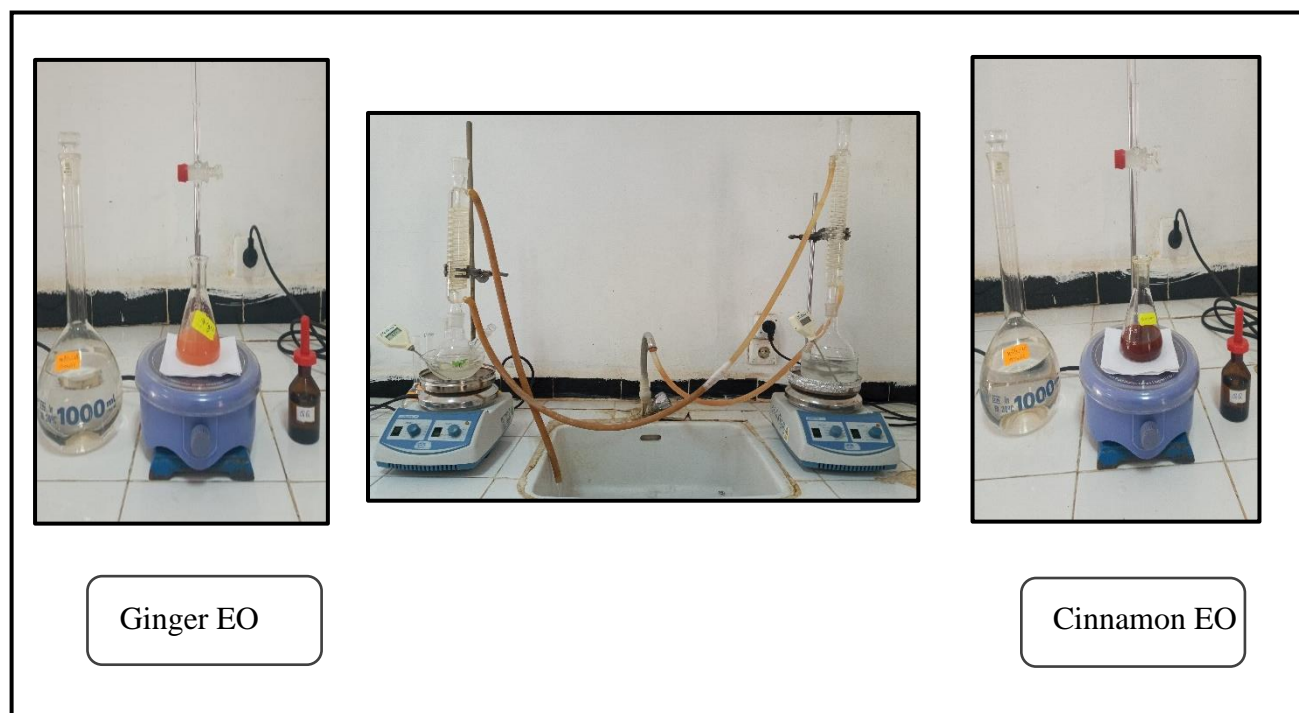


Fig.4.5 Ester value determination process.

The ester value (EV) is calculated using the following equation:

$$EV = \left(\frac{56.11 \times M}{W} \right) \times (V_0 - V_1) - AV \quad (\text{Eq4.6})$$

Where:

- M: Molarity of the base (mol).
- W: Weight of essential oil sample (g).
- V: Volume in ml of the HCl solution (0.1 N) measured for the blank test.
- V: Volume in ml of the HCl solution (0.1 N) measured for the calculation.
- Av: Acid value.

4.4.2.5. Saponification Value

The saponification value (1) is the number that expresses in milligrams the quantity of potassium hydroxide needed to neutralise the free acids and saponify the esters present in 1g of the substance [120, 121].

The saponification value is given by the following formula:

$$SV = AV + EV \quad (\text{Eq.4.7})$$

Where:

- SV: Saponification value
- AV: Acid value
- EV: Ester value

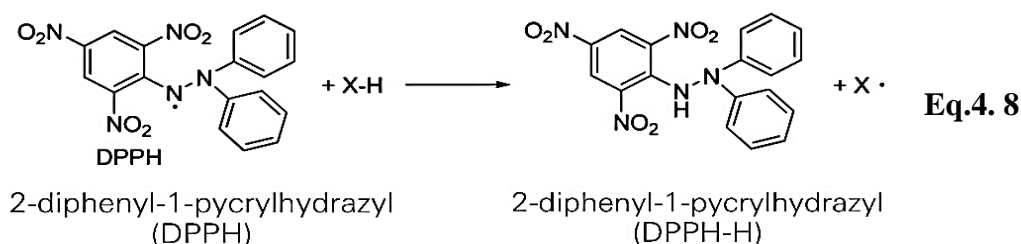
4.4.3. Biochemical activity

4.4.3.1 Determination of total flavonoids:

The aluminum trichloride method mentioned in [122], was used to quantify flavonoids in our extracts.

Aluminum chloride forms a highly stable complex with the hydroxyl (OH) groups of flavonoids. This yellow complex absorbs visible light at a wavelength of 418 nm. For this assay, 1 ml of 1% methanolic solution are combined with 0.4 mg/ml of the extract. The mixture is thoroughly mixed and incubated for 10 minutes in the absence of light.

4.4.3.2. Antioxidant activitie:



Essential oils have garnered significant attention due to their diverse biological activity and immense therapeutic potential. The antioxidant properties of essential oils are particularly intriguing, especially in the context of diseases with inflammatory components. In our thesis, we investigated the antioxidant activities of the essential oil extract using the 2,2-diphenyl-1-picrylhydrazyl (DPPH) assay.

a. Free radical scavenging activity (DPPH test):

The 1,1-diphenyl-2-picrylhydrazyl (DPPH) assay is a widely used colourimetric method to assess the radical scavenging capacity of plants and extracts. This assay is accurate, easy to perform, and cost-effective, providing a screening tool for the overall activity of antioxidants. It relies on using a sTab and synthetic radical known as DPPH [123].

b. Mechanism of DPPH test:

In this assay, an antioxidant or any molecule with a weak X–H bond reacts with the coloured and persistent DPPH radical (2,2-diphenyl-1-picrylhydrazyl), causing a change in colour from violet to yellow (Eq 4.9.) [124, 125]. The absorption maximum of the DPPH radical is observed between 515 and 517 nm.

The antioxidant activity of standard compounds or essential oils is quantified by determining the IC 50 value, which represents the concentration of the test material required to cause a 50% decrease in the initial DPPH concentration [126]. It is important to note that the IC 50 value alone does not provide sufficient information about the reactivity of the antioxidant as it depends on the

reaction time. Moreover, meaningful comparisons can only be made when the data is obtained under identical experimental conditions [127].

- **Procedure :**

The free radical-scavenging activity of cinnamon essential oil and cinnamon extract was evaluated using a modified DPPH (1,1-diphenyl-2-picrylhydrazyl) assay[128, 129], which measures the reducing ability of antioxidants towards the DPPH radical.

In brief, DPPH was prepared by weighing 4 mg of the compound using an electrical balance and dissolving it in 100 ml of methanol. Various dilutions (5%, 20%, 40%, 60%, 80%, 100%) of the cinnamon essential oil sample were prepared and mixed with 1 ml of 0.024 mmol/l methanolic DPPH solution, it's presented in the Fig.2.7. The mixture was incubated for 30 minutes at 25°C, and the absorbance at 515 nm was measured using a UV/Vis spectrophotometer. Similarly, diluted cinnamon extract was prepared and measured in a similar manner.

The decrease in absorbance at 517 nm was recorded for each essential oil and cinnamon extract sample. Ascorbic acid, a well-known antioxidant, was used as a positive control, while a mixture of DPPH radical solution and 1 ml ethanol served as the blank in the experiment[126].

The percentage of radical scavenging (%) was calculated by the following formula:

$$\% \text{ Inhibition} : ([A_{(\text{blank})} - A_{(\text{sample})}] / A_{(\text{blank})}) \times 100 \quad (\text{Eq.2.9})$$

Where :

- $A_{(\text{blank})}$: Absorbance of solution without the test material
- $A_{(\text{sample})}$: absorbance of sample.

4.4.3. Antibacterial activity :Determination of the minimum inhibitory concentration of ginger and cinnamon essential oils

The antibacterial activity is carried out by placing a sterile cellulose disk with a diameter of 6 mm (Whatman N°1) impregnated with a quantity of essential oil onto:

- ✓ A MH (Mueller Hinton) agar medium previously inoculated with a bacterial culture.
- ✓ A Sabouraud agar medium inoculated with a fungal culture.

After incubation, the results were determined by measuring the diameters of the inhibition zones in millimeters.

4.4.3.1. Selection of bacterial and fungal strains for culture media:

The bacterial strains chosen for this study are pathogenic bacteria. One Gram-positive bacterium (*Staphylococcus aureus*), one Gram-negative bacterium (*Escherichia coli*), and one fungus (*Candida albicans*), it's presented in the Tab 2.1 . These strains were provided to us by the analysis laboratory in Zibouch - Ain Defla.

Tab.4.2 List and characteristics of microorganisms tested.

Bacteria and Fungus	N ATTC American Type Culture Collection	Gram	Culture Medium	Family
<i>E. Coli</i>	25922	-	MH	Enterobacteriaceae
<i>Staphylococcus aureus</i>	25923	+	MH	Staphylococcaceae
<i>Candida albicans</i>	Purification	/	Sab	Saccharomycetaceae

4.4.3.2. Bacterial suspension preparation

Three to four colonies were picked using a sterile loop and added to a tube containing physiological water (9‰ NaCl) with vigorous agitation and homogenization (as illustrated in Fig 4.6) [130].

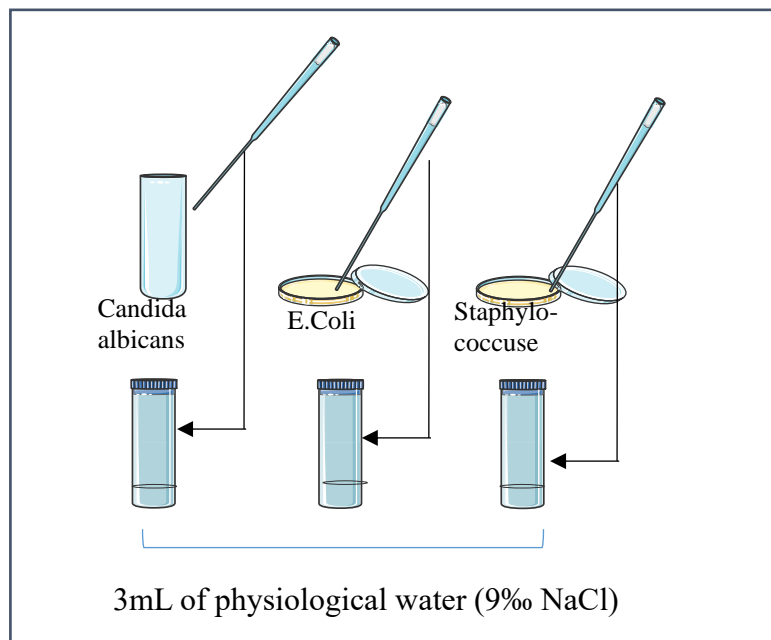


Fig.4.6 Bacterial suspension preparation

4.4.3.3. Preparation of cinnamon and ginger essential oil dilutions

To obtain different concentrations of cinnamon and ginger EO, they were diluted in DMSO (Dimethyl Sulfoxide) to the following concentrations: 100 (pure EO), 75, 50, and 25 as shown in Fig 4.7 .

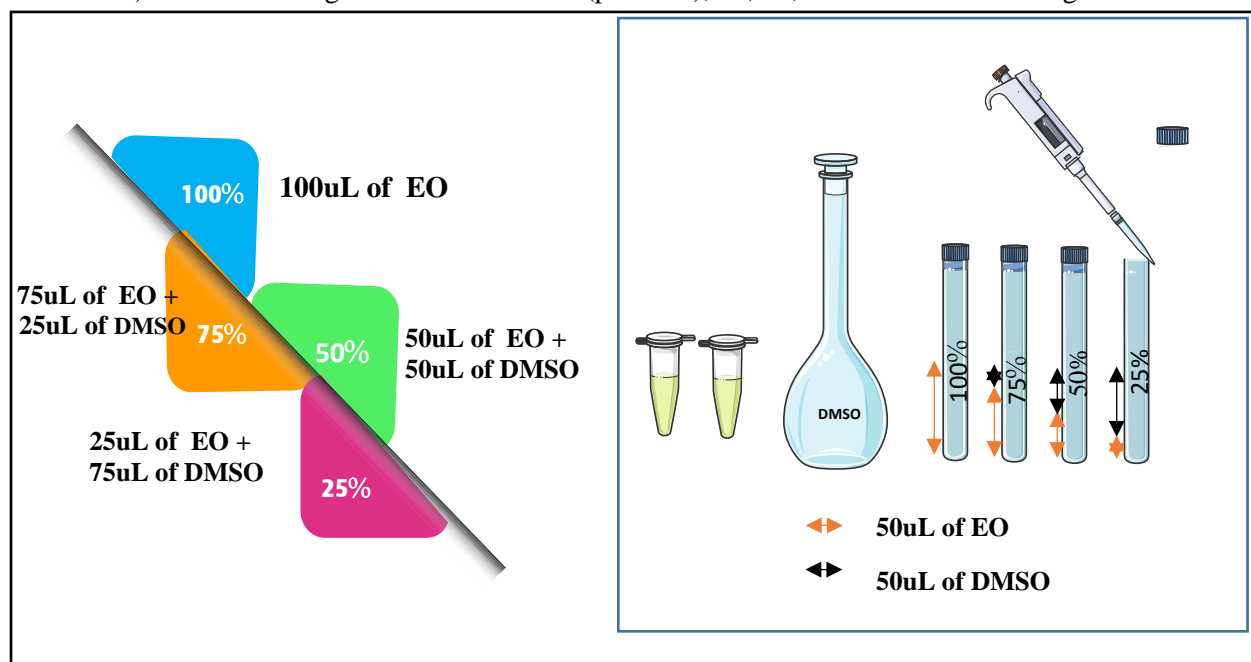


Fig.4.7 Cinnamon and Ginger essential oil dilute

- **Procedure:**

The test was performed by culturing bacteria on an MH agar medium for E. Coli ,Staphylococci and a Sabouraud medium for candida albicans.

Each 90 mm Petri dish received 20 mL of the culture medium and was inoculated with 1 to 2 μ L of the microbial suspension containing 10^7 – 10^8 cfu/ML.

Sterile disks impregnated with EO were placed on the surface of the medium and left to diffuse for 30 min . The bacterial samples were subsequently incubated in darkness at 37 °C for 24 hours in an oven, with periodic inversion., it's presented in the Fig 4.8.

The diameters of the zones of inhibition were read using a ruler.

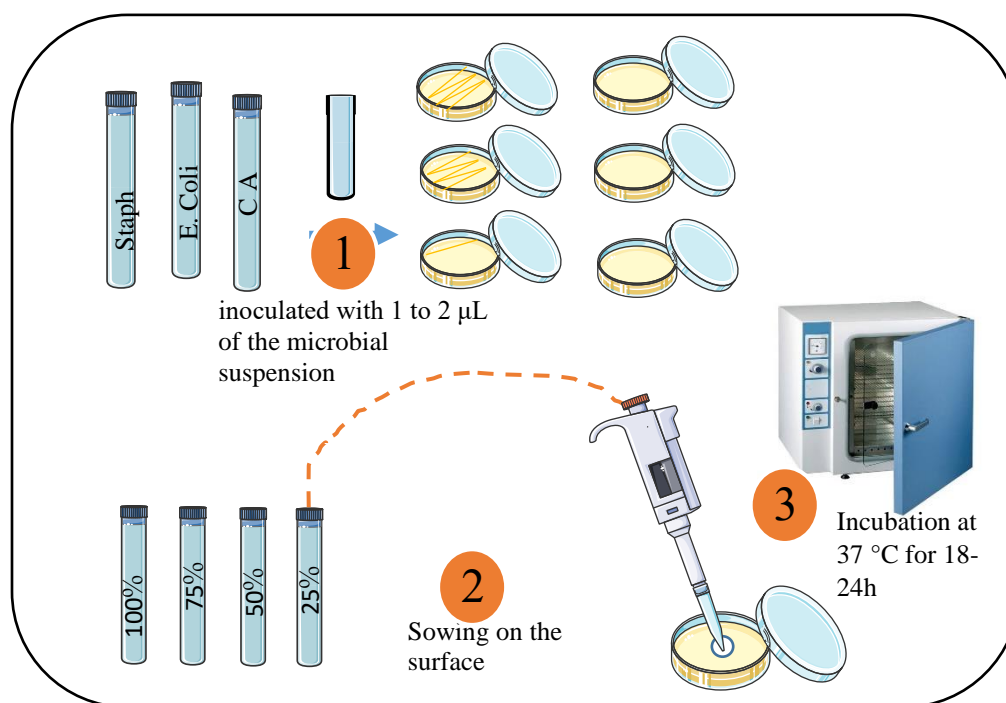


Fig.4.8 Shema of procedure of MIC(The minimum inhibitory concentration)

The minimum inhibitory concentration (MIC) is defined as the lowest concentration of EO that can have an effect. The percentage of bacterial growth inhibition is calculated using the following formula:

$$\%inhibition = (D_{test}/D_{control}) * 100 \quad (\text{Eq 4.10})$$

where:

- D_{test} : Diameter of the zone of inhibition.
- $D_{control}$: Diameter of the Petri dish.

A classification of essential oils in relation to their antimicrobial activity spectrum can be established based on the size of the inhibition zone. by ordering the four diameters of the microbial growth inhibition zones into four classes:

- ❖ Strongly inhibitory when: $\phi \geq 28$ mm of the inhibition zone.
- ❖ Moderately inhibitory when: $28 \text{ mm} > \phi > 16$ mm of the inhibition zone.
- ❖ Slightly inhibitory when: $16 \text{ mm} > \phi > 10$ mm of the inhibition zone.
- ❖ Non-inhibitory when: $\phi < 10$ mm of the inhibition zone. [131, 132]

4.5. In Silico anticancer study

4.5.1. Micro-computer

We utilized two laptops for the execution and analysis of our work, and their specifications are summarized in the following Tab.4.3 :


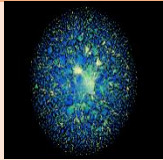

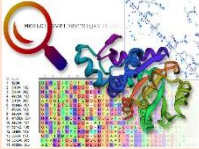

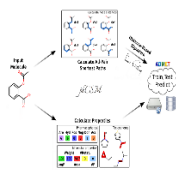

Tab.4.3 Characteristics of the laptops used in the study.

	Laptop 1	Laptop 2
Memory (RAM)	4.00 GO	8.00 GO
Operating system type	64-bit operating system	64-bit operating system
Processor	Intel(R) Pentium(R) CPU B960 @ 2.20 GHz, 2.20GHz	Intel(R) Core(TM) i7-6600U CPU @ 2.60GHz 2.81 GHz
Operating system	Windows 10 professionnall	Windows 10 professionnall

The use of several programs and the consultation of several databases and databases were necessary to carry out our practical part .

Tab.4.4 Programs used to carry out in silico study.

Programs	Using	Logo
Molecular docking		
AutoDockTools V1.5.6	An interactive graphical user interface (GUI) for coordinate preparation, docking and analysis[133] .	 AutoDock 4
Discovery Studio Visualizer V21.1.0	Molecular modeling environment for both small molecule and macromolecule applications, targeted mostly towards the needs in drug discovery and pharmaceutical industry [134].	
PyMOL Molecular Graphics System V2.3.2	A cross-platform molecular graphics tool, has been widely used for three-dimensional (3D) visualization of proteins, nucleic acids, small molecules, electron densities, surfaces, and trajectories[135] .	
AutoDock Vina V1.1.2	A turnkey computational docking program that is based on a simple scoring function and rapid gradient optimization conformational search[136] .	/
PDB Protein Data Bank	RCSB Protein Data Bank (RCSB PDB) enables breakthroughs in science and education by providing access and tools for exploration, visualization, and analysis[137].	

Modeling		
SWISS MODEL	Is a fully automated protein structure homology-modelling server, accessible via the Expasy web server, or from the program DeepView (Swiss Pdb-Viewer)[138].	 Swiss Institute of Bioinformatics
ESM 'Evolutionary scale modeling'	The ESM Metagenomic Atlas will enable scientists to search and analyze the structures of metagenomic proteins at the scale of hundreds of millions of proteins[139].	
Alpha Fold 2	AlphaFold is an AI system developed by DeepMind that predicts a protein's 3D structure from its amino acid sequence[140].	
Robetta fasta	Robetta is a protein structure prediction service that is continually evaluated through CAMEO. Features include relatively fast and accurate deep learning[141].	
ADMET		
Drulito	An open source virtual screening tool. It's calculation is based on the various druglikeness rules like Lipinski's rule, MDDR-like rule, Veber rule, Ghose filter, BBB rule, CMC-50 like rule and Quantitative Estimate of Drug-likeness (QED)[142].	
pkCSM	The pkCSM signatures were successfully used across five main different pharmacokinetic properties classes to develop predictive regression and classification models[112].	
Pass online	Pass-online is an online marketing agency specialized in digital interaction (e-marketing). and high quality performance[114].	

4.5.2. Molecular docking

4.5.2.1. Preparation of the receptor/target and ligand for the docking

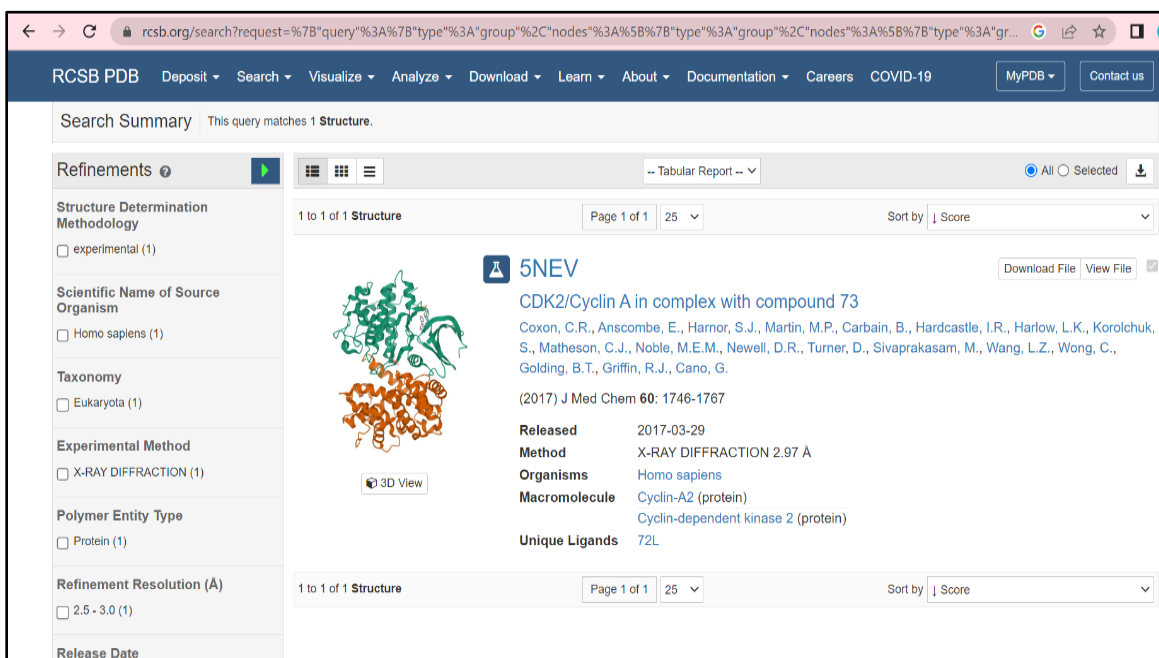
❖ Receptor preparation

In our study we will prepare the 3D structure of the target protein Cyclin-dependent kinase 2 with five methods.

A. Protein data bank

Step 1: we download the protein (CDK2) (PDB ID : 5NEV ;with resolution =2.97Å) from Protein Data Bank (www.rcsb.org).

The PDB file (5NEV.pdb) contains protein, water, ligands, cofactors, ions, etc., these protein structure inhibitors (water, ligands, cofactors, ions) were separated by releasing atomic coordinates of the PDB file [137].



The screenshot shows the RCSB PDB search results for PDB ID 5NEV. The page includes a search summary, a list of refinements, and a detailed view of the structure. The structure is shown as a 3D ribbon diagram. The title is 'CDK2/Cyclin A in complex with compound 73'. The authors are Coxon, C.R., Anscombe, E., Harnor, S.J., Martin, M.P., Carbain, B., Hardcastle, I.R., Harlow, L.K., Korolchuk, S., Matheson, C.J., Noble, M.E.M., Newell, D.R., Turner, D., Sivaprakasam, M., Wang, L.Z., Wong, C., Golding, B.T., Griffin, R.J., Cano, G. The journal reference is (2017) J Med Chem 60: 1746-1767. The release date is 2017-03-29. The method is X-RAY DIFFRACTION 2.97 A. The organisms are Homo sapiens. The macromolecule is Cyclin-A2 (protein) and Cyclin-dependent kinase 2 (protein). The unique ligands are 72L.

Fig.4.9 Downloading the PDB format file of protein.

Step 2: open autodock , and input the PDB file of the protein first click on “edit -> Delete water” than “edit >charges >add kollman charges” finely click on “ edit> hydrogens> add> and select polar only>ok” because they are required for appropriate treatment of electrostatics during docking

Step 3: Open the file by selecting “Grid>Macromolecule>chose ”, chose the types. Click “OK” to accept the changes. A window will pop up to write the PDBQT file. Click “Save” to register a file protein.pdbqt.

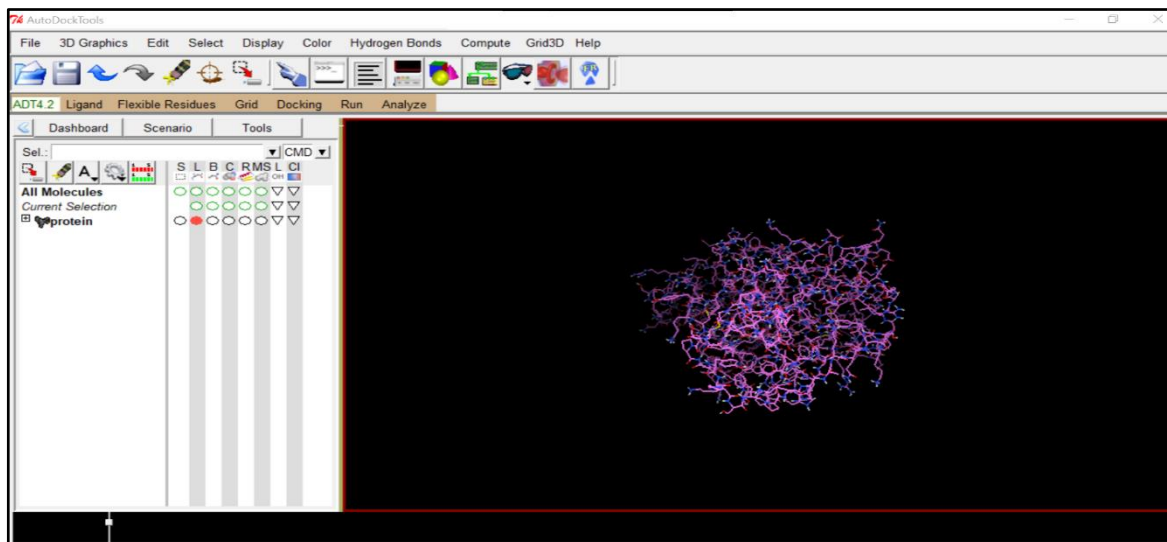


Fig.4.10 Addition of polar hydrogens to protein structure

The steps as show in Figs (4.9 ; 4.10) .

4.5.2.2. Ligand preparation

In the drug discovery field, some public repositories (e.g., PubChem) can collect and store chemical information and their biological activities in accessing free of charge to researchers. PubChem (<https://pubchem.ncbi.nlm.nih.gov/>) is a free and open resource which contains information on small molecules and their biological activities. (Fig 4.11).

The characterization of the components of essential oils using gas chromatography coupled with mass spectrometry (GC-MS) was not performed as part of our methodology. However, to continue the study, we adopted an approach based on the results previously described in scientific articles. "ginger" [143, 144] and "cinnamon" [27, 145-147]. The volatile compounds (ligands) were selected based on their therapeutic properties, particularly their anti-cancer activity.



Fig.4.11 The PubChem file

- ✓ **Step 1:** download the ligand from PubChem in sdf format.
- ✓ **Step 2:** we change its format to pdb by using a pymol program as follows :

In Pymol open the sdf file then click on File > Export Molecule > Save and enter the file name, at last, change the option of SDF and save it as ligand.pdb. The next step is the preparation ligand.pdbqt file [148]. It's presented in the Fig 2.12.

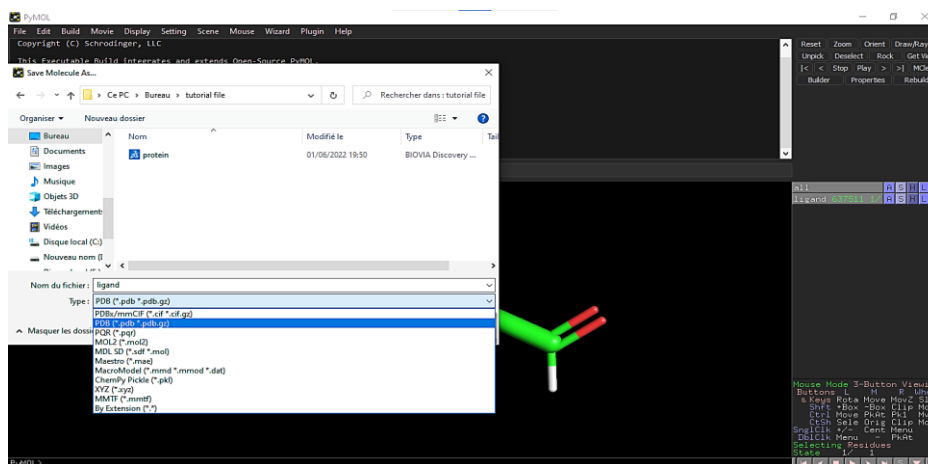


Fig.4.12 The changed of the format file on Pymol

- ✓ **Step 3:** Open AutodockTool. Introduce Ligand, select Input, and then click Open. Change the file format pdbqt to pdb in the following pop-up window. Then click Open after selecting ligand.pdb. Once more, open the Ligand menu, select Output, and save it as

PDBQT. Save the Ligand file as ligand.pdbqt in the specified working folder, where protein.pdbqt was saved.

The next stage is the preparation of the grid parameters file .

4.5.2.3. Preparation of docking parameter file

- ✓ **Step 1:** open the autodocktools and entered the protein.pdbqt and the ligand.pdbqt .

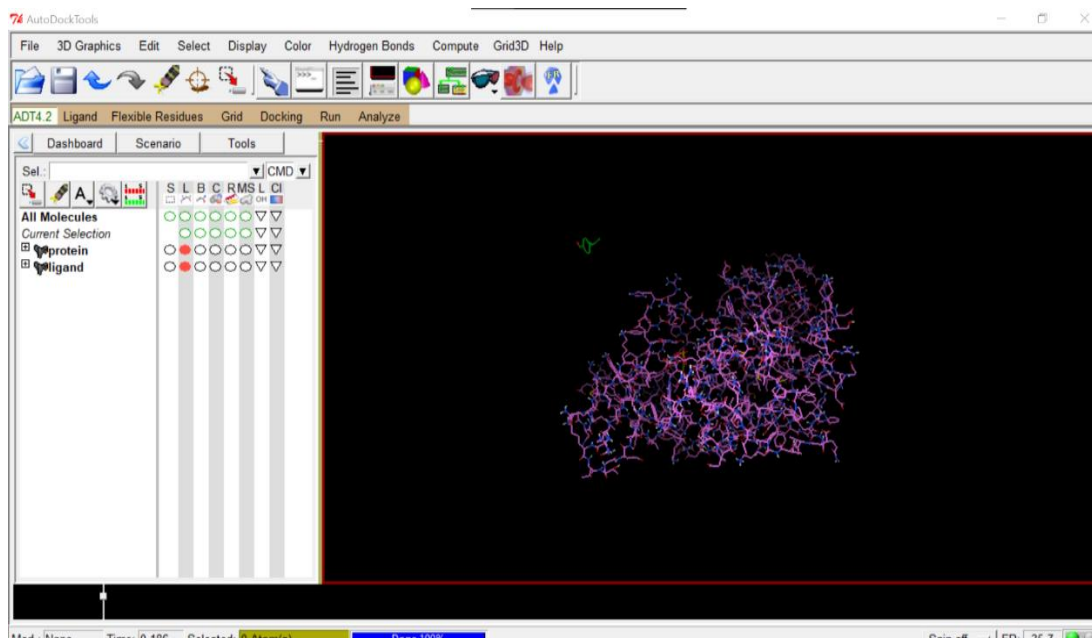
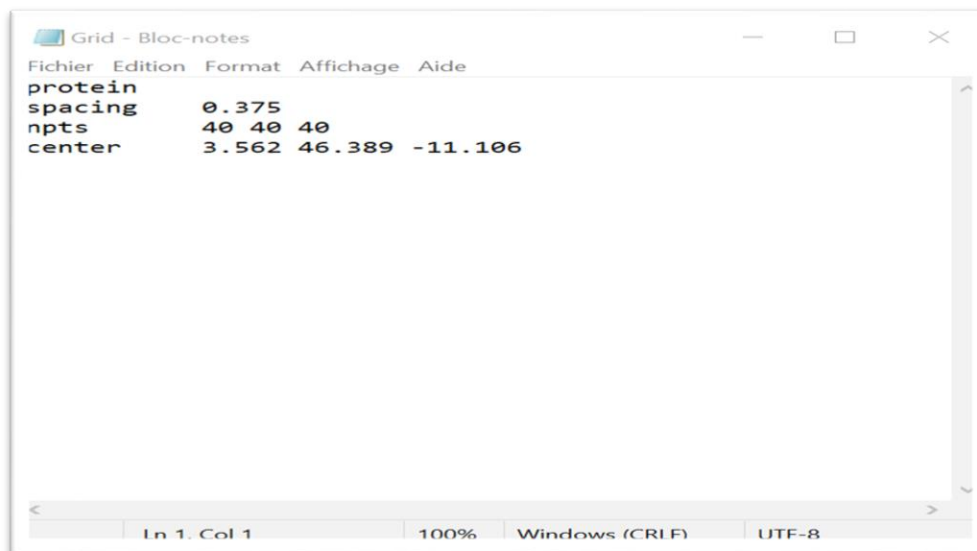


Fig.4.13 The opening of the protein and the ligand on autodocktools

- ✓ **Step2:** Select “Grid >Macromolecule > Open Protein PDBQT file, click “Yes” to preserve the existing charges in the file, and “OK” to accept. There may also be a warning window if there are slight irregularities in charges. Click “OK” if it appears .
- ✓ **Step3:** click on grid >grid box> file>output and dimensions file > save as txt file where protein.pdbqt and ligand.pdbqt was saved .

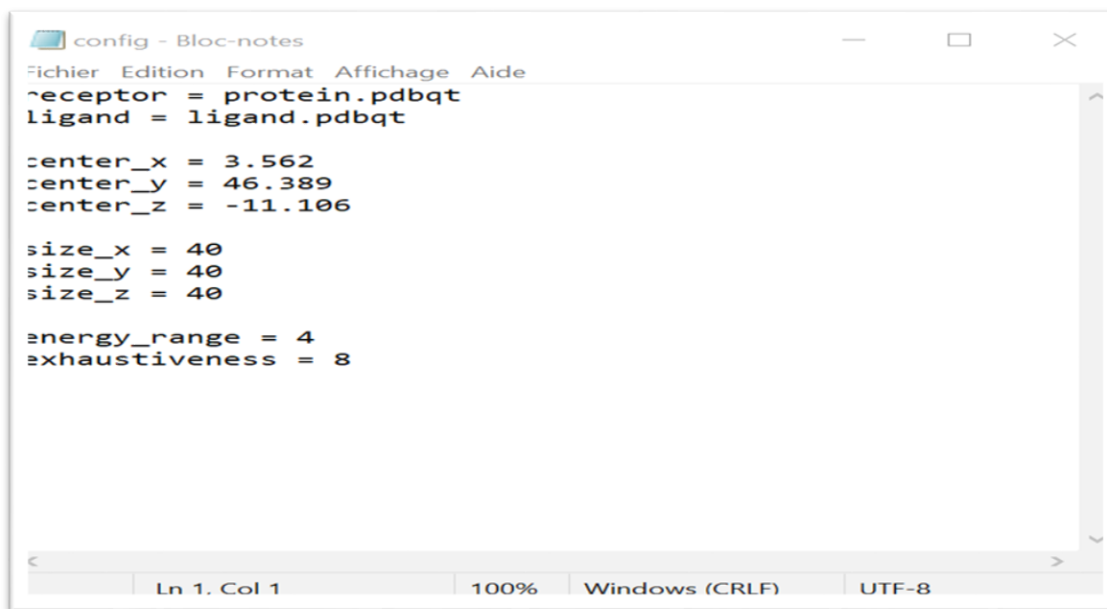


```
Grid - Bloc-notes
Fichier Edition Format Affichage Aide
protein
spacing      0.375
npts         40 40 40
center       3.562 46.389 -11.106

Ln 1, Col 1    100%    Windows (CRLF)    UTF-8
```

Fig.4.14 The dimensions file of the grid box

- ✓ **Step4:** write the conFiguRation file (Grid.txt) then click “Save”. Make sure to save conFig.txt in the same folder or working directory where protein.pdbqt and ligand.pdbqt files were already saved.



```
config - Bloc-notes
Fichier Edition Format Affichage Aide
receptor = protein.pdbqt
ligand = ligand.pdbqt

center_x = 3.562
center_y = 46.389
center_z = -11.106

size_x = 40
size_y = 40
size_z = 40

energy_range = 4
exhaustiveness = 8

Ln 1, Col 1    100%    Windows (CRLF)    UTF-8
```

Fig.4.15 The configuration file

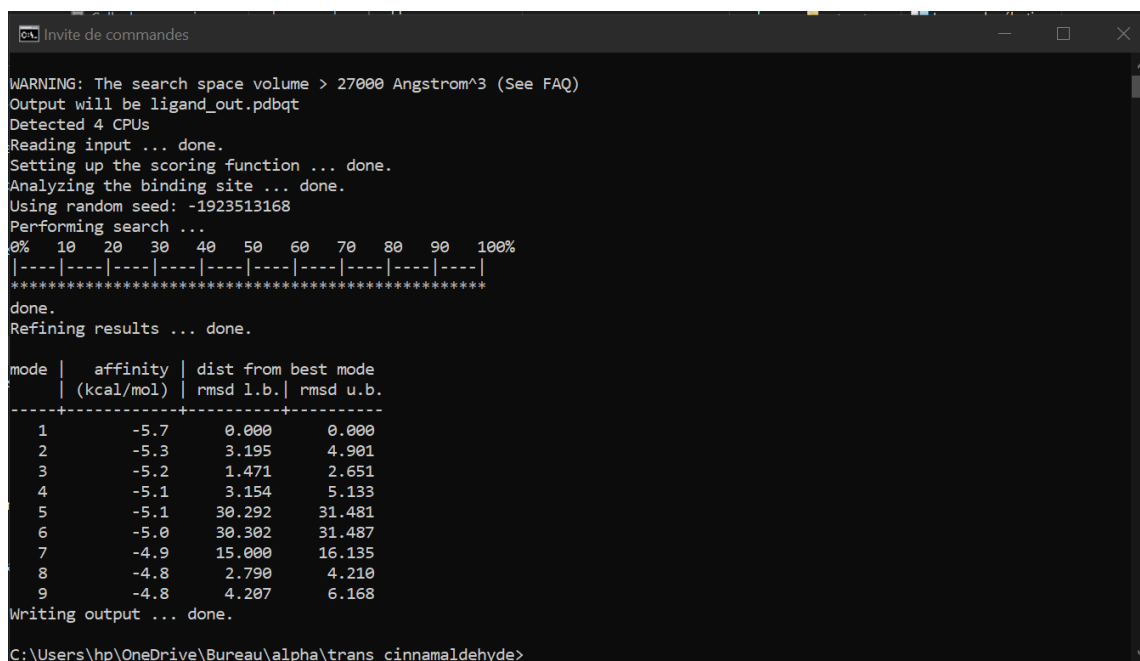
The steps as show in Fig (4.13 ; 4.15) .

4.5.2.4. Running autodock vina

- ✓ **Step 1:** Locate the installed vina in our default installation directory. The default installation directory could be "C:\Program Files (x86)\The Scripps Research Institute" Copy the vina.exe, vina_licence.rtf and vina_split.exe files from the installation folder into the working directory (In the current case, it is working directory on Desktop\tutorial file."
- ✓ **Step 2:** Run the vina command using Command Prompt (command line in a window) for Molecular Docking, Open CMD, from Window START search for CMD and click on Command prompt.

Go to the working directory where the required files are present using the command, « cd C:\Users\HP\Desktop\tutorial file ». In this case study, Press enter and then type the following commands « vina.exe - -conFig conf.txt - -log log.txt ».

Upon completion of the processing, which may range from seconds to minutes depending on system performance, the results are saved in the "log.txt" file, and the program automatically returns to the original working directory location as show in Fig 4.16 [136].



```
Invite de commandes

WARNING: The search space volume > 27000 Angstrom^3 (See FAQ)
Output will be ligand_out.pdbqt
Detected 4 CPUs
Reading input ... done.
Setting up the scoring function ... done.
Analyzing the binding site ... done.
Using random seed: -1923513168
Performing search ...
0% 10 20 30 40 50 60 70 80 90 100%
|----|----|----|----|----|----|----|----|----|
*****
done.
Refining results ... done.

mode |  affinity  |  dist from best mode
      |  (kcal/mol) |  rmsd l.b. | rmsd u.b.
-----+-----+-----+-----
  1   |    -5.7   |    0.000   |    0.000
  2   |    -5.3   |    3.195   |    4.901
  3   |    -5.2   |    1.471   |    2.651
  4   |    -5.1   |    3.154   |    5.133
  5   |    -5.1   |   30.292   |   31.481
  6   |    -5.0   |   30.302   |   31.487
  7   |    -4.9   |   15.000   |   16.135
  8   |    -4.8   |    2.790   |    4.210
  9   |    -4.8   |    4.207   |    6.168

Writing output ... done.

C:\Users\hp\OneDrive\Bureau\alpha\trans_cinnamaldehyde>
```

Fig.4.16 Result of execution of autodock vina commands

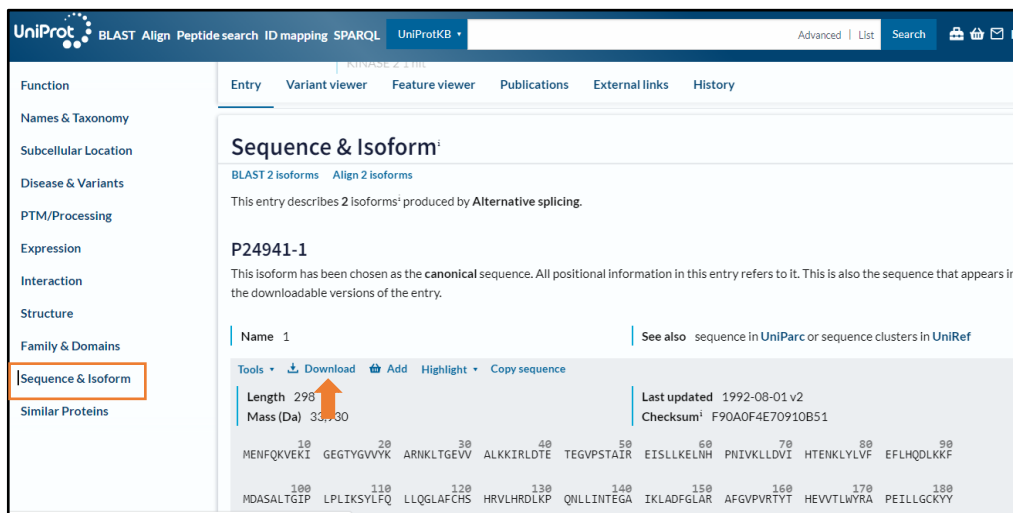
4.5.2.5. Evaluation of docking and virtual screening

- ✓ **Step 1:** Open protein.pdbqt in Discovery Studio, then drag and drop ligand.pdbqt from the working directory into the graphical window of discovery studio [134].
- ✓ **Step 2:** Click Receptor-Ligand Interactions in DS followed by clicking Ligand Interactions on left hand side to show the 3D interaction .

4.5.3. Modeling

B. Swiss model

Step1: Open the Pass web server <https://www.uniprot.org/> ,and click on ‘Sequence & Isoform’ then ‘download’ as shown in Fig 4.17 [149].



The screenshot shows the UniProt website interface. The main content area is titled 'Sequence & Isoform' and displays information for entry P24941-1. The entry is described as having 2 isoforms produced by alternative splicing. The canonical sequence is shown with its length (298) and mass (33,730). The 'Download' button is highlighted with an orange arrow. The sequence is displayed in a grid format with residue numbers 10, 20, 30, 40, 50, 60, 70, 80, 90, 100, 110, 120, 130, 140, 150, 160, 170, 180.

Residue	10	20	30	40	50	60	70	80	90
Sequence	MENFQKVEKI	EGGTYGVVYK	ARNKLTGEWV	ALKKIRLDTE	TEGVPSTAIR	EISLLKELNH	PNIVKLLDVI	HTENKLYLVP	EFLHQDLKRF
Residue	100	110	120	130	140	150	160	170	180
Sequence	MDASALTGIP	LPLIKSYLFQ	LLQGLAFCHS	HRVLHRDLKP	QNLLINTEGA	IKLADFGLAR	AFGVPVRTYT	HEWTLWYRA	PEILLGCKYY

Fig.4.17 Downloding of the sequence

- ✓ **Step2:** Open the Pass web server <https://swissmodel.expasy.org/> ,and click on ‘Start Modelling’.
- ✓ **Step3:** Paste the protein sequence or provide the UniprotKB AC (P24941) of your target sequence in the input form , It’s presented in the Fig 4.18 [138].

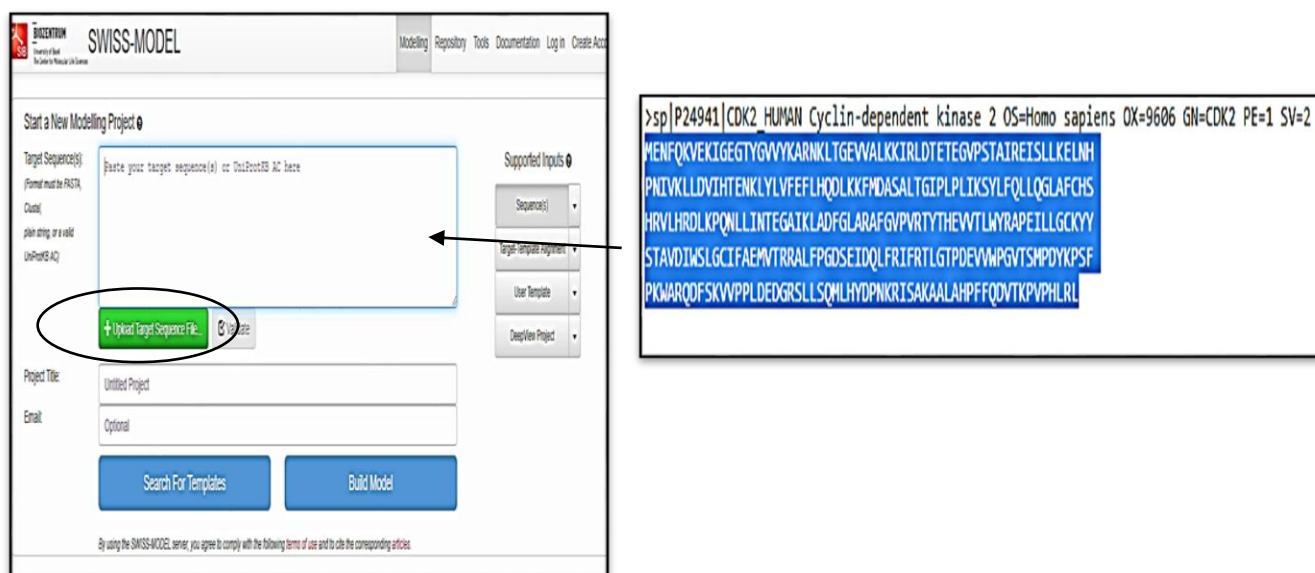


Fig.4.18 The input form of the target sequence

Step4: Click on ‘Build Model’ in order to search the template (as illustrated in Fig 4.19).



Fig.4.19 The building model on swiss model

C. Alphadatabase

- ✓ **Step1:** Open the Pass web server <https://www.uniprot.org/> ,and click on ‘Sequence & Isoform’ then ‘download’ [149].
- ✓ **Step2:** Open the Fasta web server <https://www.ebi.ac.uk/Tools/sss/fasta/>, and provide the UniprotKB AC (P24941) of your target sequence in the input form.

Fig.4.20 The input form of the target sequence on Alpha Fold

- Step3:** Click on ‘Protien Databases , choose ‘Structures’ then ‘AlphaFold DB’ [150] .

- ✓ **Step4:** Submit our job by Clicking on 'Submit'
Fig.4.21 ScreenShot of protein databases

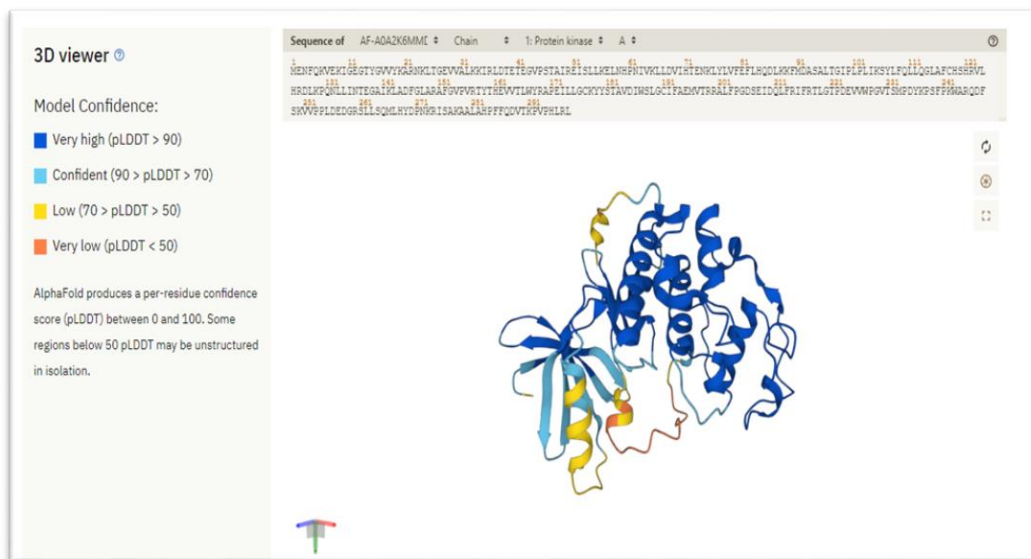


Fig .4.22 The building Model on AlphaFold

- ✓ **Step5:** Dowload the file .

Fig.4.23 The downloading file

The steps as show in Fig (4.20 ; 4.23) .

D. Evolutionary scale modeling (ESM)

- ✓ **Step1:** Open the web server <https://www.uniprot.org/>, and click on ‘Sequence & Isoform’ then ‘download’ [149].
- ✓ **Step2:** Open the Pass web server <https://esmatlas.com/>, and click on ‘Fold Sequence’ (as illustrated in Fig 4.24).

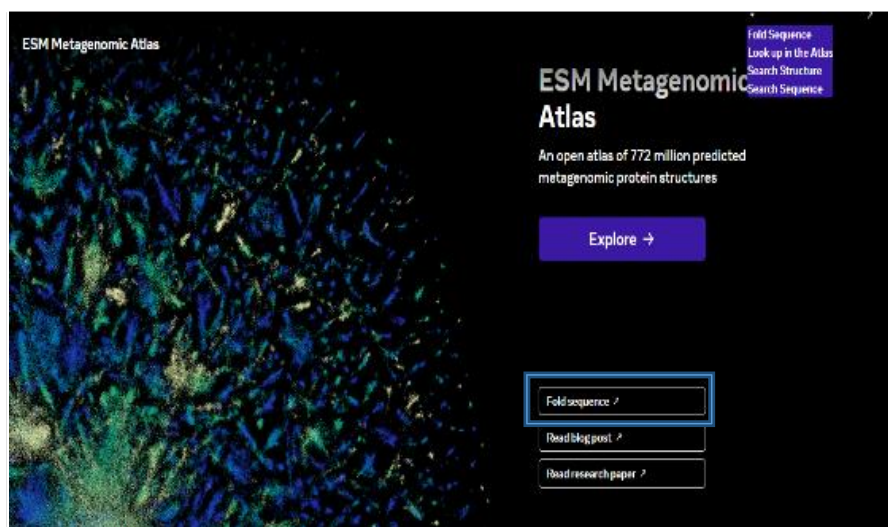


Fig.4.24 The opening of the pass web server

- ✓ **Step3:** In the input form, provide your target sequence's UniprotKB AC (P24941) look Fig 2.27 .

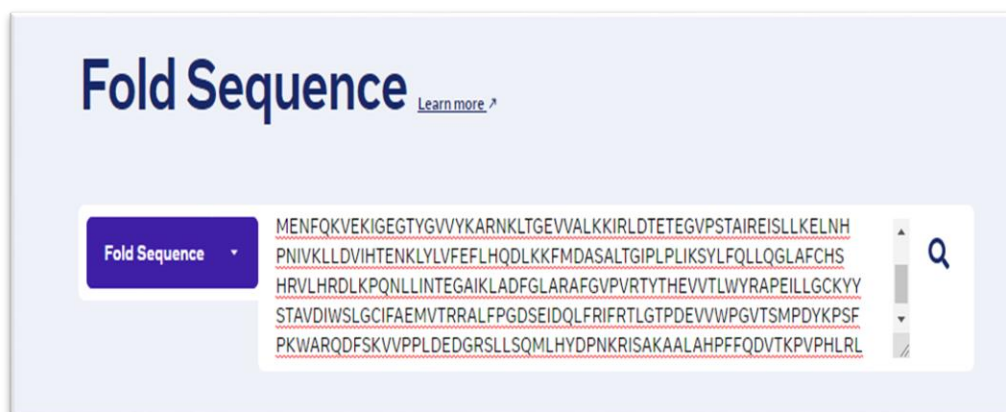


Fig.4.25 The input form of the target sequence on ESM

- ✓ **Step4:** Download the file by clicking on ‘PDB file’ as show in Fig 4.26 [139].

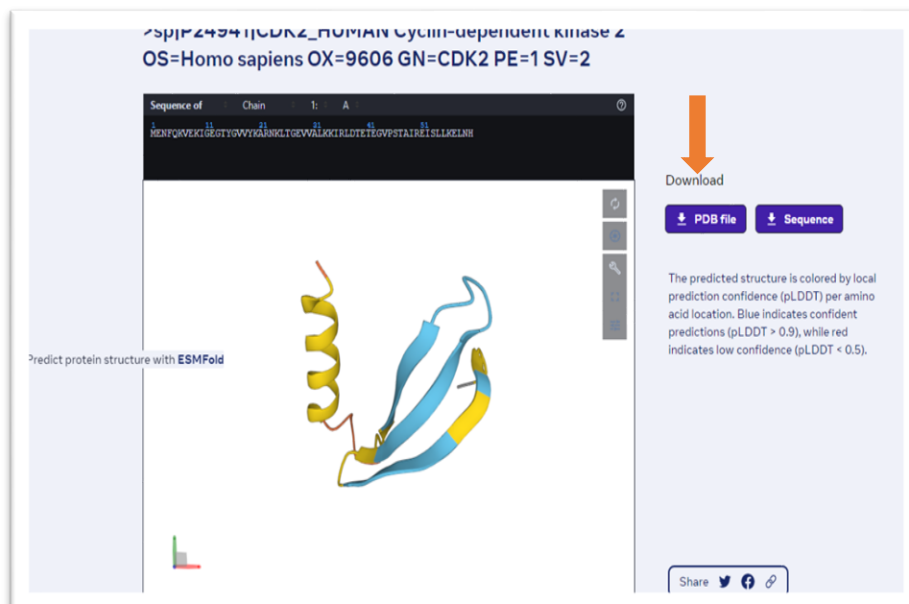


Fig.4.26 The building model on ESM

E. Robetta

- ✓ **Step 1:** Open the s web server <https://www.uniprot.org/> ,and click on ‘Sequence & Isoform’ then ‘download’ [149].
- ✓ **Step2:** Open the Pass web server <https://robetta.bakerlab.org/> and log in
- ✓ **Step3:** Click “structure prediction” than “submit” .

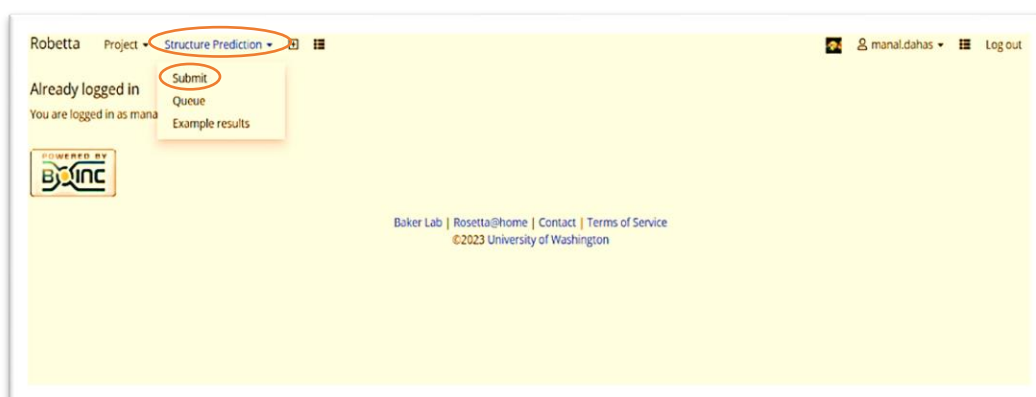
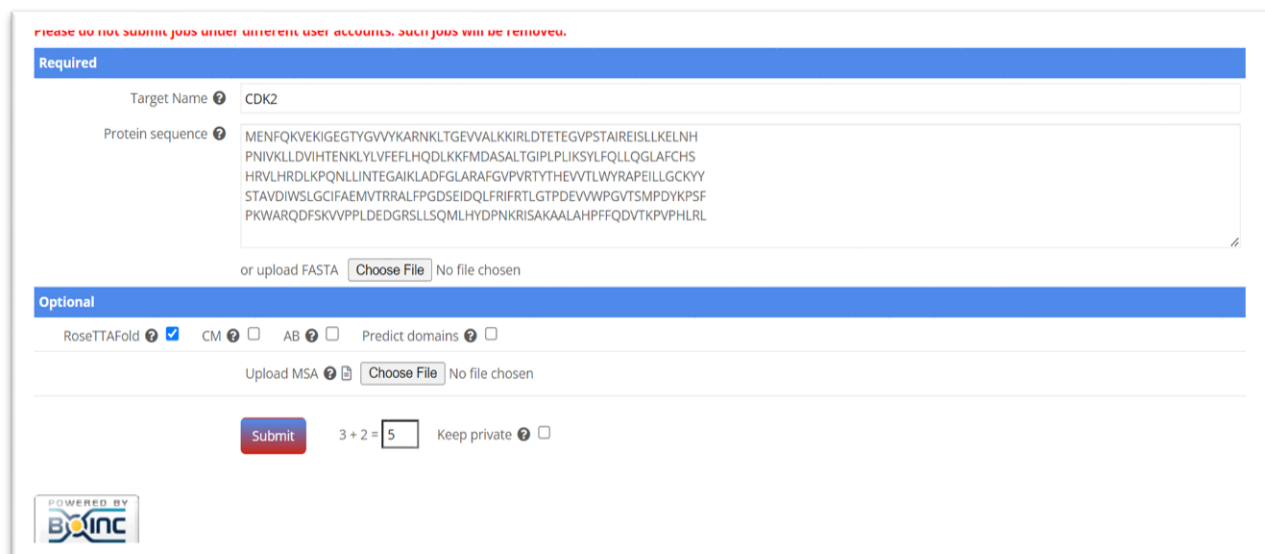


Fig.4.27 The opening of Robetta

- ✓ **Step4:** Provide your target sequence's UniprotKB AC (P24941) in the input form. Named the target to click on RoseTTAFold, and click on submit [141].



The screenshot shows the RoseTTAFold web interface. At the top, there is a warning: "Please do not submit jobs under different user accounts. Such jobs will be removed." Below this, the "Required" section contains a "Target Name" field with "CDK2" and a "Protein sequence" field with the following sequence: MENFQKVEKIGEGTYGVVYKARNKLTGEVWALKIRLDTETEGVPSTAIRESILLKELNH PNIVKLLDVIHTENKLYLVEFLHQDLKKFMDASALTGIPLPIKSYLQQLQGLAFCHS HRVLHRDLKPQNLLINTEGAIKLADFGLARAFGVPVRTYTHEVTLWYRAPELLGCKYY STAVDIWSLGCIFAEMVTRRALFPGDSEIDQLFRIFRTLGTDPDEVWPGVTSMPDYKPSF PKWARQDFSKVVPPLDEEDGRSLLSQMLHYDPNKRISAKAALAHFFQDVTKPVPHLRL. Below the sequence field, there is a "Choose File" button and the text "No file chosen". The "Optional" section includes checkboxes for "RoseTTAFold" (checked), "CM", "AB", and "Predict domains". There is also an "Upload MSA" field with a "Choose File" button and "No file chosen". At the bottom, there is a "Submit" button, a CAPTCHA "3 + 2 = 5", and a "Keep private" checkbox. A "POWERED BY" logo for "BIOIN" is visible in the bottom left corner.

Fig.4.28 The input form of the target sequence on Robetta

- ✓ **Step5:** wait for the result of the prediction on your email .

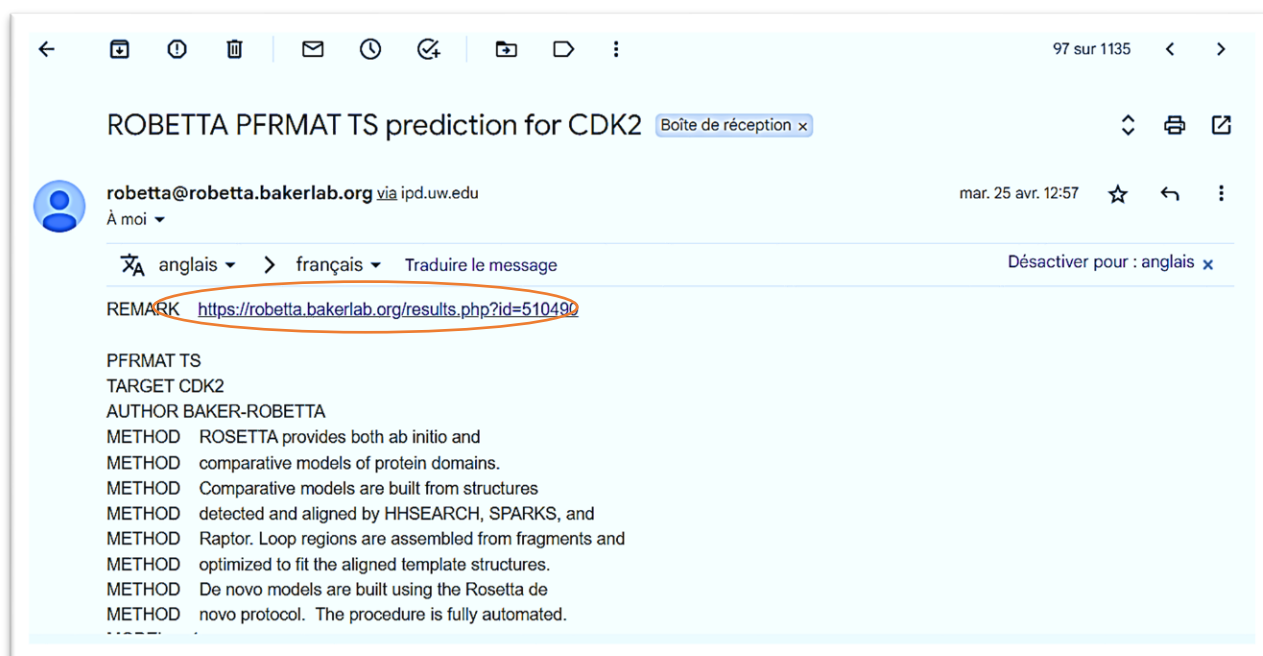


Fig.4.29 The screenshot of the E-mail

- ✓ **Step6:** click on the link and Download the file [141].

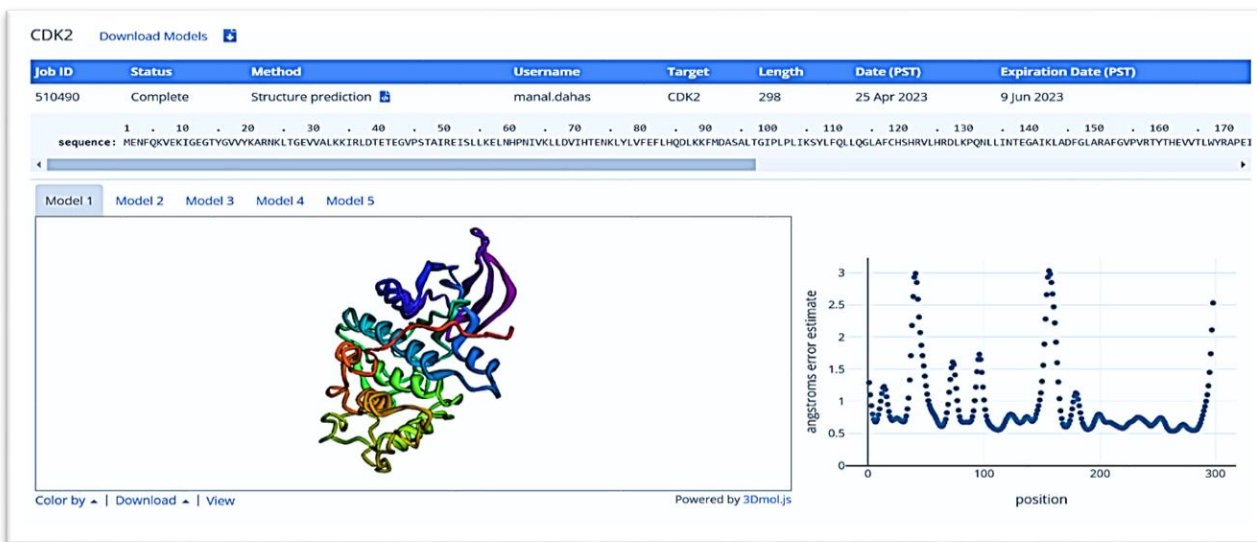


Fig.4.30 The building model on Robetta

The steps as show in Fig (4.27 ; 4.30) .

4.6. Pharmacokinetics

4.6.1. Drug likeness tool ‘Drulito’

- ✓ **Step1:** Click on ‘Browse’ button and select the molecule either in *.mol or *.sdf file format.

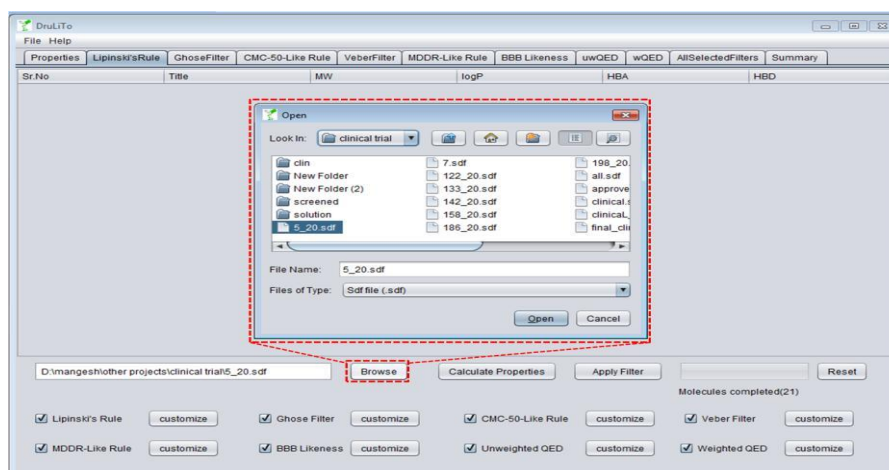


Fig.4.31 Input the SDF file of the compound on Drulito

- ✓ **Step2:** Click on the ‘Calculate Propriets’ button which calculates all the descriptors.

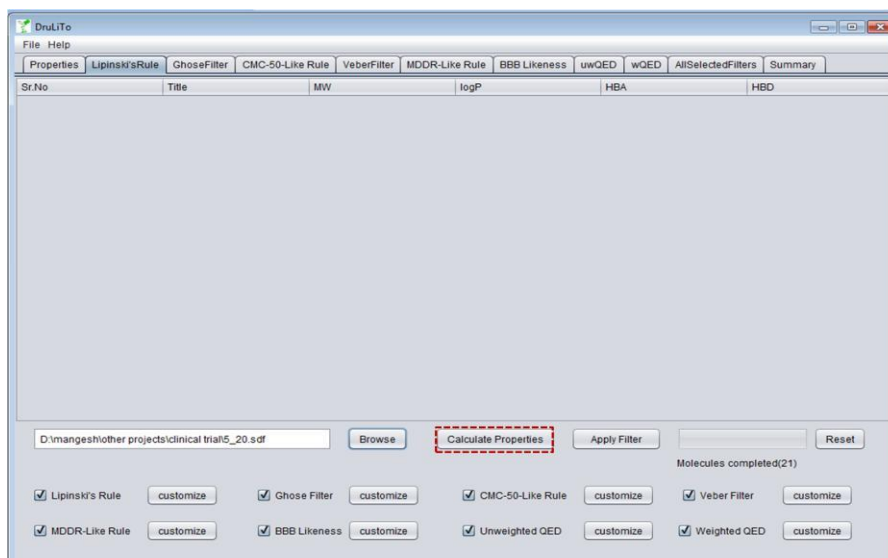


Fig.4.32 Calculate the propriets

- ✓ **Step3:** Click on the Drug likeness rule box according to the users need. The user can even customize the rules as per the need by clicking on the ‘customize’ button.

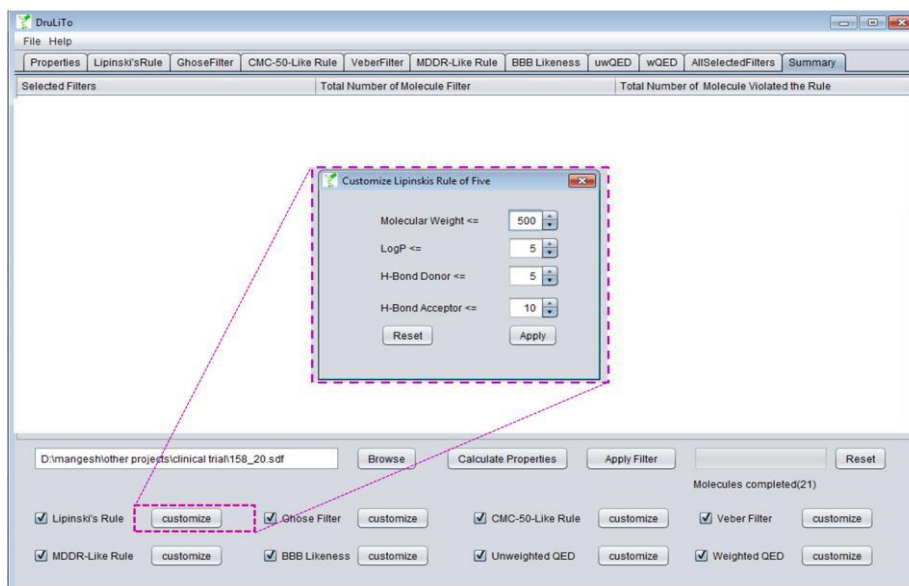


Fig.4.33 customize the rules as per the need.

- ✓ **Step4:** Click on the ‘Apply Filter’ button to apply the selected rules.

The screenshot shows the DruLiTo software interface. At the top, there are tabs for Properties, Lipinski's Rule, GhoseFilter, CMC-50-Like Rule, VeberFilter, MDDR-Like Rule, BBB Likeness, uwQED, wQED, AllSelectedFilters, and Summary. The main area contains a table with 21 rows of molecule data. Below the table, there are buttons for 'Browse', 'Calculate Properties', 'Apply Filter', and 'Reset'. At the bottom, there are checkboxes for various filters: Lipinski's Rule, Ghose Filter, CMC-50-Like Rule, Veber Filter, MDDR-Like Rule, BBB Likeness, Unweighted QED, and Weighted QED. The 'Apply Filter' button is highlighted with a dashed blue box.

Sr. No.	Title	MW	logp	Alogp	HBA	HBD	TPSA	AMR	nRB	nAtom	nAcidic...	RC	nRigidB	nAtom...	nHB	SAAlerts
1	UnTitle...	270.05	1.043	-0.387	5	3	86.99	78.92	1	30	0	3	21	2	8	1
2	DCL00...	270.05	1.043	-0.387	5	3	86.99	78.92	1	30	0	3	21	2	8	1
3	DCL00...	240.08	1.379	0.972	3	2	49.69	77.44	1	30	0	3	19	2	5	0
4	DCL00...	421.92	3.411	1.482	3	1	46.53	98.67	3	34	0	3	21	3	4	1
5	DCL00...	240.05	1.533	1.998	2	0	64.73	70.11	2	26	0	3	18	3	2	2
6	DCL00...	228.08	2.048	1.194	3	3	69.69	74.51	2	29	0	2	16	2	6	1
7	DCL00...	174.03	-0.011	0.176	3	1	54.37	50.98	0	19	0	2	14	1	4	0
8	DCL00...	204.09	0.621	-0.622	4	1	42.85	58.82	1	27	0	3	16	1	5	0
9	DCL00...	346.12	1.152	0.603	4	4	80.92	106.96	0	44	0	5	30	3	8	0
10	DCL00...	297.09	2.445	2.167	4	1	80.38	92.48	1	36	0	3	22	2	5	1
11	DPR00...	297.09	2.445	2.167	4	1	80.38	92.48	1	36	0	3	22	2	5	1
12	DCL00...	270.06	1.536	1.408	4	2	73.12	65.57	4	28	0	1	15	1	6	4
13	DCL00...	346.12	-1.192	0.027	8	4	141.94	100.77	2	40	0	4	27	4	12	0
14	DCL00...	287.06	-0.217	-0.866	6	4	142.52	63.55	3	33	0	2	18	1	10	2
15	DCL00...	288.11	-0.256	-1.24	6	2	80.85	82.9	4	37	0	3	19	1	8	1
16	DPR00...	250.09	0.197	-1.557	5	1	68.49	73.01	1	29	0	3	20	2	6	1
17	DCL00...	220.06	1.545	0.681	3	1	41.46	71.53	0	25	0	4	20	3	4	0
18	DCL00...	238.11	1.576	0.906	3	2	41.13	78.21	1	32	0	3	19	2	5	1
19	DCL00...	238.11	1.576	0.906	3	2	41.13	78.21	1	32	0	3	19	2	5	1
20	DCL00...	345.16	1.791	-0.543	6	3	80.18	102.12	5	48	0	3	22	2	9	1
21	DCL00...	343.1	0.96	-2.2	6	1	99.79	99.65	7	41	0	3	19	3	7	1

Fig.4.34 Apply the selected rules.

- ✓ **Step5:** Check the 'Summary' tab of Drug likeness rules to see the total number of candidate among the molecules passing and violating all the rules [151, 152].

The screenshot shows the DruLiTo software interface with the 'Summary' tab selected. It displays a table with three columns: 'Selected Filters', 'Total Number of Molecule Filter', and 'Total Number of Molecule Violated the Rule'. Below the table, there are buttons for 'Browse', 'Calculate Properties', 'Apply Filter', and 'Reset'. At the bottom, there are checkboxes for various filters: Lipinski's Rule, Ghose Filter, CMC-50-Like Rule, Veber Filter, MDDR-Like Rule, BBB Likeness, Unweighted QED, and Weighted QED.

Selected Filters	Total Number of Molecule Filter	Total Number of Molecule Violated the Rule
Lipinski's Rule of Five	21	0
Ghose_Filter	3	18
CMC-50 Like Rule	0	21
Vebers Rule	19	2
MDDR Like Rule	1	20
BBB Likeness Rule	0	21
Unweighted QED	20	1
Weighted QED	19	2
All Selected Filters	0	21

Fig.4.35 The total number of candidate among the molecules passing and violating all the rules.

The steps as show in Fig (4.31 ; 4.35).

4.6.2. Pharmacokinetics models for small molecule(PKCSM)

- ✓ **Step1:** Open the web page <https://biosig.lab.uq.edu.au/pkcsm/> , and choose ‘PKCSM’ .
- ✓ **Step2,3:** provide either an input file with a list of molecules (2) in smiles format (up to a maximum of 100 molecules) or supply a single smiles string (3).

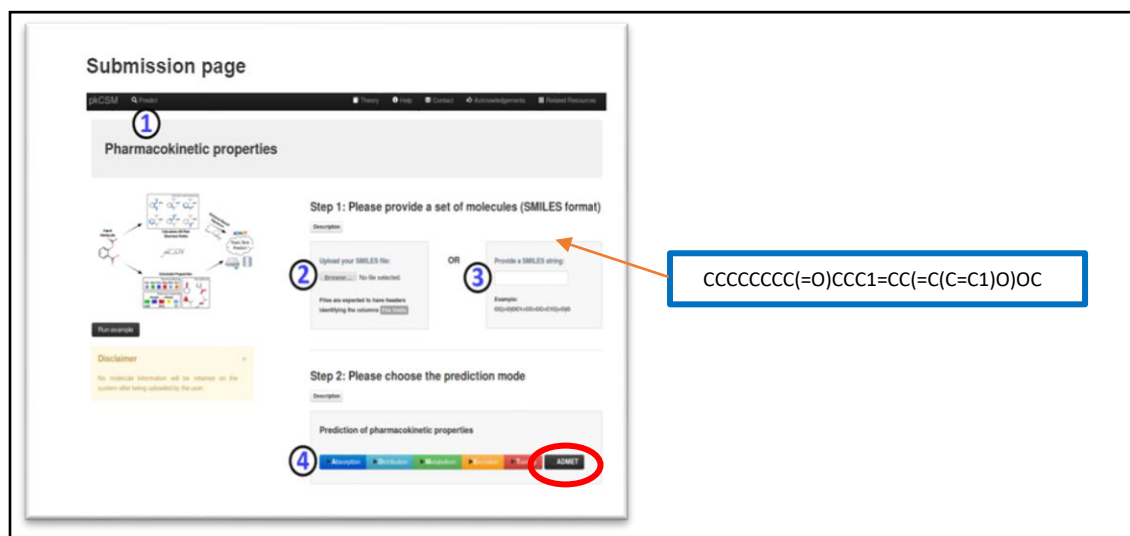


Fig.4.36 Input the smile file on PKCSM

- ✓ **Step4:** Choose the prediction mode. Users can choose between the main admet property classes (absorption, distribution, metabolism, excretion and toxicity) by clicking its corresponding button or systematically evaluating all predictive models [112].

The result are shown in Fig 4.37 .

Category	Descriptor	Value	Unit
Absorption	Skin Permeability	-2.781	Numeric (log Kp)
	P-glycoprotein substrate	Yes	Categorical (Yes/No)
	P-glycoprotein I inhibitor	Yes	Categorical (Yes/No)
Distribution	P-glycoprotein II inhibitor	No	Categorical (Yes/No)
	VDss (human)	0.588	Numeric (log L/kg)
	Fraction unbound (human)	0.183	Numeric (Fu)
Metabolism	BBB permeability	-0.794	Numeric (log BB)
	CNS permeability	-2.789	Numeric (log PS)
	CYP2D6 substrate	No	Categorical (Yes/No)
	CYP3A4 substrate	Yes	Categorical (Yes/No)
	CYP1A2 inhibitor	Yes	Categorical (Yes/No)
	CYP2C19 inhibitor	Yes	Categorical (Yes/No)
Excretion	CYP2C9 inhibitor	Yes	Categorical (Yes/No)
	CYP2D6 inhibitor	No	Categorical (Yes/No)
	CYP3A4 inhibitor	No	Categorical (Yes/No)
Excretion	Total Clearance	1.4	Numeric (log ml/min/kg)

Fig.4.37 The result of Pharmacokinetics

4.6.3. Pass Online

- ✓ **Step1:** Open the Pass web server <http://www.way2drug.com/passonline/>, and click on 'GO for prediction'.
- ✓ **Step2:** Choose 'Predict New Compound' (a in Fig 4.38), then input your molecule using its SMILES code (b in Fig 4.38) or upload a structure file in SDF or MOL format.

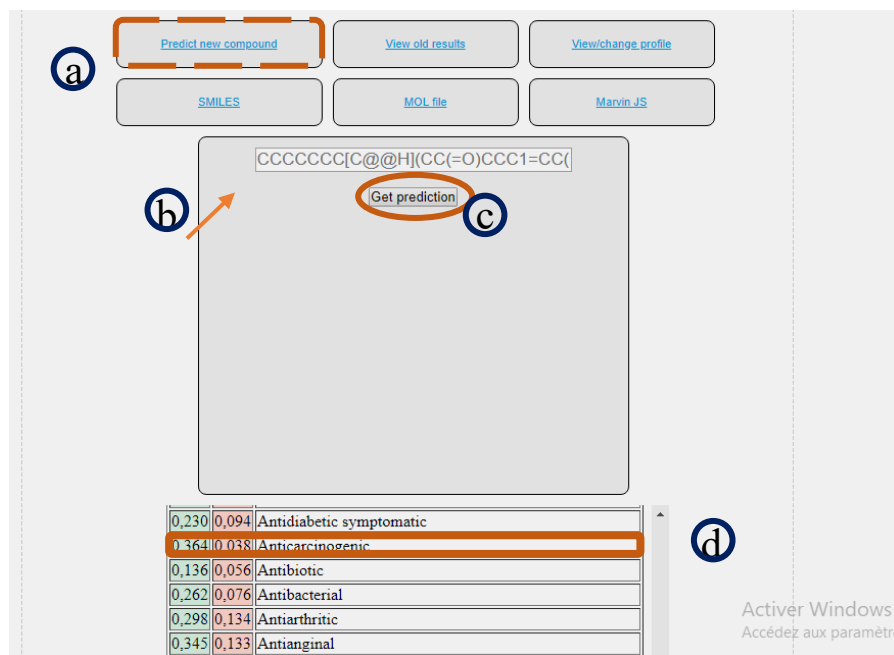
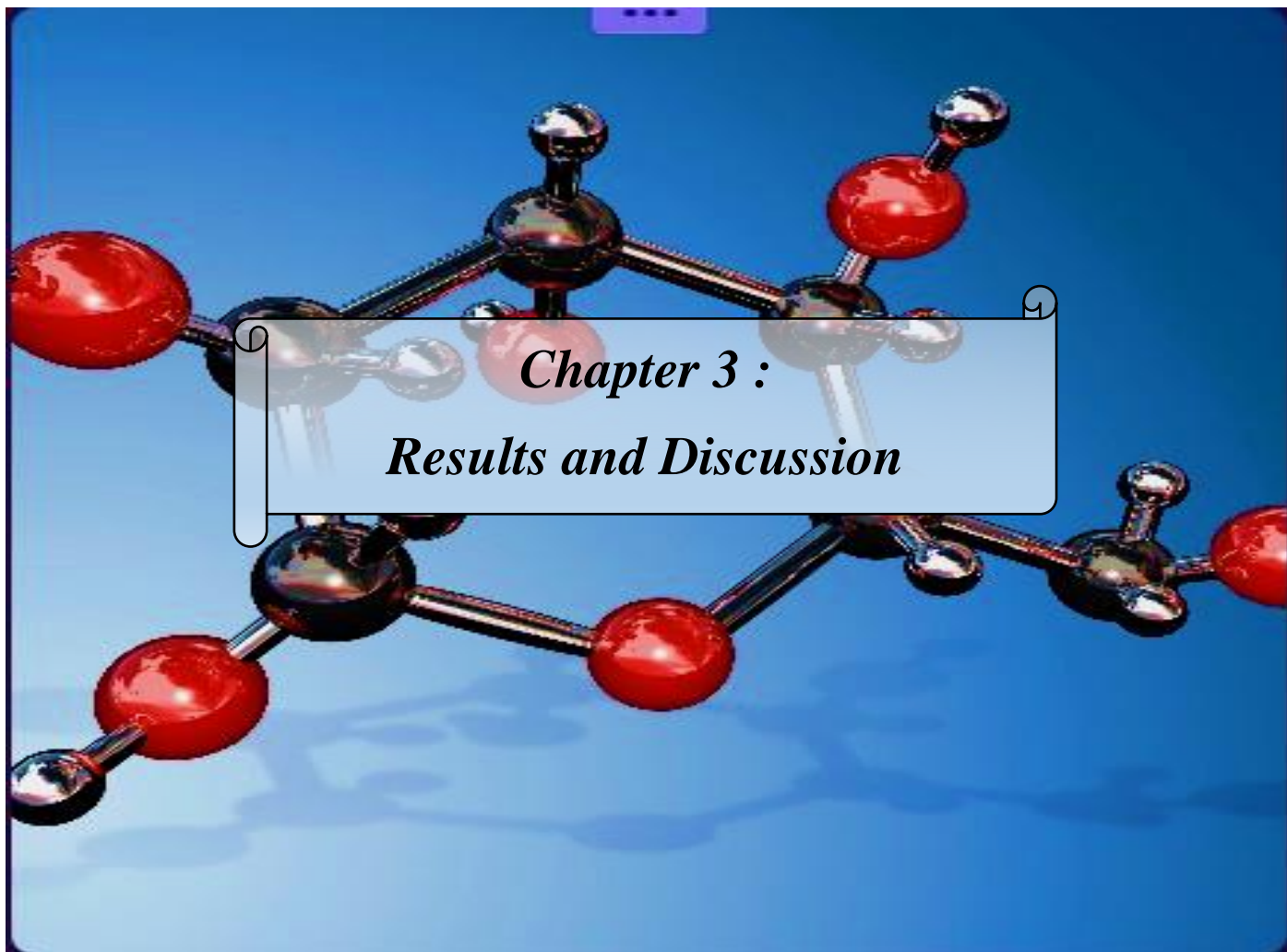


Fig.4.38 The result of the pass online

- ✓ **Step3:** Click on 'Get Prediction'(c in Fig 4.38), Choose the activity classes you want to predict from the list of available options. we choose 'Anticancer'(d in Fig 4.38) [151].

4.7. Conclusion

In this chapter, we provided a detailed description of the materials used and the methods employed in this study to extract essential oils from cinnamon and ginger, as well as to examine their properties and evaluate their potential anticancer effects.



Chapter 5: Results and discussion

5.1. Introduction

This study involved the results extraction of essential oils from cinnamon and ginger, followed by a comprehensive analysis encompassing organoleptic properties, physico-chemical characteristics, biochemical activities, and biological activities, which were investigated through in vitro experiments using cell cultures and in silico simulations to assess the anticancer effects.

5.2. Extraction “Hydrodistillation”

The initial assessment to be performed involves determining the essential oil yield through steam distillation. To obtain the percentage of cinnamon and ginger essential oil yield, the weight of the essential oil is compared to the dry weight of the bark powder mass utilized in the steam distillation process [153, 154]. The outcomes are displayed in Tab 5.1 and Fig 5.1.

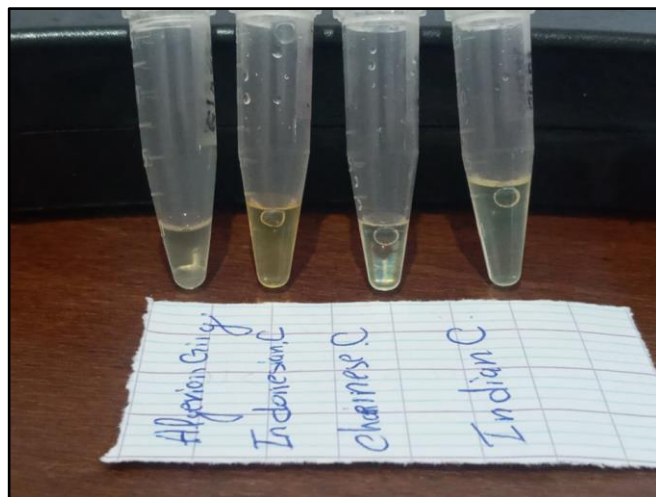
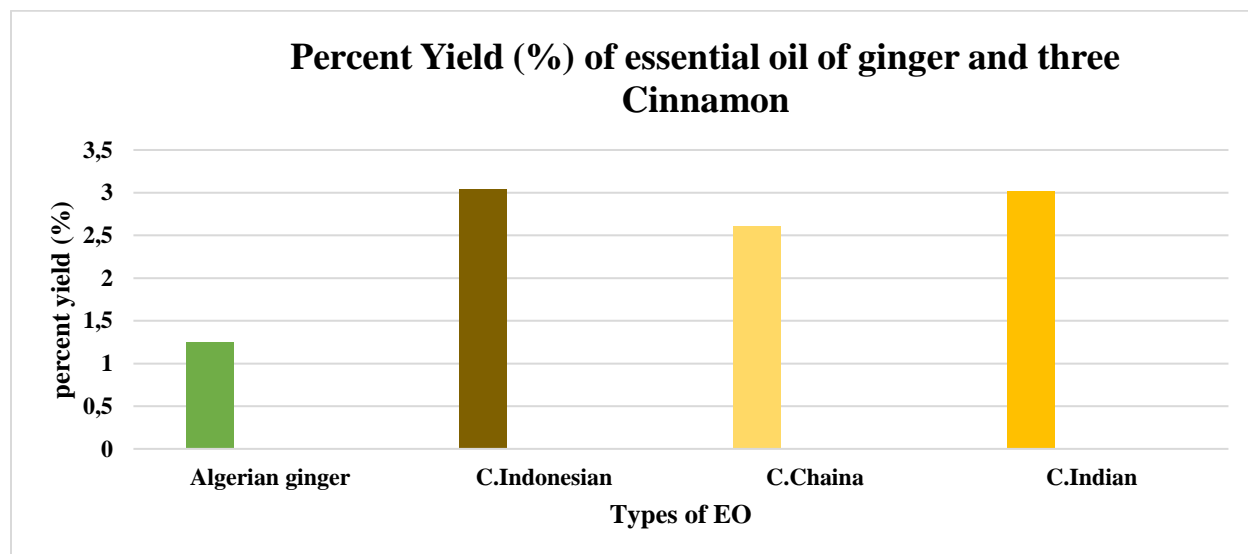


Fig.5.1. Essential oil obtained of ginger and cinnamon by steam distillation.

Tab.5.1. Yield result by steam distillation method

Plant	Mass of initial plant (g)	Mass of the extracted oil (g)	The yield %	standards
Algerian Ginger	70	0.87	1.24%	0,5 -2% [155]
Indonesian cinnamon	50	1.52	3.04%	2-4% [155]
Chines cinnamon	50	1.3	2.6%	2-4% [155]
Indian cinnamon	50	1.51	3.02%	2-4% [155]

**Fig.5.2** Graphic representation of the different yields (%) of the essential oils of ginger and the three types of cinnamon.

Based on the results in the Tab 5.1 and in the graphic of the Fig 5.2 for cinnamon, it seems that the highest yield is obtained from Indonesian cinnamon, followed by Indian cinnamon and Chinese cinnamon. These values indicate the proportion of essential oil obtained compared to the dry weight of the bark mass used in the steam distillation process.

Comparing the ginger oil yield to the cinnamon oil yields, we can observe that the yield of ginger oil is lower than that of cinnamon oil. This suggests that the steam distillation of Algerian ginger resulted in a lower extraction efficiency compared to the steam distillation of cinnamon.

It's worth noting that the yield can be influenced by various factors such as the quality and variety of the plant material, the extraction technique, and the conditions during distillation. These factors can vary between different plant species and regions, which might explain the variation in the oil yields between the different types of cinnamon and ginger in this case.

5.3. Characteristics of essential oil

5.3.1. Organoleptic properties

Tab.5.2 The Organoleptic properties of ginger and cinnamon essential oils

	Ginger	Cinnamon	standards
Taste	Spicy and sweet.	Spicy, pungent, hot, and biting	AFNOR
Textur	Mobile and mildly viscous liquid	Mobile and mildly viscous liquid	AFNOR
Color	Golden Yellow	Pale yellow	AFNOR
Aroma	Good smell and woody	Penetrating.	AFNOR

These organoleptic properties play a significant role in the culinary and aromatic applications of cinnamon and ginger. They contribute to the overall sensory experience when these ingredients are used in cooking, baking, or in the production of various products such as perfumes, soaps, and aromatherapy oils.

5.3.2. Physico-chemical properties of essential oil

5.3.3.1. Relative density

Relative density, also known as specific gravity, is a measure of the density of a substance relative to the density of a reference substance.

Tab.5.3 Relative density of ginger and cinnamon essential oils.

Sample type	Relative density	Standars
Algerian ginger	0.85	0,842 à 0,894[156]
Indonesian cinnamon	1.07	1,052 à 1,070[157]
Chinese cinnamon	1.06	1,052 à 1,070[157]
Indian cinnamon	1.05	1,052 à 1,070[157]

Based on the values of the Tab 5.3, we can observe that the relative densities of cinnamon essential oils are slightly higher than 1, indicating that they are denser than water. On the other hand, the relative density of Algerian ginger essential oil is lower than 1, indicating that it is less dense than water [156] [157].

Relative density can provide information about the concentration or purity of a substance.

5.3.3.2. pH value

pH is a measure of the acidity or alkalinity of a solution. It is determined on a scale from 0 to 14, where pH 7 is considered neutral, values below 7 are acidic, and values above 7 are alkaline or basic.

Tab.5.4. pH value of ginger and cinnamon essential oils.

Sample type	Ph
Indian cinnamon	5.5
Chinese cinnamon	6.2
Indonesian cinnamon	5.4
Algerian ginger	5.8
mixteur of ginger and cinnamon	5.3

Based on the pH values, it appears that all the samples, including the individual cinnamon and ginger samples and the mixture of ginger and cinnamon, have a slightly acidic pH of 5 or 6. This suggests that these samples are slightly acidic in nature.

It's important to note that pH can influence the stability, functionality, and sensory characteristics of substances. For instance, a specific pH range might be optimal for certain applications such as drug formulations or cosmetic formulations [158].

5.3.3.3. Acid value (neutralization number)

The results of acid value are shown in Tab 5.5 and in Fig 5.3,5.4:

Tab.5.5 Acid value of cinnamon and ginger essential oil.

Sample types	Volume	AV	stadars
Algarian Ginger EO	1.1 ml	62.15 mgKOH/g	68,44[159]
Indonesian Cinnamon EO	0.27 ml	15.26 mgKOH/g	<20 [160]
Chinese Cinnamon EO	0.26 ml	14.7 mgKOH/g	<20 [160]
Indian Cinnamon EO	0.28 ml	15.82 mgKOH/g	<20 [160]

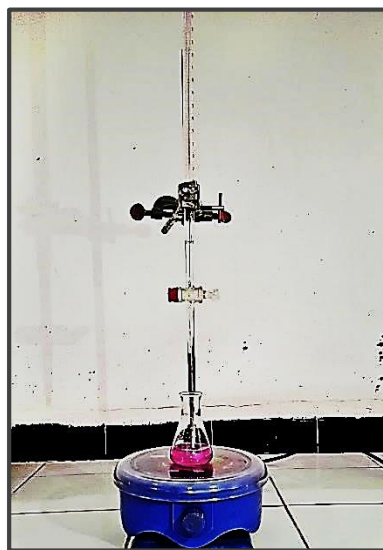


Fig.5.3 Acid value results.

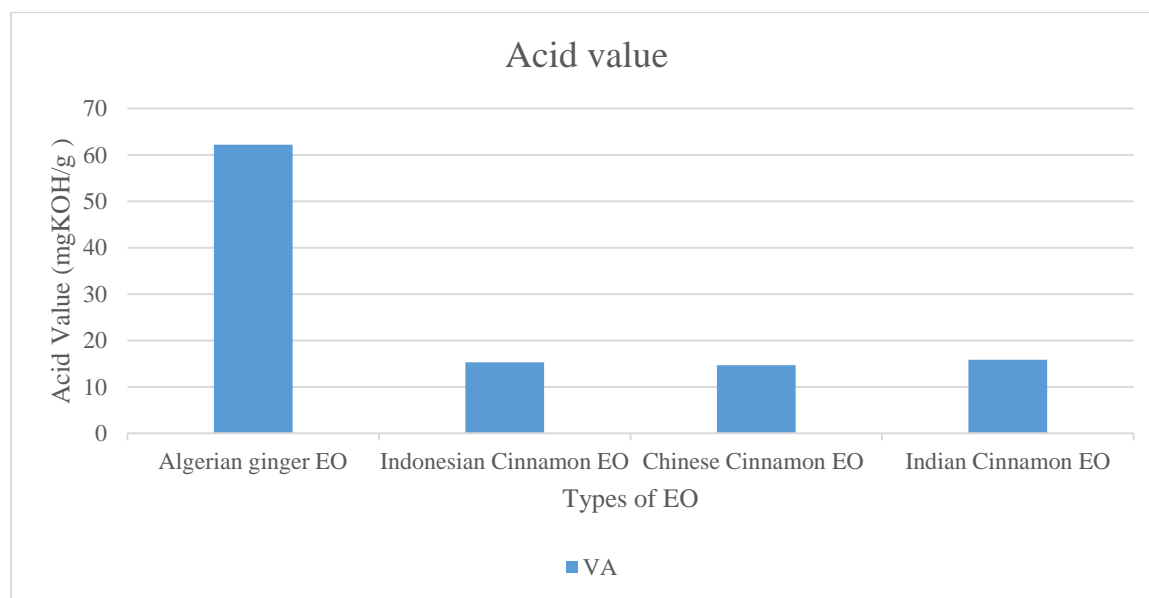


Fig.5.4 Variation in acid value according to the types of EO.

The obtained acid index results are 62.15 / 15.26 , 14.7 and 15.82 mgKOH/g for ginger/ Indonesian cinnamon, Chinese cinnamon and indian cinnamon, respectively, and they comply with the standards. This acid index indicates the behavior and quantity of free acids present in our oil, providing information about the quality and susceptibility of essential oils to undergo alterations.

Indeed, a higher acid index corresponds to lower quality of essential oils as it represents the total concentration of free fatty acids present. This acidity is influenced by microorganisms, their enzymes, and the water content found in the oil [161]. According to our results, the Indian cinnamon essential oil exhibits a higher acid index compared to Indonesian and Chinese cinnamon essential oil. The Algerian ginger essential oil has a lower acid index compared to Chinese ginger. This shows that our essential oil has a good storage quality.

5.3.3.4. Ester value

The results of ester value are shown in Tab 5.6 and in Fig 5.5, 5.6 :

Tab.5.6 Ester value of ginger and cinnamon EO

Sample types	Volume	EV	standars
Blank sample	20.7ml	/	/
Algerian Ginger EO	21.25 ml	92.07mgKOH/g	99,86[159]
Indonesian Cinnamon EO	20.9 ml	40.82mgKOH/g	20.14 [162]
Chinese Cinnamon EO	20.9 ml	41.38mgKOH/g	20.14 [162]
Indian Cinnamon EO	20.9 ml	40.26mgKOH/g	20.14 [162]

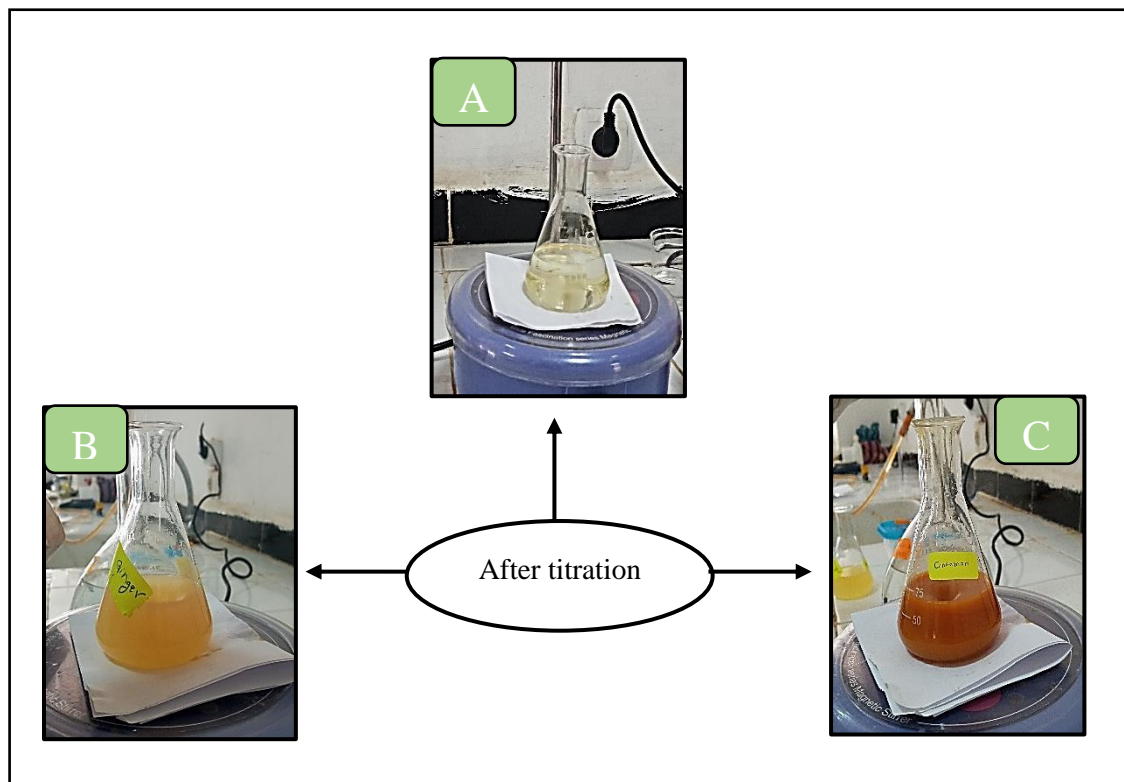


Fig.5.5 Ester value for titration of the blank and for titration of the essential oils.

Where:

A : Blank sample without essential oil.

B : Sample with Ginger essential oil.

C: Sample with Cinnamon essential oil.

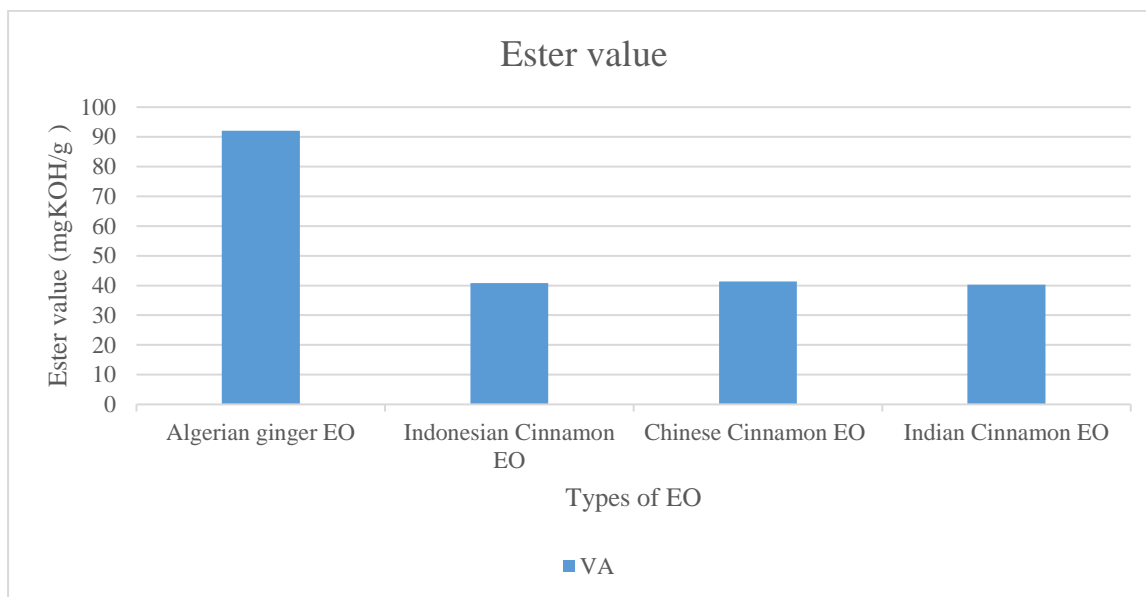


Fig.5.6 Variation in ester value according to the types of EO.

The obtained result shows that ester index, measured at a temperature of 23 °C, is higher compared to the maximum value specified in the pharmacopoeia standard, which are 99,86 ; 20.14 mgKOH/g. This indicates that studied EO is rich in esters. The ester index values suggest that all oils contain a certain amount of free acid [163].

This result suggests a high proportion of fatty acids combined in the form of triglycerides.

5.3.3.6. Saponification value

The results of saponification value are shown in Tab 5.7 and in Fig 5.7 :

Tab.5.7 Saponification value of ginger and cinnamon EO

Sample types	SV(mgKOH/g)	stadars
Algarian Ginger EO	154.22	168,3 [159]
Indonesian Cinnamon EO	56.08	33.6 [164]
Chinese Cinnamon EO	56.08	33.6 [164]
Indian Cinnamon EO	56.08	33.6 [164]

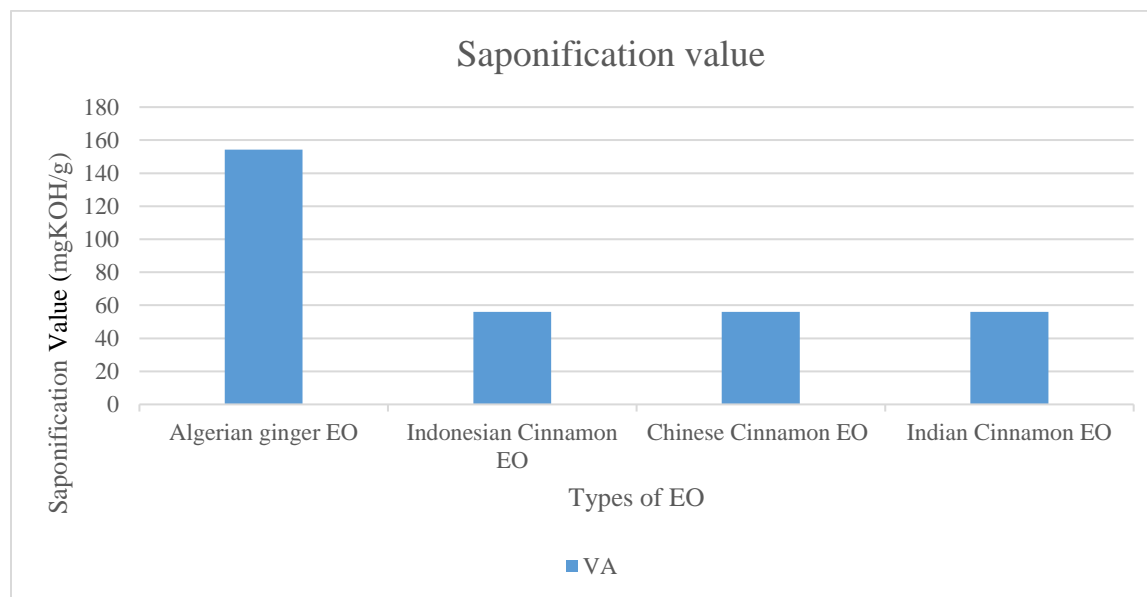


Fig.5.7 Variation in saponification value according to the types of EO.

The determination of saponification indices for oils yielded the values presented in Tab 5.7, which show that Algerian ginger has a higher saponification index (SI) of 154.22 mgKOH/g compared to cinnamon, which has an SI of 56.08 mgKOH/g. The saponification index is a test that indicates the quantity of fatty acids and provides information about the chain length of the fatty acids present in the analyzed oil. The higher the saponification index, the lower the fatty acid chain length. It reflects the average weight of the fat and is inversely proportional to it. The higher the molecular weight, the lower the saponification index [165]. This indicates that the EO could be used in soap making since its saponification value is high.

5.3.4. Biochemical activity

5.3.4.1. Flavonoids test

The quantitative study of aqueous extracts using spectrophotometric assays, according to the aluminum trichloride ($AlCl_3$) method, aimed at determining the total content of flavonoids. A calibration curve (Fig 5.8) was plotted for this purpose, established with quercetin at different concentrations. Density measurements were taken at 418 nm. The corresponding quantities of

flavonoids were reported in milligram equivalents of quercetin per gram of extract (HE) and determined using the equation of the form: $y = ax + b$.

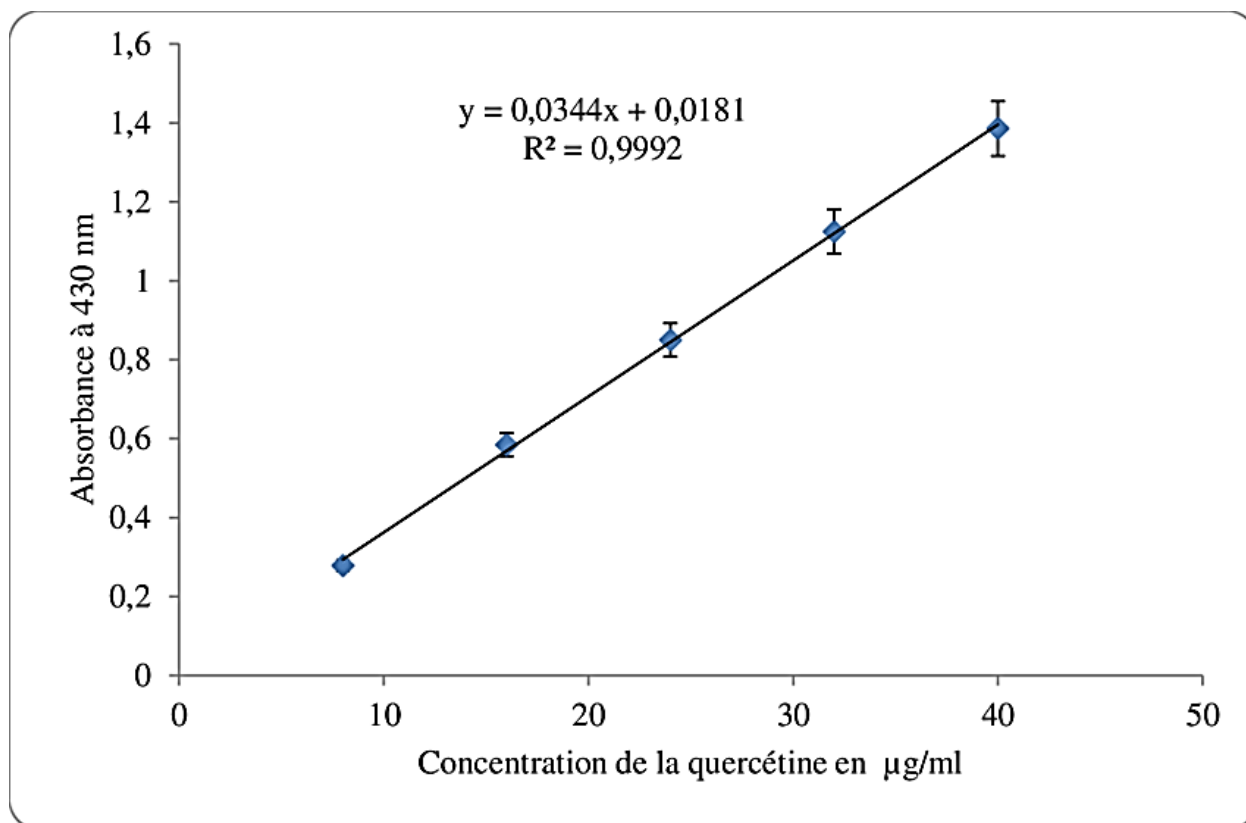


Fig.5.8 Calibration Curve of Flavonoids

Tab.5.8 Quantification of flavonoids in the hydrodistillation extract.

Sample types	Extraction method	Absorbance (Abs)	Concentration $\mu\text{g/ml}$
Algerian ginger	hydrodistillation extract	0.134	3.36
Indonesian Cinnamon		0.161	4.15

The dosage results indicate the presence of flavonoids in both extracts, but the concentration of EO of Algerian ginger is lower than that of EO of Indonesian Cinnamon. Absorbance is proportional to concentration. The properties of flavonoids are extensively studied in the medical field, where they are recognized for their antiviral, antioxidant, antiallergic, antitumor, anti-inflammatory, and anticancer activities [166].

5.3.4.2. Antioxidant activity

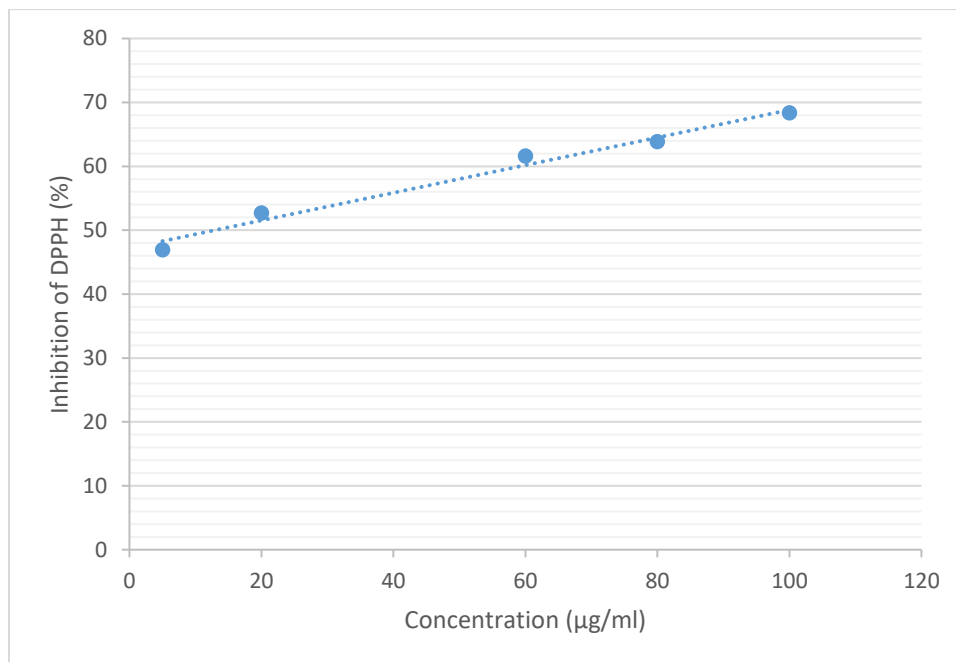


Fig.5.9 Percentage inhibition of cinnamon essential oil by DPPH test.

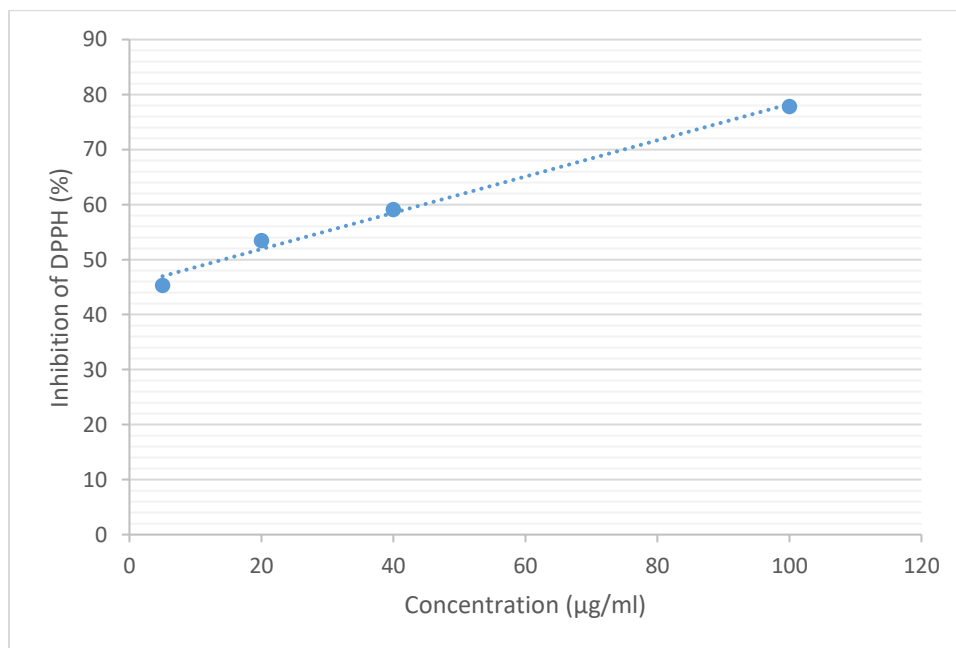


Fig.5.10 Percentage inhibition of ginger essential oil by DPPH test.

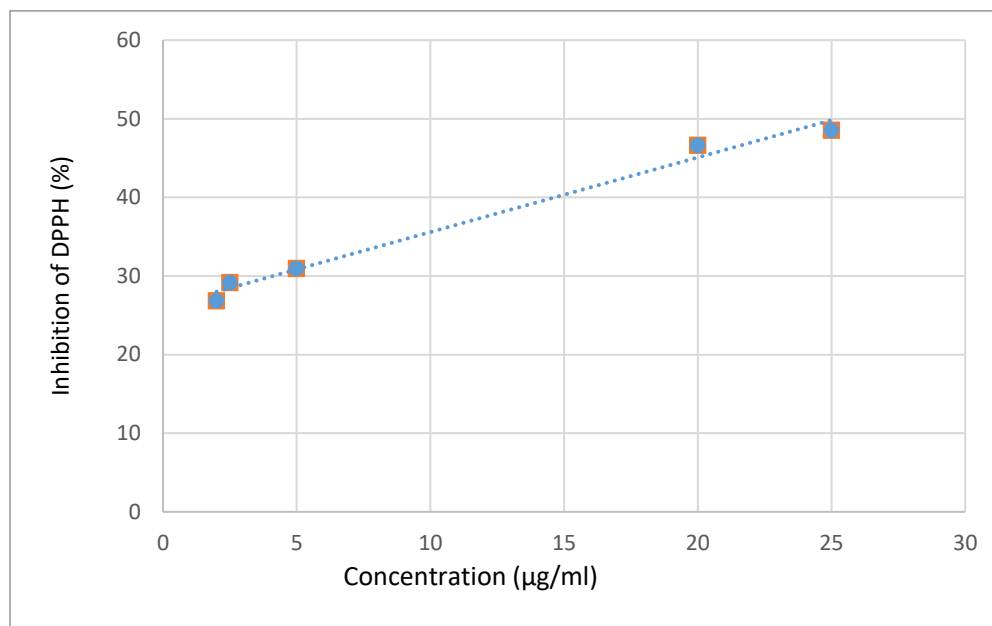


Fig.5.11 Percentage inhibition of ascorbic acid by DPPH test.

Tab.5.9 Linear regression equations obtained for antioxidant activity of cinnamon and ginger

	Regression equation	Linearity (r ²)	IC 50(µg/ml)
Cinnamon EO	$y = 0,2162x + 47,204$	$R^2 = 0,9808$	12,9324
Ginger EO	$y = 0,3296x + 45,32$	$R^2 = 0,9902$	14,1990
Ascorbic acid	$y = 0,9496x + 26,096$	$R^2 = 0,9864$	25,1727

The IC 50 value is a measure of the antioxidant activity of a substance. It represents the concentration of the substance required to inhibit 50% of a specific biological or chemical activity [167]. In this case, the IC 50 values are being used to compare the antioxidant activity of cinnamon, ginger, and ascorbic acid. Based on the given IC 50 values showed in the Tab 5.9.

The IC 50 value of cinnamon is 12,9324 µg/ml. This means that cinnamon requires a concentration of approximately 12,9324 µg/ml to inhibit 50% of the tested activity. A lower IC 50 value indicates higher antioxidant activity. Therefore, cinnamon has a stronger antioxidant activity compared to both ginger and ascorbic acid. Where the IC 50 value of ginger is 14,1990 µg/ml. This suggests that ginger requires a concentration of approximately 14,1990 µg/ml to inhibit 50% of the tested

activity. Although ginger has a higher IC 50 value compared to cinnamon, it still indicates a significant level of antioxidant activity. However, ginger's antioxidant activity is slightly lower than that of cinnamon.

Ascorbic acid, also known as vitamin C, is a well-known antioxidant. However, in this comparison, ascorbic acid has the highest IC 50 value among the three substances [168]. This indicates that it requires a higher concentration, approximately 25,1727 $\mu\text{g/ml}$, to inhibit 50% of the tested activity compared to both cinnamon and ginger. While ascorbic acid still possesses antioxidant activity, the given data suggests that cinnamon and ginger have stronger antioxidant properties in this particular assay.

5.3.5. Antibacterial activity

The antibacterial activity of essential oils (ginger and cinnamon) is evaluated using the diffusion technique, also known as the aromatogram method. The results are presented in (Tab 5.12), (Tab5.10) and (Fig 5.13),(Fig 5.14).

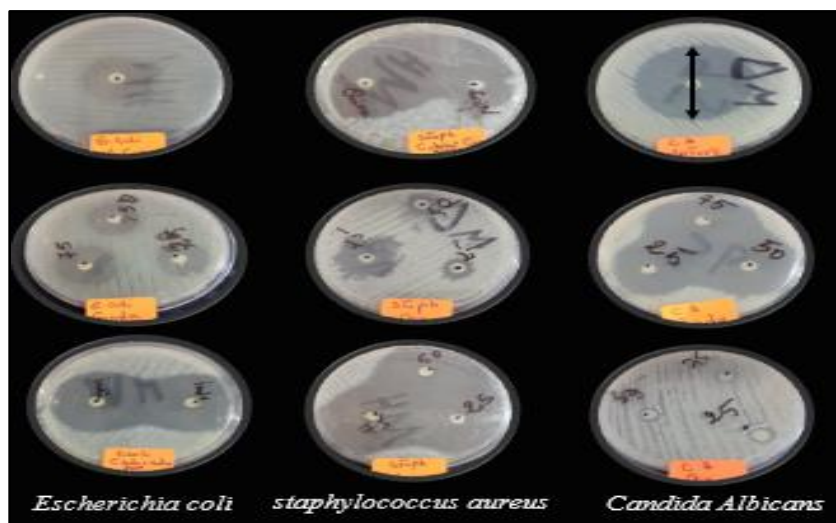
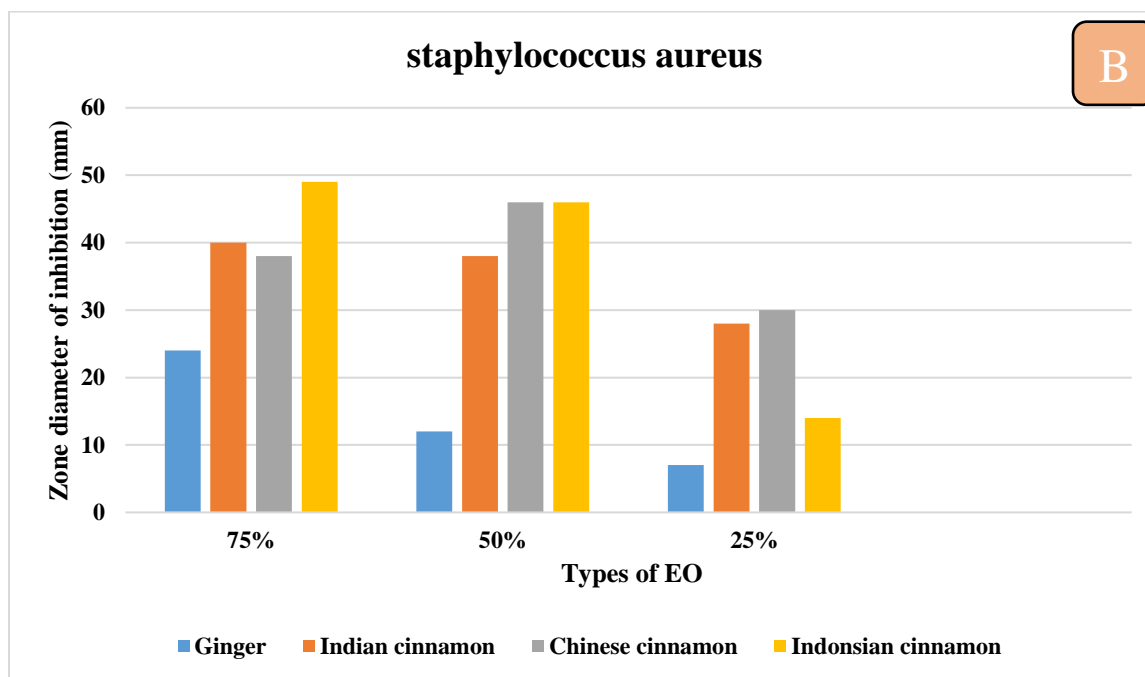
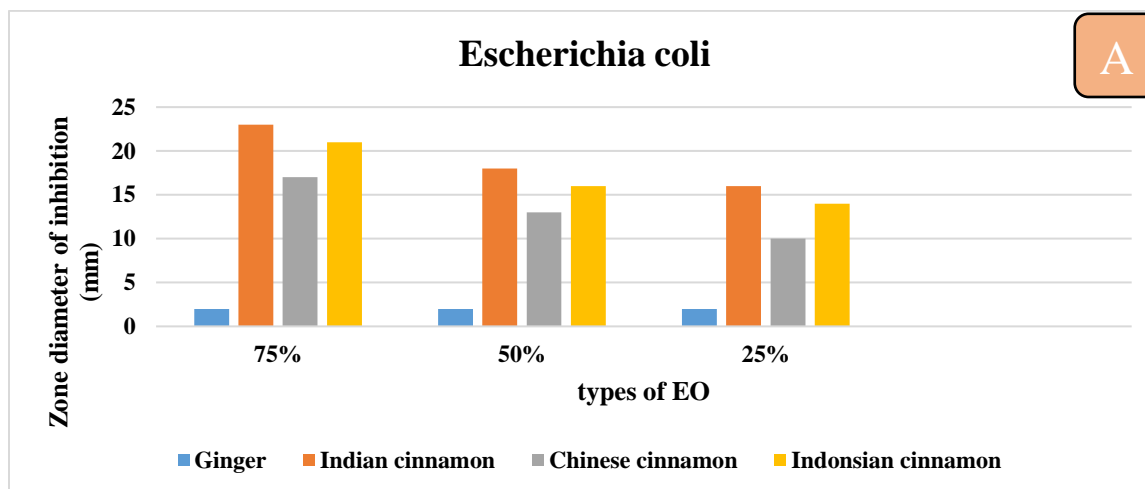


Fig.5.12 Zones of inhibition results of each strain.

Tab.5.10 Antibacterial activity result for essential oil of Ginger and Cinnamon

Strain	concentration	Zone diameter of inhibition (mm)					mixte	DMSO
		Ginger	Cinnamon					
			Indonsian	India	Chaina			
<i>Escherichia coli</i>	100%	2 mm	19 mm	20mm	23 mm	22 mm	0 mm	
	75%	2 mm	21 mm	23 mm	17 mm			
	50%	2 mm	16 mm	18 mm	13 mm			
	25%	2 mm	14 mm	16 mm	10 mm			
<i>staphylococcus aureus</i>	100%	25 mm	34 mm	41 mm	40 mm	38 mm	0 mm	
	75%	24 mm	49 mm	40 mm	38 mm			
	50%	12 mm	46 mm	38 mm	46 mm			
	25%	7 mm	35 mm	28 mm	30 mm			
<i>Candida Albicans</i>	100%	6 mm	41 mm	42 mm	40 mm	44 mm	0 mm	
	75%	2 mm	40 mm	49 mm	50 mm			
	50%	2 mm	34 mm	40 mm	46 mm			
	25%	2 mm	30 mm	38 mm	32 mm			



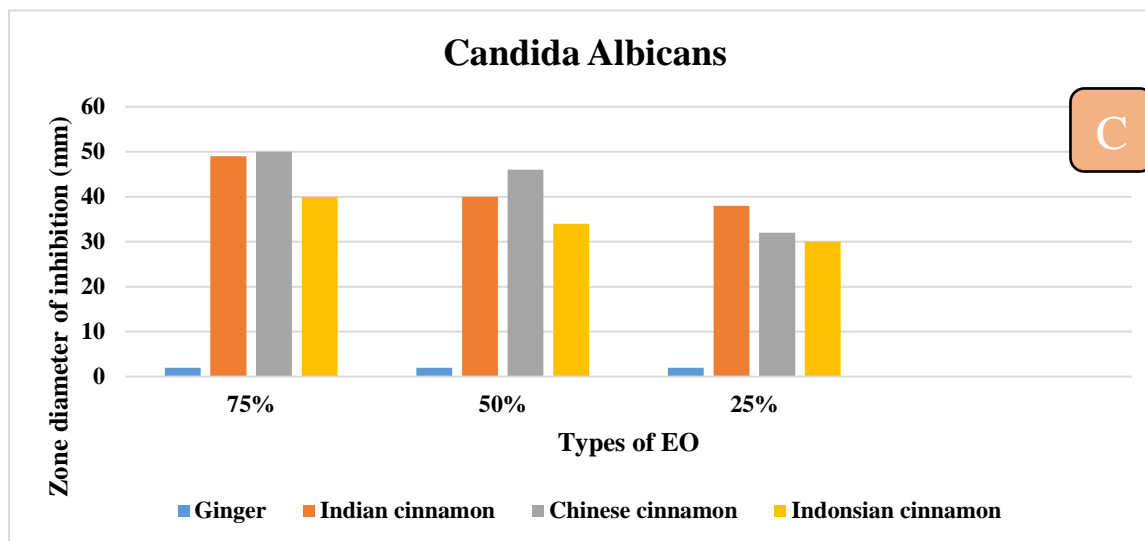


Fig.5.13 Variation in zone diametre of inhibition according to the type of dilute oil and type of strain.

Where :

A : *Escherichia coli*.

B: *staphylococcus aureus*.

C: *Candida Albicans*.

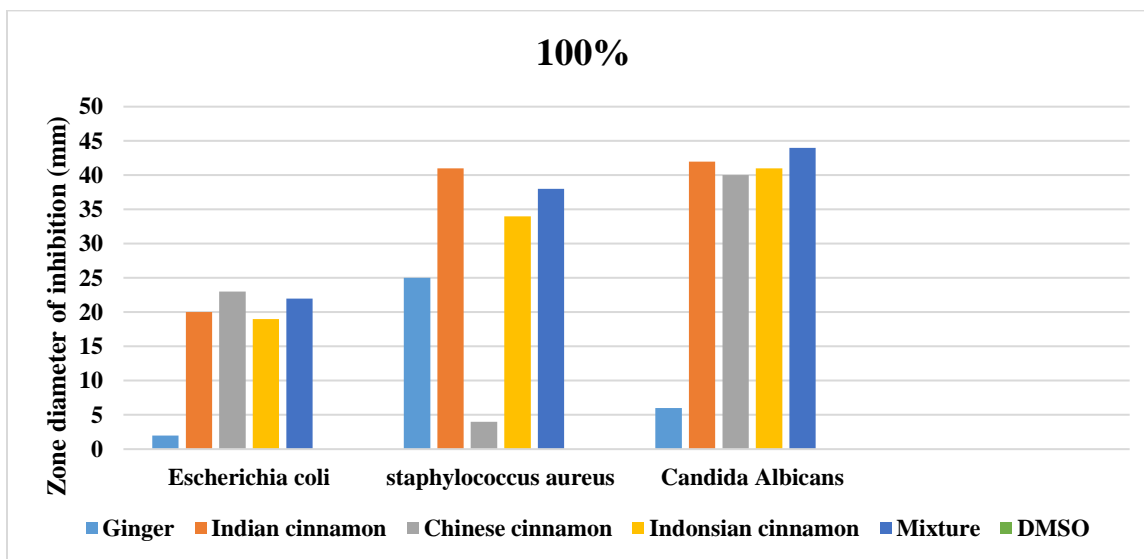


Fig.5.14 Variation in zone diametre of inhibition according to the type of oil (100%) and type of strain

Tab.5.11 % inhibition result for essential oil of Ginger and Cinnamon

Strain	concentration	% inhibition					mixte	DMSO
		Ginger	Cinnamon					
			Indonsian	India	Chaina			
<i>Escherichia coli</i>	100%	2.22	21.11	22.22	25.55	24.44	0	
	75%	2.22	23.33	25.55	18.88			
	50%	2.22	17.77	22.22	14.44			
	25%	2.22	15.55	17.77	11.11			
<i>staphylococcus aureus</i>	100%	27.77	37.77	45.55	44.44	42.22	0	
	75%	26.66	54.44	44.44	42.22			
	50%	13.33	51.11	42.22	51.11			
	25%	7.77	38.88	31.11	33.33			
<i>Candida Albicans</i>	100%	6.66	45.55	46.66	44.44	48.88	0	
	75%	2.22	44.44	54.44	55.55			
	50%	2.22	37.77	44.44	51.11			
	25%	2.22	33.33	42.22	35.55			

Fig.5.15 Variation in zone diametre of inhibition according to the type of extract.

A classification of essential oils in relation to their antimicrobial activity spectrum can be established based on the size of the inhibition zone [169] [170].

Tab.5.12 Estimation of the antibacterial activity of EO and various CE.

Strain	concentration	classification of essential oils					
		Ginger	Cinnamon			Mixte	DMSO
			Indonsian	India	Chaina		
<i>Escherichia coli</i>	100%	-	++	++	++	++	-
	75%	-	++	++	++		
	50%	-	++	++	+		
	25%	-	+	++	+		
<i>staphylococcus aureus</i>	100%	++	+++	+++	+++	+++	-
	75%	++	+++	+++	+++		
	50%	+	+++	+++	+++		
	25%	-	+++	++	+++		
<i>Candida Albicans</i>	100%	-	+++	+++	+++	+++	-
	75%	-	+++	+++	+++	+++	
	50%	-	+++	+++	+++		
	25%	-	+++	+++	+++		

Based on the results ,we obseved that the essential oil of Cinnamon has very good antibacterial activity (where we can see a variation in the zone diameter of inhibition of which prevented the growth all of strains tested) compared to the essential oil of Ginger We also observed that staphylococcus aureus and Candida Albicans were the most senistive strains among the tested strains .

The mixture had a good antibacterial activity on E.coli, Staphylococcus aureus and Cabdida albicans was dominated by the antibacterial activity of Cinnamon .

DMSO , it had no antibacterial activity.

Ginger essential oil has demonstrated antibacterial activity specifically against Staphylococcus aureus, with an inhibition rate of 27.77% (25mm). However, its effectiveness against other strains

of bacteria was negligible, as the inhibition zones were consistently less than 10 cm across different concentrations tested .

As for the cinnamon essential oil it showed antibacterial activity on all strains. We noticed that at a concentration of 100% (pure oil), Chinese cinnamon recorded the highest inhibition value for E.coli and Staphylococcus aureus by 25.55% (25 mm), followed by Indian cinnamon, then Indonesian cinnamon. for dilute concentrations , the inhibition value decreased to 19 mm.

In contrast, Chinese cinnamon (dilute concentrations) showed greater activity on Candida albicans with an estimated inhibition rate of 55.55. At a concentration of 100, Indian cinnamon had a slightly greater effect than Chinese and Indonesian cinnamon.

It can explain the results of antibacterial for defferent concentration;

For ginger ,the antibacterial activity of ginger essential oil against Staphylococcus aureus can be attributed to its chemical composition. Ginger essential oil contains various bioactive compounds, including gingerols, shogaols, and zingerone, which are known for their antimicrobial properties [171].

These compounds have been shown to have antibacterial effects against a range of bacteria, including Staphylococcus aureus. They can interfere with the bacterial cell membrane, inhibit the synthesis of bacterial proteins, and disrupt essential enzymatic processes, leading to the inhibition of bacterial growth and viability.

Additionally, ginger essential oil possesses other properties that contribute to its antibacterial activity. It has antioxidant and anti-inflammatory properties, which can support the body's immune response and help combat bacterial infections. Gingerols, specifically, have been found to have immunomodulatory effects, which can further enhance the antibacterial activity against Staphylococcus aureus [171].

For Cinnamon ; Cinnamon essential oil contains several bioactive compounds, such as cinnamaldehyde and eugenol, which contribute to its antibacterial activity against Staphylococcus aureus, E. coli, and Candida albicans.

Cinnamaldehyde: This is the main component of cinnamon essential oil and has been found to possess strong antimicrobial properties. It can inhibit the growth and proliferation of various bacteria, including *Staphylococcus aureus* and *E. coli*, as well as *Candida albicans*.

Eugenol: Another significant compound found in cinnamon essential oil, eugenol, has been reported to exhibit broad-spectrum antibacterial and antifungal activity. It can effectively inhibit the growth of *Staphylococcus aureus*, *E. coli*, and *Candida albicans*.

These compounds work by disrupting the cellular membranes and metabolic processes of the microorganisms, ultimately leading to their inhibition or death [172].

It's important to note that the effectiveness essential oil may vary depending on factors such as;


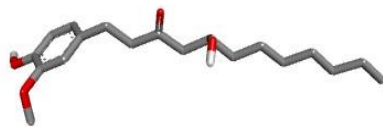

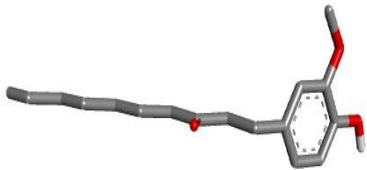
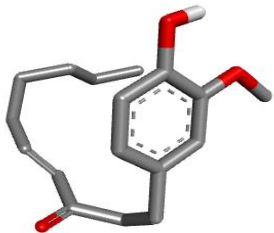
- The composition and solubility of the essential oil.
- The microorganism and the speed of its growth .


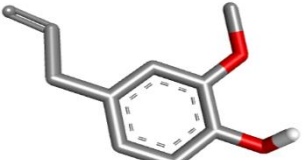
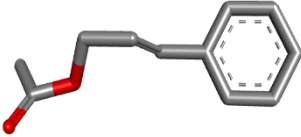
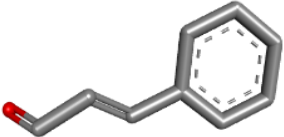
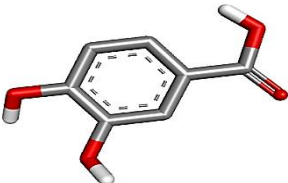
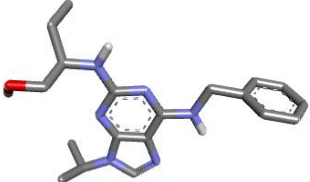
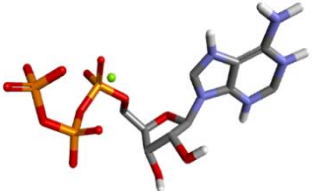
5.4. In Silico anti-cancer study

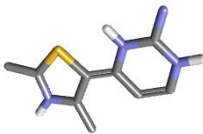
5.4.1. Molecular docking:

The results of in silico study of the essential oil of ginger and cinnamon using molecular docking with autodock tools autodock vina pymol and discovery studio are presented in the Tab (5.13), (5.14) preceded by a presentation of the ligands and targets used in this study.


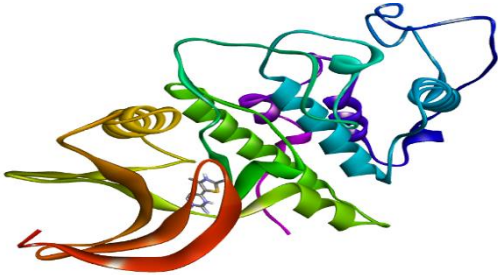
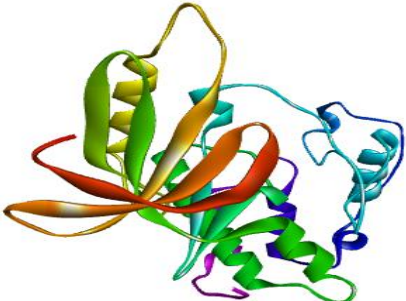
Tab.5.13 Presentation of ligands

Ligands	Formula	IUPAC	PDBQT format 3D
<i>Ginger</i>			
6-Gingerol (PubChem ID : 442793)	C ₁₇ H ₂₆ O ₄	(5S)-5-hydroxy-1-(4hydroxy-3-methoxyphenyl)decan-3-one	
8-Gingerol (PubChem ID : 168114)	(PubChem ID : 168114) C ₁₉ H ₃₀ O ₄	5S)-5-hydroxy-1-(4-hydroxy-3methoxyphenyl)dodecan-3 -one	
10-Gingerol (PubChem ID : 168115)	C ₂₁ H ₃₄ O ₄	(5S)-5-hydroxy-1-(4hydroxy-3methoxyphenyl)tetradecan-3-one	
6-Paradol (PubChem ID : 94378)	C ₁₇ H ₂₆ O ₃	1-(4-hydroxy-3methoxyphenyl)decan-3one	
6-Shogaol (PubChem ID : 5281794)	C ₁₇ H ₂₄ O ₃	(E)-1-(4-hydroxy-3methoxyphenyl)dec-4-en-3-one	
<i>Cinnamon</i>			

Cuminaldehyde (PubChem ID : 326)	C ₁₀ H ₁₂ O	4-propan-2-ylbenzaldehyde	
Eugenol (PubChem ID : 3314)	C ₁₀ H ₁₂ O ₂	2-methoxy-4-prop-2-enylphenol	
(E)-cinnamyl acetate (PubChem ID : 5282110)	C ₁₁ H ₁₂ O ₂	[(E)-3-phenylprop-2-enyl] acetate	
TransCinnamaldehyde (PubChem ID : 637511)	C ₉ H ₈ O	(E)-3-phenylprop-2-enal	
Protocatechuic Acid (PubChem ID : 72)	C ₇ H ₆ O ₄	3,4-dihydroxybenzoic acid	
Witness			
Roscovitine (PubChem ID: 160355)	C ₁₉ H ₂₆ N ₆ O	(2R)-2-[[6-(benzylamino)-9-propan-2-yl]purin-2-yl]amino]butan-1-ol	
Ligand			
Ligand of PDB	C ₂₃ H ₁₈ NO ₂ S	4-[[6-(3-phenylphenyl)-7~H-purin-2-yl]amino]benzenesulfonamide	

Ligand of Swiss model	C ₉ H ₁₆ N ₄ S ₁	(4Z)-4-(2,4-dimethyl-1,3-thiazolidin-5-ylidene)-1,2,3,4-tetrahydropyrimidin-2-amine	
------------------------------	--	---	---

Tab.5.14 Presentation of Targets

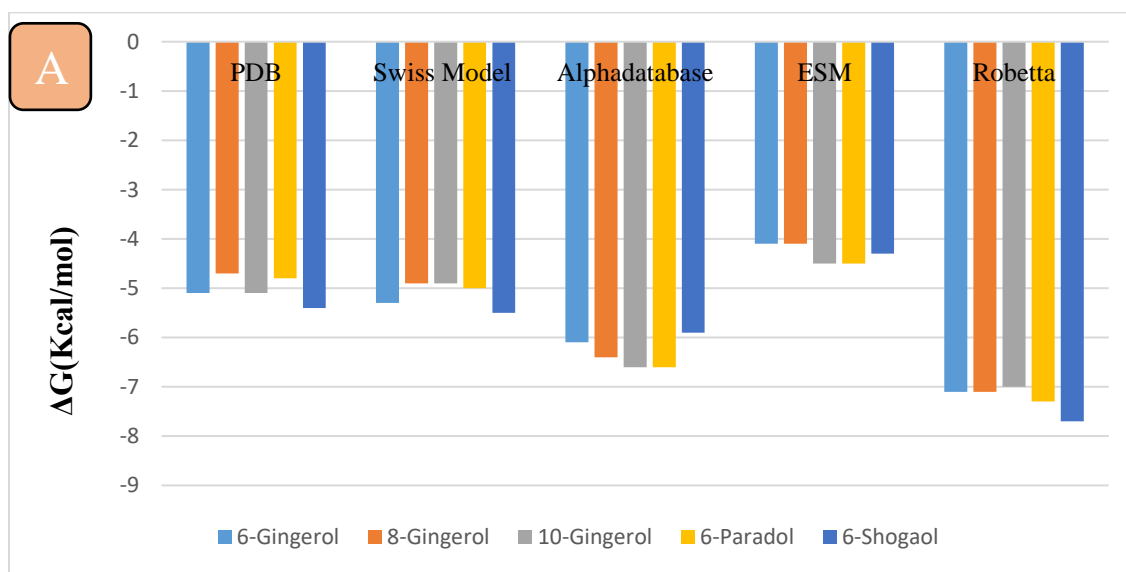
Target	PDBQT
PDB	
Modeling	
SWISS MODEL	
ALPHA FOLD	



Tab.5.15 Molecular docking binding affinity of ginger and cinnamon compounds, ranked free energy of binding (ΔG) and inhibition constant (K_i)

C o d e		PDB		SWISS		ALPHA		ESM		ROBETTA	
		ΔG (Kcal/ mol)	K_i (nM)	ΔG (Kcal/ mol)	K_i (nM)	ΔG (Kcal/ mol)	K_i (nM)	ΔG (Kcal/ mol)	K_i (nM)	ΔG (Kcal/ mol)	K_i (nM)
<i>Ginger</i>											
S1	6-Gingerol	-5.1	5503	-5.3	7714	-6.1	29788	-4.1	1016	-7.1	161246
S2	8-Gingerol	-4.7	3925	-4.9	3925	-6.4	49440	-4.1	1016	-7.1	161246
S3	10-Gingerol	-5.1	5503	-4.9	3925	-6.6	69305	-4.5	1997	-7.0	136190
S4	6-Paradol	-4.8	3316	-5.0	4648	-6.6	6935	-4.5	1997	-7.3	226037
S5	6-Shogaol	-5.4	9133	-5.5	10813	-5.9	21249	-4.3	1425	-7.7	444182
<i>Cinnamon</i>											
S6	Cuminaldehyd	-5.1	5648	-5.2	6691	-6.4	2.33	-3.4	317	-6.8	100593
S7	Eugenol	-5.0	4768	-4.8	3398	-5.9	21249	-3.5	375	-6.0	25943
S8	(E)-cinnamyl acetate	-5.2	6691	-5.0	4768	-6.0	25943	-3.5	375	-6.8	100593

S9	trans-Cinnamaldehyde	-4.5	2044	-4.7	2868	-5.7	15607	-3.1	190	-6.0	25943
S10	Protocatechuic Acid	-5.7	15607	-5.2	6691	-5.6	13176	-3.3	267	-6.2	36405
Witness											
W	Roscovitine	-5.9	21250	-6.2	35268	-7.8	525903	-5.0	4648	-8.1	872852
Ligands											
L1	Ligand of pdb	-2.9	133	/	/	/	/	/	/	/	/
L2	Ligand of swiss model	/	/	-4.8	3315	/	/	/	/	/	/



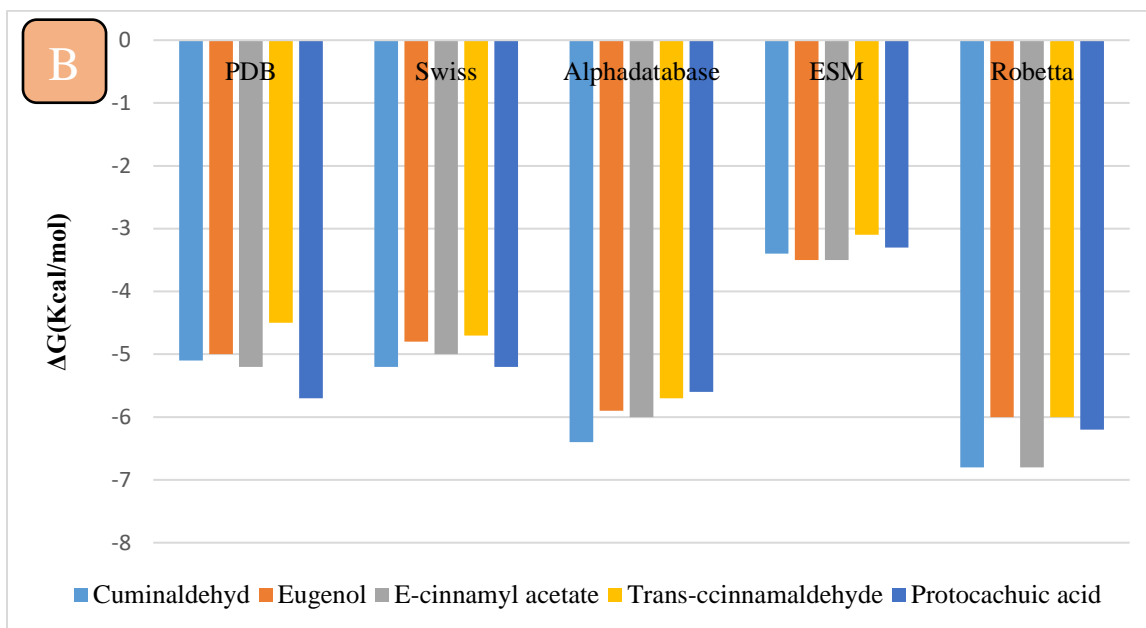


Fig.5.16 Molecular docking binding affinity of ginger[A] and cinnamon[B] compounds

Tab.5.16 parameters of the grids box

	Grid center (x y z)	npts	spacing
PDB	1.523 30.136 21.495	40 40 40	0.375
Swiss model	3.562 46.389 -11.106	40 40 40	0.375
Alpha fold	-0.754 0.619 1.070	40 40 40	0.375
Ems	0.437 -20.985 19.785	40 40 40	0.375
robetta	-0.754 0.619 1.070	40 40 40	0.375

Docking was carried out using Autodock version 4.2 software. The artemisinin compounds were docked to realize the smallest binding energy using AutoDock vina calculation method, on grid box x, y, and z showed in the Tab 5.15. From the re-docking results, the RMSD value have to be < 2 and is illustrated by the overlay structure between the natural ligands and re-docking results. According to the docking procedure, the elimination of water molecules surrounding the clusters of compounds and receptors is conducted first to prevent water-mediated interactions that can increase entropy and decrease free energy, ultimately stabilizing the drug-receptor complex. This procedure also facilitates the formation of hydrogen bonds crucial for compound-receptor interactions. Analyzing the docking results of ginger and cinnamon compounds against cyclin-dependent kinase CDK2 in Tab 5.16, adherence to the rules indicates that compounds

demonstrating lower binding free energy (ΔG) exhibit stronger and more stable interactions with CDK2, suggesting their potential as effective drug-receptor interactions.

However, in this case, we consider the CDK2 downloaded from PDB as a reference because it is the closest example to the actual enzyme in the human body, whereas the others are merely predictions. Based on the results shown in the Tab5.15, it appears that the predictions of Swiss-Model for the CDK2 enzyme are similar to the results obtained from the CDK2 enzyme downloaded from PDB. While it can be seen that Protocatechuic Acid (cinnamon) and 6-Shogaol (ginger) have a lower binding free energy (ΔG) with CDK2 from both PDB and Swiss-Model compared to the other compounds. Therefore, both of them can be expected to have activity as an anticancer candidate. If the free energy binding was lower, it means the drug-receptor interaction was better and more stable. In addition to the free energy binding value, in Tab 5.16 the value of the constant of inhibition (K_i) can also be seen. The enzyme inhibition constant (K_i), also known as the inhibitor dissociation constant, is an equilibrium constant of a reversible inhibitor for complexation with its target enzyme. Unless otherwise specified, all inhibitors described hereafter are reversible inhibitors. K_i is associated with thermodynamic parameters in $\Delta G = -RT \ln(K_i)$, where ΔG , R , and T are the absolute binding free energy, the gas constant, and the absolute temperature, respectively. From the reaction equilibrium among the receptor and the compound, the lesser the K_i value the more the reaction equilibrium leans to favor the formation of receptor–compound complexes [137].

5.4.1.1. Protein data bank:

The interactions between the target CDK2 from PDB and ligands of cinnamon and ginger compounds are shown in the Fig 5.18, 5.19, 5.20, 5.21, 5.22 and the Tab 5.17.

Tab.5.17 Interaction details of the target enzyme CDK2 (CDK2 from PDB)

Compounds	Receptor pocket	Interactions Category	Distance (Å)	Witness	Ligand PDB	Hot spot of CDK2
		<i>Ginger</i>				
6-Gingerol	GLU 113	Conventional Hydrogen Bond	2,07	THR218 VAL251	LYS33 LYS129	I10 V18
	ALA 282	Conventional Hydrogen Bond	3,07	THR198 ARG214	MG382 THR14	E81 L83
	LEU 281	Alkyl	3,67	LYS250 ARG200	ASN132 GLU81	H84 Q85
	ALA 116	Alkyl	4,08	PRO253	ASP86	K89
	LYS 278	Alkyl	4,44		LEU83	L134
	ALA 116	Pi-Alkyl	4,08		ATP381	D145
	LEU 281	Pi-Alkyl	5,45		TYR15	
	PHE 109	Pi-Alkyl	4,62			
8-Gingerol	ARG 126	Conventional Hydrogen Bond	2,35			
	VAL 154	Conventional Hydrogen Bond	2,33			
	ARG 126	Carbon Hydrogen Bond	3,78			
	LEU 124	Alkyl	5,26			
	LEU 124	Alkyl	4,10			
	TYR 180	Pi-Alkyl	4,24			
	TYR 180	Pi-Alkyl	5,21			
	ARG 150	Pi-Alkyl	5,25			
10-Gingerol	THR 198	Conventional Hydrogen Bond	2,08			
	ARG 214	Conventional Hydrogen Bond	2,17			
	VAL 251	Carbon Hydrogen Bond	3,71			
	LYS 250	Alkyl	4,74			
	VAL 251	Alkyl	5,15			
	VAL 251	Alkyl	3,94			
	LEU 202	Alkyl	4,29			
	ARG 200	Pi-Alkyl	4,96			

6-Paradol	LYS 250	Conventional Hydrogen Bond	2,10
	VAL 251	Carbon Hydrogen Bond	3,48
	ARG 214	Alkyl	3,72
	ARG 217	Alkyl	4,84
	VAL 251	Pi-Alkyl	4,68
6-Shogaol	LYS250	Conventional Hydrogen Bond	2,28
	ALA201	Conventional Hydrogen Bond	2,93
	VAL251	Carbon Hydrogen Bond	3,59
	ARG214	Alkyl	4,16
	ARG217	Alkyl	4,45
	VAL251	Pi-Alkyl	4,66
<i>Cinnamon</i>			
Cuminaldehyde	ASP 86	Carbon Hydrogen bond	3.65
	ILE 10	Pi-Sigma	3.99
(E)-cinnamyl acetate	ASN 62	Conventional hydrogen bond	2.45
	VAL 289	Pi-Alkyl	5.15
	LYS 291	Pi-Alkyl	4.50
	LYS 291	Alkyl	5.39
	LYS 291	Conventional hydrogen bond	2.74
Eugenol	ARG 150	Pi- Alkyl	3.97
	ARG150	Conventional hydrogen bond	2.73
	LEU 124	Pi-Alkyl	3.83
	LEU 124	Alkyl	4.49
	LEU124	Conventional hydrogen bond	2.71
	TYR 180	Pi-Alkyl	4.24
trans- Cinnamaldehyde	ARG 126	Pi- Alkyl	5.25
	ARG 150	Pi- Alkyl	3.90
	LEU124	Pi- Alkyl	3.79

Protocatechuic Acid	ILE 10 ASP 86	Pi-Sigma Conventional hydrogen bond	3.83 2.20			
----------------------------	------------------	---	--------------	--	--	--

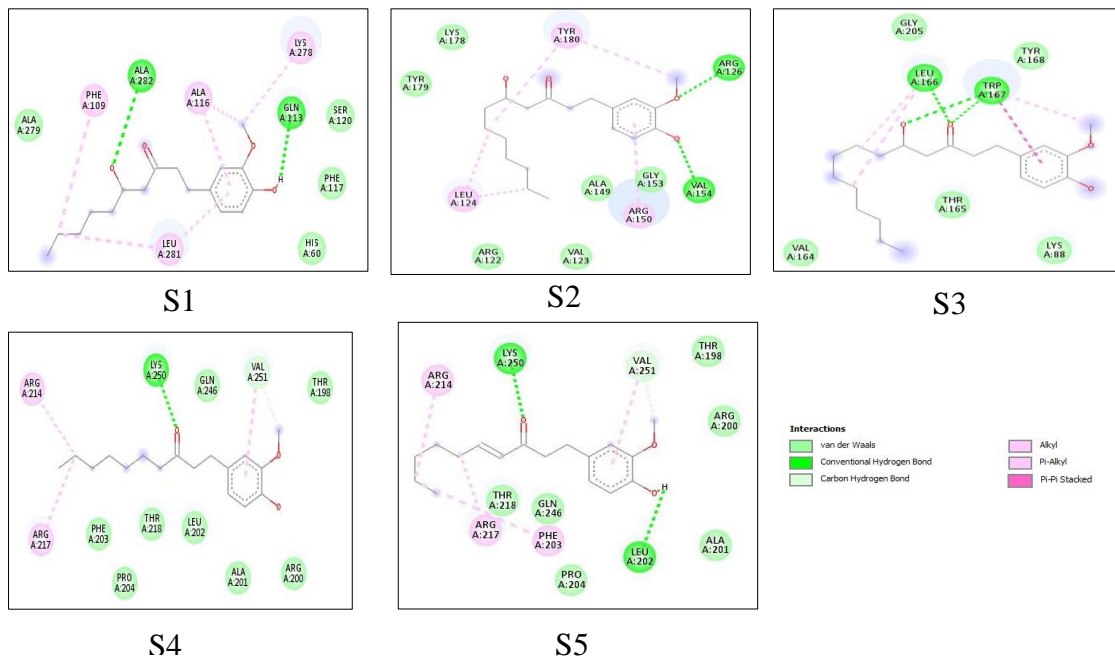


Fig.5.17 Interaction of CDK2 from PDB with ginger compounds (2D)

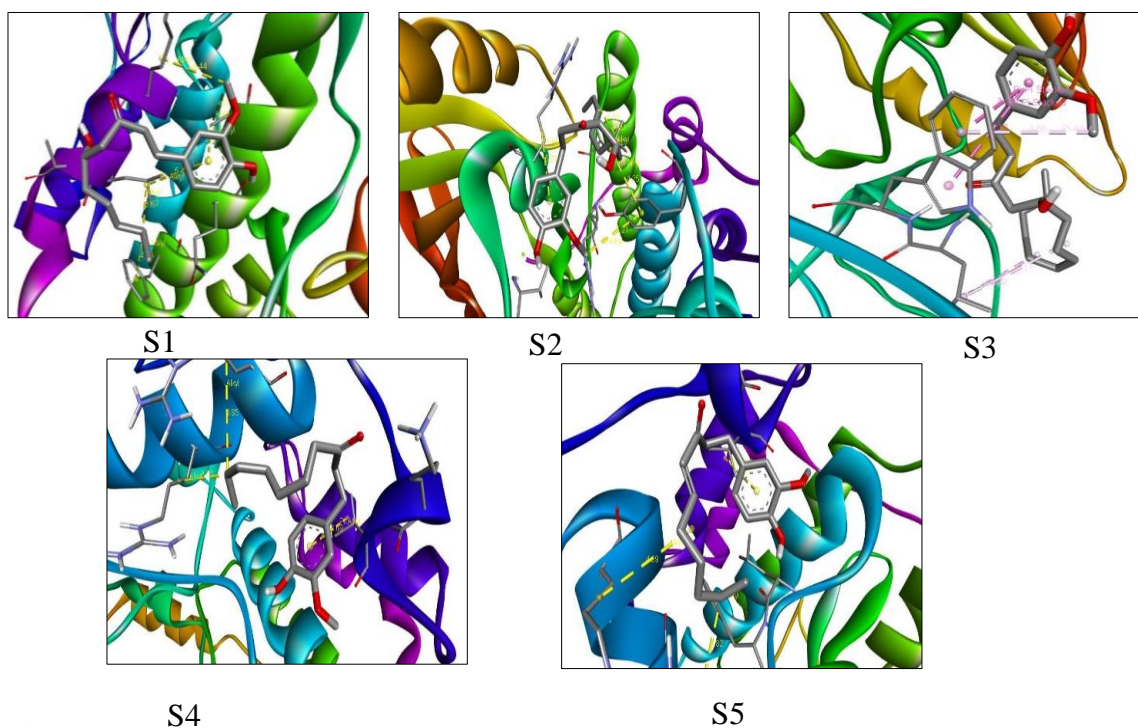


Fig.5.18 Interaction of CDK2 from PDB with ginger compounds (3D)

a. The result of the interaction between CDK2 and ginger:

Based on the information giving in the Fig 5.17. and Fig 5.18. , it appears that the ginger compounds 6-gingerol, 8-gingerol, 10-gingerol, and 6-paradol interact with different residues of CDK2 through conventional hydrogen bonds, carbon hydrogen bonds, alkyl interactions, and pi-alkyl interactions.

Specifically, 6-gingerol interacts with GLU113, ALA282, LEU281, ALA116, LYS278, and PHE109; 8-gingerol interacts with ARG126, VAL154, LEU124, TYR180, and ARG150; 10-gingerol interacts with THR198, ARG214, VAL251, LYS250, LEU202, and ARG200; and 6-paradol interacts with LYS250, VAL251, ARG214, ARG217, and ALA201

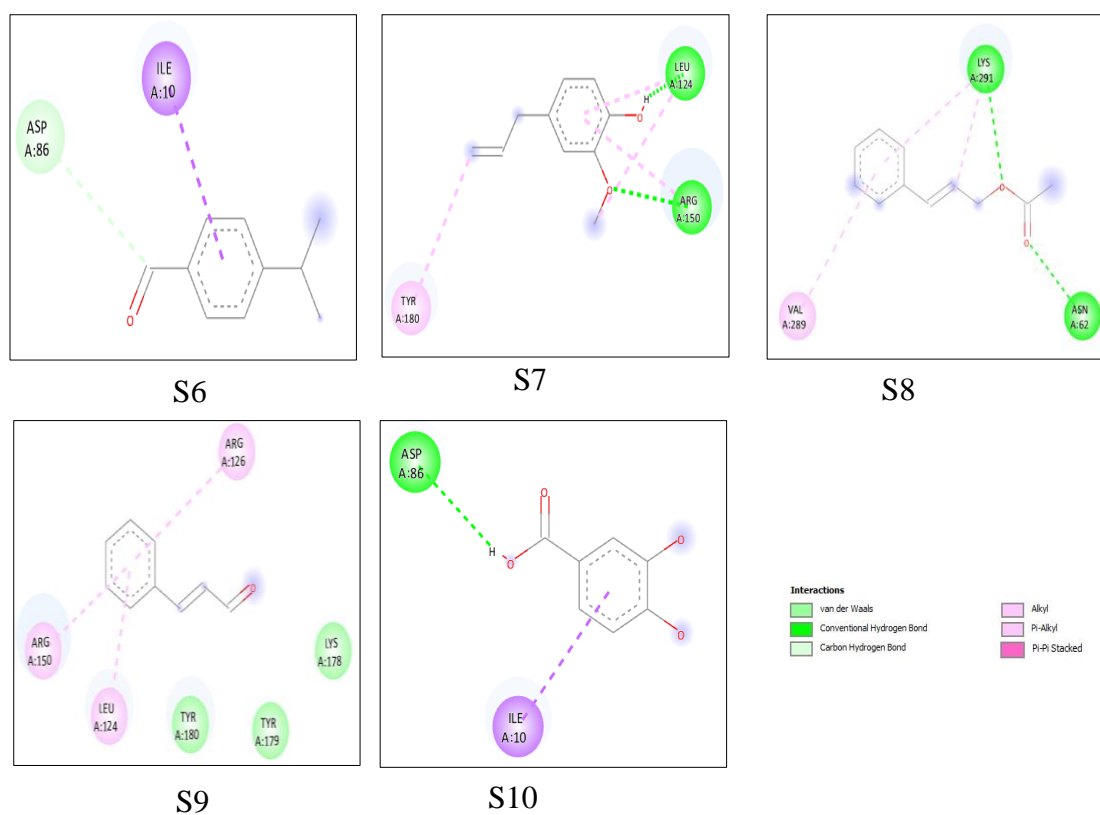


Fig.5.19 Interaction of CDK2 from PDE with cinnamon compounds (2D)

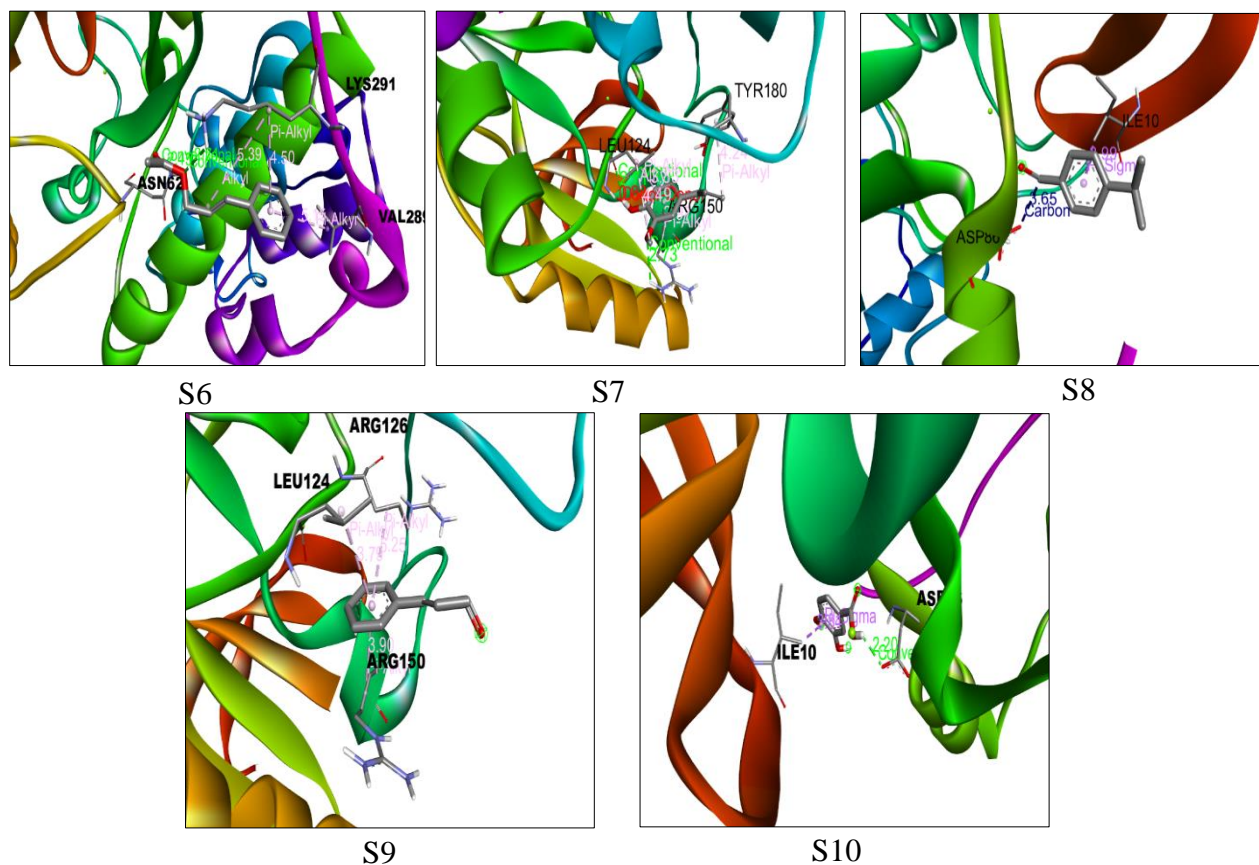


Fig.5.20 Interaction of CDK2 from PDB with cinnamoyl compounds (3D)

b. Interactin between CDK2 and cinnamon

According to the result showed in the Fig 5.18 and Fig 5.19. It can notes that Cuminaldehyde interacts with ILE 10 through a Pi-Sigma interaction, which is one of the "hot spot" residues identified as important for inhibitor binding. This suggests that cuminaldehyde may have some potential inhibitory activity against CDK2.

(E)-cinnamyl acetate interacts with LYS 89 through a Pi-Alkyl interaction, but this residue is not one of the "hot spot" residues identified. However, it also interacts with LYS 291 and VAL 289, which are nearby residues that could potentially contribute to inhibitor binding.

Eugenol interacts with H84, L83, and L134 through Pi-Alkyl and Alkyl interactions, which are all "hot spot" residues. It also interacts with ARG 150 through a Pi-Alkyl and Conventional hydrogen bond, which is not a "hot spot" residue but could still contribute to inhibitor binding.

Trans-Cinnamaldehyde interacts with L134 through a Pi-Alkyl interaction, which is a "hot spot" residue for inhibitor binding. It also interacts with ARG 126 and ARG 150 through Pi-Alkyl interactions, which are not "hot spot" residues but could contribute to binding affinity.

Protocatechuic acid interacts with ILE 10 through a Pi-Sigma interaction, which is a "hot spot" residue for inhibitor binding. It also interacts with ASP 86 through a Conventional hydrogen bond, which is not a "hot spot" residue but could still contribute to binding affinity.

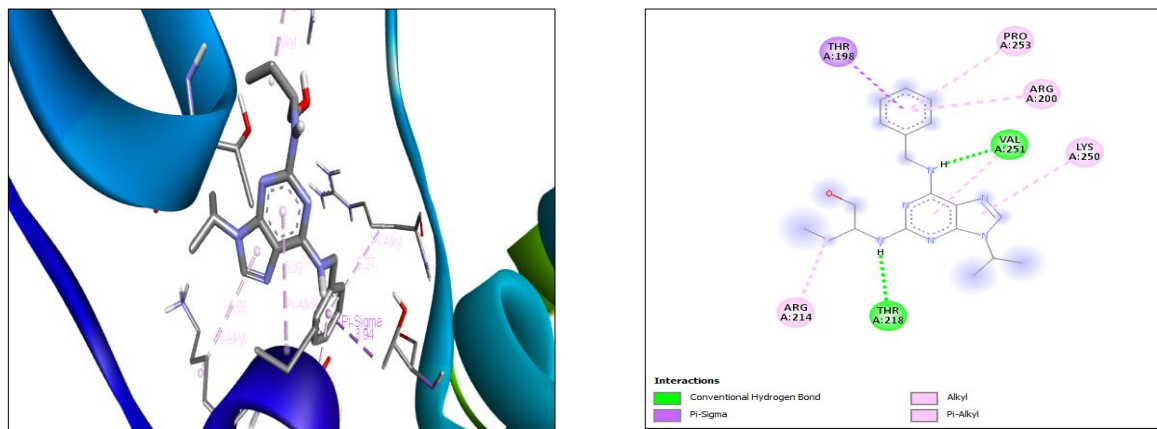


Fig.5.21 Interaction of CDK2 from PDB with Roscovitine.

The prediction of the 3D structure of proteins based on their amino acid sequence has made considerable progress in recent years with the advent of methods based on deep learning. In this study, we compare the reliability of the Swiss model, AlphaFold, ESM and Robetta algorithms' predictions for a new set of membrane proteins involved in human pathologie

Tab.5.18 Parameters of programme of protein prediction

Programme of protein prediction	Time of prediction	Number of amino acid sequence
Swiss model	3 min	298
AlphaFold	5 min	298
ESM	2 seconds	60
Robetta	2 hours	298

In addition to the differences in prediction times and the number of amino acid sequences showed in the Tabs 5.18, it's likely that the protein structures predicted by the different programs may also

vary. Since each program utilizes different algorithms, approaches, and databases, their predictions may produce different structural models for the same protein sequence. As it can be showed in Tab 5.14.

The variations in the predicted protein structures could be due to the differences in the underlying methods used by each program, as well as the training data and algorithms employed. It's important to note that protein structure prediction is a challenging task, and different prediction programs may have varying levels of accuracy and reliability. Therefore, when comparing protein structure predictions from different programs, it's advisable to consider multiple factors, such as the consensus among different methods or experimental validation, to assess the likelihood and reliability of the predicted structures. In fact, there is a very large part of the human proteome comprising intrinsically disordered proteins, i.e., proteins having no ordered structure, or having at least one disordered part [173]. Thanks to genome sequencing data and prediction algorithms, it has been estimated that IDPs (Intrinsically Disordered Proteins) represent about 40% of all proteins, constituting the “unfoldome”, which corresponds to the set of disordered proteins [174].

3.5.1.2. Swiss model

The interactions between the target CDK2 from Swiss model and the ligands of ginger and cinnamon compounds are showed in the Figs 5.23, 5.24, 5.25, 5.26, 5.27 and in the Tab 5.19

Tab.5.19 Interaction details of the target enzyme CDK2 (swiss model)

Compounds	Receptor pocket	Interactions Category	Distance (Å)	Witness	Hot spot of CDK2	Ligand swiss
Ginger				LEU83 GLU81 LEU134 PHE80 ALA144 VAL64 VAL18	I10 V18 E81 L83 H84 Q85 K89 L134 D145	LEU83 GLU81 LEU134 PHE80 ALA144 VAL64 VAL18 ALA31
6-Gingerol	GLU 28	Conventional Hydrogen Bond	4,85			
	PHE 82	Conventional Hydrogen Bond	2,80			
	GLU 81	Carbon Hydrogen Bond	2,46			
	VAL 29	Pi-Alkyl	3,63			

8-Gingerol	ARG 169	Conventional Hydrogen Bond	2,22			
	VAL 146	Conventional Hydrogen Bond	2,12			
	LEU 166	Pi-Sigma	3,79			
	LEU 166	Pi-Sigma	3,99			
	TRP 167	Pi-Sigma	3,77			
	LEU 166	Alkyl	4,26			
	TRP 167	Pi-Alkyl	4,76			
	TRP 167	Pi-Alkyl	4,12			
	TRP 167	Pi-Alkyl	4,70			
	TRP 167	Pi-Alkyl	4,16			
10-Gingerol	LEU 166	Alkyl	1,99			
	TRP 167	Alkyl	1,96			
	TRP 167	Conventional Hydrogen Bond	2,52			
	TRP 167	Conventional Hydrogen Bond	5,32			
	TRP 167	Conventional Hydrogen Bond	3,95			
	LEU 166	Pi-Alkyl	5,16			
	LEU 166	Pi-Pi Stacked	4,46			
	TRP 167	Pi-Pi Stacked	4.66			
6-Paradol	ARG 214	Conventional Hydrogen Bond	2,71			
			4,50			
	VAL 251	Alkyl	5,37			
	LEU 202	Alkyl	4,24			
	ARG 200	Alkyl	5,19			
	LEU 202	Alkyl	4,72			
	PRO 204	Alkyl	5,21			
	ARG 217	Pi-Alkyl				
6-Shogaol	ARG50	Conventional Hydrogen Bond	2,13			
	ARG5	Conventional Hydrogen Bond	1,87			
	TYR159	Conventional Hydrogen Bond	2,81			
	THR160	Conventional Hydrogen Bond	2,16			
	HIS161	Conventional Hydrogen Bond	2,16			
	TYR159	Pi-Pi Stacked	4,22			
	LEU148		5,49			

	VAL163 TYR159	Alkyl Alkyl Pi-Alkyl	4,65 5,28			
<i>Cinnamon</i>						
Cuminaldehyde	GLN 131	Conventional hydrogen bond	2,14			
	TRP 167	Pi-Pi stacked	4,33			
	TRP 167	Pi-Sigma	3,80			
	TRP 167	Pi-Alkyl	4,59			
(E)-cinnamyl acetate	TRP 167	Pi-Pi stacked	5,10			
	TRP 167	Pi-Pi stacked	4,00			
	TRP 167	Pi-Alkyl	3,69			
	TRP 167	Pi-Alkyl	4,36			
Eugenol	HIS 161	Conventional hydrogen bond	1,90			
	TYR 159	Pi-Alkyl	4,42			
	TYR 159	Pi-Pi stacked	4,23			
	THR 160	Conventional hydrogen bond	2,28			
	THR 160	Conventional hydrogen bond	2,26			
trans-Cinnamaldehyde	TRP 167	Pi-Pi Stacked	5,23			
	TRP167	Pi-Pi Stacked	4,04			
	THR 165	Conventional hydrogen bond	3,03			
	LEU 166	Conventional hydrogen bond	1,96			
Protocatechuic Acid	TRP 167	Pi-Pi Stacked	3,99			
	TRP 167	Pi-Pi Stacked	4,52			
	TRP 167	Conventional hydrogen bond	2,24			
	LEU 166	Conventional hydrogen bond	1,93			
	GLN 131	Conventional hydrogen bond	2,19			
	GLN 131	Conventional hydrogen bond	1,85			

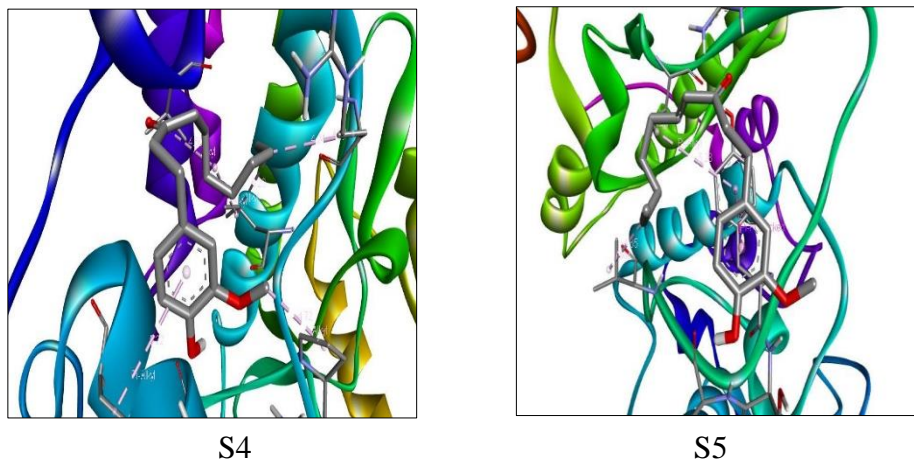


Fig.5.23 Interaction of CDK2 from swiss model with ginger compound (3D)

a. Interaction of CDK2 from swiss model with target of ginger compounds:

(6-gingerol, 8-gingerol, 10-gingerol, 6-paradol, and 6-shogaol) interact with CDK2 through various types of interactions, including conventional hydrogen bonds, carbon hydrogen bonds, pi-alkyl interactions, and pi-pi stacked interactions.

Specifically, 6-gingerol interacts with CDK2 through a conventional hydrogen bond with GLU 28 and PHE 82, a carbon hydrogen bond with GLU 81, and a pi-alkyl interaction with VAL 29.

8-gingerol interacts with CDK2 through conventional hydrogen bonds with ARG 169 and VAL 146, pi-sigma interactions with LEU 166 and TRP 167, and pi-alkyl interactions with LEU 166, TRP 167, and ARG 150.

10-gingerol interacts with CDK2 through an alkyl interaction with LEU 166, conventional hydrogen bonds with TRP 167, and a pi-pi stacked interaction with LEU 166 and TRP 167.

6-paradol interacts with CDK2 through a conventional hydrogen bond with ARG 214, and alkyl interactions with VAL 251, LEU 202, ARG 200, PRO 204, and ARG 217.

Finally, 6-shogaol interacts with CDK2 through conventional hydrogen bonds with ARG50, ARG5, THR160, HIS161, and TYR159, as well as a pi-pi stacked interaction with TYR159, and alkyl interactions with LEU148 and VAL163.

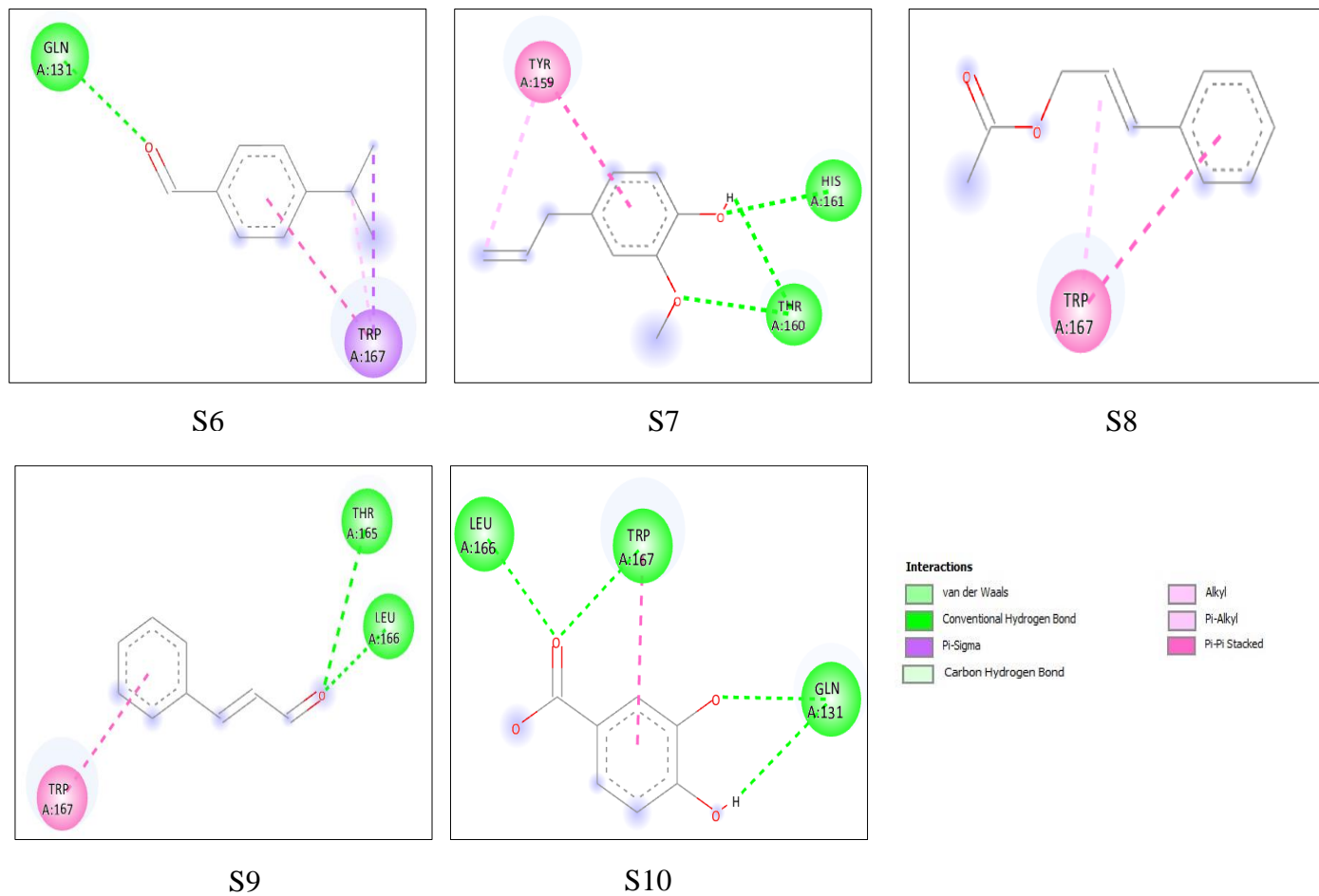
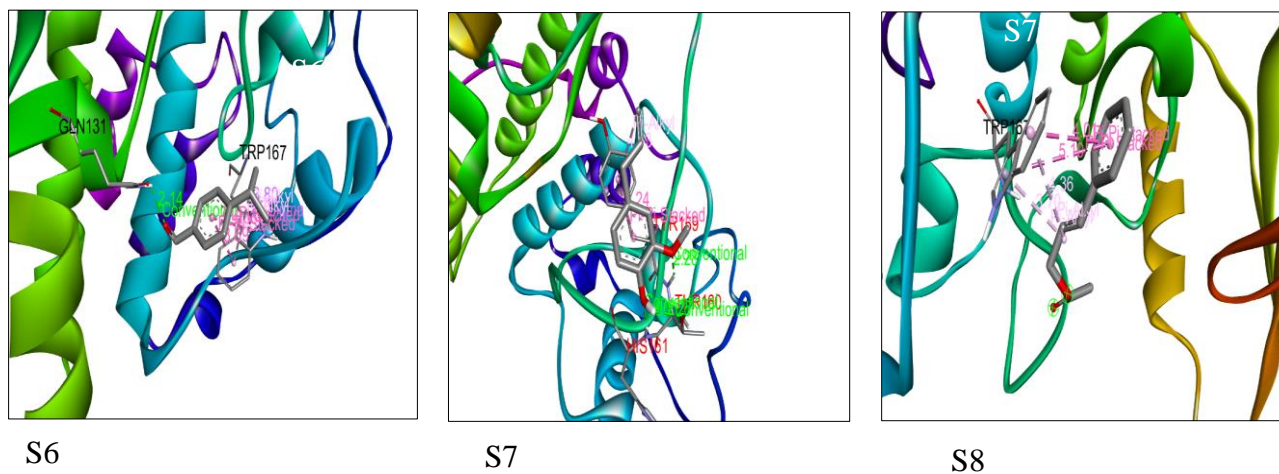


Fig.5.24 Interaction of CDK2 from swiss model with cinnamon compounds (2D)



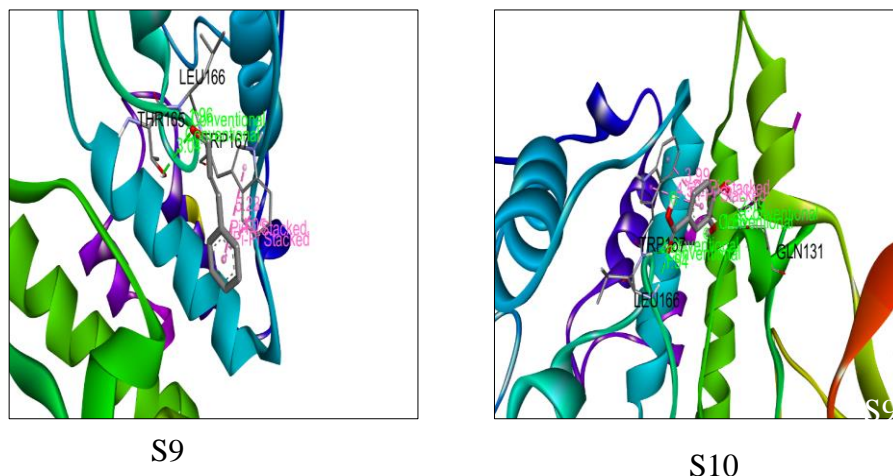


Fig.5.25 Interaction of CDK2 from swiss model with cinnamoyl compounds (3D)

b. Interactin between CDK2 from swiss model and cinnamoyl :

Based on the results, it appears that the hot spot residues involved are TRP 167, HIS 161, TYR 159, THR 160, THR 165, LEU 166, GLN 131, and E81. These residues are involved in various types of interactions such as Pi-Pi stacking, conventional hydrogen bonds, and Pi-Alkyl interactions.

Cuminaldehyde forms Pi-Sigma and Pi-Alkyl interactions with GLN 131 and TRP 167, respectively. (E)-cinnamyl acetate forms two Pi-Pi stacked interactions with TRP 167 and TRP 167, respectively, as well as Pi-Alkyl interactions with TRP 167. Eugenol forms conventional hydrogen bonds with HIS 161 and THR 160, and Pi interactions with TYR 159. trans-Cinnamaldehyde forms two Pi-Pi stacked interactions with TRP 167, a conventional hydrogen bond with THR 165, and a conventional hydrogen bond with LEU 166. Protocatechuic acid forms two Pi-Pi stacked interactions with TRP 167, as well as conventional hydrogen bonds with TRP 167, LEU 166, and GLN 131.

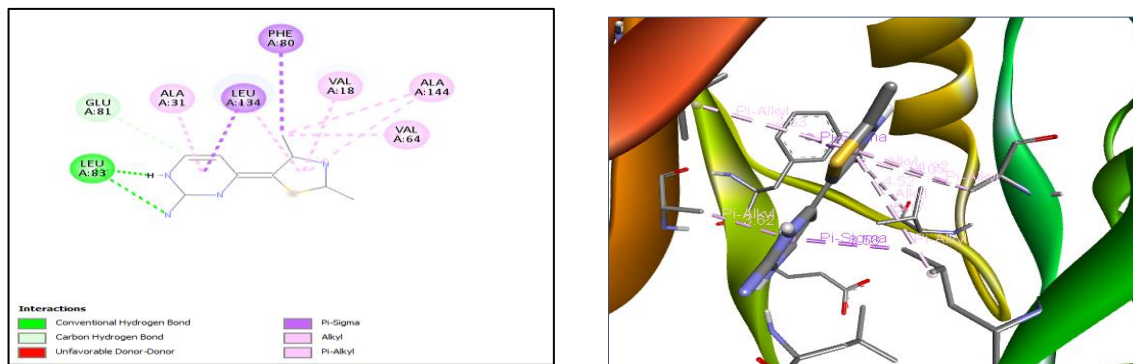


Fig.5.26 Interaction of CDK2 from swiss model with Roscovitine

3.5.1.3. Alphadatabase

The interactions between the target CDK2 from AlphaFold and the ligands of ginger and cinnamon compounds are showed in the Figs 5.28, 5.29, 5.30 , 5.31, 5.32 and in the Tab 5.20.

Tab.5.20 Interaction details of the target enzyme CDK2 (alphadatabase)

Compounds	Receptor pocket	Interactions Category	Distance (Å)	Witness	Hot spot of CDK2
<i>Ginger</i>					
6-Gingerol	LEU83	Alkyl	1,96	LYS33	I10
	ILE10	Alkyl	2,58	GLN131	V18
	GLU 81	Alkyl	2,34	ASN132	E81
	LEU134	Conventional Hydrogen Bond	3,53	ILE10	L83
				LEU134	H84
				LEU134	Q85
				ALA144	K89
	ALA144	Conventional Hydrogen Bond	4,38	VAL64	L134
				PHE80	D145
			VAL18		
			ALA31		
	VAL64	Pi-Alkyl	4,34		
	PHE80	Pi-Alkyl	4,04		
	VAL18	Pi-Alkyl	4,78		

	ALA31	Pi-Sigma	4,08			
8-Gingerol	LEU134	Pi-Sigma	3,98			
	PHE80	Pi-Sigma	3,54			
	VAL18	Alkyl	4,92			
	ALA31	Alkyl	3,45			
	LEU134	Alkyl	5,02			
	ALA144	Alkyl	4,70			
	ALA144	Alkyl	3,66			
	VAL64	Alkyl	3,80			
	ILE10	Alkyl	5,16			
	LEU134	Alkyl	5,42			
	PHE82	Pi-Alkyl	4,45			
	ILE10	Pi-Alkyl	5,12			
	10-Gingerol	LYS89	Conventional Hydrogen Bond	2,77		
LYS89		Conventional Hydrogen Bond	2,35			
LEU83		Conventional Hydrogen Bond	1,97			
ASP145		Conventional Hydrogen Bond	2,03			
PHE80		Pi-Sigma	3,71			
ILE10		Alkyl	5,01			
VAL18		Alkyl	5,01			
VAL18		Alkyl	5,08			
ALA31		Alkyl	4,99			
ALA31		Alkyl	5,01			
VAL64		Alkyl	5,48			
LEU134		Alkyl	4,64			
ALEU134		Alkyl	5,01			
ALA144		Alkyl	4,34			
ALA144		Alkyl	3,66			
VAL64		Alkyl	4,18			
VAL18		Alkyl	4,63			
PHE80		Pi-Alkyl	5,36			
6-Paradol		HIS84	Conventional Hydrogen Bond	2,28		
		PHE80	Pi-Sigma	3,64		
	VAL18	Alkyl	4,04			
	ALA31	Alkyl	4,73			
	LYS33	Alkyl	5,08			
	ALA144	Alkyl	3,75			

	VAL64 ILE10 LEU134	Alkyl Pi-Alkyl Pi-Alkyl	4,14 5,19 4,99	
6-Shogaol	LYS89 GLU81 VAL18 VAL18 VAL18 ALA31 VAL64 LEU134 PHE80 ALA31 LEU134	Alkyl Alkyl Alkyl Alkyl Carbon Hydrogen Bond Conventional Hydrogen Bond Pi-Alkyl Pi-Alkyl Pi-Alkyl Pi-Sigma Pi-Sigma	2,39 3,54 3,66 3,96 4,98 3,85 4,15 4,97 5,03 4,96 5,25	
<i>Cinnamon</i>				
cuminaldehyd	Val 18 ALA 31 VAL 64 LEU 134 ALA 144 ASP 145	Pi-alkyl Pi-alkyl Pi-alkyl Pi-sigma Pi-alkyl Carbon hydrogen bond	5.14 4.44 5.28 3.74 4.76 3.29	
E-cinnamyl acetate	ILE 10 PHE 80 LEU 134	Pi-sigma Pi-sigma Pi-alkyl	3.53 3.54 5.36	
Eugenol	VAL 18 ALA 31 VAL 64 PHE 80 LEU 134 ALA 144 ASP 145	Pi-alkyl Pi-alkyl Alkyl Pi-alkyl Pi-sigma Alkyl	4.55 5.07 4.12 3.61 3.63 3.75 3.67	

		Carbon hydrogen bond			
trans cinnamaldehyde	VAL 18 ALA 31 LEU 134 ASP 145	Pi-alkyl Pi-alkyl Pi-sigma Carbon hydrogen bond	4.43 4.66 3.75 3.35		
protocatechuic acid	VAL 18 ALA 31 LYS 33 LEU 134 ASP 145	Pi-alkyl Pi-alkyl Pi-alkyl Pi-alkyl Conventional hydrogen bond	4.58 4.49 5.54 5.34 1.95		

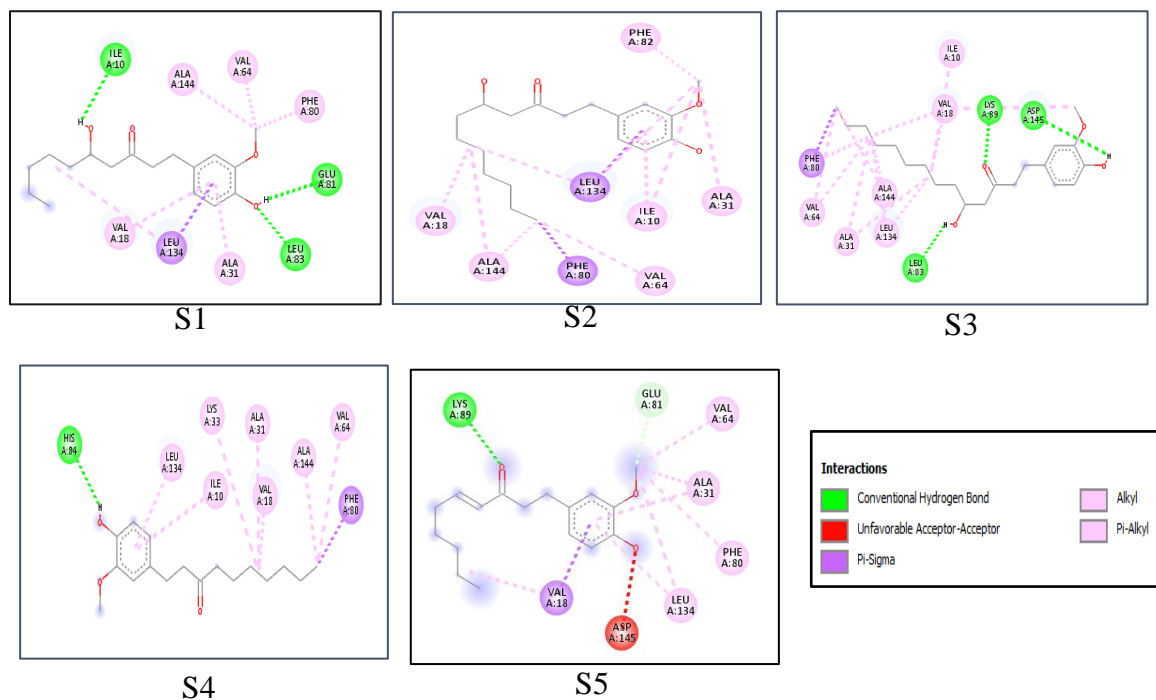


Fig.5.27 Interaction of CDK2 from Alphadatabase with ginger compounds (2D)

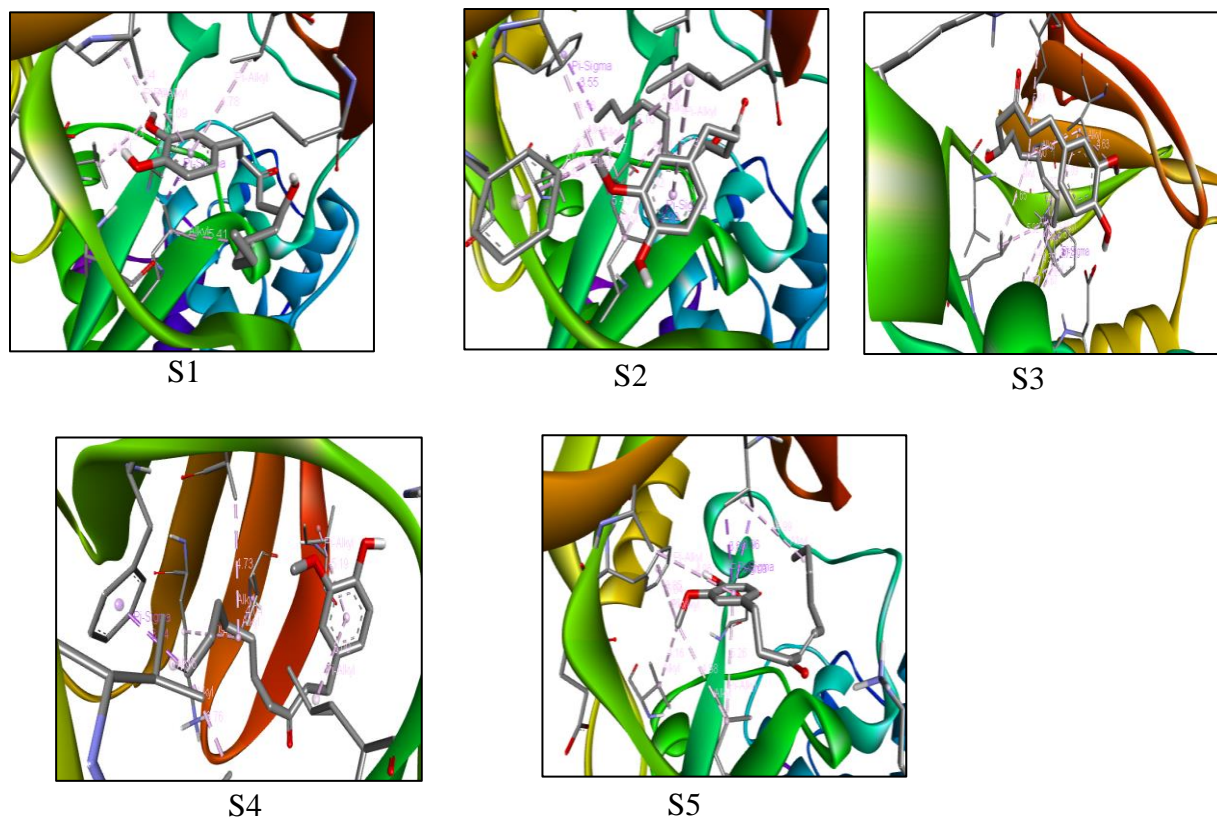


Fig.5.28. Interaction of CDK2 from Alphadatdbase with Ginger compounds (3D)

a. Interaction of CDK2 from Alphadatdbase with target of Ginger

Based on the interactions listed on the Figs 5.28 , 5.29 , it appears that the ginger compounds 6-gingerol, 8-gingerol, 10-gingerol, 6-paradol, and 6-shogaol are capable of interacting with CDK2 through a variety of different interactions, including conventional hydrogen bonds, pi-alkyl interactions, pi-sigma interactions, and carbon hydrogen bonds.

Specific amino acids that appear to be involved in these interactions include LEU83, ILE10, GLU81, LEU134, ALA144, VAL64, PHE80, VAL18, ALA31, LYS33, HIS84, and ASP145

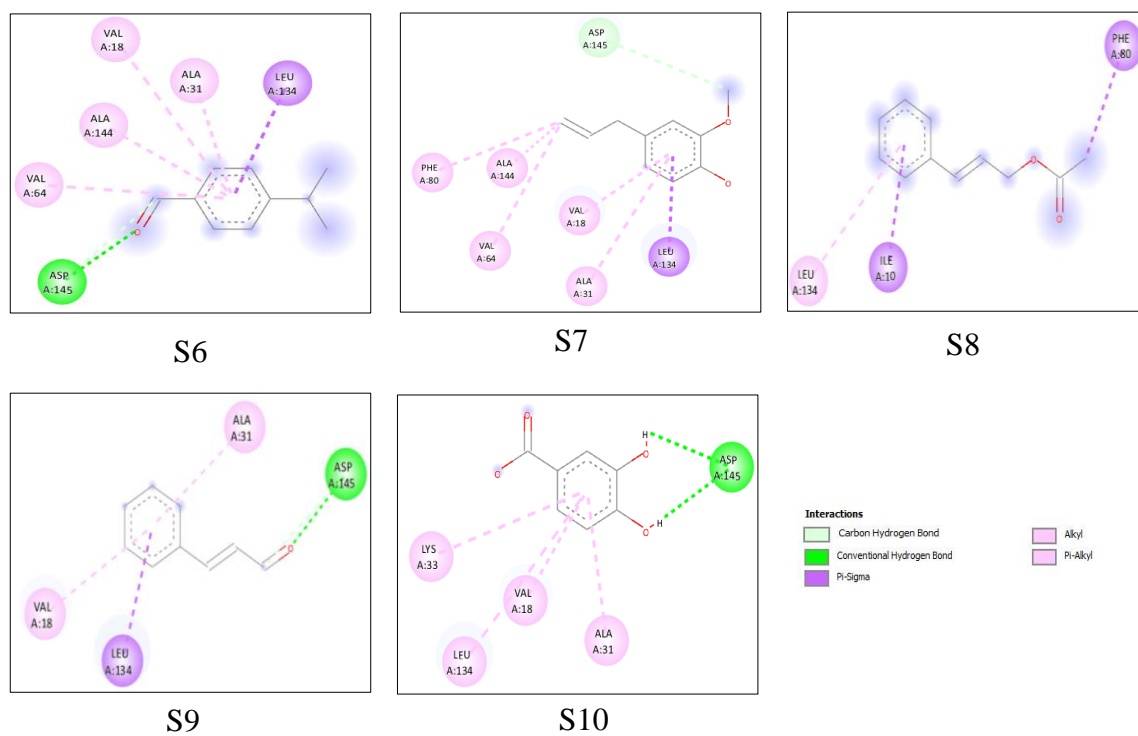


Fig.5.29 Interaction of CDK2 from Alphadatabase with cinnamion compounds (2D).

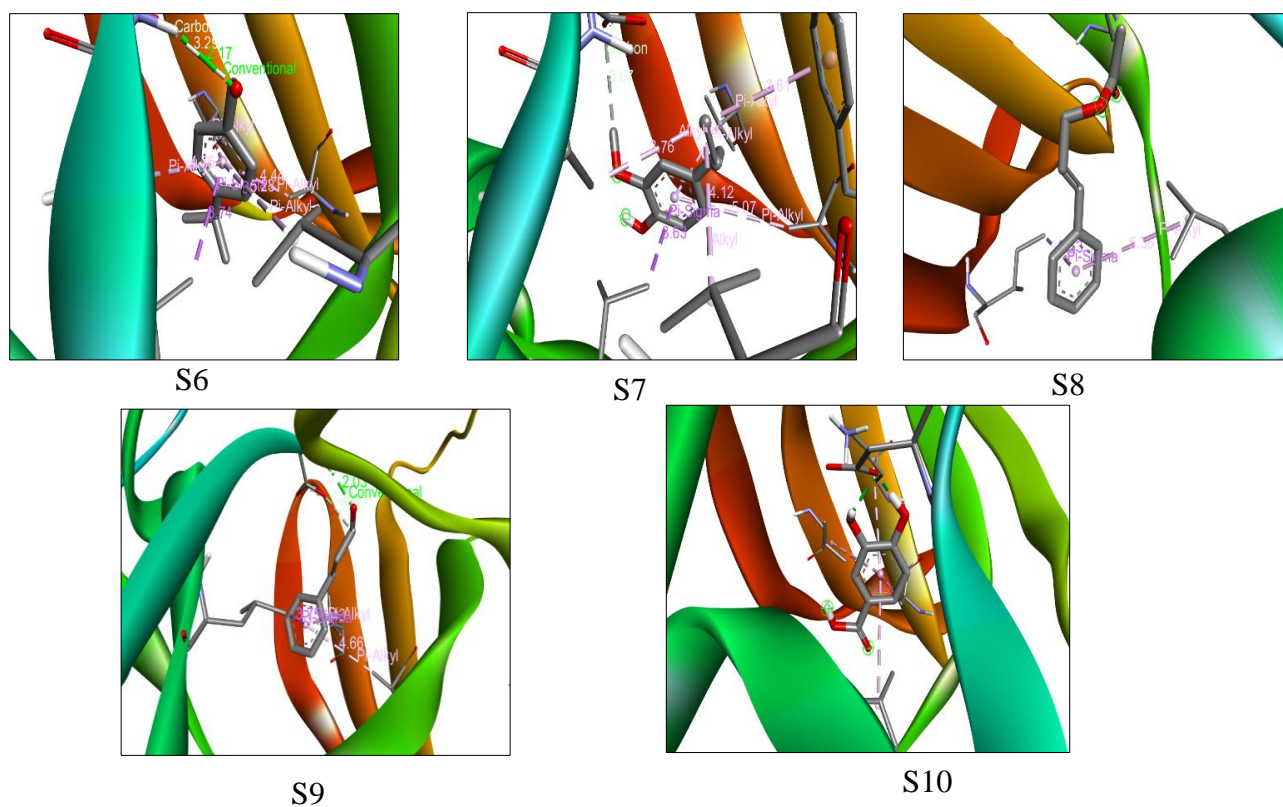


Fig.5.30 Interaction of CDK2 from Alphadatabase with cinnamion compounds (3D).

a. Interaction of CDK2 from Alphadatabase with target of cinnamon:

Based on the results provided in the Figs 5.30, 5.31, it seems that all of the cinnamon compounds interact with CDK2 from alpha fold through pi-alkyl or pi-sigma interactions with several residues, including Valine 18, Alanine 31, and Leucine 134. Additionally, most of the compounds form conventional hydrogen bonds with Aspartic Acid 145. However, there are some differences in the specific residues involved in the interactions between the different compounds and CDK2.

For example, Cuminaldehyde and Eugenol interact with Valine 64 and Phenylalanine 80, respectively, while Protocatechuic acid forms a pi-alkyl interaction with Lysine 33. Overall, these interactions suggest that the cinnamon compounds have the potential to bind to and modulate the activity of CDK2

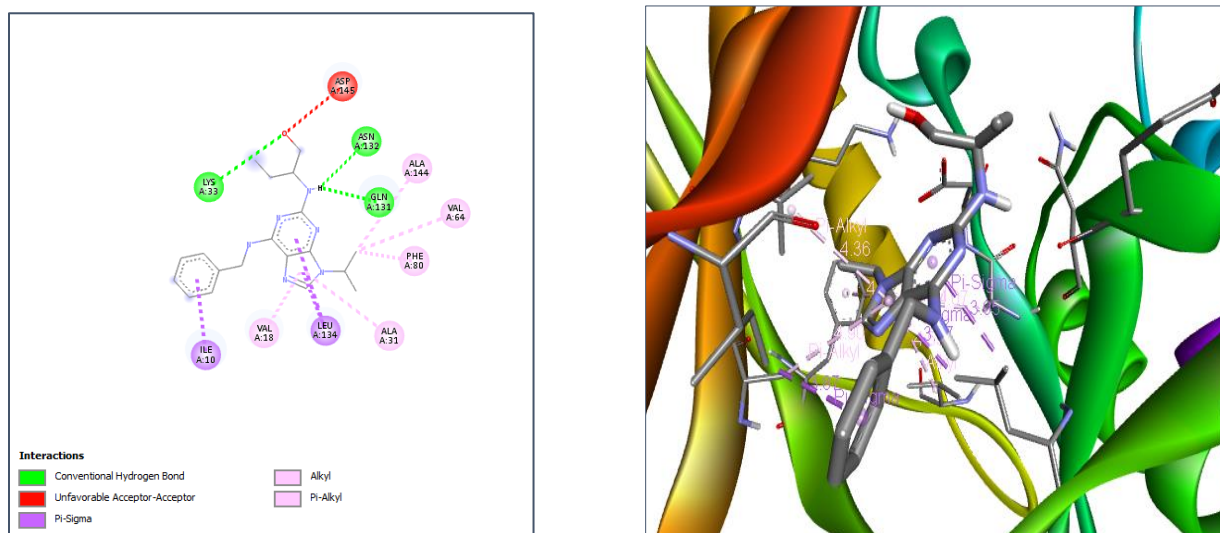


Fig.5.31 Interaction of CDK2 from Alphadatabase with Roscovitine

3.5.1.4. Evolutionary scale modeling ESM

The interactions between the target CDK2 from ESM and the ligands of ginger and cinnamon compounds are shown in the Figs 5.33, 5.34, 5.35, 5.36, 5.37 and in the Tab 5.21.

Tab.5.21 Interaction details of the target enzyme CDK2 (ESM)

Compounds	Receptor pocket	Interactions Category	Distance (Å)	Witness	Hot spot of CDK2
<i>Ginger</i>				LYS33 LYS34 ILE35 LEU37 ILE52 LEU55 MET1 LEU32	I10 V18 E81 L83 H84 Q85 K89 L134 D145
6-Gingerol	LYS33	Conventional Hydrogen Bond	2,25		
	ASN59	Conventional Hydrogen Bond	2,50		
	ALA31	Alkyl	3,85		
	ILE52	Alkyl	4,35		
	LYS33	Alkyl	4,62		
8-Gingerol	ASN59	Conventional Hydrogen Bond	2,34		
	LYS33	Conventional Hydrogen Bond	2,35		
	LYS33	Alkyl	5,30		
	LEU55	Alkyl	4,74		
	ILE52	Pi-Alkyl	4,49		
10-Gingerol	ASN59	Conventional Hydrogen Bond	2,40		
	ASN59	Conventional Hydrogen Bond	2,44		
	LYS33	Conventional Hydrogen Bond	2,68		
	VAL18	Alkyl	3,96		
	ALA31	Alkyl	3,72		
	LYS33	Alkyl	4,15		
	LYS33	Alkyl	5,11		
	LEU55	Alkyl	4,17		
	VAL18	Alkyl	4,58		
	ILE52	Pi-Alkyl	4,10		
LEU55	Pi-Alkyl	4,42			
6-Paradol	THR41	Conventional Hydrogen Bond	2,70		
	THR47	Conventional Hydrogen Bond	2,49		
	THR41	Conventional Hydrogen Bond	2,49		

	GLY43:	Conventional Hydrogen Bond	2,48		
	PRO45	Alkyl	4,30		
	TYR15	Pi-Alkyl	5,08		
	PRO45	Pi-Alkyl	4,05		
6-Shogaol	ALA31	Conventional Hydrogen Bond	2,07		
	LYS56	Alkyl	3,72		
	LEU32	Alkyl	4,17		
	ILE52	Alkyl	4,59		
	LEU55	Alkyl	5,32		
	LEU55	Alkyl	4,75		
	LYS33	Pi-Alkyl	4,37		
<i>Cinnamon</i>					
cummaldehyd	LYS 6	Conventional hydrogen bond	2.43		
	VAL 7	Conventional hydrogen bond	2.34		
E-cinnamyl acetate	MET 1	Pi-sulfur	5.87		
	GLN 5	Carbon hydrogen bond	3.44		
	LYS 6	Conventional hydrogen bond	2.26		
	VAL 7	Conventional hydrogen bond	2.06		
eugenol	MET 1	Alkyl	5.28		
	PHE 4	Conventional hydrogen bond	2.22		
	LYS 6	Conventional hydrogen bond	2.82		
	VAL7	Carbon hydrogen bond	3.80		
	TYR19	Pi-donor hydrogen bond	3.57		
trans cinnamaldehyde	LYS 6	Pi-alkyl	4.00		
	LYS 20	Carbon hydrogen bond	3.44		

protocatechuic acid	MET 1	Conventional hydrogen bond	2.62		
	LYS 6	Unfavorable donor-donor	1.69		
	VAL 7	Pi-sigma	3.59		
	VAL 7	Unfavorable acceptor-acceptor	2.88		

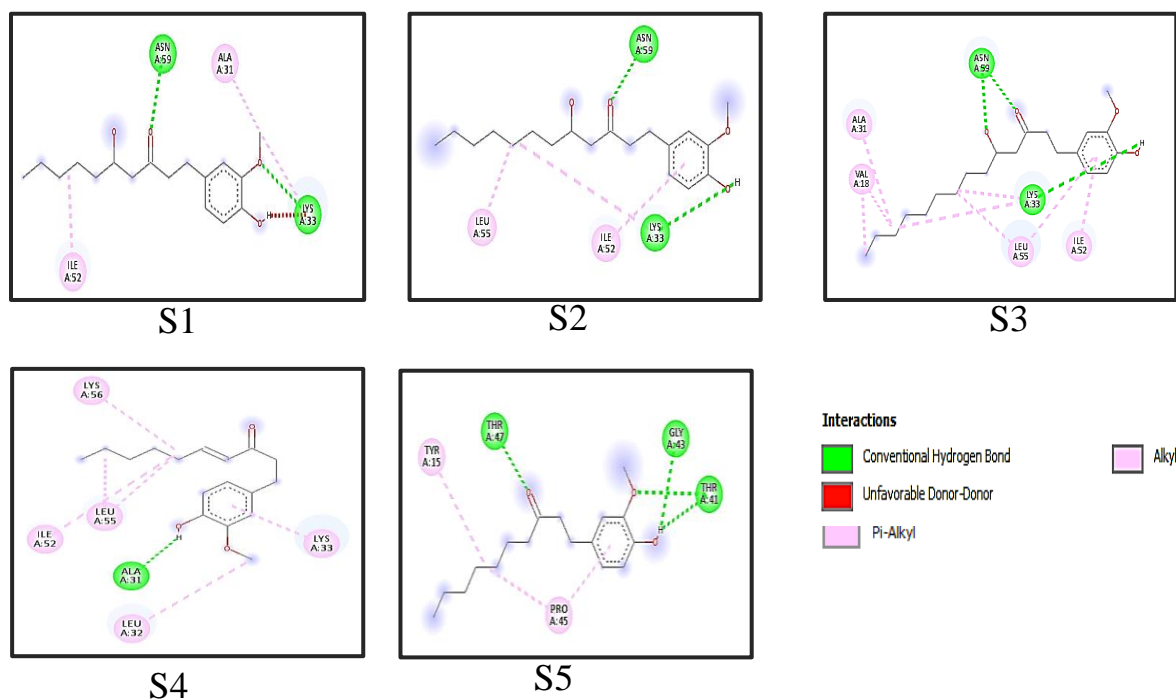


Fig.5.32 Interaction of CDK2 from ESM with ginger compounds (2D)

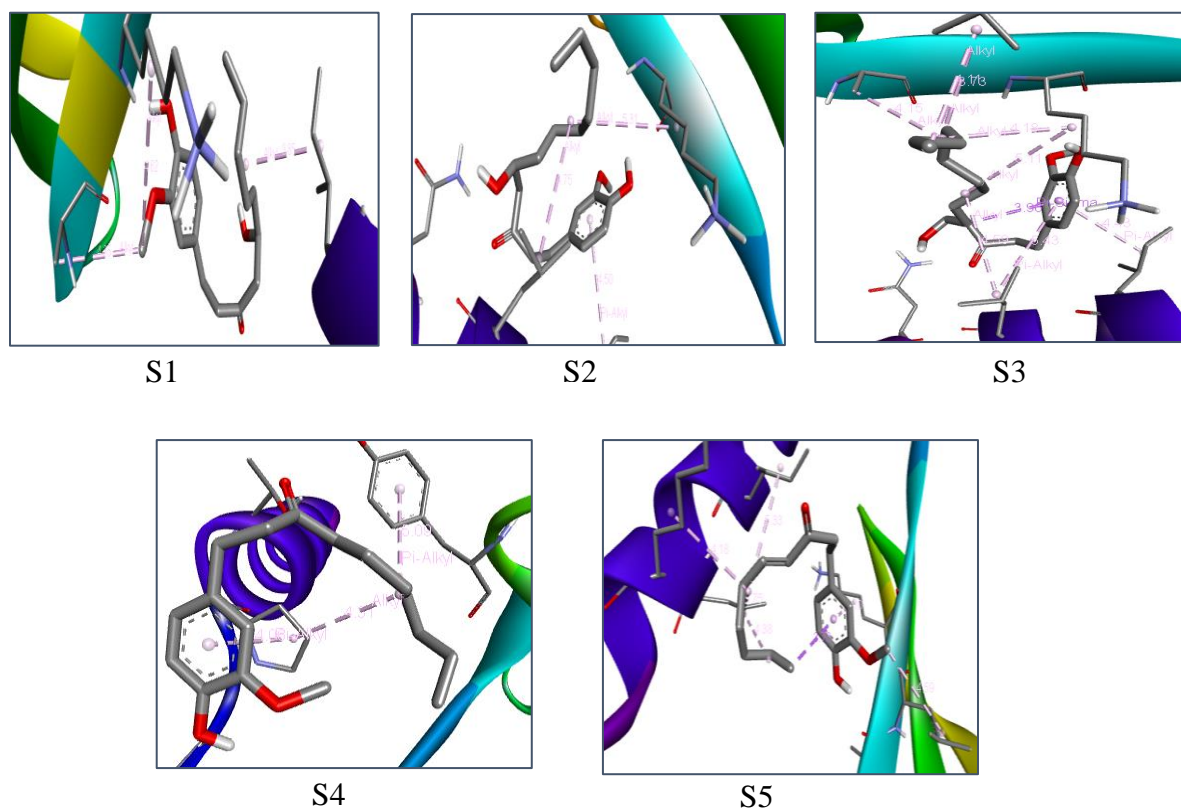


Fig.5.33 Interaction of CDK2 from ESM with ginger compounds (3D)

a. Interaction of CDK2 from ESM with ginger compounds:

The results of the interaction between ginger compounds and CDK2 showed in the Fig 5.33,5.34 suggest that these compounds can bind to the active site of CDK2 and potentially inhibit its activity. The specific interactions observed with each compound may contribute to its binding affinity and potency as a CDK2 inhibitor. For example, the conventional hydrogen bonds formed between 6-Gingerol and CDK2 may contribute to its strong binding affinity. Meanwhile, the pi-alkyl interactions observed with 8-Gingerol and 10-Gingerol may also contribute to their binding affinity. Overall, these findings suggest that ginger compounds may have potential as CDK2 inhibitors.

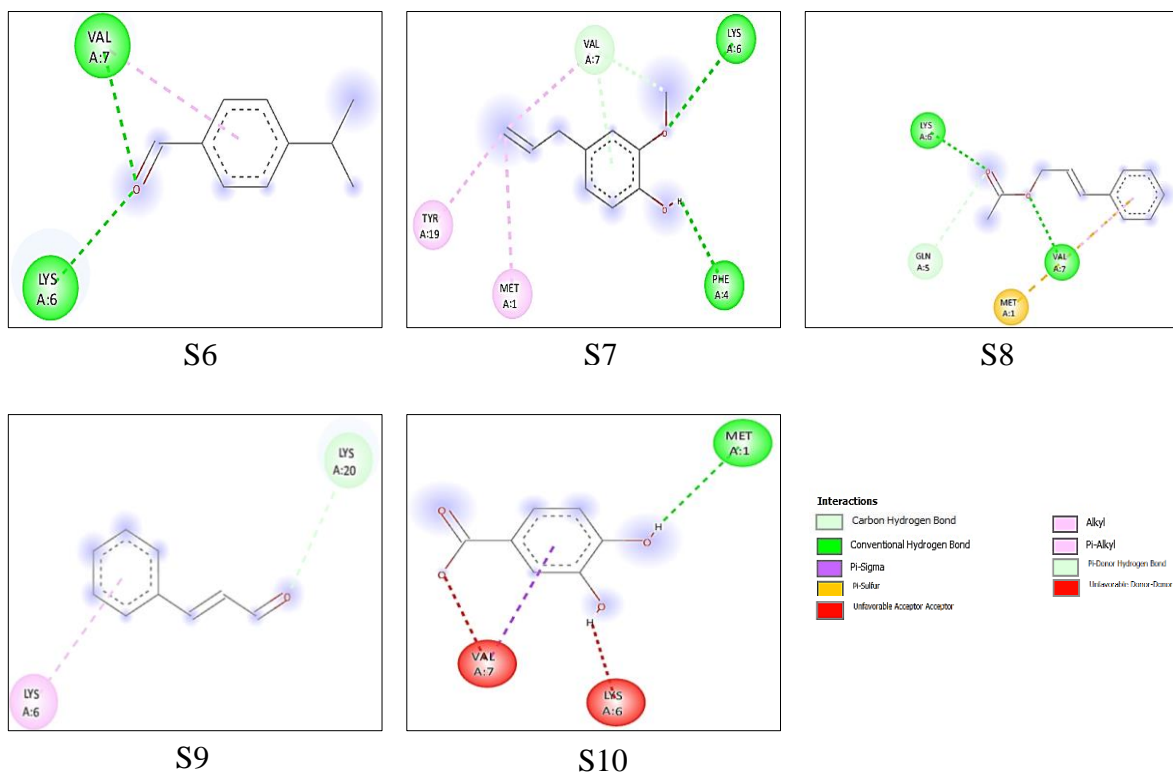


Fig.5.34 Interaction of CDK2 from ESM with cinnamon compounds (2D)

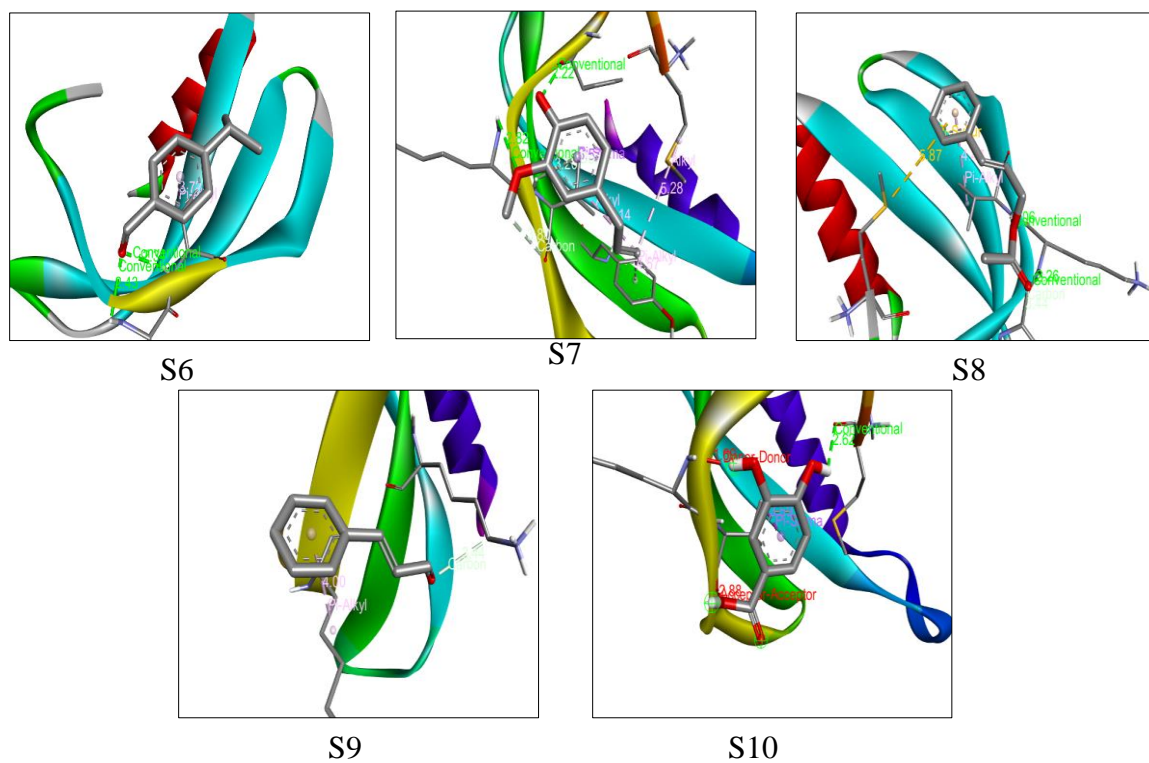


Fig.5.35 Interaction of CDK2 from ESM with cinnamon compounds (3D)

b. Interaction of CDK2 from ESM with cinnamon compounds:

Based on the information showed in the Figs 5.35, 5.36, it seems that the cinnamon compounds cuminaldehyde, E-cinnamyl acetate, eugenol, and trans cinnamaldehyde interact with CDK2 through various amino acid residues. The specific residues involved in the interactions are LYS 6, VAL 7, MET 1, GLN 5, PHE 4, TYR 19, and LYS 20.

However, it is important to note that the results do not provide a clear indication of the strength or significance of the interactions between the cinnamon compounds and CDK2. It is also not clear if these interactions occur specifically within the nine residues identified as hot spots of inhibitor-CDK2.

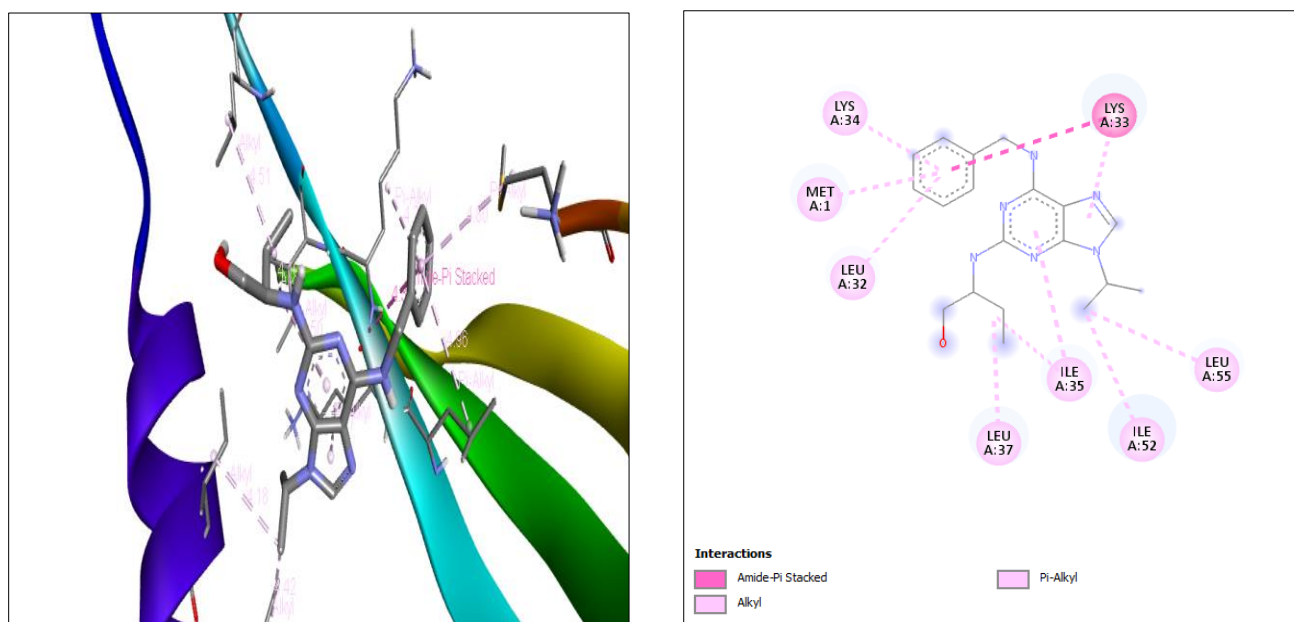


Fig.5.36 Interaction of CDK2 from ESM with Roscovitine

3.5.1.5. Robetta

The interactions between the target CDK2 from Robetta and the ligands of ginger and cinnamon compounds are shown in the Figs 5.38, 5.39, 5.40, 5.41, 5.42 and in the Tab 5.22.

Tab.5.22 Interaction details of the target enzyme CDK2 (Robetta)

Compounds	Receptor pocket	Interactions Types	Distance (Å)	Witness	Hot spot of CDK2
Ginger					
6-Gingerol	GLU12	Conventional Hydrogen Bond	2,45	LEU83 ILE10	I10 V18
	ASP86	Conventional Hydrogen Bond	2,46	GLU12 ALA144	E81 L83
	ILE10	Pi-Sigma	3,96	LEU134 VAL18	H84 Q85
	LEU134	Pi-Sigma	3,54	LYS33	K89
	VAL18	Alkyl	4,38		L134
	LEU134	Alkyl	5,04		D145
	ALA144	Alkyl	3,99		
	VAL18	Alkyl	3,80		
	LYS33	Alkyl	3,77		
	PHE80	Pi-Alkyl	4,12		
8-Gingerol	ASP86	Conventional Hydrogen Bond	2,56		
	ASN132	Conventional Hydrogen Bond	2,84		
	LEU83	Conventional Hydrogen Bond	2,48		
	LEU134	Pi-Sigma	3,43		
	VAL18	Alkyl	4,54		
	ALA31	Alkyl	4,05		
	ALA31	Alkyl	4,85		
	LYS33	Alkyl	4,36		
	LYS33	Alkyl	4,64		
	ALA144	Alkyl	4,82		
	VAL64	Alkyl	4,41		
	LEU134	Alkyl	3,92		
	PHE80	Alkyl	5,12		
	PHE80	Pi-Alkyl	4,36		
ILE10	Pi-Alkyl	4,21			
10-Gingerol	GLU12	Conventional Hydrogen Bond	1,94		
	GLU12	Carbon Hydrogen Bond	3,64		
	ASP86	Carbon Hydrogen Bond	3,60		

	ILE10	Pi-Sigma	3,79
	LEU134:	Pi-Sigma	3,78
	LEU134	Pi-Sigma	3,75
	VAL18	Alkyl	4,56
	LYS33	Alkyl	5,13
	ALA144	Alkyl	4,23
	VAL18	Pi-Alkyl	4,80
6-Paradol	ASP86	Conventional Hydrogen Bond	2,35
	ILE10	Carbon Hydrogen Bond	3,79
	LEU134	Pi-Sigma	3,53
	VAL18	Alkyl	4,70
	VAL18	Alkyl	5,01
	ALA31	Alkyl	4,30
	LYS33	Alkyl	4,45
	VAL64	Alkyl	4,76
	ALA144	Alkyl	4,46
	ALA144	Alkyl	4,49
	LEU134	Alkyl	5,14
	PHE80	Pi-Alkyl	4,85
	PHE80	Pi-Alkyl	4,45
	ILE10	Pi-Alkyl	4,53
6-Shogaol	HIS84	Carbon Hydrogen Bond	3,55
	LEU134	Pi-Sigma	3,53
	VAL18	Alkyl	4,55
	ALA31	Alkyl	3,68
	LYS33	Alkyl	4,23
	ILE10	Alkyl	3,65
	VAL64	Alkyl	4,10
	LEU83	Alkyl	5,39
	LEU134	Alkyl	4,93
	PHE80	Pi-Alkyl	5,06
	PHE82	Pi-Alkyl	4,84
	ILE10	Pi-Alkyl	5,09
<i>Cinnamon</i>			
cumnaldehyd	VAL 18	Pi-sigma	3.47
	ALA 31	Pi-alkyl	4.80
	PHE 80	Pi-sigma	3.68
	LEU 134	Pi-sigma	3.42

E-cinnamyl acetate	VAL 18	Pi-alkyl	4.59
	ALA 31	Pi-alkyl	5.37
	PHE 80	Pi-pi t-shaped	4.77
	ASP 86	Conventional hydrogen bond	2.66
	LEU 134	Pi-alkyl	5.38
	ALA 144	Pi-alkyl	4.09
Eugenol	ILE 10	Alkyl	4.11
	VAL18	Pi-alkyl	4.35
	VAL 64	Alkyl	3.93
	PHE 80	Pi-alkyl	3.65
	GLN 131	Conventional hydrogen bond	2.04
	LEU 134	Pi-sigma	3.59
	ALA 144	Alkyl	4.59
		Pi-alkyl	4.95
		Alkyl	3.76
trans cinnamaldehyde	VAL 18	Pi-sigma	3.97
	LYS 33	Pi-alkyl	5.08
	PHE 80	Pi-pi t-shaped	5.00
	ALA144	Pi-alkyl	4.29
protocatechuic acid	VAL 18	Pi-alkyl	5.09
	LYS 33	Pi-alkyl	5.02
	VAL 64	Pi-alkyl	5.36
	PHE 80	Pi-pi stacked	3.81
	ALA 144	Pi-alkyl	4.26
	ASP 145	Conventional hydrogen bond	1.97

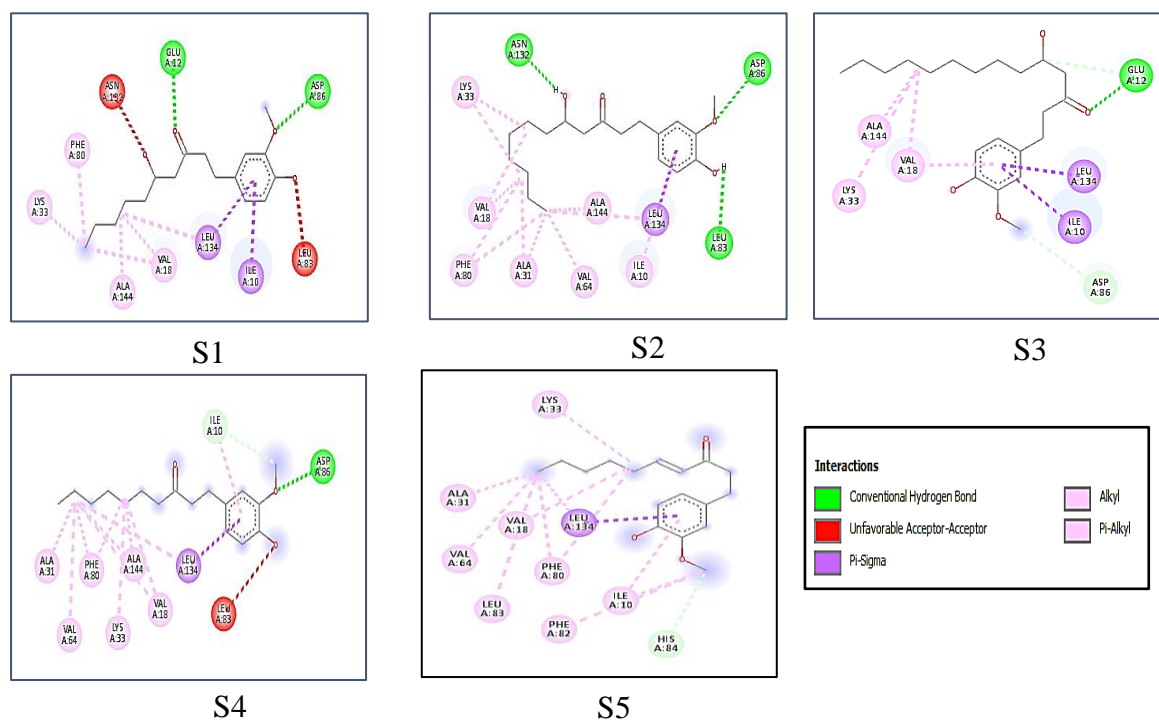


Fig.5.37 Interaction of CDK2 from Robetta with ginger compounds (2D)

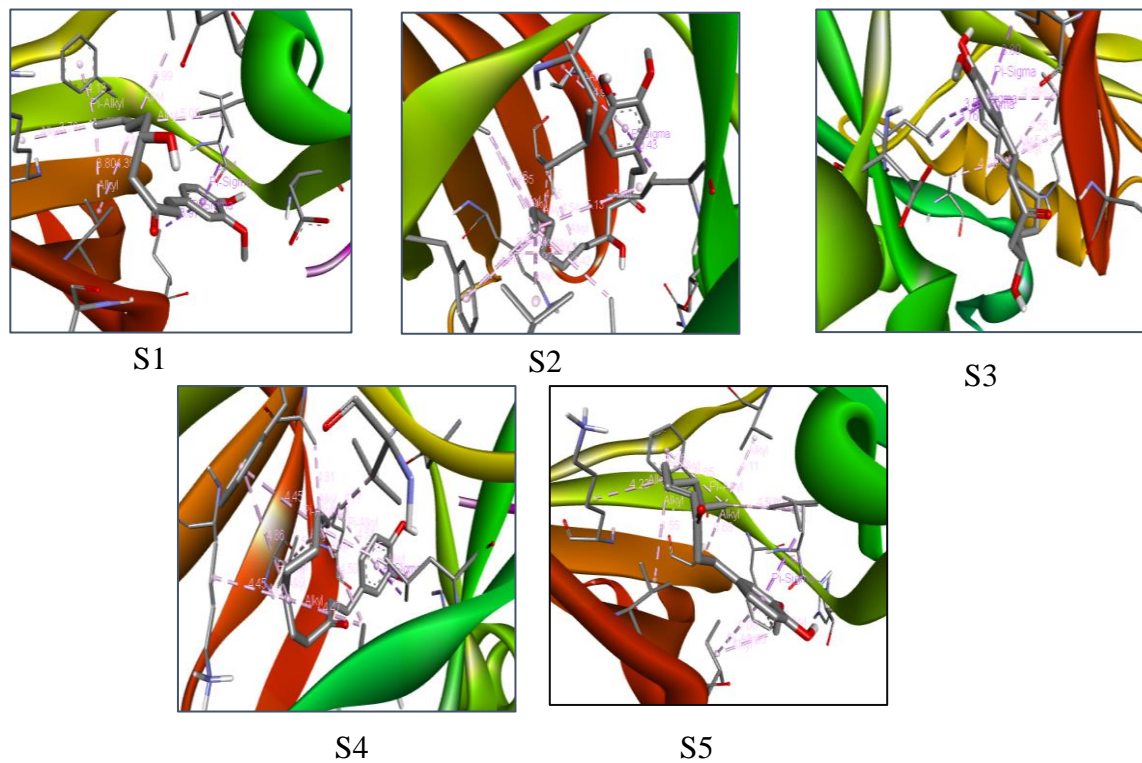


Fig.5.38 Interaction of CDK2 from Robetta with ginger compounds (3D)

a. Interaction of CDK2 from Robetta with ginger

The results of the interaction between the ginger compounds and CDK2 show that all four compounds interact with several amino acid residues of CDK2 through a combination of conventional hydrogen bonds, carbon hydrogen bonds, pi-sigma interactions, alkyl interactions, and pi-alkyl interactions.

In particular, 6-gingerol interacts with GLU12, ASP86, ILE10, LEU134, VAL18, ALA144, LYS33, and PHE80. 8-gingerol interacts with ASP86, ASN132, LEU83, LEU134, VAL18, ALA31, LYS33, ALA144, VAL64, and PHE80. 10-gingerol interacts with GLU12, ASP86, ILE10, LEU134, VAL18, LYS33, ALA144, and VAL18. 6-paradolol interacts with ASP86, ILE10, LEU134, VAL18, ALA31, LYS33, VAL64, ALA144, LEU134, PHE80, and PHE80. Finally, 6-shogaol interacts with HIS84, LEU134, VAL18, ALA31, LYS33, ILE10, VAL64, LEU83, LEU134, PHE80, PHE82, and ILE10.

Overall, the results suggest that ginger compounds have the potential to interact with CDK2, which is a key player in cell cycle regulation and cancer progression. These interactions could have implications for the development of novel cancer therapies.

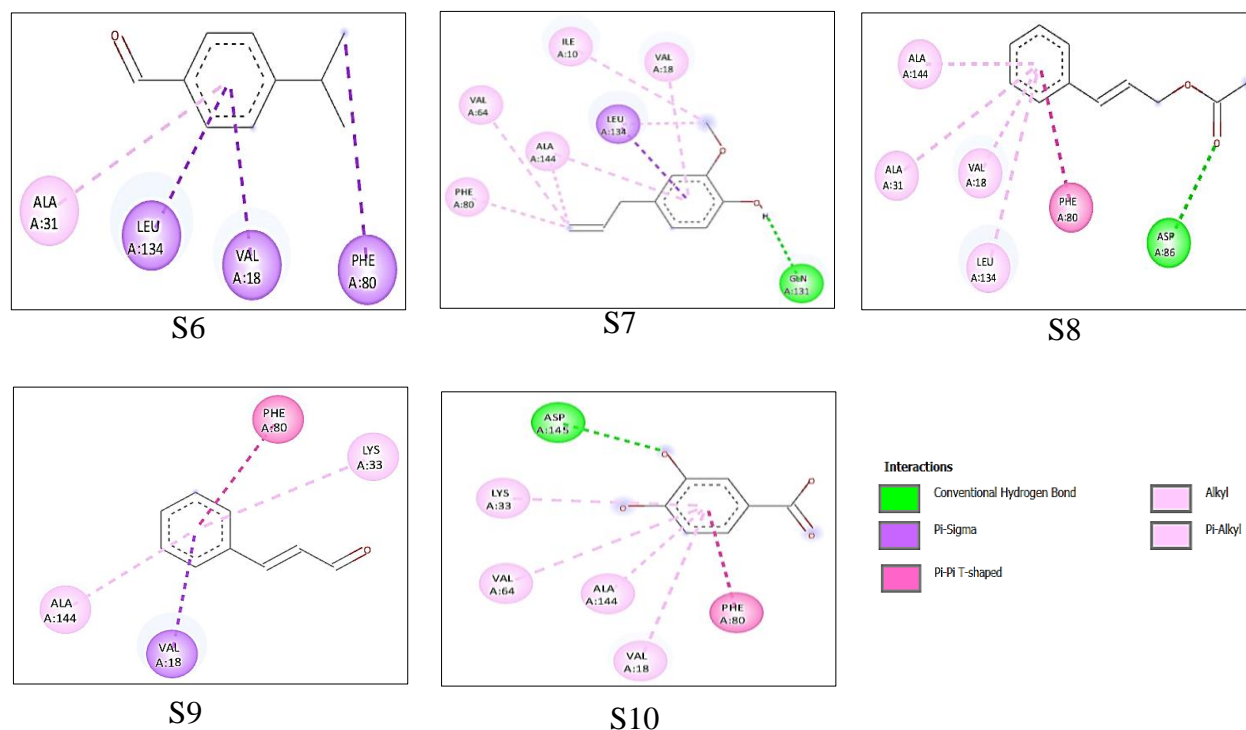


Fig.5.39 Interaction of CDK2 from Robetta with cinnamon compounds (2D)

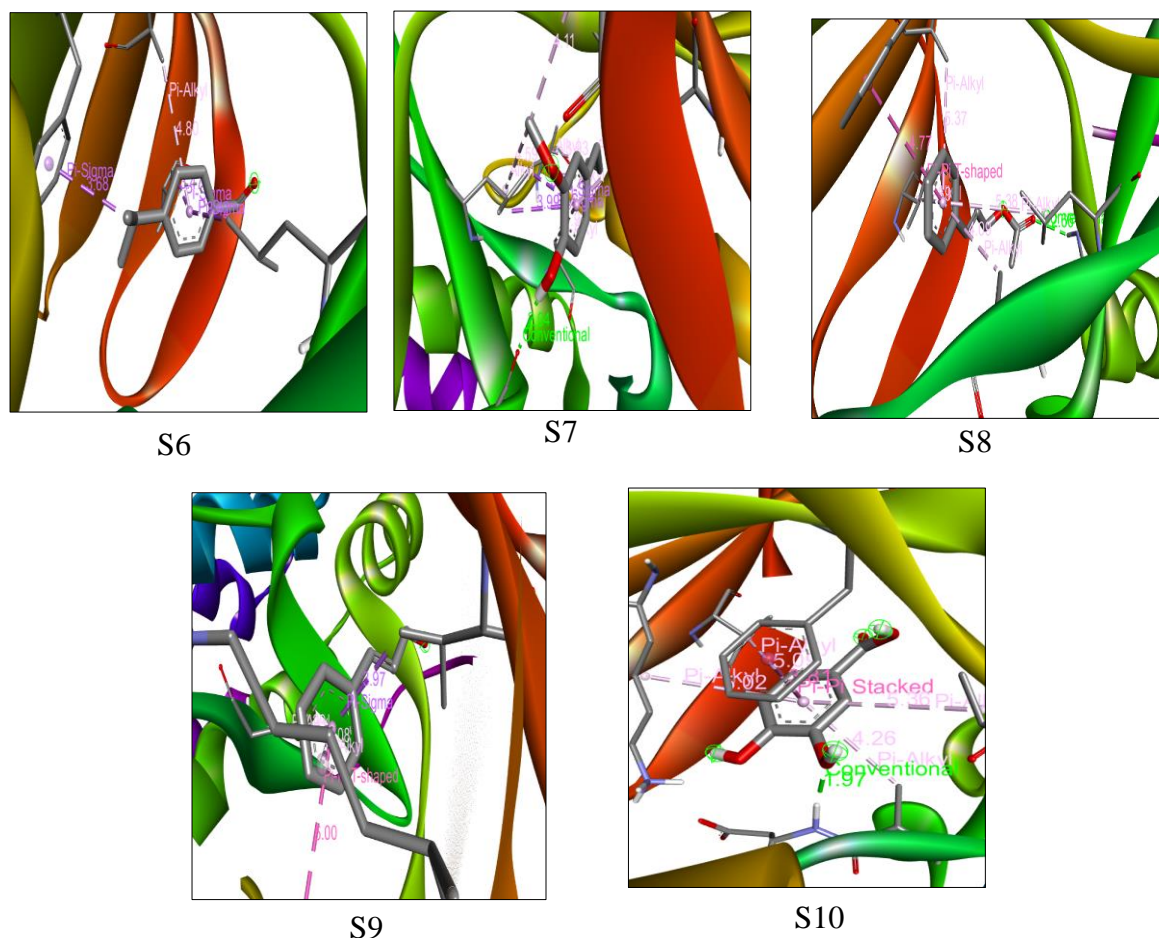


Fig.5.40 Interaction of CDK2 from Robetta with cinnamyl compounds (3D)

c. Interaction of CDK2 from Robetta with cinnamyl

Based on the interactions observed in the Figs 5.39, 5.40, it can be concluded that Cuminaldehyde interacts with CDK2 mainly through Pi-sigma interactions at residue VAL18 and LEU134, and Pi-alkyl interactions at residues ALA31 and PHE80. E-cinnamyl acetate interacts with CDK2 through Pi-alkyl interactions at residues VAL18 and ALA31, and Pi-pi T-shaped interactions at residue PHE80. Additionally, a conventional hydrogen bond is formed with residue ASP86. Eugenol interacts with CDK2 through alkyl interactions at residues ILE10, VAL18, VAL64, and LEU134, as well as a Pi-alkyl interaction at residue ALA144. A conventional hydrogen bond is also formed with residue GLN131. Protocatechuic acid interacts with CDK2 through Pi-alkyl interactions at residues VAL18, LYS33, and VAL64, a Pi-pi stacked interaction at residue PHE80,

and Pi-alkyl interactions at residue ALA144. Additionally, a conventional hydrogen bond is formed with residue ASP145. Trans-cinnamaldehyde interacts with CDK2 mainly through Pi-sigma interactions at residue VAL18, Pi-alkyl interactions at residue LYS33, Pi-pi T-shaped interactions at residue PHE80, and Pi-alkyl interactions at residue ALA144. Overall, the cinnamom compounds exhibit a variety of interactions with CDK2, including Pi-sigma, Pi-alkyl, Pi-pi T-shaped, and conventional hydrogen bonds. These interactions could potentially affect the binding affinity and inhibitory activity of the compounds towards CDK2.

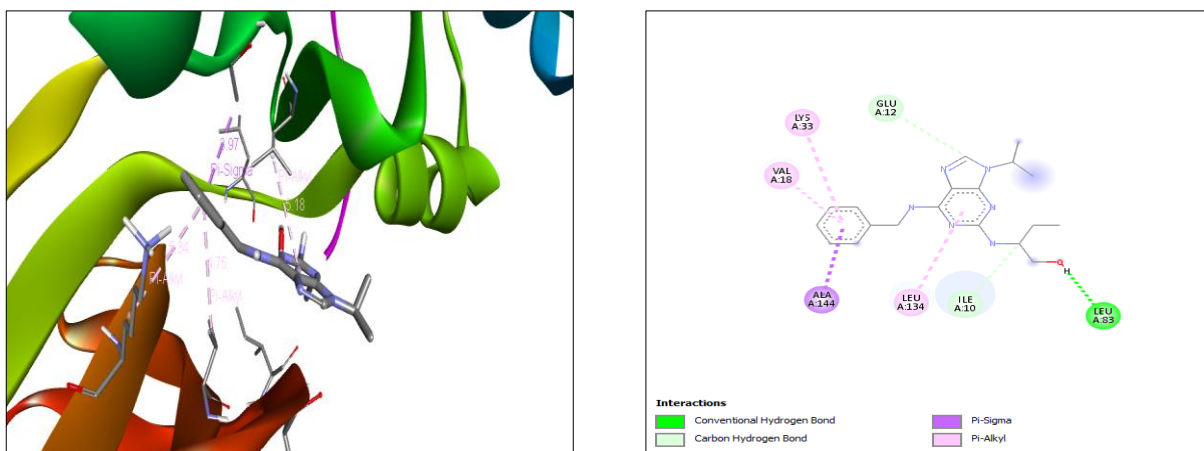


Fig.5.41 Interaction of CDK2 from Robetta with Roscovitine

5.4.2. Comparison of interaction results

The compounds interacted with different residues in the active site of CDK2 through conventional hydrogen bonds, carbon-hydrogen bonds, hydrophobic bonds; Pi interactions, and van der Waals interactions.

It can be observed that the amino acids differ in each CDK2 prediction case. In the case of CDK2 from PDB, it is noticed that THR 198, ARG 214, VAL 251, LYS 250, ARG 200, ARG 150, LEU 124, and ARG 126 are repeated in most compounds of the two plates (cinnamon and ginger). In the case of Swiss-Model, the most frequently occurring amino acids are LEU 166, TRP 167, GLN 131, and GLU 81. On the other hand, the most repeated amino acids in the case of CDK2 from AlphaFold are ILE10, LEU134, ALA144, VAL64, PHE80, VAL18, and ALA31. Similarly, in the case of CDK2 from Robetta, the most repeated amino acids are ILE10, LEU134, ALA144,

VAL64, PHE80, VAL18, and ALA31. However, in the case of ESM, there are no common amino acids between the compounds of cinnamon and ginger.

AlphaFold are ILE10, LEU134, ALA144, VAL64, PHE80, VAL18, and ALA31. Similarly, in the case of CDK2 from Robetta, the most repeated amino acids are ILE10, LEU134, ALA144, VAL64, PHE80, VAL18, and ALA31. However, in the case of ESM, there are no common amino acids between the compounds of cinnamon and ginger.

When it compare with roscovitine ,we find that the major amino acids are common in the two models alphafold and robetta. However, there is a lesser occurrence of these common amino acids in the PDB, Swiss and ESM models

5.5. Pharmacokinetics

5.5.1. Drug likeness tool

The resulte shown in the Tab 5.23

Tab.5.23 Prediction of Druglikeness with DruLiTo program.

Code	MW	LogP	HBA	HBD	TPSA	AMR	nRB	nAtom	Lipinski's Rule	Ghose Filter	Weber Rule
<i>Ginger</i>											
S1	294.18	2.437	4	2	66.76	80.8	10	47	1	0	1
S2	322.21	3.575	4	2	66.76	86.63	12	53	1	1	0
S3	350.25	4.713	4	2	66.76	92.45	14	59	1	1	0
S4	278.19	3.889	3	1	46.53	77.75	10	46	1	1	1
S5	276.17	3.775	3	1	46.53	82.07	9	44	1	1	1

<i>Cinnamon</i>											
S6	148.09	2.423	1	0	17.07	49.08	2	23	1	0	1
S7	164.08	2.223	2	1	29.46	52.89	3	24	1	1	1
S8	176.2	2.531	2	0	26.3	56.48	4	25	1	1	1
S9	132.2	1.968	1	0	17.07	46.27	2	18	1	0	1
S10	154.03	0.616	4	3	77.76	40.17	1	17	1	0	1
<i>Witness</i>											
W	354.22	1.693	7	3	84.51	104.86	8	52	1	1	1
<i>Ligand</i>											
L1	442.12	1.72	8	3	129.68	132.53	5	50	1	0	0
L2	199.01	0.868	4	3	75.61	33.55	1	17	1	0	1

3.6.1.1. Drulito interpretation:

The prediction results of physico-chemical properties based on several drug-likeness rules (Tab 5.23) shown that two compound from Ginger (6-Paradol ,6-Shogaol) and cinnamon(Eugenol, (E)-cinnamyl acetate) albums did comply with Lipinski's rule, Ghose's filter and Veber's rule .

There is one compound(S1) that does not comply with Ghose rule, and two last (S2,S3) did not comply with Veber's rule from Ginger . As for Cinnamon compounds there is three compounds that did not comply with Ghose rule, (S6,S9,S10). It does not mean that « 6,8 and 10-Gingerol » & « Protocatechuic Acid ,trans-Cinnamaldehyde and Cuminaldehyd » are unable to penetrate cell membranes because the drug can penetrate cell membranes if it complies with at least 2 of Lipinski's rules. Compared to the results of roscovitine and the ligands, W and L2 have the ability to penetrate cell membranes, while L1 doesn't penetrate cell membranes [151].

5.5.2. Pharmacokinetics models for small molecules

The result shown in the Tab 5.24

Tab.5.24 Prediction of pKCSM

Code	Intestinal Absorption (humanà)	Skin permeability	VD _{ss} (human)	BBB Permeability	CYP2D6 Substrate	CYP2D6 inhibitor	Total Clearance	Renal OCT2 Substrate	Ames Toxicity	Hepato - toxicity
<i>Ginger</i>										
S1	92.416	-2.817	0.524	-0.727	No	No	1.339	No	No	No
S2	91.716	-2.781	0.588	-0.794	No	No	1.41	No	No	No
S3	91.029	-2.759	0.605	-0.877	No	No	1.462	No	No	No
S4	92.18	-2.587	0.549	-0.223	No	No	1.411	No	No	No
S5	92.686	-2.584	0.501	-0.197	No	No	1.44	No	No	No
<i>Cinnamon</i>										
S6	92.041	-2.207	0.324	-0.438	No	No	0.227	No	No	No
S7	94.148	-1.437	0.24	-0.374	No	No	0.282	No	Yes	No
S8	93.665	-2.735	-1.953	-0.423	No	No	0.28	No	Yes	No
S9	95.015	-2.355	0.266	-0.436	No	No	0.208	No	No	No
S10	71.174	-2.727	-1.298	-0.683	No	No	0.551	No	No	No
<i>Witness</i>										
W	89.24	-2.735	0.418	-1.199	No	No	0.95	Yes	Yes	Yes
<i>Ligand</i>										
L1	0	-2.735	-0.287	-3.691	No	No	-0.315	No	No	No
L2	73.502	-2.843	0.184	-0.341	No	No	0.652	No	No	No

3.6.2.1. Pharmacokinetics models for small molecules interpretation

Pharmacokinetics prediction can be seen from Tab 5.24. Where the prediction of absorption is expressed by the value of intestinal absorption, the distribution is expressed by the value of VD_{ss} and BBB permeability, metabolism is expressed by CYP2D6 substrate and inhibitor, excretion is expressed by the value of total clearance, and toxicity is expressed by hepatotoxicity and LD 50. For a given compound it predicts the percentage that will be absorbed through the human intestine, a molecule with an absorbance of less than 30% is considered to be poorly absorbed. For ginger compounds, it can be seen that the intestinal absorption (human) value of the tested compounds is around 91.029% - 92.686%. For cinnamon compounds, the intestinal absorption value of the tested compounds is around 71.174% - 95.014% (trans-cinnamaldehyde has better intestinal absorption), so it can be predicted that the ten compounds will be absorbed well in the human intestine, it's better than drscovitine and ligands (ligand protein data bank can't will be absorbed in the human intestine). A compound is considered to have a relatively low skin permeability if it has a logK_p > -2.5. Therefore, all compounds have relatively high skin permeability, as their log K_p values are greater than -2.5 except three cinnamon compounds (Cuminaldehyd, Eugenol and trans-Cinnamaldehyde) their log K_p > -2.5 have low skin permeability. The VD_{ss} is a steady-state volume of distribution that predicts the value total dose of the drug would need to be uniformly distributed to give the same concentration as in blood plasma. The higher the VD is, the more of a drug is distributed in tissue rather than plasma. It can be affected by renal failure and dehydration. VD_{ss} is considered low if below 0.71 L/kg (log VD_{ss} < -0.15) and high if above 2.81 L/kg (log VD_{ss} > 0.45). The test ginger compounds VD_{ss} are ranged from 0.524 to 0.605 (log L/kg), as for cinnamon compounds from -1.953 to 0.324 (log L/kg). The predicted results showed VD_{ss} relatively low.

The brain is protected from exogenous compounds by the blood-brain barrier (BBB). The ability of a drug to cross into the brain is an important parameter to consider to help reduce side effects and toxicities or to improve the efficacy of drugs whose pharmacological activity is within the brain. For a given compound, a logBB > 0.3 considered to readily cross the blood-brain barrier while molecules with logBB < -1 are poorly distributed to the brain. The BBB values of ten compounds above -1 (from -0.877 to -0.197 for « Ginger compounds ») and (from -0.683 to -0.374 for « Cinnamon compounds »), which means that they can penetrate the BBB moderately.

The cytochrome P450's responsible for are metabolism of many drugs. However inhibitors of the P450's can dramatically alter the pharmacokinetics of these drugs. It is therefore important to assess whether a given compound is likely to be a cytochrome P450 substrate. One of the major isoforms responsible for drug metabolism is 2D6. In the Tab, it can be seen that none of the ten compounds act as substrates or inhibitors of CYP2D6, so it can be predicted that all test compounds to be metabolized by the enzyme cytochrome P450. The total Clearance value of the test compounds ranges from 0.205 to 0.784 for ginger compounds, as for cinnamon compounds, its value ranges from 0.227 to 0.551. So from these values it can be predicted the compound's excretion. OCT2(Renal Organic Cation Transporter 2) in the kidney plays an important role in the disposition and clearance of endogenous drugs and compounds. It is clear from the Tab that all compounds do not affect the OCT2 substrate. Therefore, there are no harmful effects or usage restrictions. The Ames test is a widely employed method to assess a compounds mutagenic potential using bacteria. A positive test indicates that the compound is mutagenic and therefore may act as a carcinogen. From the results Tab 5.24 shows that two cinnamon compounds (Eugenol(E)-cinnamyl acetate) are predicted to be active to cause mutagenic effects and all the ten compounds from ginger and cinnamon are non-hepatotoxic but roscovitine show a toxicity (hepatotoxicity ,Ames toxicity and renal toxicity) [113, 175, 176].

5.5.3. Pass online

The result shown in the Tab 5.25

Tab.5.25 The PASS onliane result.

Anticarcinogenic			
Code	Compound Name	Pa	Pi
<i>Ginger</i>			
S1	6-Gingerol	0.364	0.038
S2	8-Gingerol	0.364	0.038
S3	10-Gingerol	0.364	0.038

S4	6-Paradol	0.415	0.028
S5	6-Shogaol	0.475	0.022
<i>Cinnamon</i>			
S6	Cuminaldehyd	0.255	0.080
S7	Eugenol	0.459	0.023
S8	(E)-cinnamyl acetate	0.466	0.023
S9	trans-Cinnamaldehyde	0.341	0.044
S10	Protocatechuic Acid	0.387	0.033
<i>Witness</i>			
W	Roscovitine	0.254	0.183
<i>Ligand</i>			
L1	Ligand of PDB	0.550	0.015
L2	Ligand of Swiss model	/	/

3.6.3.1. Pass online interpretation:

The Pa value is the possibility of a compound being active in carrying out biological activities in laboratory experiments, while the Pi value is the opposite. If a compound has a value of $Pa > Pi$, then the compound has the potential to have this activity. And it has medium potential on a laboratory scale because the Pa value > 0.3 , the pa value of ginger compounds are between (0.364-0.475) and of cinnamon compounds are between (0.255-0.466), roscovitine have $pa=0.254$, it's less than the ten compounds but ligand PDB have a good $pa \geq 0.5$. While all the compounds have under activity except Cuminaldehyd ($pa = 0.255$). But it has the same value with the witness *Roscovitine* ($pa = 0.254$) so we can say that cuminaldehyd has the same activity. While the ligand of swiss model don't have any activity as an anticarcinogenic [114, 151].

5.6. Conclusion

In conclusion, The investigation of cinnamon and ginger extracts in this chapter unveiled their organoleptic, physicochemical, biochemical, and antibacterial properties, showcasing promising prospects for their utilization in the fields of cosmetics and pharmaceuticals.

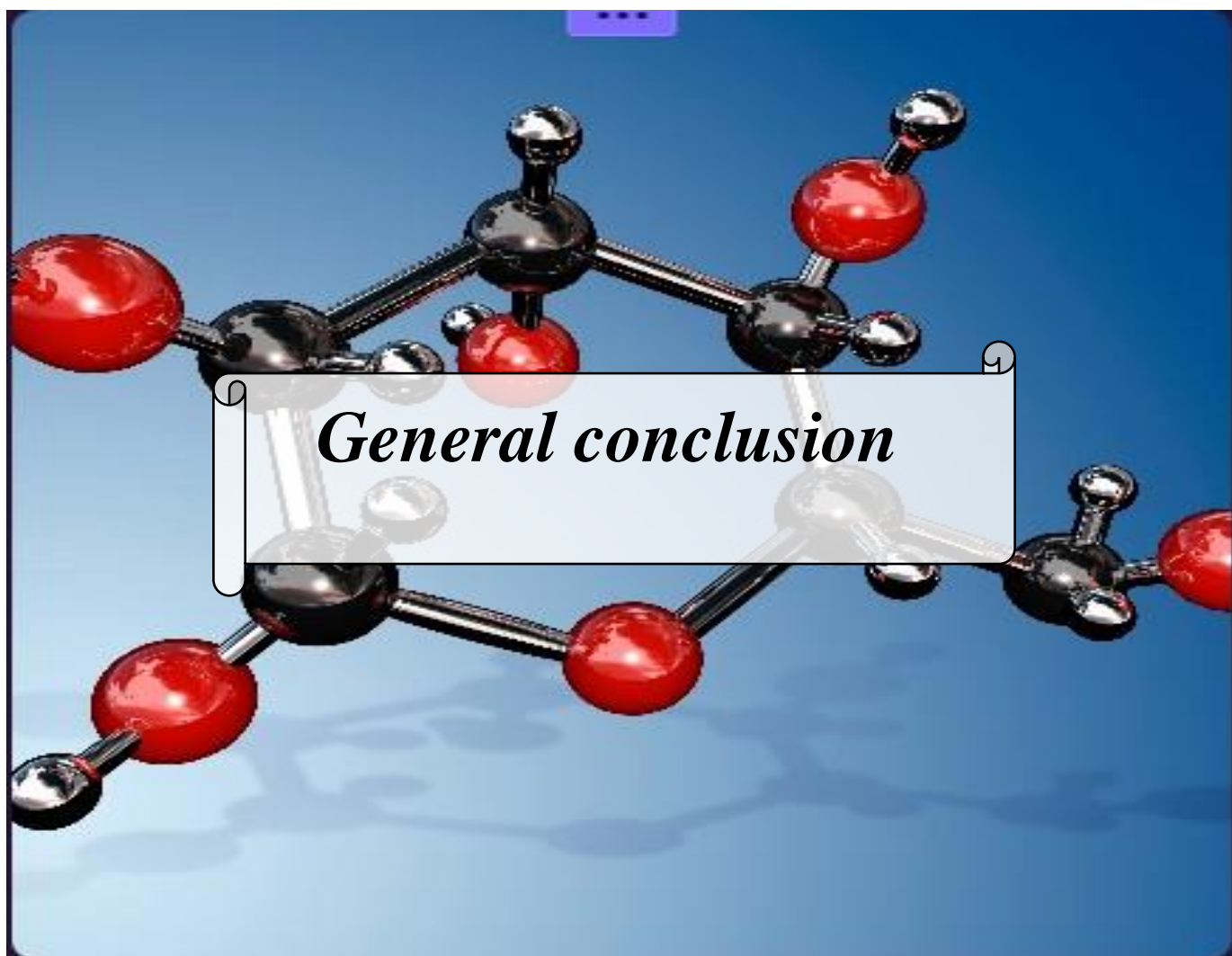
The in silico study conducted using AutoDock and protein prediction programs provided valuable insights into the interaction between bioactive compounds present in cinnamon and ginger extracts with the target protein CDK2. This computational approach allows for a deeper understanding of the molecular mechanisms underlying the observed anticancer activities.

According to the results of molecular docking, it can be concluded that the better compound from cinnamon is 6-shogaol, while from ginger it is Protocatechuic Acid.

Although the comparison based on the PDB results suggests that SWISS-MODEL is the ideal Model, if the objective is to select the model with better ΔG results, ROBETTA would be the preferred option based on the given comparison. It is important to consider the specific requirements and context of the study when choosing the most appropriate model for protein modeling and ΔG calculations.

Among the models studied, the fusion of the ten compounds resulted in a lack of agreement with the results obtained from the drug in both the Robetta and AlphaFold models, unlike the other models assessed. However, the ultimate judgment on this matter will rely solely on the experiment, as the results obtained are mere expectations that can only be validated or disproven through experimental investigation.

Lastly, the ADMET prediction offered an assessment of the extracts' pharmacokinetic and toxicological properties, providing essential information for future drug development and safety considerations.



General conclusion

General conclusion

The objective of our study is to investigate the potential anticancer activity of ginger and cinnamon specifically targeting cyclin dependent kinase 2 (CDK2). CDK2 is a protein involved in cell cycle regulation, and its dysregulation is often associated with cancer. By examining the effects of ginger and cinnamon on CDK2, we aim to determine if these natural substances have the ability to inhibit CDK2 and potentially exert anti-cancer effects. This research may contribute to the development of new therapeutic approaches or compounds derived from ginger and cinnamon that could be used in cancer treatment strategies targeting CDK2. During our research, we have directed our attention towards two plant species: cinnamon originating from three different countries - Indonesia, India, and China, and locally cultivated ginger of Algerian origin.

In this context, we conducted a study on the organoleptic and physicochemical characteristics of the plants. Subsequently, we determined the flavonoid content. Additionally, we investigated the antibacterial and antioxidant activities of different essential oil extracts.

The physical properties of cinnamon indicated that it has a density (Approximately 1.06) greater than ginger (0.85). the pH value of oils is 5 to 6 which indicates its purity. In terms of their chemical properties, the analysis revealed that cinnamon essential oil has a lower free acid content compared to ginger essential oil. However, both essential oils are abundant in esters, with cinnamon containing 41% and ginger containing 92.07%. The saponification values (SV) were measured as 56.08 mgKOH/g for cinnamon and 154.22 mgKOH/g for ginger.

Furthermore, cinnamon essential oil exhibited significantly higher antioxidant activity than ginger essential oil. Both oils had similar IC 50 values, with cinnamon at 12.93 µg/ml and ginger at 14.19 µg/ml. However, it is important to note that the concentration of flavonoids in Algerian ginger essential oil was lower compared to Indonesian cinnamon essential oil.

In this study, we conducted an in vitro evaluation of the antibacterial activity of essential oils on three different bacterial strains: *Escherichia coli*, *Staphylococcus aureus*, and *Candida albicans*. The results of our study indicated that our cinnamon Essential Oil exhibited a high inhibitory effect

against all three bacterial strains. However, the ginger Essential Oil showed inhibitory activity only against the *Staphylococcus aureus* strain.

Using an *in silico* approach, we investigated the potential anti-cancer effects of Cinnamon and ginger essential oils by studying their interactions with the protein CDK2. Specifically, we evaluated the binding affinity and molecular interactions between these essential oils and CDK2 protein. In this *in silico* analysis, we focused on compounds from ginger and cinnamon essential oils. After screening, we identified 10 compounds with good glide scores that showed potential interactions with the target protein CDK2. During the docking process, we observed that the ligands formed various bonds with specific amino acid residues of the target protein. These bonds included conventional hydrogen bonds, carbon hydrogen bonds, alkyl interactions, Pi-Pi stacked, Pi-Sigma and pi-alkyl interactions. Notably, compounds such as 6-gingerol, 8-gingerol, 10-gingerol, 6-paradol, and 6-shogaol from ginger, as well as Cuminaldehyde, Eugenol, (E)-cinnamyl acetate, trans-Cinnamaldehyde, and Protocatechuic Acid from cinnamon, formed significant hydrogen bonds with specific amino acids it differ in each CDK2 prediction case. In the case of CDK2 from PDB, it is noticed that THR 198, ARG 214, VAL 251, LYS 250, ARG 200, ARG 150, LEU 124, and ARG 126 are repeated in most compounds of the two plates (cinnamon and ginger). In the case of Swiss-Model, the most frequently occurring amino acids are LEU 166, TRP 167, GLN 131, and GLU 81. On the other hand, in the case of CDK2 from Robetta, the most repeated amino acids are ILE10, LEU134, ALA144, VAL64, PHE80, VAL18, and ALA31. However, in the case of ESM, there are no common amino acids between the compounds of cinnamon and ginger. When it's compared with roscovitine we find that the common amino acid are major in Robetta model. Based on the docking results, two compounds stood out among the others. Protocatechuic Acid from cinnamon achieved a ΔG score of -5.7 (Kcal/mol) with K_i of 15607nm, indicating a stronger binding affinity compared to the other ligands. Similarly, 6-shogaol from ginger exhibited a ΔG score of -5.4 (Kcal/mol) with K_i of 9133 nm, suggesting a highly favorable binding interaction, when compared with a roscovitine drug, we find that the results of ΔG are very close, estimated at -5.9 Kcal/mol with K_i of 21250 nm. The more negative the ΔG score and the smaller the K_i value, the stronger the complex formed between the ligand and the

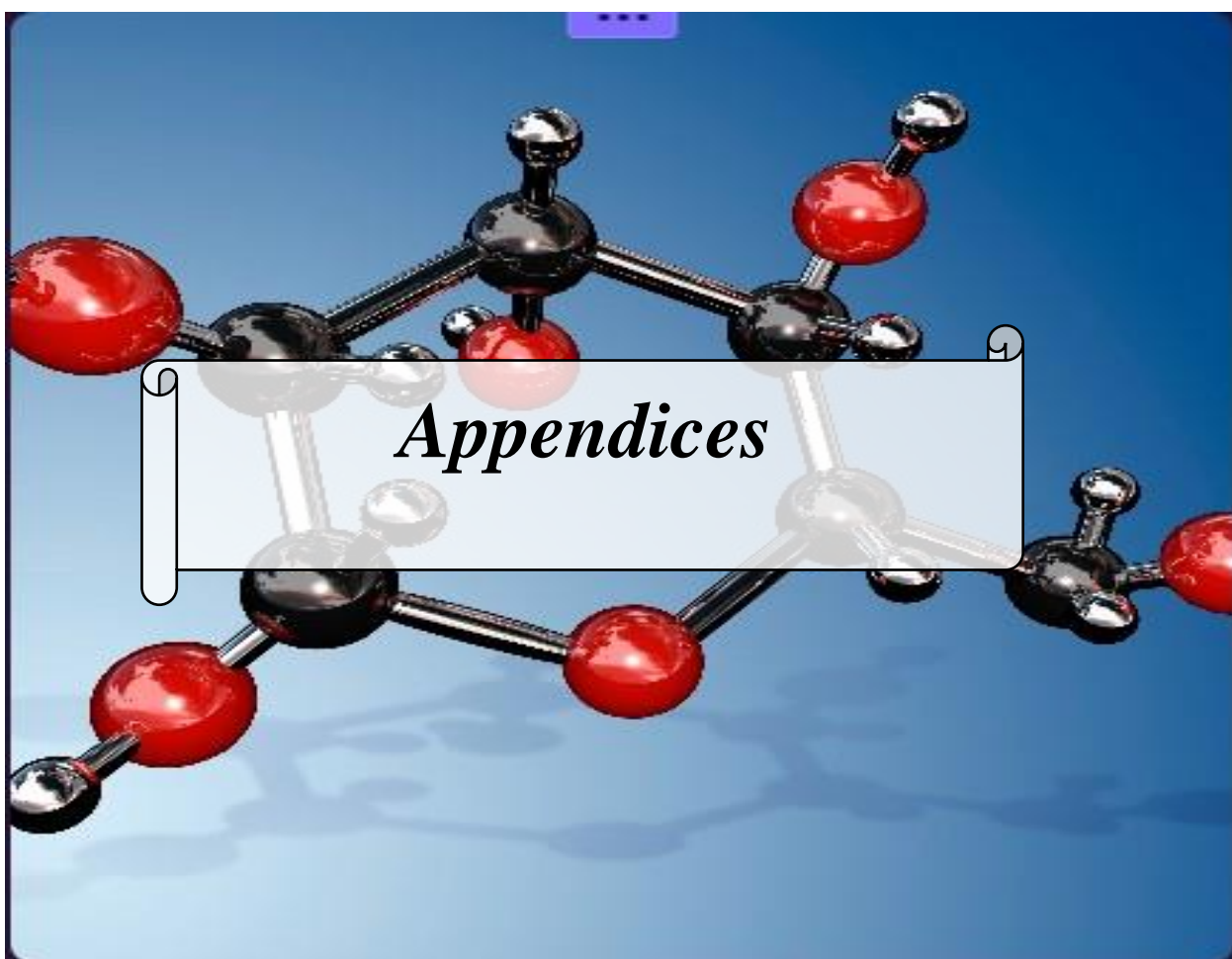
target protein. In this case, protocatechuic acid from cinnamon and 6-shogaol from ginger displayed the most promising binding affinities among the tested compounds.

According to the pharmacokinetics results and ADMET predictions, the tested compounds exhibited varying levels of intestinal absorption in humans, ranging from 31.11% to 100%. The volume of distribution at steady state (VD_{ss}) for the compounds ranged from -0.55 to 0.01 (log L/kg), indicating relatively low values. The predicted blood-brain barrier (BBB) values for nine compounds were above -1.15, suggesting moderate penetration potential into the brain. Additionally, all ten compounds from ginger and cinnamon were predicted to be non-hepatotoxic.

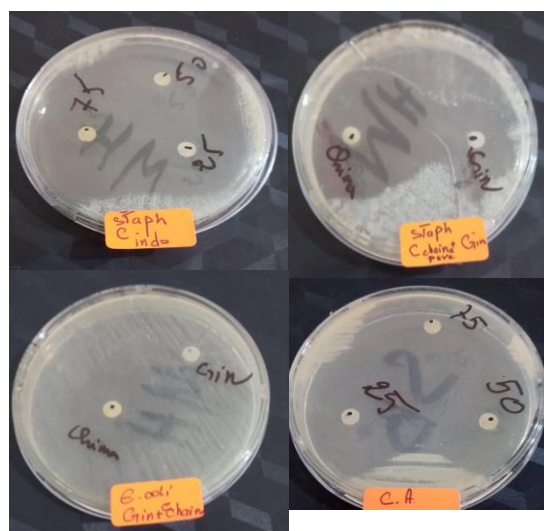
The physicochemical properties of the compounds, as assessed by several drug-likeness rules, indicated their ability to penetrate cell membranes. The pass online analysis revealed that the partition coefficient (p_a) values for the ginger compounds ranged from 0.364 to 0.475, while for the cinnamon compounds, the values ranged from 0.255 to 0.466. Notably, roscovitine had a p_a value of 0.254, indicating marginal activity. All the compounds, except for Cuminaldehyde (p_a=0.255), exhibited p_a values below the threshold for activity.

Regarding the prediction results, we find that Swiss-Model showed superiority in PDB-based comparisons, while Robetta excelled in ΔG results. It is important to note that these results are subject to the limitations of computational modeling and should be further validated through experimental studies.

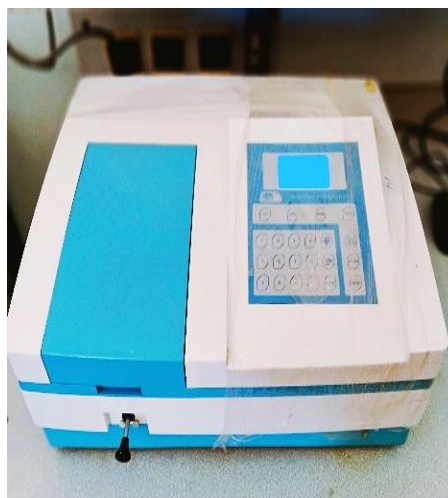
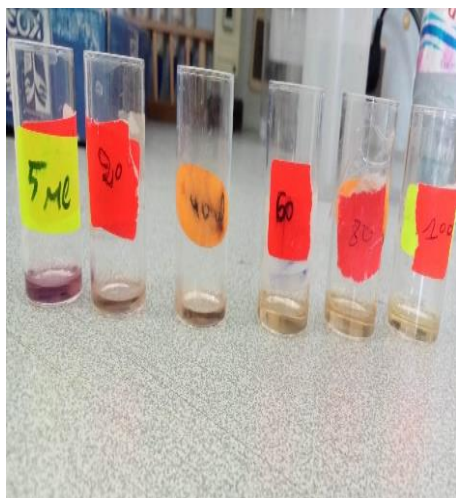
Therefore, it can be concluded that the flavonoid, phenolic acids compounds from ginger and cinnamon. Album has the potential as a promising anti-cancer drug candidate, where the best candidate is Protocatechuic Acid (cinnamon) then 6-Shogaol from ginger. However, further studies of flavonoid, phenolic acid compounds from *Syzygium cumini* var. Album are need.



Appendices



Antibacterial Activity



Antioxydant test

Bibliographic references

- [1. Muggleton, S., *Alan Turing and the development of Artificial Intelligence*. AI communications, 2014. **27**(1): p. 3-10.
2. Lamberti, M.J., et al., *A study on the application and use of artificial intelligence to support drug development*. Clinical therapeutics, 2019. **41**(8): p. 1414-1426.
3. Smith, R.G. and A. Farquhar, *The road ahead for knowledge management: an AI perspective*. AI magazine, 2000. **21**(4): p. 17-17.
4. Ramesh, A., et al., *Artificial intelligence in medicine*. Annals of the Royal College of Surgeons of England, 2004. **86**(5): p. 334.
5. Miles, J. and A.J. Walker. *The potential application of artificial intelligence in transport*. in *IEE Proceedings-Intelligent Transport Systems*. 2006. IET.
6. Wirtz, B.W., J.C. Weyerer, and C. Geyer, *Artificial intelligence and the public sector—applications and challenges*. International Journal of Public Administration, 2019. **42**(7): p. 596-615.
7. Yang, Y. and K.L. Siau, *A qualitative research on marketing and sales in the artificial intelligence age*. 2018.
8. Ashburn, T.T. and K.B. Thor, *Drug repositioning: identifying and developing new uses for existing drugs*. Nature reviews Drug discovery, 2004. **3**(8): p. 673-683.
9. Cui, W., et al., *Discovering anti-cancer drugs via computational methods*. Frontiers in pharmacology, 2020. **11**: p. 733.
10. Zhang, M., et al., *CDK inhibitors in cancer therapy, an overview of recent development*. American journal of cancer research, 2021. **11**(5): p. 1913.
11. Tadesse, S., et al., *Targeting CDK2 in cancer: challenges and opportunities for therapy*. Drug discovery today, 2020. **25**(2): p. 406-413.
12. Rao, P.V. and S.H. Gan, *Cinnamon: a multifaceted medicinal plant*. Evidence-Based Complementary and Alternative Medicine, 2014. **2014**.
13. Cabello, C.M., et al., *The cinnamon-derived Michael acceptor cinnamic aldehyde impairs melanoma cell proliferation, invasiveness, and tumor growth*. Free Radical Biology and Medicine, 2009. **46**(2): p. 220-231.
14. Davidson-Hunt, I., *Ecological Ethnobotany: Stumbling Toward New Practices and Paradigms*.
15. Lucy, H. and J. Edgar, *Medicinal plants: A reemerging health aid, division of life sciences UNESCO*. 1999.
16. Singh, R., *Medicinal plants: A review*. Journal of plant sciences, 2015. **3**(1-1): p. 50-55.
17. Vergine, M., et al., *Secondary metabolites in Xylella fastidiosa–plant interaction*. Pathogens, 2020. **9**(9): p. 675.
18. Mohammed, A.H., *Importance of medicinal plants*. Research in Pharmacy and Health Sciences, 2019. **5**(2): p. 124-125.
19. Rasool Hassan, B., *Medicinal plants (importance and uses)*. Pharmaceut Anal Acta, 2012. **3**(10): p. 2153-435.
20. Krishnaiah, D., R. Sarbatly, and R. Nithyanandam, *A review of the antioxidant potential of medicinal plant species*. Food and bioproducts processing, 2011. **89**(3): p. 217-233.
21. Ravindran, P., K. Nirmal-Babu, and M. Shylaja, *Cinnamon and cassia: the genus Cinnamomum*. 2003: CRC press.
22. Barceloux, D.G., *Cinnamon (cinnamomum species)*. Disease-a-month, 2009. **6**(55): p. 327-335.

23. Felter, H. and J. Lyod, *King's American Dispensatory Eclectic Medical Publications*. 1898, Portland.
24. Stevens, N. and K. Allred, *Antidiabetic potential of volatile cinnamon oil: A review and exploration of mechanisms using in silico molecular docking simulations*. *Molecules*, 2022. **27**(3): p. 853.
25. Senanayake, U.M., T.H. Lee, and R.B. Wills, *Volatile constituents of cinnamon (Cinnamomum zeylanicum) oils*. *Journal of agricultural and food chemistry*, 1978. **26**(4): p. 822-824.
26. Singh, G., et al., *A comparison of chemical, antioxidant and antimicrobial studies of cinnamon leaf and bark volatile oils, oleoresins and their constituents*. *Food and chemical toxicology*, 2007. **45**(9): p. 1650-1661.
27. Delgado, Y., et al., *Biomedical effects of the phytonutrients turmeric, garlic, cinnamon, graviola, and oregano: A comprehensive review*. *Applied Sciences*, 2021. **11**(18): p. 8477.
28. Semwal, R.B., et al., *Gingerols and shogaols: Important nutraceutical principles from ginger*. *Phytochemistry*, 2015. **117**: p. 554-568.
29. Ok, S. and W.-S. Jeong, *Optimization of extraction conditions for the 6-shogaol-rich extract from ginger (Zingiber officinale Roscoe)*. *Preventive Nutrition and Food Science*, 2012. **17**(2): p. 166.
30. Chen, X.-W., K. B Sneed, and S.-F. Zhou, *Pharmacokinetic profiles of anticancer herbal medicines in humans and the clinical implications*. *Current medicinal chemistry*, 2011. **18**(21): p. 3190-3210.
31. Butt, M.S. and M.T. Sultan, *Ginger and its health claims: molecular aspects*. *Critical reviews in food science and nutrition*, 2011. **51**(5): p. 383-393.
32. Govindarajan, V. and D. Connell, *Ginger—chemistry, technology, and quality evaluation: part 1*. *Critical Reviews in Food Science & Nutrition*, 1983. **17**(1): p. 1-96.
33. Prakash, J., *Chemical composition and antioxidant properties of ginger root (Zingiber officinale)*. *Journal of Medicinal Plants Research*, 2010. **4**(24): p. 2674-2679.
34. Ling, H., et al., *6-Shogaol, an active constituent of ginger, inhibits breast cancer cell invasion by reducing matrix metalloproteinase-9 expression via blockade of nuclear factor- κ B activation*. *British journal of pharmacology*, 2010. **161**(8): p. 1763-1777.
35. Kim, E.-C., et al., *[6]-Gingerol, a pungent ingredient of ginger, inhibits angiogenesis in vitro and in vivo*. *Biochemical and biophysical research communications*, 2005. **335**(2): p. 300-308.
36. Kim, S.O., et al., *Inhibitory effects of [6]-gingerol on PMA-induced COX-2 expression and activation of NF- κ B and p38 MAPK in mouse skin*. *Biofactors*, 2004. **21**(1-4): p. 27-31.
37. Shukla, Y. and M. Singh, *Cancer preventive properties of ginger: a brief review*. *Food and chemical toxicology*, 2007. **45**(5): p. 683-690.
38. Kaewpiboon, C., et al., *Studies of the in vitro cytotoxic, antioxidant, lipase inhibitory and antimicrobial activities of selected Thai medicinal plants*. *BMC complementary and alternative medicine*, 2012. **12**: p. 1-8.
39. XU, J.-K. and Y.-L. WANG, *Advances in the study uptake and accumulation of heavy metal in rice (Oryza sativa) and its mechanisms*. *Chinese Bulletin of Botany*, 2005. **22**(05): p. 614.
40. Arkin, N., et al., *Nutrition in critically ill patients with COVID-19: challenges and special considerations*. *Clinical Nutrition*, 2020. **39**(7): p. 2327-2328.
41. Abdullah, S., et al., *Ginger extract (Zingiber officinale) triggers apoptosis and G0/G1 cells arrest in HCT 116 and HT 29 colon cancer cell lines*. *Afr J Biochem Res*, 2010. **4**(4): p. 134-142.
42. Bidinotto, L.T., et al., *Effects of ginger (Zingiber officinale Roscoe) on DNA damage and development of urothelial tumors in a mouse bladder carcinogenesis model*. *Environmental and molecular mutagenesis*, 2006. **47**(8): p. 624-630.
43. Rahman, M.M., et al., *Docosahexaenoic acid inhibits UVB-induced activation of NF- κ B and expression of COX-2 and NOX-4 in HR-1 hairless mouse skin by blocking MSK1 signaling*. *PloS one*, 2011. **6**(11): p. e28065.

44. Bounedjar, A., et al., *Incidence of lung cancer in males and females in Algeria: The lung cancer registry in Algeria (LuCaReAl)*. *Cancer Epidemiology*, 2020. **69**: p. 101799.
45. Tsai, L.-H., et al., *The cdk2 kinase is required for the G1-to-S transition in mammalian cells*. *Oncogene*, 1993. **8**(6): p. 1593-1602.
46. Colas, P., *Cyclin-dependent kinases and rare developmental disorders*. *Orphanet Journal of Rare Diseases*, 2020. **15**(1): p. 1-14.
47. Upadhyay, A., *Cancer: An unknown territory; rethinking before going ahead*. *Genes & Diseases*, 2021. **8**(5): p. 655-661.
48. Varricchio, C.G., *A cancer source book for nurses*. 2004: Jones & Bartlett Learning.
49. Patel, A., *The Cell Biological Basis of Cancer*. *Zoology (major)*, 2012.
50. Bounedjar, A., et al., *General Oncology Care in Algeria*, in *Cancer in the Arab World*. 2022, Springer Singapore Singapore. p. 15-30.
51. Are, C., *Cancer on the global stage: Incidence and cancer-related mortality in Afghanistan*. 2016.
52. Irvin Jr, W.J. and L.A. Carey, *What is triple-negative breast cancer?* *European journal of cancer*, 2008. **44**(18): p. 2799-2805.
53. Goodman, J.E., et al., *Recommendations for further revisions to improve the International Agency for Research on Cancer (IARC) Monograph program*. *Regulatory Toxicology and Pharmacology*, 2020. **113**: p. 104639.
54. Schabath, M.B. and M.L. Cote, *Cancer progress and priorities: lung cancer*. *Cancer epidemiology, biomarkers & prevention*, 2019. **28**(10): p. 1563-1579.
55. Sung, H., et al., *Global cancer statistics 2020: GLOBOCAN estimates of incidence and mortality worldwide for 36 cancers in 185 countries*. *CA: a cancer journal for clinicians*, 2021. **71**(3): p. 209-249.
56. Biller, L.H. and D. Schrag, *Diagnosis and treatment of metastatic colorectal cancer: a review*. *Jama*, 2021. **325**(7): p. 669-685.
57. Malumbres, M., *Cyclin-dependent kinases*. *Genome biology*, 2014. **15**(6): p. 1-10.
58. Peyressatre, M., et al., *Targeting cyclin-dependent kinases in human cancers: from small molecules to peptide inhibitors*. *Cancers*, 2015. **7**(1): p. 179-237.
59. Malumbres, M., et al., *Cyclin-dependent kinases: a family portrait*. *Nature cell biology*, 2009. **11**(11): p. 1275-1276.
60. Orzáez, M., M.S. Medina, and E. Pérez-Payá, *Cyclin-dependent Kinase (CDK) Inhibitors: Methods and Protocols*. 2016: Springer.
61. Kalra, S., et al., *Structural insights of cyclin dependent kinases: implications in design of selective inhibitors*. *European journal of medicinal chemistry*, 2017. **142**: p. 424-458.
62. Roncato, R., et al., *CDK4/6 inhibitors in breast cancer treatment: potential interactions with drug, gene, and pathophysiological conditions*. *International journal of molecular sciences*, 2020. **21**(17): p. 6350.
63. Giordano, A. and G. Romano, *Cell Cycle Control and Dysregulation Protocols*. Vol. 285. 2008: Springer Science & Business Media.
64. Rodriguez-Acevedo, A., et al., *Indoor tanning prevalence after the International Agency for Research on Cancer statement on carcinogenicity of artificial tanning devices: systematic review and meta-analysis*. *British Journal of Dermatology*, 2020. **182**(4): p. 849-859.
65. Demetrick, D., H. Zhang, and D. Beach, *Chromosomal mapping of human CDK2, CDK4, and CDK5 cell cycle kinase genes*. *Cytogenetic and Genome Research*, 1994. **66**(1): p. 72-74.
66. Pines, J. and T. Hunter, *Human cyclin A is adenovirus E1A-associated protein p60 and behaves differently from cyclin B*. *Nature*, 1990. **346**(6286): p. 760-763.

67. Lees, E., et al., *Cyclin E/cdk2 and cyclin A/cdk2 kinases associate with p107 and E2F in a temporally distinct manner*. *Genes & Development*, 1992. **6**(10): p. 1874-1885.
68. Xu, M., et al., *Cyclin A/CDK2 binds directly to E2F-1 and inhibits the DNA-binding activity of E2F-1/DP-1 by phosphorylation*. *Molecular and cellular biology*, 1994. **14**(12): p. 8420-8431.
69. Hinds, P.W., *Cdk2 dethroned as master of S phase entry*. *Cancer cell*, 2003. **3**(4): p. 305-307.
70. Schulze-Gahmen, U., et al., *Multiple modes of ligand recognition: crystal structures of cyclin-dependent protein kinase 2 in complex with ATP and two inhibitors, olomoucine and isopentenyladenine*. *Proteins: Structure, Function, and Bioinformatics*, 1995. **22**(4): p. 378-391.
71. De Azevedo, W.F., et al., *Inhibition of cyclin-dependent kinases by purine analogues: crystal structure of human cdk2 complexed with roscovitine*. *European journal of biochemistry*, 1997. **243**(1-2): p. 518-526.
72. Gray, N.S., et al., *Exploiting chemical libraries, structure, and genomics in the search for kinase inhibitors*. *Science*, 1998. **281**(5376): p. 533-538.
73. de Azevedo Jr, W.F., et al., *Structural basis for specificity and potency of a flavonoid inhibitor of human CDK2, a cell cycle kinase*. *Proceedings of the National Academy of Sciences*, 1996. **93**(7): p. 2735-2740.
74. Hoessel, R., et al., *Indirubin, the active constituent of a Chinese antileukaemia medicine, inhibits cyclin-dependent kinases*. *Nature cell biology*, 1999. **1**(1): p. 60-67.
75. Spangler, J.B., et al., *Insights into cytokine-receptor interactions from cytokine engineering*. *Annual review of immunology*, 2015. **33**: p. 139-167.
76. Gilson, M.K., et al., *BindingDB in 2015: a public database for medicinal chemistry, computational chemistry and systems pharmacology*. *Nucleic acids research*, 2016. **44**(D1): p. D1045-D1053.
77. Muratov, E.N., et al., *A critical overview of computational approaches employed for COVID-19 drug discovery*. *Chemical Society Reviews*, 2021. **50**(16): p. 9121-9151.
78. Krejsa, C.M., et al., *Predicting ADME properties and side effects: the BioPrint approach*. *Current opinion in drug discovery and development*, 2003. **6**(4): p. 470-480.
79. Hansch, C., A. Leo, and D. Hoekman, *Exploring QSAR: hydrophobic, electronic, and steric constants*. Vol. 2. 1995: American Chemical Society Washington, DC.
80. Hansen, C., B.R. Telzer, and L. Zhang, *Comparative QSAR in toxicology: examples from teratology and cancer chemotherapy of aniline mustards*. *Critical reviews in toxicology*, 1995. **25**(1): p. 67-89.
81. Bradbury, S.P., *Quantitative structure-activity relationships and ecological risk assessment: an overview of predictive aquatic toxicology research*. *Toxicology letters*, 1995. **79**(1-3): p. 229-237.
82. Vučković, V., *Teorijske osnove i pristupi u QSAR modeliranju*. 2016, University of Split. Faculty of Chemistry and Technology. Division of Chemistry.
83. Perkins, R., et al., *Quantitative structure-activity relationship methods: Perspectives on drug discovery and toxicology*. *Environmental Toxicology and Chemistry: An International Journal*, 2003. **22**(8): p. 1666-1679.
84. Morris, G.M., R. Huey, and A.J. Olson, *Using autodock for ligand-receptor docking*. *Current protocols in bioinformatics*, 2008. **24**(1): p. 8.14. 1-8.14. 40.
85. Kitchen, D.B., et al., *Docking and scoring in virtual screening for drug discovery: methods and applications*. *Nature reviews Drug discovery*, 2004. **3**(11): p. 935-949.
86. Berman, H.M., et al., *The protein data bank*. *Nucleic acids research*, 2000. **28**(1): p. 235-242.
87. Trott, O. and A.J. Olson, *AutoDock Vina: improving the speed and accuracy of docking with a new scoring function, efficient optimization, and multithreading*. *Journal of computational chemistry*, 2010. **31**(2): p. 455-461.

88. Halperin, I., et al., *Principles of docking: An overview of search algorithms and a guide to scoring functions*. Proteins: Structure, Function, and Bioinformatics, 2002. **47**(4): p. 409-443.
89. Fuxreiter, M., et al., *Malleable machines take shape in eukaryotic transcriptional regulation*. Nature chemical biology, 2008. **4**(12): p. 728-737.
90. Feng, Y., et al., *Docking and scoring for nucleic acid–ligand interactions: Principles and current status*. Drug Discovery Today, 2022. **27**(3): p. 838-847.
91. Sousa, S.F., et al., *Protein-ligand docking in the new millennium—a retrospective of 10 years in the field*. Current medicinal chemistry, 2013. **20**(18): p. 2296-2314.
92. Morris, G.M., et al., *Automated docking using a Lamarckian genetic algorithm and an empirical binding free energy function*. Journal of computational chemistry, 1998. **19**(14): p. 1639-1662.
93. Wang, Y., et al., *The diagnostic value of ultrasound-based deep learning in differentiating parotid gland tumors*. Journal of Oncology, 2022. **2022**.
94. Cavasotto, C.N. and A.J. W Orry, *Ligand docking and structure-based virtual screening in drug discovery*. Current topics in medicinal chemistry, 2007. **7**(10): p. 1006-1014.
95. Wang, R., L. Lai, and S. Wang, *Further development and validation of empirical scoring functions for structure-based binding affinity prediction*. Journal of computer-aided molecular design, 2002. **16**: p. 11-26.
96. Cohen, M.H., et al., *FDA drug approval summary: gefitinib (ZD1839)(Iressa®) tablets*. The oncologist, 2003. **8**(4): p. 303-306.
97. Adnane, L., et al., *Sorafenib (BAY 43-9006, Nexavar®), a dual-action inhibitor that targets RAF/MEK/ERK pathway in tumor cells and tyrosine kinases VEGFR/PDGFR in tumor vasculature*. Methods in enzymology, 2006. **407**: p. 597-612.
98. Ahmad, N.M. and J.J. Li, *Venetoclax (Venclexta): A BCL-2 Antagonist for Treating Chronic Lymphocytic Leukemia*. Current Drug Synthesis, 2022: p. 143-163.
99. Deeks, E.D., *Olaparib: first global approval*. Drugs, 2015. **75**: p. 231-240.
100. Markham, A. and S. Dhillon, *Acalabrutinib: first global approval*. Drugs, 2018. **78**: p. 139-145.
101. Waterhouse, A., et al., *SWISS-MODEL: homology modelling of protein structures and complexes*. Nucleic acids research, 2018. **46**(W1): p. W296-W303.
102. Biasini, M., et al., *SWISS-MODEL: modelling protein tertiary and quaternary structure using evolutionary information*. Nucleic acids research, 2014. **42**(W1): p. W252-W258.
103. Peitsch, M.C., et al., *Automated modelling of the transmembrane region of G-protein coupled receptor by Swiss-model*. Receptors & channels, 1996. **4**(3): p. 161-164.
104. Chiereghin, C., et al., *In-depth genetic and molecular characterization of diaphanous related formin 2 (DIAPH2) and its role in the inner ear*. Plos one, 2023. **18**(1): p. e0273586.
105. Kumar, P., et al., *In-silico Identification and Analysis of Hub Proteins for Designing Novel First-line Anti-seizure Medications*. Letters in Drug Design & Discovery, 2023. **20**(6): p. 662-673.
106. Singh, J., et al., *SPOT-Contact-LM: improving single-sequence-based prediction of protein contact map using a transformer language model*. Bioinformatics, 2022. **38**(7): p. 1888-1894.
107. Clifford, J.N., et al., *BepiPred-3.0: Improved B-cell epitope prediction using protein language models*. Protein Science, 2022. **31**(12): p. e4497.
108. Oladejo, D.O., et al., *In silico Structure Prediction, Molecular Docking, and Dynamic Simulation of Plasmodium falciparum AP2-I Transcription Factor*. Bioinformatics and Biology Insights, 2023. **17**: p. 11779322221149616.
109. Park, H., et al., *Automatic structure prediction of oligomeric assemblies using Robetta in CASP12*. Proteins: Structure, Function, and Bioinformatics, 2018. **86**: p. 283-291.

110. Jia, C.-Y., et al., *A drug-likeness toolbox facilitates ADMET study in drug discovery*. Drug discovery today, 2020. **25**(1): p. 248-258.
111. Pangastuti, A., et al., *Natural bioactive compound from Moringa oleifera against cancer based on in silico screening*. Jurnal Teknologi, 2016. **78**(5).
112. Pires, D.E., T.L. Blundell, and D.B. Ascher, *pkCSM: predicting small-molecule pharmacokinetic and toxicity properties using graph-based signatures*. Journal of medicinal chemistry, 2015. **58**(9): p. 4066-4072.
113. Lohohola, P.O., et al., *In Silico ADME/T properties of quinine derivatives using SwissADME and pkCSM webservers*. International Journal of TROPICAL DISEASE & Health, 2021. **42**(11): p. 1-12.
114. Filimonov, D., et al., *Prediction of the biological activity spectra of organic compounds using the PASS online web resource*. Chemistry of Heterocyclic Compounds, 2014. **50**: p. 444-457.
115. Pogodin, P.V., et al., *How to achieve better results using PASS-based virtual screening: Case study for kinase inhibitors*. Frontiers in chemistry, 2018. **6**: p. 133.
116. Ban, L., et al., *Antioxidant activities from different rosemary clonal lines*. Food chemistry, 2016. **201**: p. 259-263.
117. Naviglio, D., et al., *Rapid Solid-Liquid Dynamic Extraction (RSLDE): A powerful and greener alternative to the latest solid-liquid extraction techniques*. Foods, 2019. **8**(7): p. 245.
118. Xiao, P., et al., *Effect of relative density and biocementation on cyclic response of calcareous sand*. Canadian Geotechnical Journal, 2019. **56**(12): p. 1849-1862.
119. Wenzl, T.G., et al., *Indications, methodology, and interpretation of combined esophageal impedance-pH monitoring in children: ESPGHAN EURO-PIG standard protocol*. Journal of pediatric gastroenterology and nutrition, 2012. **55**(2): p. 230-234.
120. Blotska, O., *EUROPEAN PHARMACOPOEIA OF 8-TH EDITION: MAJOR CHANGES IN THE CHAPTER "VACCINES FOR VETERINARY USE"*. Ветеринарна біотехнологія, 2015(27): p. 321-325.
121. Змеева, О.Н., et al., *Lotus corniculatus L.-перспективный вид рода Lotus L. Химия растительного сырья*, 2017(4): p. 5-14.
122. Djeridane, A., et al., *Antioxidant activity of some Algerian medicinal plants extracts containing phenolic compounds*. Food chemistry, 2006. **97**(4): p. 654-660.
123. Onimpandresena, T., *ÉTUDE DE L'ACTIVITE CICATRISANTE DE L'EXTRAIT HT 15 CHEZ LE RAT*. 2016, UNIVERSITE D 'ANTANANARIVO.
124. Bozin, B., et al., *Antimicrobial and antioxidant properties of rosemary and sage (Rosmarinus officinalis L. and Salvia officinalis L., Lamiaceae) essential oils*. Journal of agricultural and food chemistry, 2007. **55**(19): p. 7879-7885.
125. Viuda-Martos, M., et al., *Antioxidant activity of essential oils of five spice plants widely used in a Mediterranean diet*. Flavour and Fragrance Journal, 2010. **25**(1): p. 13-19.
126. Mkaddem, M., et al., *Chemical composition and antimicrobial and antioxidant activities of Mentha (longifolia L. and viridis) essential oils*. Journal of food science, 2009. **74**(7): p. M358-M363.
127. Amorati, R., M.C. Foti, and L. Valgimigli, *Antioxidant activity of essential oils*. Journal of agricultural and food chemistry, 2013. **61**(46): p. 10835-10847.
128. Brand-Williams, W., M.-E. Cuvelier, and C. Berset, *Use of a free radical method to evaluate antioxidant activity*. LWT-Food science and Technology, 1995. **28**(1): p. 25-30.
129. Gardeli, C., et al., *Essential oil composition of Pistacia lentiscus L. and Myrtus communis L.: Evaluation of antioxidant capacity of methanolic extracts*. Food chemistry, 2008. **107**(3): p. 1120-1130.
130. Ouraïni, D., et al., *Study of the activity on the various stages of development of dermatophytes of essential oils from aromatic Plants with antifungal properties*. Phytotherapie, 2005. **3**: p. 147-157.

131. Chahbi, A., et al., *Research Article Chemical Composition and Antimicrobial Activity of the Essential Oils of Two Aromatic Plants Cultivated in Morocco (Cinnamomum cassia and Origanum compactum)*. 2020.
132. Saeed, M., et al., *Antimicrobial activity of Syzygium aromaticum extracts against food spoilage bacteria*. Afr. J. Microbiol. Res, 2013. **7**(41): p. 4848-4856.
133. Forli, S., et al., *Computational protein–ligand docking and virtual drug screening with the AutoDock suite*. Nature protocols, 2016. **11**(5): p. 905-919.
134. Jejurikar, B.L. and S.H. Rohane, *Drug designing in discovery studio*. 2021.
135. Schiffrin, B., et al., *PyXlinkViewer: A flexible tool for visualization of protein chemical crosslinking data within the PyMOL molecular graphics system*. Protein Science, 2020. **29**(8): p. 1851-1857.
136. Eberhardt, J., et al., *AutoDock Vina 1.2. 0: New docking methods, expanded force field, and python bindings*. Journal of chemical information and modeling, 2021. **61**(8): p. 3891-3898.
137. Richardson, J.S., D.C. Richardson, and D.S. Goodsell, *Seeing the PDB*. Journal of Biological Chemistry, 2021. **296**.
138. Kiefer, F., et al., *The SWISS-MODEL Repository and associated resources*. Nucleic acids research, 2009. **37**(suppl_1): p. D387-D392.
139. Lin, Z., et al., *Evolutionary-scale prediction of atomic-level protein structure with a language model*. Science, 2023. **379**(6637): p. 1123-1130.
140. David, A., et al., *The AlphaFold database of protein structures: a biologist’s guide*. Journal of molecular biology, 2022. **434**(2): p. 167336.
141. Oladejo, D.O., et al., *Structure Prediction, Molecular Docking, and Dynamic Simulation of AP2-I Transcription Factor*. 2023.
142. Mignani, S., et al., *Present drug-likeness filters in medicinal chemistry during the hit and lead optimization process: how far can they be simplified?* Drug discovery today, 2018. **23**(3): p. 605-615.
143. Hussain, S., et al., *Phytochemical Composition of Ginger, its Nutritional and Pharmacological Importance*. Lahore Garrison University Journal of Life Sciences, 2020. **4**(01): p. 17-31.
144. Singh, R. and K. Singh, *Zingiber officinale: a spice with multiple roles*. Research Journal of Life Sciences, Bioinformatics, Pharmaceutical and Chemical Sciences, 2019. **5**(2): p. 113-125.
145. Gotmare, S. and E. Tambe, *Identification of chemical constituents of cinnamon bark oil by GCMS and comparative study garnered from five different countries*. Global Journal of Science Frontier Research: C Biological Science, 2019. **19**(1): p. 34-42.
146. Wang, R., R. Wang, and B. Yang, *Extraction of essential oils from five cinnamon leaves and identification of their volatile compound compositions*. Innovative Food Science & Emerging Technologies, 2009. **10**(2): p. 289-292.
147. Chairunnisa, C., H.A. Tamhid, and A.T. Nugraha. *Gas chromatography–Mass spectrometry analysis and antibacterial activity of Cinnamomum burmanii essential oil to Staphylococcus aureus and Escherichia coli by gaseous contact*. in *AIP Conference Proceedings*. 2017. AIP Publishing.
148. Wang, Y., et al., *PubChem: a public information system for analyzing bioactivities of small molecules*. Nucleic acids research, 2009. **37**(suppl_2): p. W623-W633.
149. Boutet, E., et al., *UniProtKB/Swiss-Prot: the manually annotated section of the UniProt KnowledgeBase*. Plant bioinformatics: methods and protocols, 2007: p. 89-112.
150. Jumper, J., et al., *Applying and improving AlphaFold at CASP14*. Proteins: Structure, Function, and Bioinformatics, 2021. **89**(12): p. 1711-1721.

151. Andhiarto, Y. and E.N. Praditapuspa, *In Silico Analysis and ADMET Prediction of Flavonoid Compounds from Syzigium cumini var. album on α -Glucosidase Receptor for Searching Anti-Diabetic Drug Candidates*. Pharmacognosy Journal, 2022. **14**(6).
152. Maingi, V., et al., *Dendrimer building toolkit: Model building and characterization of various dendrimer architectures*. Journal of computational chemistry, 2012. **33**(25): p. 1997-2011.
153. Cheng, D.M., et al., *In vivo and in vitro antidiabetic effects of aqueous cinnamon extract and cinnamon polyphenol-enhanced food matrix*. Food chemistry, 2012. **135**(4): p. 2994-3002.
154. Roy, B.C., M. Goto, and T. Hirose, *Extraction of ginger oil with supercritical carbon dioxide: experiments and modeling*. Industrial & Engineering Chemistry Research, 1996. **35**(2): p. 607-612.
155. Amira Ghislaine, D., et al., *Biochemical Parameters and Antioxidant Activity of Fresh and Dry Ginger Rhizomes (Zingiber officinale). Comparative Study*. Egyptian Academic Journal of Biological Sciences. C, Physiology and Molecular Biology, 2022. **14**(2): p. 185-196.
156. Khedis, L. and A. Aid, *Caractérisation phytochimique et activité antibactérienne de curcuma longa*. 2020.
157. Dohroo, N., . *Diseases of Ginger*, in *Ginger*. 2016, CRC Press. p. 325-360.
158. Wang, Y., et al., *Physical characterization and pork packaging application of chitosan films incorporated with combined essential oils of cinnamon and ginger*. Food and Bioprocess Technology, 2017. **10**: p. 503-511.
159. Setiyoningrum, F., G. Priadi, and F. Afati. *Supplementation of ginger and cinnamon extract into goat milk kefir*. in *AIP Conference Proceedings*. 2019. AIP Publishing LLC.
160. Couic-Marinier, F. and A. Lobstein, *Mode d'utilisation des huiles essentielles*. Actualités pharmaceutiques, 2013. **52**(525): p. 26-30.
161. Mraicha, F., et al., *Effect of olive fruit fly infestation on the quality of olive oil from Chemlali cultivar during ripening*. Food and chemical toxicology, 2010. **48**(11): p. 3235-3241.
162. BENCHEIKH, S.E., *Etude de l'activité des huiles essentielles de la plante Teucrium polium ssp Aurasianum Labiatae*. 2017.
163. Warabi, Y., D. Kusdiana, and S. Saka, *Reactivity of triglycerides and fatty acids of rapeseed oil in supercritical alcohols*. Bioresource technology, 2004. **91**(3): p. 283-287.
164. Bourrinet, P., *La pharmacie à l'aube du 3e millénaire*. Académie nationale de pharmacie, *La Pharmacie à l'aube du 3e millénaire, réalisation Regimedia*, 2010. Revue d'Histoire de la Pharmacie, 2011. **98**(370): p. 290-290.
165. Wu, H., et al., *Essential oil extracted from peach (Prunus persica) kernel and its physicochemical and antioxidant properties*. LWT-Food Science and Technology, 2011. **44**(10): p. 2032-2039.
166. Villaño, D., et al., *Radical scavenging ability of polyphenolic compounds towards DPPH free radical*. Talanta, 2007. **71**(1): p. 230-235.
167. Li, X., X. Wu, and L. Huang, *Correlation between antioxidant activities and phenolic contents of radix Angelicae sinensis (Danggui)*. Molecules, 2009. **14**(12): p. 5349-5361.
168. Khalaf, N.A., et al., *Antioxidant activity of some common plants*. Turkish Journal of Biology, 2008. **32**(1): p. 51-55.
169. Jehl, F., A. Chabaud, and A. Grillon, *L'antibiogramme: diamètres ou CMI?* Journal des Anti-infectieux, 2015. **17**(4): p. 125-139.
170. Friedman, M., et al., *Antibacterial activities of plant essential oils and their components against Escherichia coli O157: H7 and Salmonella enterica in apple juice*. Journal of agricultural and food chemistry, 2004. **52**(19): p. 6042-6048.
171. Wang, X., et al., *Antibacterial activity and mechanism of ginger essential oil against Escherichia coli and Staphylococcus aureus*. Molecules, 2020. **25**(17): p. 3955.

172. Zhu, H., et al., *Bactericidal effects of Cinnamon cassia oil against bovine mastitis bacterial pathogens*. Food Control, 2016. **66**: p. 291-299.
173. Uversky, V.N., *Dancing protein clouds: the strange biology and chaotic physics of intrinsically disordered proteins*. Journal of Biological Chemistry, 2016. **291**(13): p. 6681-6688.
174. Uversky, V.N., *The mysterious unfoldome: structureless, underappreciated, yet vital part of any given proteome*. Journal of Biomedicine and Biotechnology, 2010. **2010**.
175. Yeni, Y. and R.A. Rachmania, *The Prediction of Pharmacokinetic Properties of Compounds in Hemigraphis alternata (Burm. F.) T. Ander Leaves Using pkCSM*. Indonesian Journal of Chemistry.
176. Prasetyanti, I.K., *ADMET prediction and in silico analysis of mangostin derivatives and sinensetin on maltase-glucoamylase target for searching anti-diabetes drug candidates*. Pharmacognosy Journal, 2021. **13**(4).

List of tables

Tab 1.1: Chemical constituents of different parts of cinnamon.....	11
Tab 1.2: The Chemical Composition of Ginger Rhizome and Uses of Ginger.....	17
Tab 1.3: Anticancer Activity of Ginger and Compounds of Ginger against Cancer.....	18
Tab 3.1: Wib sice of the main molecular docking programs.....	42
Tab 4.1	54
Tab 4.2: List and characteristics of microorganisms tested.....	64
Tab 4.3: The characteristics of used laptops used in the stade.....	67
Tab 4.4: Programs used to carry out in silico study.....	68
Tab 5.1: Yield result by steam distillation method.....	90
Tab 5.2: The Organoleptic properties of ginger and cinnamon essential oils.....	91
Tab 5.3: Relative density of ginger and cinnamon essential oils.	92
Tab 5.4: pH value of ginger and cinnamon essential oils.....	93
Tab 5.5: Acid value of cinnamon and ginger essential oil.....	93
Tab 5.6: Ester value of ginger and cinnamon EO.....	95
Tab 5.7: Saponification value of ginger and cinnamon EO.....	97
Tab 5.8: Quantification of flavonoids in the hydrodistillation extract.	99
Tab 5.9: Linear regression equations obtained for antioxidant activity of cinnamon and ginger	101
Tab 5.10: Antibacterial activity result for essential oil of Ginger and Cinnamon.....	103
Tab 5.11: % inhibition result for essential oil of Ginger and Cinnamon.....	106
Tab 5.12: Estimation of the antibacterial activity of our EO and various CE.....	107
Tab 5.13: Presentation of ligands.....	110
Tab 5.14: Presentation of Targets	112
Tab 5.15: Molecular docking binding affinity of ginger and cinnamon compounds, ranked free energy of binding (ΔG) and inhibition constant (K_i).....	113
Tab 5.16: parameters of the grids box.....	115
Tab 5.17: Interaction details of the target enzyme CDK2 (CDK2 from PDB).....	117
Tab 5.18: Parameters of programme of protein prediction.....	122
Tab 5.19: Interaction details of the target enzyme CDK2 (swiss model).....	123
Tab 5.20: Interaction details of the target enzyme CDK2 (alphadatabase).....	130

Tab 5.21: Interaction details of the target enzyme CDK2 (ESM).....	137
Tab 5.22: Interaction details of the target enzyme CDK2 (Robetta).....	143
Tab 5.23: Prediction of Druglikeness with DruLiTo program.....	150
Tab 5.24: Prediction of pKCSM.....	152
Tab 5.25: The PASS online result.....	154

List of figures

Fig 1.1: Secondary metabolites.....	08
Fig 1.2: Clinical Significance of Cinnamon.....	10
Fig 1.3: Cinnamyl group-containing compounds.....	12
Fig 1.4: Clinical Significance of Ginger.....	14
Fig 1.5: Major chemical constituents of ginger.....	16
Fig 2.1: Features of Cancer - Major changes occurring in a cell undergoing malignant change.....	25
Fig 2.2: Schematic diagram depicting how metastasis from tumor occurs.....	26
Fig 2.3: Top 10 Cancers by Incidence-Current Rates in Algeria	27
Fig 2.4: Classification of CDKs.....	31
Fig 2.5: Representation of CDK2 as a prototype CDK protein bound with cyclin A and ATP and Tloop helps activate the ATP binding site when it gets bound to the CDK.	32
Fig 2.6: Illustrative view of cell cycle along with CDKs involved in cell cycle progression.....	33
Fig 2.7: inhibitors CDKs.....	34
Fig 2.8: crystallographic structure of CDK2 without and with cyclin A.	35
Fig 2.9: Action mechanism of CDK2 at the cell level	36
Fig 3.1: molecular bonding purchase of docking programs.....	42
Fig 3.2: Swiss Model	46
Fig 3.3: Drug likeness tools	49
Fig 3.4: PKCSM	50
Fig 4.1 : Flowchart representing the preparation of the plants.....	55
Fig 4.2 : Steam extraction process.....	56
Fig 4.3 : Separation the essential oil of cinnamon.....	56
Fig 4.4 : Volumetric analysis process.....	59
Fig 4.5 : Ester value determination process.....	60

Fig 4.6 : Bacterial suspension preparation.....	65
Fig 4.7 : Cinnamon and Ginger essential oil dilute.....	65
Fig 4.8 : Shema of procedure of MIC.....	66
Fig 4.9 : Downloading the pdb format file of protein.....	70
Fig 4.10 : Addition of polar hydrogens to protein structure.....	71
Fig 4.11 : The PubChem file.....	72
Fig 4.12 : The changed of the format file on Pymol.....	72
Fig 4.13 : The opening of the protein and the ligand on autodocktools.....	73
Fig 4.14 : The dimensions file of the grid box.....	74
Fig 4.15 : The configuration file.....	74
Fig 4.16 : Result of execution of autodock vina commands.....	75
Fig 4.17 : Downlodng of the sequence	76
Fig 4.18 : The input form of the target sequence.....	77
Fig 4.19 : The building Model on swiss model.....	77
Fig 4.20 : The input form of the target sequence on Alpha Fold.....	78
Fig 4.21: ScreenShot of protein databases.....	78
Fig 4.22: The building Model on AlphaFold.....	79
Fig 4.23: The downloading file.....	79
Fig 4.24: The opening of the pass web server.....	80
Fig 4.25: The input form of the target sequence on ESM.....	80
Fig 4.26: The building model on ESM.....	81
Fig 4.27: The opening of Robetta.....	81
Fig 4.28: The input form of the target sequence on Robetta.....	82
Fig 4.29: The screenshot of the E-mail.....	82
Fig 4.30: The building model on Robetta.....	83
Fig 4.31: Input the SDF file of the compound on Drulito.....	84
Fig 4.32: calcul the propriets.....	84
Fig 4.33: customize the rules as per the need.....	84
Fig 4.34: apply the selected rules.....	85
Fig 4.35: the total number of candidate among the molecules passing and violating all the rules.....	85
Fig 4.36: Input the smile file on PKCSM.....	86

Fig 4.37: The result of ADMET.....	86
Fig 4.38: The result of the pass online.....	87
Fig 5.1: Essential oil obtained of ginger and cinnamon by steam distillation.....	89
Fig 5.2: Graphic representation of the different yields (%) of the essential oils of ginger and the three types of cinnamon.....	90
Fig 5.3: Acid value results.....	94
Fig 5.4: Variation in acid value according to the types of EO.....	94
Fig 5.5: Ester value for titration of the blank and for titration of the essential oils.....	96
Fig 5.6: Variation in ester value according to the types of EO.....	97
Fig 5.7: Variation in saponification value according to the types of EO.....	98
Fig 5.8: Calibration Curve of Flavonoids.....	99
Fig 5.9: Percentage inhibition of cinnamon essential oil by DPPH test.....	100
Fig 5.10: Percentage inhibition of ginger essential oil by DPPH test.....	100
Fig 5.11: Percentage inhibition of ascorbic acid by DPPH test.....	102
Fig 5.12: Zones of inhibition results of each strain.....	101
Fig 5.13: Variation in zone diametre of inhibition according to the type of dilute oil and type of strain.....	105
Fig 5.14: Variation in zone diametre of inhibition according to the type of oil (100%) and type of strain.....	105
Fig 5.16: Molecular docking binding affinity of ginger[A] and cinnamon[B] compounds...	115
Fig 5.17: Interaction of CDK2 from PDB with ginger compounds (2D).....	118
Fig 5.18: Interaction of CDK2 from PDB with ginger compounds (3D).....	118
Fig 5.19: Interaction of CDK2 from PDB with cinnamon compounds (2D).....	120
Fig 5.20: Interaction of CDK2 from PDB with cinnamon compounds (3D).....	121
Fig 5.21: Interaction of CDK2 from PDB with Roscovitine.....	122
Fig 5.22: Interaction of CDK2 from swiss model with ginger compounds (2D)	126
Fig 5.23 : Interaction of CDK2 from swiss model with ginger compound (3D)	127
Fig 5.24: Interaction of CDK2 from swiss model with cinnamon compounds (2D)	128
Fig 5.25: Interaction of CDK2 from swiss model with cinnamon compounds (3D).....	129

Fig 5.26: Interaction of CDK2 from swiss model with Roscovitine.....	130
Fig 5.27: Interaction of CDK2 from Alphadatabase with ginger compounds (2D)	133
Fig 5.28: Interaction of CDK2 from Alphadatabase with Ginger compounds (3D)	134
Fig 5.29: Interaction of CDK2 from Alphadatabase with cinnamon compounds (2D)	135
Fig 5.30: Interaction of CDK2 from Alphadatabase with cinnamon compounds (3D).....	135
Fig 5.31: Interaction of CDK2 from Alphadatabase with Roscovitine.....	136
Fig 5.32: Interaction of CDK2 from ESM with ginger compounds (2D)	139
Fig 5.33: Interaction of CDK2 from ESM with ginger compounds (3D)	140
Fig 5.34: Interaction of CDK2 from ESM with cinnamon compounds (2D).....	141
Fig 5.35: Interaction of CDK2 from ESM with cinnamon compounds (3D)	141
Fig 5.36: Interaction of CDK2 from ESM with Roscovitine.....	142
Fig 5.37: Interaction of CDK2 from Robetta with ginger compounds (2D)	146
Fig 5.38: Interaction of CDK2 from Robetta with ginger compounds (3D)	146
Fig 5.39: Interaction of CDK2 from Robetta with cinnamon compounds (2D)	147
Fig 5.40: Interaction of CDK2 from Robetta with cinnamon compounds (3D)	148
Fig 5.41: Interaction of CDK2 from Robetta with Roscovitine.....	149

List of equation

Equation 4.1 : The essential oil yield percentage	56
Equation 4.2 : Relative density	57
Equation 4.3 : Potassium hydroxide reacts with acid	58
Equation 4.4 : The acid value	59
Equation 4.5 : Ester equation	59
Equation 4.6 : The ester value.....	60
Equation 4.7 : The saponification value	61
Equation 4.8 : DPPH equation	62
Equation 4.9 : The percentage of radical scavenging	63
Equation 4.10 : The percentage of bacterial growth inhibition	67

List of abbreviations

- **ADP** : Adenosine Diphosphate
- **AFDB** : AlphaFold Database
- **AMR**: Atom Molar Refractivity
- **ATM** : Ataxia Telangiectasia Mutated
- **ATP** : Adenosine Triphosphate
- **AV** : Acid Value
- **BBB** : Blood-Brain Barrier
- **BCL-2** : B-cell lymphoma 2
- **BIOVIA** : Biology + Virtual Integrated Applications
- **BTK** : Bruton's Tyrosine Kinase
- **CCTOP** : Consensus Constrained TOPology Prediction
- **CDK2** : Cyclin-Dependent kinase 2
- **CDK5R1** : Cyclin-Dependent Kinase 5 Regulatory Subunit 1
- **CDKs** : Cyclin-Dependent kinases
- **CLL** : Chronic Lymphocytic Leukemia
- **C-MY** : Cellular Myelocytomatosis
- **COX2** : Cyclooxygenase-2
- **CPU** : Central Processing Unit
- **CYC** : Cyclin
- **Deep TMHMM** : Deep Transmembrane Hidden Markov Model
- **DFG** : Aspartate (D), Phenylalanine (F), and Glycine (G)
- **DMSO** : Dimethyl Sulfoxide
- **DNA** : Deoxyribonucleic Acid
- **DS** : Discovery Studio
- **DSSP** : Dictionary of Secondary Structure of Proteins
- **E2F** : Transcription Factors
- **EBV-EA** : Epstein-Barr Virus - Early Antigens

- **EGFR** : Epidermal Growth Factor Receptor
- **EMBL** : European Molecular Biology Laboratory
- **EV** : Ester Value
- **GC** : Gas Chromatography
- **GNs** : Gingerols
- **GPX** : Glutathione Peroxidase
- **GR** : Glutathione Reductase
- **GST** : Glutathione S-transferase
- **HBA**: H-Bond Acceptor,
- **HBD**: H-Bond Donor,
- **HDL** : High-Density Lipoprotein
- **HL** : Human Leukemia
- **HPLC** : High Performance of Liquid Chromatography
- **HTC15** : Homo Sapiens Colon Carcinoma Cell line 15
- **IC 50** : 50% of Inhibitory Concentration
- **IL-8** : Interleukin-8
- **KDa** : Kills Deaths Assists.
- **Kin** : Kinase
- **LD50** : Lethal Dose 50.
- **LogP**: Partition coefficient,
- **MCF7** : Michigan Cancer Foundation-7
- **MCSM** : Manhattan Center for Science and Mathematics
- **MDA-MB-231** : Metastatic Ductal Adenocarcinoma-Michigan Cancer Foundation-Breast Cancer 231
- **MDDR** : Medicinal Data for Drug Discovery and Research
- **MDM** : Mouse Double Minute
- **MLH** : MutL Homolog
- **MMP-9** : Matrix Metalloproteinase-9
- **mRNA** : *Messenger RiboNucleic Acid*
- **MSH** : MutS Homolog

- **MVD** : Molegro Virtual Docker
- **MW-HD/A-LR** : Molecular Weight, Hydrogen Bond Donor and Acceptor, Lipophilicity, and RotaTab Bonds
- **nAtom**: Number of Atoms.
- **NF-KB** : Nuclear Factor-kappa B
- **NMR** : Nuclear Magnetic Resonance
- **nRB**: Number of RotaTab Bond,
- **NSCLC** : Non-Small Cell Lung Cance
- **P** : Protein
- **Pa** : Probability of Activity
- **PARP** : Poly Adenosine Diphosphate Ribose
- **PDB** : Protein Data Bank
- **Ph** : Potential of Hydrogen.
- **Pi** : Probability of Inactivity
- **pKB** : Protein Kinase B
- **PKCSM** : Pharmacokinetic and Pharmacodynamic Simulator
- **pRb** : Retinoblastoma Protein
- **QED** : Quantitative Estimate of Drug-likeness
- **QSAR** : Quantitative Structure–Activity Relationship
- **RAF** : Rapidly Accelerated Fibrosarcoma
- **Renal OCT2** : Renal Organic Cation Transporter 2
- **ROS** : Reactive Oxygen Species
- **S/TPXK/R** : S/T is the phosphorylated serine or threonine, P is proline, X is any amino acid, K is lysine, and R is arginine
- **SBDD** : Structure-Based Drug Design
- **SGs** : Shogaols
- **SK-MEL2** : Sloan-Kettering Melanoma Cell line 2
- **SV** : Saponification Value
- **TGF** : Transforming Growth Factor
- **TLC** : Thin Layer Chromatography

- **TM** : Transmembrane
- **TMDET** : TransMembrane Protein DETection
- **TNF- α** : Tumor Necrosis Factor-alpha
- **TOPCONS2** : Topological Consensus Prediction
- **TPSA**: Total Polar Surface Area
- **UNESCO** : United Nations Educational, Scientific, and Cultural Organization
- **UV** : Ultraviolet
- **VDss** : Volume of Distribution at Steady State
- **VEGF** : Vascular Endothelial Growth Factor
- **WHO** : World Health Organization